



INVESTIGATING THE ROLE OF REACTIVE METABOLITES AND PARENT COMPOUND
IN DRUG INDUCED LIVER INJURY

Thesis submitted in accordance with the requirements of the University of Liverpool
for the degree of Doctor of Philosophy

By

Nicola Marie Tidbury
September 2012

DECLARATION

This thesis is the result of my own work. The material contained within this thesis has not been presented, nor is it currently being presented, either wholly or in part for any degree or other qualification.

Nicola Marie Tidbury

This research was carried out in the Department of Molecular and Clinical Pharmacology, The University of Liverpool

CONTENTS

Acknowledgements		<i>iv</i>
Publications		<i>v</i>
Abbreviations		<i>vi</i>
Abstract		<i>ix</i>
Chapter 1	General introduction	1
Chapter 2	Nefazodone and buspirone: reactive metabolite formation and irreversible binding in liver	40
Chapter 3	Nefazodone and buspirone: reactive metabolite formation and toxicity to hepatocytes	75
Chapter 4	Phenformin: Parent compound and its role in mitochondrial toxicity	133
Chapter 5	Concluding discussion	163
Appendices	AUC values of metabolites	176
Bibliography		181

ACKNOWLEDGEMENTS

I would like to thank my PhD supervisors, Dr. Dominic Williams and Prof. Kevin Park, for their support and advice throughout the PhD.

I would like to express my gratitude to Pfizer for their sponsorship and the help, advice and support that were provided at my time spent in Kent. I would particularly like to thank Kathryn and Jon for their help with culturing rat hepatocytes and Gareth for his help with Cellomics.

A massive thank you to all the PhD students, post-docs and staff within the pharmacology department at the University of Liverpool. Particularly to Dr James Maggs for his MS assistance and advice. I would like to say a huge thank you to Dr Sophie Regan, for giving me so much of her time, help and advice and for putting up with my never ending questions!

Thank you to my family for their love and encouragement during my PhD, especially my mom and dad for always encouraging me to achieve as much as possible. Most importantly, thank you to my husband, Laurence, for always being there for me and providing constant support, encouragement and love.

PUBLICATIONS

Papers

Nicola Tidbury, James Maggs, R. Scott Obach, Iain Gardner, B. Kevin Park, Dominic P. Williams. Metabolism and toxicity of nefazodone in rat liver microsomes and hepatocytes. Chemical Research in Toxicology. *Manuscript in preparation*

Book Chapters

Webb, H. M., Regan, S., Antoine, D. J., **Lane, N.**, Walsh, R. J., Srivastava, A., Starkey-Lewis, P., Benson, C., Williams, D. P., Lavery, H., Goldring, C. and Park, B. K. 2012. Drug Bioactivation and Oxidative Stress. Encyclopedia of Drug Metabolism and Interactions.

Abstracts

Tidbury N, Williams D and Park K (2010) Comparison of non-clinical drug safety signals with nefazodone and buspirone. *Proceedings of the British Pharmacological Society* at <http://www.pA2online.org/abstracts/Vol8Issue1abst061P.pdf>

Lane N, Maggs J, Park K and Williams D (2010) Investigation into the metabolism and toxicity of nefazodone and buspirone. *Toxicology* **278**: 365-366.

ABBREVIATIONS

1-PP	1-pyrimidinylpiperazine
ABC	ATP-binding cassette
ABT	1-aminobenzotriazole
ACN	Acetonitrile
ADR	adverse drug reaction
AMP	adenosine 5'-monophosphate
AMPK	AMP-activated protein kinase
Apaf-1	apoptosis activating factor 1
ATP	adenosine 5'-triphosphate
AUC	area under the curve
β	Beta
Bax	Bcl-2 associated X protein
Bcl-2	B cell lymphoma 2
BCRP	breast cancer resistance protein
BSEP	bile salt export pump
$^{\circ}\text{C}$	degrees centigrade
^{14}C	carbon 14
Ci	Curie
C _{max}	maximum drug concentration
CO ₂	carbon dioxide
CoA	coenzyme A
CYP450	cytochrome P450
Δ	Delta
Δp	proton motive force
$\Delta\Psi$	mitochondrial membrane potential
Da	Dalton
dH ₂ O	distilled water
DILI	drug induced liver injury
DMSO	dimethyl sulfoxide
DTNB	5,5'-dithio-bis (2-nitrobenzoic acid)
EDTA	ethylenediaminetetra acetic acid
ER	estrogen receptor
EtOH	ethanol
ETC	electron transport train
FAD	flavin adenine dinucleotide
FAO	fatty acid oxidation
FDA	food and drug administration

FMO	flavin monooxygenase
γ	gamma
GAPDH	glyceraldehyde 3-phosphate dehydrogenase
γ -GCL	gamma-glutamyl cysteinyl ligase
GCT	gamma-glutamyl transpeptidase
GSH	glutathione
GSSG	oxidised glutathione
HCl	hydrochloric acid
HEPE	S 4-(2-hydroxyethyl)-1-piperazineethansulphonic acid
HPLC	high performance liquid chromatography
IC ₅₀	half maximal inhibitory concentration
LC	liquid chromatography
LC-MS	liquid chromatography – mass spectrometry
m/z	mass to charge ratio
mCPP	meta-chlorophenylpiperazine
MDRP	multidrug resistance protein
MeOH	methanol
MPT	mitochondrial permeability transition
MS	mass spectrometry
NAD	nicotinamide adenine nucleotide
NADPH	nictotinamide adenine dinucleotide phosphate (reduced)
NaOH	sodium hydroxide
NAPQI	n-acetyl-p-benzoquinone-imine
NIDDM	non-insulin dependent diabetes mellitus
NSAID	non-steroidal anti-inflammatory drug
NTCP	sodium taurochlorate co-transporting polypeptide
OCT1	organic cation transporter 1
OH	hydroxyl
OXPPOS	oxidative phosphorylation
Ψ	Psi
ROS	reactive oxygen species
Rpm	revolutions per minute
SEM	standard error of the mean
SLC	solute carrier
SSA	5'-sulphosalicylic acid
TIC	total ion chromatogram

Tmax	time of maximum drug concentration
TNF	tumour necrosis factor
XIC	extracted ion current

ABSTRACT

Adverse drug reactions (ADRs) are a major problem for drug companies and healthcare providers alike. Although ADRs can present anywhere in the body, the liver frequently effected, due to the relatively large concentrations of drugs it encounters. Drug induced liver injury (DILI) can occur through several different mechanisms. Bioactivation of drugs to reactive metabolites is believed to be a crucial step in the development of many cases of DILI. Nefazodone, an anti-depressant which was withdrawn due to hepatotoxicity, has been shown to be bioactivated to a reactive quinone-imine. The role of the mitochondria and their involvement in DILI is being increasingly recognised. The biguanides are known mitochondrial toxins, and phenformin and buformin were removed from the market due to unacceptably high incidents of lactic acidosis. The aims of this thesis were two-fold; to assess the bioactivation and irreversible binding of nefazodone and its safer analogue buspirone and to use the biguanides to assess mitochondrial toxicity in primary hepatocytes.

In liver microsomes, both nefazodone and buspirone demonstrated NADPH-dependent irreversible binding, however, nefazodone irreversible binding was 9-fold that of buspirone. The metabolism of both nefazodone and buspirone was extensive and consisted mainly of hydroxylation and *N*-dealkylation reactions. In rat and human liver microsomes supplemented with GSH, nefazodone formed GSH conjugates with *m/z* 791 and *m/z* 807. This implied that the conjugates were formed from bioactivation of *para*-hydroxy nefazodone and dihydroxy-nefazodone. In rat liver microsomes, buspirone did not form any GSH conjugates.

Further investigations of nefazodone and buspirone were carried out in freshly isolated rat hepatocytes. Metabolism of nefazodone and buspirone was investigated and revealed extensive metabolism of both compounds; however, GSH conjugates of neither compound were discovered. At 6 hours, both nefazodone and buspirone demonstrated significant irreversible binding (117.54 ± 15.32 pmol equiv./mg protein and 84.43 ± 30.93 pmol equiv./mg protein respectively) but only nefazodone demonstrated a significant decrease in cell viability (19.25 ± 18.26 % control viability). Inhibition studies, using ABT, significantly reduced the irreversible binding of nefazodone (49.34 ± 4.64 pmol equiv./mg protein) but did not decrease cytotoxicity. This indicated that in rat hepatocytes the parent compound may be responsible for toxicity.

Mitochondrial toxicity was investigated using the model mitochondrial toxins the biguanides. Initially, studies in cultured primary rat hepatocytes demonstrated that phenformin was the most potent mitochondrial toxin and dissipated the mitochondrial membrane potential, as measured by TMRM, within 24 hours ($1.028 \pm 0.39\%$ control fluorescence). This was taken forward to investigate mitochondrial toxicity in primary rat hepatocytes. Investigations into phenformin in rat hepatocytes demonstrated a high turnover to glucuronide metabolites and the novel metabolites [O, OMe] phenformin glucuronide and [2O] phenformin glucuronide were identified. Inhibition studies of CYP450 2D were undertaken using quinine (100 μ M) and this demonstrated significant inhibition of phenformin up to 200 μ M (AUC 47.30 ± 47.30 without quinine vs AUC 648.80 ± 121.28 with quinine). Despite increased phenformin concentrations, inhibition of phenformin metabolism

did not produce overt cytotoxicity, however, lactate concentrations correlated with increased phenformin concentration.

The work presented here highlights the need for a greater understanding of the role of bioactivation and irreversible binding in hepatotoxicity. It also demonstrates that whilst irreversible binding can help inform decisions as to whether a compound progresses into clinical trials, it should be made in the context of other safety assessments. Investigations into phenformin mitochondrial toxicity, illustrates the need to assess drugs and systems fully, to establish model compounds to investigate mechanisms of ADRs. A greater understanding of *in vitro* systems and the tools utilised to assess them, will benefit drug discovery and development. Ultimately, understanding these *in vitro* tests and the model compounds used to assess them, will help bridge the gap to man.

CHAPTER 1

GENERAL INTRODUCTION

Contents

1.1	INTRODUCTION.....	3
1.2	ADVERSE DRUG REACTIONS.....	5
1.3	DRUG INDUCED LIVER INJURY	6
1.4	METABOLISM, REACTIVE METABOLITE FORMATION, COVALENT BINDING AND DILI	7
1.4.1	Phase I and II metabolism	8
1.4.2	GSH conjugation.....	10
1.4.3	Reactive metabolites and covalent binding.....	12
1.5	MITOCHONDRIAL TOXICITY AND DILI	16
1.5.1	Mitochondrial physiology and function	16
1.5.2	Mitochondria and cell death.....	18
1.5.3	Mechanisms of drug induced mitochondrial injury.....	20
1.6	HEPATIC TRANSPORTERS AND DILI.....	22
1.6.1	Drug transporters in the liver	22
1.6.2	Bile acid transport and DILI.....	24
1.7	NEFAZODONE.....	25
1.7.1	Nefazodone induced hepatotoxicity.....	26
1.7.2	Metabolism and bioactivation of nefazodone and its involvement in DILI	26
1.7.3	Parent compound and its involvement in DILI.....	28
1.8	BUSPIRONE.....	29
1.9	BIGUANIDES	31
1.9.1	Biguanides and lactic acidosis.....	32
1.10	TOOLS USED TO INVESTIGATE METABOLISM AND TOXICITY	35
1.10.1	Inhibitors used to investigate mechanisms of toxicity	35
1.10.2	Stains and dyes for investigating cell toxicity	37
1.11	AIMS.....	38

INTRODUCTION

Adverse drug reactions (ADRs) are of great concern to the pharmaceutical industry and place a burden on medical services. Most ADRs are predictable, resulting from extension of the primary pharmacology of the drug, and come to light during pre-clinical safety assessments and clinical trials. They often result from drug-drug interactions or a prescribing error (Olson et al. 2000). Idiosyncratic or unpredictable ADRs rarely come to light during clinical trials and are only detected once the drug has reached the wider market.

Idiosyncratic reactions are generally considered to have different initiating factors, one of which is linked to the formation of reactive metabolites, which bind to proteins leading to toxicity. Many drugs that cause idiosyncratic reactions are now linked to reactive metabolite formation (Park et al. 2005). Detoxification of many reactive metabolites occurs via GSH conjugation (DeLeve, Kaplowitz 1991), and depletion of GSH is often required for toxicity to transpire. The irreversible binding of radiolabelled compounds or the identification of a GSH adduct of a drug in pre-clinical testing, is now seen as a hazard signal for the potential of a drug to undergo bioactivation and therefore cause toxicity (Park et al. 2011). Of the drugs that are bioactivated, many contain ‘structural alerts’, chemical moieties that are often associated with bioactivation and resultant toxicity (Kalgutkar et al. 2005a). As such one approach to designing safer drugs is to avoid the use of structural alerts in drug design (Kalgutkar, Soglia 2005, Edwards, Sturino 2011). This is not always possible however, as the structural alert may be a vital part of the pharmacology of the drug. The use of structural alerts is further complicated by the fact that not all drugs with structural alerts are bioactivated and not all drugs that are bioactivated are toxic (Kalgutkar, Didiuk 2009).

Drugs that contain moieties associated with the formation of electrophilic quinones, quinone-imines and quinone-methides, such as phenols, hydroquinones, *o*-aminophenols, *p*-aminophenols, alkylphenols and 5-oxo-indoles, are well established structural alerts (Edwards, Sturino 2011, Edwards, Sturino 2011). Quinone-imine formation has been well characterised through the model hepatotoxin, paracetamol. *n*-acetyl-*p*-benzoquinone-imine (NAPQI), the quinone-imine metabolic product of paracetamol has been shown to irreversibly bind to cellular proteins causing cell death through a variety of mechanisms (Bulera et al. 1995, Corcoran, Chung & Salazar 1987, Dietze et al. 1997a, Landin, Cohen & Khairallah 1996, Matthews et al. 1997, Parmar et al. 1995, Tirmenstein, Nelson 1989). Nefazodone, an anti-depressant withdrawn in 2004, has been demonstrated to form quinone-imine reactive metabolites following hydroxylation *para* to nitrogen on the chlorophenylpiperazine ring system. It is thought that this metabolism is responsible for the idiosyncratic hepatotoxicity observed in man (Kalgutkar et al. 2005b, Bauman et al. 2008a). In contrast, buspirone, an anxiolytic agent, has the potential to be bioactivated on its pyrimidinylpiperazine moiety and yet appears not to be (Kalgutkar et al. 2005b), and there have been no reports of buspirone induced hepatotoxicity. There are also reports that the parent nefazodone structure is the toxic entity eliciting mitochondrial toxicity or BSEP inhibition (Dykens et al. 2008, Kostrubsky et al. 2006). Investigating the link between nefazodone toxicity and bioactivation, alongside the non-hepatotoxin buspirone, will help to further elucidate the structure-toxicity relationship of nefazodone.

Although several drugs that cause idiosyncratic toxicity are thought to be due to reactive metabolite formation, metabolism is normally a detoxification process and the parent compound can also be involved in idiosyncratic toxicity. The biguanides

are anti-diabetic drugs, of which two, phenformin and buformin, have been withdrawn due to unacceptably high levels of lactic acidosis (Brown et al. 1998). It has been demonstrated that phenformin accumulates in mitochondria at concentrations up to 100-fold that in the cytosol (Davidoff 1971). It is not clear however why some patients developed lactic acidosis. Phenformin is metabolised by CYP450 2D6, a highly polymorphic enzyme, and it is a possibility that CYP450 2D6 poor metabolisers are at increased risk of phenformin toxicity (Idle et al. 1981, Shah, Evans & Oates 1985, Shah et al. 1980). As an AMPK-activator, phenformin has been recommended for clinical trials in triple-negative and ER-positive breast cancer (Caraci et al. 2003, Appleyard et al. 2012) and identification of patients that are liable to develop lactic acidosis could aid a re-introduction into the clinic.

The work presented in this thesis uses nefazodone, buspirone and phenformin to investigate the roles of reactive metabolite formation and parent compounds in drug induced toxicity, and the systems and biomarkers used to detect such toxicity.

1.2 ADVERSE DRUG REACTIONS

Adverse drug reactions (ADRs) are of great concern to the pharmaceutical industry and the medical profession. In the pharmaceutical industry 50% of drug candidates that enter pre-clinical trial studies fail to make it to clinical trial. Of those that advance to clinical testing, a further 30% are terminated due to unforeseen adverse effects (Kramer, Sagartz & Morris 2007). Of the drugs that do make it to market, in the 25 year period from 1975-2000 over 10% (56 of 548) of newly approved drugs were given a black box warning and a further 2.9% (16 of 548) had to be withdrawn from the market (Lasser et al. 2002). In the UK approximately 6.5% of hospital

admissions are as a result of an ADR (Pirmohamed et al. 2004) and as such are a financial burden to the NHS.

ADRs can broadly be split into two categories, on-target and off-target reactions. On-target reactions are predictable and result from an extension of the known primary or secondary pharmacology of the drug (eg bleeding in a warfarin patient). These reactions show a clear dose-dependent relationship and can be avoided by lowering the dose. These reactions are rarely life threatening, and account for 80% of all drug reactions (Williams 2006). Off-target (idiosyncratic) reactions are not related to the primary or secondary pharmacology of the drug and show a complex dose relationship. Idiosyncratic reactions normally occur at therapeutic doses after an initial delay or latency period, which may range from a few days to several months. They occur at a frequency of 1 in 100 to 1 in 100,000 patients and are often related to the host-dependent factors such as genetic disposition and metabolism. It is unclear why so many idiosyncratic reactions occur, but they have been associated with the formation of reactive metabolites which may result in cell death or immune mediated reactions.

1.3 DRUG INDUCED LIVER INJURY

Drug induced liver injury (DILI) is the most frequent reason for black box warnings or withdrawal from the market and although only 10-20% of cases of DILI are deemed to be idiosyncratic; 75% of idiosyncratic reactions result in liver transplantation or death (Ostapowicz et al. 2002). DILI has become a major problem for clinicians, the pharmaceutical industry and regulatory agencies worldwide, not least because it is poorly predictable from pre-clinical animal studies. Acute liver failure is also not normally present in clinical trial phases of the drug due to the large

numbers of patients that would be required to participate for such an incidence to occur, therefore, DILI is normally not indicated as a problem until the post-marketing stage. Between 1975 and 1999, 548 new drugs were approved by the FDA, of which 10 received a black box warning for hepatotoxicity and a further four were withdrawn (Lasser et al. 2002).

In the clinic, DILI can either occur as an allergic or non-allergic reaction and may resemble other forms of liver disease including hepatitis and cholestasis. Allergic reactions are characterised by the presence of fever, rash, eosinophilia, a relatively short latency period (1-6 weeks) and rapid reoccurrence of the reaction (although this is normally deemed unethical). Autoantibodies directed towards the drug or a metabolite may also be present. Allergic DILI may also be accompanied by other severe reactions such as Steven Johnson syndrome. Non-allergic DILI is characterised by consistent absence of the above features of allergic reactions, tending to have a much longer latency period (1 month – 1 year) and unlike allergic reactions, may not produce a consistent reaction upon re-challenge.

1.4 METABOLISM, REACTIVE METABOLITE FORMATION, COVALENT BINDING AND DILI

Drug metabolism generally makes a drug less reactive and assists excretion of the drug from the body through increasing its lipophilicity. Occasionally metabolism causes bioactivation of a drug into a reactive metabolite. Reactive metabolites are normally deactivated by conjugation to GSH, however, if cell defences are impaired or overwhelmed these reactive metabolites are free to bind to cellular macromolecules and cause toxicity through a number of mechanisms (figure 1.1). This is particularly evident in the liver, which is the main site of metabolism. All

drugs administered orally pass through the liver via the portal vein before reaching the systemic circulation, therefore, the liver is often the site of ADRs. Post 1950, 13 out of 21 (62%) of drugs withdrawn from the market or given a black box warning due to hepatotoxicity have been shown to produce reactive metabolites (Walgren, Mitchell & Thompson 2005) which have been implicated as a major cause of DILI.

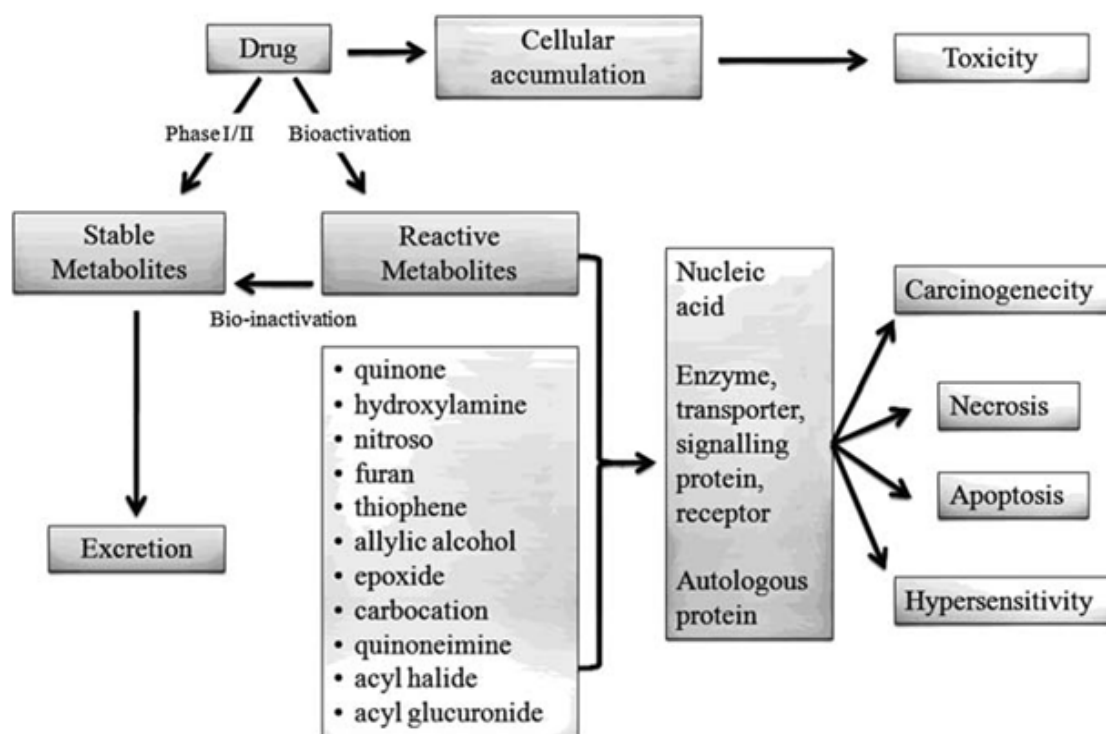


Figure 1.1. Schematic of metabolism and reactive metabolite formation. Following phase I metabolism, some molecules can be bioactivated to reactive metabolites. If these are not detoxified they can bind to macromolecules resulting in cell death, hypersensitivity reactions or carcinogenicity.

1.4.1 Phase I and II metabolism

The liver is the primary site of metabolism and receives 80% of its blood supply from the gut and so has a high metabolic capacity. Drug metabolism normally takes place in two stages. Initially, drugs undergo phase I metabolism. This is usually an oxidative process which adds or unmask a functional group so that the molecule can undergo conjugation reactions or phase II metabolism, this makes the drug

Phase I reactions	Phase II reactions
Oxidation	Glucuronidation/glucosylation
Reduction	Sulphation
Hydrolysis	Methylation
Hydration	Acetylation
Dethioacetylation	Amino acid conjugation
Isomerisation	Fatty acid conjugation
	Condensation

Table 1.1 Summary of phase I and II reactions.

more hydrophilic and therefore easier to excrete. The cytochrome P450 (CYP450) enzyme family are the most important of the oxidative enzymes responsible for phase I metabolism. They are able to metabolise a huge array of structurally diverse compounds, where the only common factor is a relatively high degree of lipophilicity. Although there are many CYP450 enzymes present in the liver the most abundant is CYP3A4 which is responsible for the metabolism of many xenobiotics (Gibson, Skett 2001). Although most phase I metabolites are unreactive, some are bioactivated to chemically reactive metabolites such as quinone-imines, which can cause cell damage and death.

Following phase I metabolism, many compounds undergo phase II conjugation reactions such as glucuronidation, sulfation and acetylation. These reactions involve a diverse group of enzymes and the above conjugation reactions are carried out by UDP-glucuronyltransferases, sulfotransferases and *N*-acetyltransferases respectively (Jancovaa, Anzenbacherb & Anzenbacherovaa 2010). These reactions generally lead

to a more water soluble compound, for easier excretion in the bile or urine as well as the metabolic inactivation of pharmacologically active compounds (Gibson, Skett 2001). Phase II reactions are not commonly associated with the same bioactivation reactions as phase I metabolism, however some phase II metabolites such as troglitazone sulphate (Funk et al. 2001b) and acyl glucuronides (Regan et al. 2010) have been implicated in the toxicity of compounds. Common phase I and phase II reactions are summarised in table 1.1.

1.4.2 GSH conjugation

GSH is a tripeptide and is probably the most important antioxidant that is produced by cells. It not only neutralises endogenously produced electrophiles and free radicals but also bioactivated xenobiotics. GSH is synthesised by the formation of a peptide bond between glutamic acid and cysteine, catalysed by γ -glutamylcysteine synthetase, then subsequent addition of glycine by GSH synthetase (figure 1.2). It is the redox and conjugation reactions that take place on the sulfhydryl group of cysteine that are thought to be the most important in its detoxifying actions (Forman, Zhang & Rinna 2008). During times of oxidative stress and GSH depletion in the cell GSH synthesis can be induced by a variety of transcription factors (Copple et al. 2008). The transcription factors that control the expression of the enzymes involved in GSH synthesis can be induced by the conjugation of GSH to electrophiles. In most cell types GSH exists at a concentration of 1-2mM but in hepatocytes the concentration may be as high as 10mM (Yuan, Kaplowitz 2008). Due to the high levels of GSH in hepatocytes GSH conjugation may occur spontaneously but is more

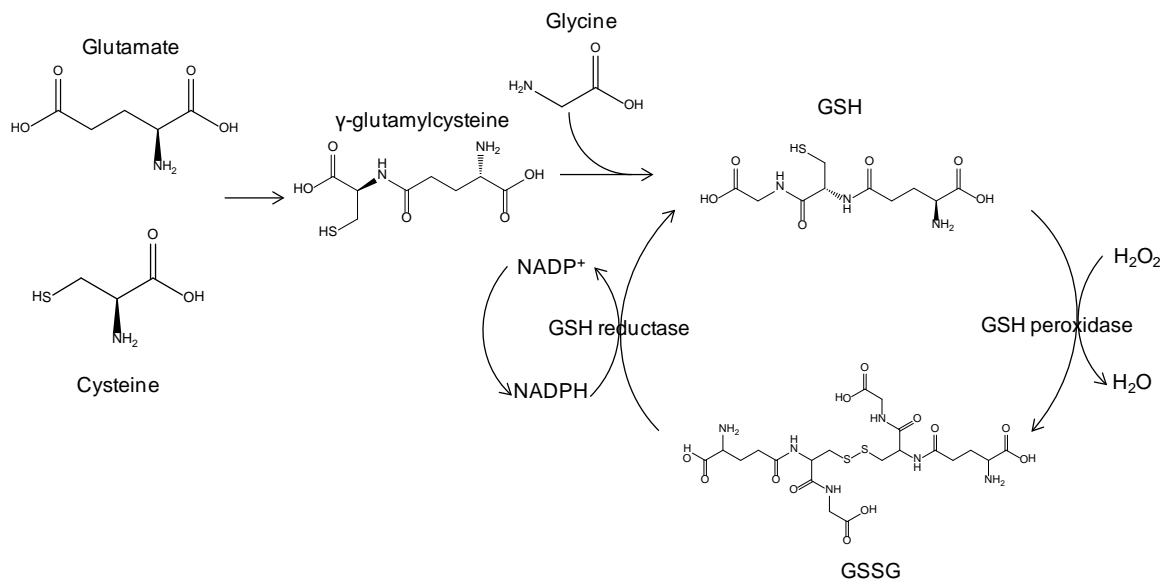


Figure 1.2. GSH synthesis. γ -glutamylcysteine is formed from glutamate and cysteine, catalysed by γ -glutamate cysteine ligase. Glycine is then added to γ -glutamylcysteine, a reaction that is catalysed by GSH synthetase. Redox cycling between GSH and GSSG occurs and is mediated by GSH reductase and GSH peroxidase.

efficient if carried out by GSH-S-transferases (GSTs). GSTs are located in both membrane and cytosolic fractions of the cell. Within the cell it is predominantly cytosolic and soluble GSTs that carry out the conjugation of GSH to xenobiotics (Salinas, Wong 1999). GSH can conjugate to a broad spectrum of electrophilic species including electrophilic carbon, nitrogen, oxygen and sulphur atoms. As GSH exists in such high levels in hepatocytes and because of transcriptional activity, it is hard to deplete GSH in cells. Redox cycling of xenobiotics in hepatocytes and chronic dosing of drugs can deplete GSH to a level where reactive metabolites may react with proteins and nucleic acids (Han et al. 2006). Depletion of intracellular GSH also leaves reactive oxygen species (ROS) that are endogenous to the cell, or that may have been induced by xenobiotics, free to react with lipid and other membranes, leading to cellular damage including lipid peroxidation, protein oxidation, DNA oxidation and mitochondrial damage (Toyokuni 1999). GSH exists in the cell in both the reduced (GSH) and oxidised (GSSG) forms. The ratio between the two forms is important in determining the redox status of the cell (Meister,

Anderson 1983). It is the oxidation or conjugation of the reduced form that is important for quenching ROS and conjugation of molecules. GSSG can be recycled back to GSH by the enzyme GSH reductase.

1.4.3 Reactive metabolites and covalent binding

Reactive metabolites normally have a low electron density (electrophiles) and seek out molecules with a high electron density to form adducts. Electrophiles can be classed as either 'hard' or 'soft' electrophiles. 'Hard' electrophiles have a high positive charge density or a formal positive charge, while 'soft' electrophiles are those with a low positive charge density. Examples of soft and hard electrophiles can be found in table 1.2. Soft electrophiles tend to form adducts with proteins, whereas hard electrophiles are more likely to target nucleic acids.. Much of the time soft electrophiles can be detoxified through conjugation with GSH (Williams et al. 2002). However, if GSH is depleted then reactive metabolites are free to react with proteins. This may cause either direct modification of the protein or oxidation of redox-sensitive thiol or amine groups contained within the protein or may cause an immune response.

Direct modification of proteins such as, for example, inhibition of γ -GCS, GAPDH and $\text{Ca}^{2+}/\text{Mg}^{2+}$ ATPase (Parmar et al. 1995, Dietze et al. 1997b) will severely impair the function of the cell through mitochondrial uncoupling, GSH depletion and perturbation of Ca^{2+} homeostasis (Park et al. 2005). All of these can lead to initiation of apoptosis and necrosis in hepatocytes.

Soft electrophiles	Hard electrophiles
Epoxide	Alkyl carbonium ions
Enones	Benzylic carbonium ions
Quinone-imines	Iminium ions
Quinone methides	Aldehydes
Michael acceptors	

Table 1.2 Summary of hard and soft electrophiles formed from bioactivation.

Immunoallergic hepatitis is also observed following covalent binding to proteins. Proteins that are modified through covalent binding can be internalised by Kupffer cells and presented to helper T-cells. This can result in the formation of cytotoxic T-cells and antibody producing B lymphocytes. The autoantibodies that are produced can initiate apoptosis in cells through TNF and Fas pathways. An example of immunoallergic hepatitis is halothane. A significant proportion of patients that underwent halothane anaesthesia develop asymptomatic rises in liver transaminases but did not develop fulminant liver failure. However, upon repeated exposure to halothane the risk of liver failure increases from 1:35,000 to 1:3700 (Park et al. 2005). Halothane is bioactivated by CYP450 2E1 to a trifluoroacetyl radical, which may modify lysine residues in a number of hepatic proteins. This leads to the production of autoantibodies against trifluoroacetylated hepatic proteins and CYP450 2E1, causing destruction to the hepatocyte (Eliasson, Kenna 1996, Martin et al. 1993, Vergani, Mieli-Vergani & Alberti 1980).

The covalent binding of several compounds to macromolecules has been linked to their toxicity, a selection of some of these compounds and their resulting toxicities

are identified in table 1.3. However, covalent binding is not always indicative of toxicity and recently studies have been undertaken to try and gain a greater understanding of the relationship between covalent binding and toxicity. There are two approaches to identifying reactive metabolites that are commonly used within the pharmaceutical industry; covalent binding using radiolabelled compound and GSH trapping and identification of reactive metabolites through mass spectrometry (Baillie, Davis 1993). The first attempt to set a quantitative limit as a guideline for industry was a paper by Evans *et al* (Evans et al. 2004). This set a limit for binding at 50pmol equiv/mg protein as a flag for toxicity, however this has not necessarily been implemented due to the complex and uncertain relationship between covalent binding and toxicity. Although covalent binding of a drug to protein may identify a risk due to its bioactivation potential, this risk may not be translated into the clinic. A good example of this is the difference between the hepatotoxicity of paracetamol and its structural isomer AMAP. Both of these compounds irreversibly bind to cellular proteins, in fact at one hour AMAP has greater levels of binding than paracetamol although this is reversed at 24 hours (Rashed, Myers & Nelson 1990). This is due to the different organelles or macromolecules that the drugs bind to within the cell. AMAP binds largely to cytosolic proteins, whilst paracetamol binds predominantly to mitochondrial proteins (Tirmenstein, Nelson 1989) that are important in mechanisms of cell death. This demonstrates it is not necessarily the amount of covalent binding that causes toxicity but where in the cell the drug binds. Attempts to determine acceptable levels of covalent binding in pre-clinical testing have led to the comparison of covalent binding to the daily dose of the compound (Nakayama et al. 2009). This gives a much better correlation between those drugs that cause idiosyncratic toxicity and those that bind but do not cause idiosyncratic toxicity,

General introduction

Drug	Reactive metabolites	Activating enzyme(s)	Proteins targeted	Toxicity	References
Paracetamol	NAPQI	CYP450 1A2, 2E1, 3A4	Glutamine synthetase,, glutamate dehydrogenase, aldehyde dehydrogenase, Mg ²⁺ ATPase, Ca ²⁺ /Mg ²⁺ ATPase, Na ⁺ /K ⁺ ATPase, γ -glutamylcysteinyl synthetase, GSH-S-transferase, GAPDH	Hepatotoxicity	(Gupta et al. 1997)(Bulera et al. 1995) (Dietze et al. 1997a, Kitteringham et al. 2000)(Park et al. 2005, Landin, Cohen & Khairallah 1996, Parmar et al. 1995, Ozdemirler et al. 1994, Halmes et al. 1996, Tsokos-Kuhn et al. 1988)(Corcoran, Chung & Salazar 1987)
Sulfamethoxazole (SMX)	SMX-HA, SMX-NO, N-chloroSMX, 3-chloroSMX	CYP450 2C9	Liver microsomal proteins, neutrophils, cellular proteins, keratinocytes, lymphoid cellular proteins, HSA, Hb	Hypersensitivity, hepatotoxicity	(Cribb et al. 1996, Cribb, Spielberg & Griffin 1995)(Gill et al. 1997)(Manchanda et al. 2002)(Miller, Trepanier 2002)(Naisbitt et al. 2002)(Reilly et al. 2000, Summan, Cribb 2002, Uetrecht, Shear & Zahid 1993)
Clozapine	Desmethyloclozapine	CYPs, MPO	GSH, MPO, other neutrophil proteins	Agranulocytosis	(Gardner et al. 1998, Zhao Chao Liu, Uetrecht 1995, Maggs et al. 1995, Pirmohamed et al. 1995, Williams et al. 1997, Williams et al. 2000)
Troglitazone	Benzoquinone, quinone-epoxide	CYP450 3A4	GSH, BSEP	Hepatotoxicity	(Funk et al. 2001b, Funk et al. 2001a, Kassahun et al. 2001, Kawai et al. 1997, Kostrubsky et al. 2001, Prabhu et al. 2002, Preininger et al. 1999, Tettey et al. 2001)
Halothane	TFA	CYP450 2E1	CYP450 2E1, protein disulfide isomerase, carboxylesterase, calreticulin, GST, glucosyl transferase, GRP78, GRP94	Hepatitis	(Martin et al. 1993, Vergani, Mieli-Vergani & Alberti 1980, Bourdi et al. 1996, Hayden et al. 1991, Kenna 1997, Martin et al. 1991)

Table 1.3. Table of compounds where reactive metabolite formation and subsequent protein binding is known to result in cytotoxicity.

however, it is well established that a link exists between high doses of compounds and toxicity.

1.5 MITOCHONDRIAL TOXICITY AND DILI

Drug induced mitochondrial toxicity was first described in 1954, when it was noted that CCl₄ reduced mitochondrial enzyme activity (Christie, Judah 1954). Since then, mitochondrial dysfunction has increasingly been seen as an important mechanism through which drugs and their metabolites can cause liver injury. Mitochondria are involved in nearly all mechanisms of DILI, either primary mitochondrial toxicity or secondarily through initiation of the cell death pathways in which mitochondria are instrumental. Mitochondrial toxicity can occur in several ways, many of which have distinct hallmarks of toxicity such as steatosis caused by disruption of β -oxidation pathways and metabolic acidosis due to perturbation of the mitochondrial respiratory chain.

1.5.1 Mitochondrial physiology and function

Mitochondria contain two membranes, one of which separates the mitochondria from the cytoplasm, whilst the other contains the matrix. In between the two membranes is the inter-membrane space (PALADE 1953). The outer membrane is mainly smooth and consists of a lipid bilayer that contains cholesterol whilst the inner membrane consists of several folds called cristae (PALADE 1953). The number of the cristae depends on the mitochondrial function, as although their main function in each tissue is to provide cellular energy through adenosine triphosphate (ATP) synthesis, mitochondria have a variety of different functions in different tissues (Dyken, Will 2008). The outer membrane contains mitochondrial porin, which allows the diffusion of neutrally charged molecules, cations and selected anions up to a molecular weight

of 5000Da into the inter-membrane space, making this very much like the cytosol in terms of low molecular weight compounds (Dyken, Will 2008). The inner membrane is highly selective and unlike the outer membrane contains the unique mitochondrial protein cardiolipin (Houtkooper, Vaz 2008).

The mitochondria produce 95% of a cells ATP through oxidative phosphorylation (OXPHOS). The electron transport chain (ETC) (figure 1.6) consists of four complexes that sit in the inner membrane of the mitochondria. Electrons pass down the chain from complexes I to IV, and each step is coupled to the expulsion of protons across the membrane. This acts as a proton pump catalysed by translocating enzymes from the matrix to the intermembrane space, creating the proton motive force Δp . This is a combination of two different potentials that are formed from the translocation of the protons; $\Delta\Psi$ which is a result of the differing distribution of electrical charges across the membrane and ΔpH which reflects the difference in chemical potential across the membrane. Δp then drives mitochondrial ATP synthase (or complex V) which is the driving force of ATP synthesis from ADP and phosphate (Dyken, Will 2008).

Mitochondria are also responsible for the β -oxidation of fatty acids, which occurs in the mitochondrial matrix. To do this, the fatty acid must be activated by forming a thioester link with Coenzyme A (CoA), this is catalysed by CoA synthase which is located on the outer mitochondrial membrane. Small and medium chain acyl CoA molecules are then able to diffuse across the inner mitochondrial membrane. Longer chain molecules are conjugated to a polar carnitine molecule and then transported into the matrix through a carnitine shuttle. Once in the mitochondrial matrix the fatty acid is broken down by 'rounds' of degradation. Each round consists of oxidation by

FAD, followed by hydration, then oxidation by NAD^+ before the final step of thiolysis.

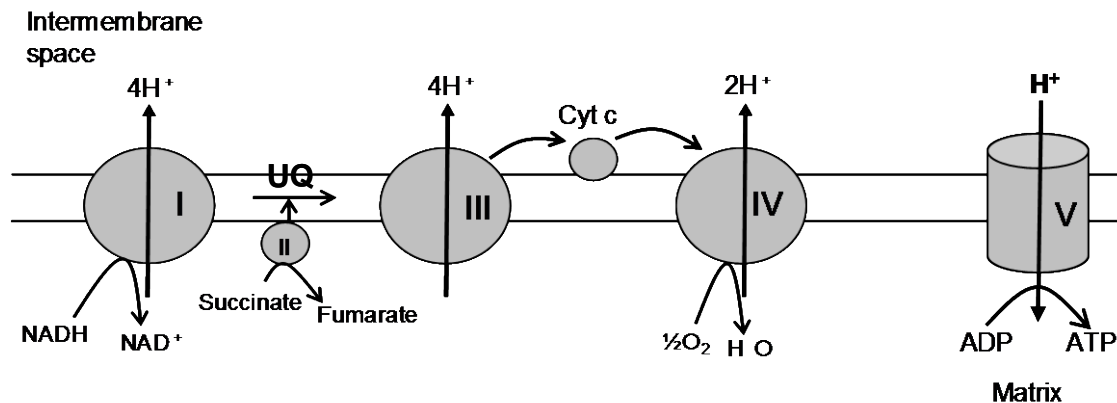


Figure 1.6. A summary of the mitochondrial respiratory chain. For every pair of electrons that flow from NADH to oxygen there are 10 protons translocated from the matrix to the intermembrane space. The movement of H^+ from the matrix into the inter-membrane space creates the proton motive force (Δp) made up of two different potentials, the electrical potential ($\Delta \Psi$) and the chemical potential (ΔpH). The protons then move back into the matrix via complex V (ATP synthase). The movement of protons drives complex V to produce ATP from ADP.

This removes two-carbon acetyl CoA molecules sequentially from the fatty acid chain until the acyl CoA has all been converted to acetyl CoA. The acetyl CoA then enters the citric acid cycle. Some drugs can impair mitochondrial fatty acid oxidation (FAO) causing the accumulation of triglycerides in the cytoplasm of hepatocytes (Fromenty, Pessayre 1995).

1.5.2 Mitochondria and cell death

Cells can undergo cell death via two distinct mechanisms; apoptosis and necrosis. Apoptosis is an energy requiring process that results in characterised by cell shrinkage, nuclear and cytoplasmic condensation, chromatin fragmentation and phagocytosis. Necrosis is a passive form of cell death associated with inflammation, cellular and organelle swelling, rupture of the plasma membrane and spilling of the

cellular contents into the extracellular milieu (Orrenius 2004). Activation of cell death via apoptosis may result from death receptors signaling from death receptors, damaged nuclear DNA, lysosomes or stressed endoplasmic reticulum. Bcl-2-associated x protein (Bax) then translocates from the cytoplasm to the mitochondria.

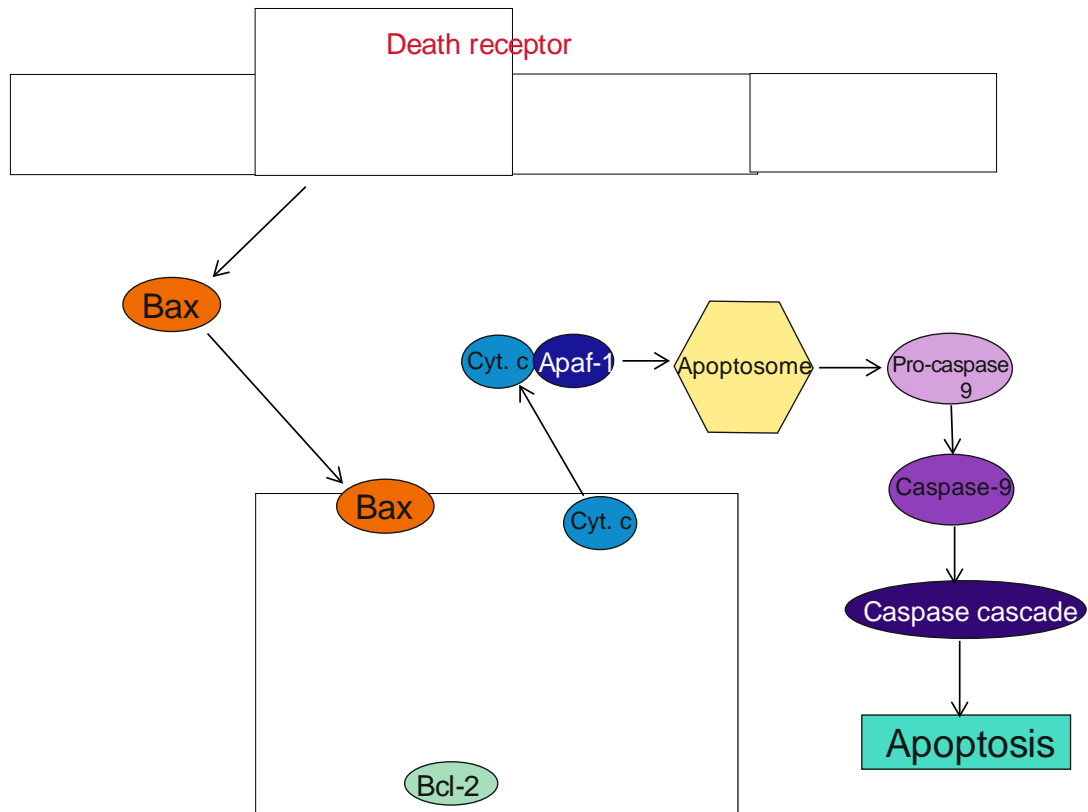


Figure 1.4. Mitochondrial mediated apoptosis. Signals from death receptors lead to the dimerisation and translocation of Bax so that it is inserted into the outer mitochondrial membrane. This triggers cytochrome c release from the mitochondrial membrane. Once in the cytosol cytochrome c binds to Apaf-1 forming the apoptosome. This promotes pro-caspase-9 activation to caspase-9 triggering the caspase cascade resulting in apoptosis.

The BCL-2 family contains both pro-apoptotic and anti-apoptotic proteins. If only a few molecules of the pro-apoptotic Bax are present, they are sequestered by Bcl-XL, an anti-apoptotic member of the BCL-2 family, allowing the cell to live. However, when there are too many Bax molecules to be sequestered, they form dimers and insert into the outer mitochondrial membrane causing it to become permeable (Gross

et al. 1998, Robertson, Orrenius 2000). This allows cytochrome c release from the intermembrane space into the cytosol. Once cytochrome c is in the cytosol it interacts with apoptosis activating factor-1 (apaf-1), forming the apoptosome which triggers the auto-activation of caspase-9 from pro-caspase-9.. Caspase-9 then activates the caspase cascade that cuts cytoplasmic and nuclear proteins that leads to apoptosis (Li et al. 1997) (figure 1.4). Cytochrome c also activates inositol (1,4,5) triphosphate receptors which triggers an efflux of Ca^{2+} which may enter intact mitochondria. An increase in mitochondrial Ca^{2+} and ROS, through inhibition of the mitochondrial respiratory chain, may also cause opening of the mitochondrial permeability transition (MPT) pore. In the normal state MPT pores are kept closed maintaining $\Delta\Psi$, however if the MPT pores open, a massive re-entry of protons leads to water accumulation causing the mitochondria to expand and rupture (Robertson, Orrenius 2000, Robertson, Orrenius & Zhivotovsky 2000, Crompton 1999). This leads to the release of cytochrome c from these mitochondria. If pore opening occurs in all mitochondria at once, this causes severe ATP depletion which results in necrosis rather than apoptosis. If the MPT pore only opens in certain mitochondria the remaining mitochondria are able to continue producing ATP, leading to apoptotic cell death (Leist et al. 1997).

1.5.3 Mechanisms of drug induced mitochondrial injury

There are several mechanisms by which drugs can cause mitochondrial injury and it is likely that this occurs through several, simultaneous mechanisms. Drugs can cause mitochondrial dysfunction through direct and indirect mechanisms.

Some drugs may lead to the opening of MPT pores. The drugs that affect MPT pores normally result in 'cytolytic' hepatitis, which may lead to fulminant liver failure. Although it is poorly understood how drugs can trigger MPT pore opening it is

believed that they may directly trigger MPT pore opening such as the NSAID diclofenac (Masubuchi, Nakayama & Horie 2002). Other drugs may cause indirect opening of the MPT pores through the JNK signalling pathway as with paracetamol (Gunawan et al. 2006) or through the increase of cytosolic calcium that enters through protein damage caused by the extensive formation of reactive metabolites.

Other compounds directly influence OXPHOS. Cationic, amphiphilic drugs such as amiodarone and perhexiline can first be protonated in the intermembrane space of the mitochondria resulting in their transport across the mitochondrial membrane potential ($\Delta\Psi$). This transfer across the membrane dissipates $\Delta\Psi$ and increases the basal respiration. Carboxylic acids such as NSAIDs, and other acids can also uncouple OXPHOS and are known as anionic uncouplers. These anionic uncouplers exist as an uncharged species which can easily cross the lipid bilayer of the inner mitochondrial membrane (Dyken, Will 2008). Once they have reached the more alkaline matrix they dissociate into their anionic form and a proton. The anionic form is then extruded into the intermembrane space where a neutral molecule is formed once more, which can then undergo another cycle of transportation. This again dissipates the membrane potential causing electrons to flow through the ETC, bypassing ATP synthase, hence no ATP is produced. Severe uncoupling can therefore decrease cellular ATP content causing mitochondrial dysfunction and cell death (Labbe, Pessayre & Fromenty 2008). OXPHOS uncoupling may also occur through direct inhibition of the ETC, although little is known about this mechanism of mitochondrial injury.

Fatty acid oxidation (FAO) can be impaired in different ways by different drugs. Some drugs can directly impair mitochondrial FAO by inhibiting FAO enzymes or by sequestering the FAO cofactors, L-carnitine and coenzyme A (Becker, Harris

1983, Corkey et al. 1988). ETC inhibition can also lead to FAO impairment by decreasing the regeneration of the oxidised cofactors which are required for β -oxidation. Severe inhibition of mitochondrial β -oxidation can lead to microvesicular steatosis, which is characterised by the presence of many small lipid droplets in the cytoplasm of hepatocytes. A less severe but chronic inhibition can cause macrovesicular steatosis, a single, large lipid vacuole in the cytoplasm of hepatocytes. In the short-term this is normally a benign liver lesion, but can result in steatohepatitis if the problem persists over several years (Fromenty, Berson & Pessayre 1997).

1.6 HEPATIC TRANSPORTERS AND DILI

Hepatic transport proteins are becoming increasingly recognised as a site that drugs and/or their metabolites are able to interact with possibly leading to toxic response. Basolateral transporters are important in the transport from the blood, whereas canalicular transporters are involved in the elimination of drugs and bile acids across the canalicular membrane and into the bile. Phase II metabolism generally renders the drug too hydrophilic to diffuse across the canalicular membrane into the bile or across the hepatic basolateral membrane into sinusoidal blood, carrier-mediated transport is therefore required to cross out of the hepatocyte.

1.6.1 Drug transporters in the liver

The major drug transporters in cell membranes belong to two superfamilies, the ATP-binding cassette (ABC) family, which are involved in primary active transport, and the solute carrier (SLC) family of transporters, which is involved in secondary active transport (Scherrmann 2009). The ABC transporters use ATP as an energy source to transport the molecule, while the SLC transporters are co-transporters and

use an ion and/or voltage gradient to transport both ions and solutes together. The transporters have broad overlapping substrates and drugs may be transported by many different proteins (fig 1.5). Influx transporters in the liver belong to the SLC superfamily and includes the four most defined transporter families. This includes sodium-dependent taurocholate cotransporting protein (NTCP), which recognises drugs with a similar structure to bile acids or drugs that are bound to taurocholate. The organ anion transporting polypeptides (OCTPs) and the organic anion transporters (OATs) also belong to this superfamily and are mainly responsible for the transport of organic anions. Organic cation transporters (OCTs) are the last of these families and are specific transporters for organic cation transport. These families mainly reside in the sinusoidal membrane and uptake xenobiotics from the blood and into the liver.

The efflux transporters, with the exception of MATE1, belong to the ABC superfamily and help with the removal of drugs from hepatocytes into the blood or bile. The major ABC transporters that are responsible for pumping substrates back into the blood belong to the family of multi-drug resistance associated proteins (MRPs). MRP1, MRP3, MRP4, MRP5 and MRP6 reside on the lateral membrane and are all involved in efflux transport back to the blood. On the canilicular membrane, MRP2 effluxes drugs into the bile. The multi-drug-resistance proteins (MDRs) can also be found here including P-glycoprotein (P-gp or MDR1) and MDR3, breast cancer resistance protein (BCRP) can also be involved in the transport of substrates. The bile salt export pump (BSEP) is also present on the canalicular membrane and mainly mediates the biliary excretion of substrates.

Drugs such as cyclosporine may inhibit several influx and efflux transporters such as OATP1B3, OATP2B1, P-gp and MRP2, which causes potential drug interactions particularly with the statins.

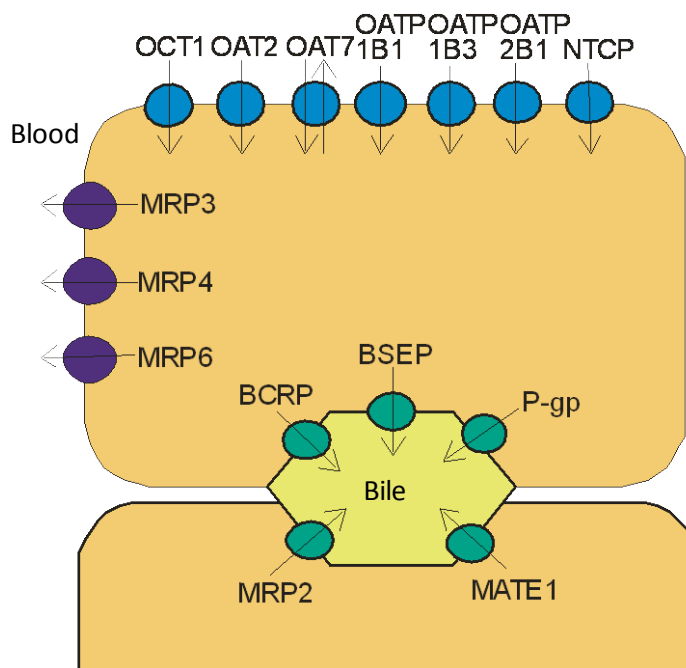


Figure 1.5. Influx and efflux transporters in hepatocytes. Influx transporters are highlighted in blue. Efflux transporters that transport substances into the sinusoid are in purple and efflux transporters that transport substances into the bile are in green.

1.6.2 Bile acid transport and DILI

NTCP accounts for the uptake of 80% of bile acids into hepatocytes from the blood and transports both conjugated and unconjugated bile acids (Nicolaou et al. 2012). OATPs are also involved in the uptake of bile salts into the hepatocyte. Whereas multiple bile transporters uptake bile acids from the blood into the hepatocytes, the main transporter involved in the efflux of bile acids is the bile salt export pump (BSEP) (Stieger, Meier & Meier 2007). Although BSEP is not thought to be

involved in the transport of phase II drugs into the bile numerous xenobiotics have been recorded as inhibiting BSEP function. Bile acids in high concentrations are themselves hepatotoxic and therefore inhibition of BSEP can cause toxicity through accumulation of bile acids (Palmeira, Rolo 2004). An example of this is troglitazone, which was withdrawn from the market following cases of severe hepatotoxicity. The phase II metabolite of troglitazone, troglitazone sulphate, is excreted from the liver into the bile via Mrp-2. If Mrp-2 does not remove the troglitazone sulfate then it can accumulate in the liver where it can reach concentrations that inhibit BSEP hence causing an increase in bile acids and hepatotoxicity (Funk et al. 2001b, Funk et al. 2001a, Kostrubsky et al. 2001).

1.7 NEFAZODONE

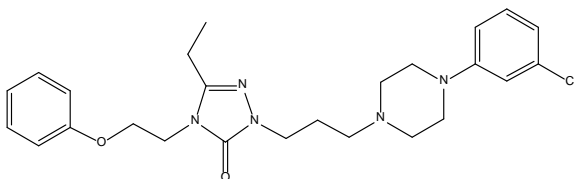


Figure 1.6. Structure of nefazodone

Nefazodone is an antidepressant that was first marketed in 1994. A phenylpiperazine derivative, it was chemically unrelated to other anti-

depressants available on the market, the serotonin re-uptake inhibitors (SSRIs), monoamine oxidase (MAO) inhibitors and the tricyclic antidepressants (TCAs). Its mechanism of action is thought to be through inhibition of serotonin and noradrenalin re-uptake by antagonising the post-synaptic 5-HT₂ and α ₁-adrenergic receptors (Davis, Whittington & Bryson 1997). The daily dose of nefazodone was up to 600mg/day, typically divided into two doses of up to 300mg. In 2004 it was voluntarily withdrawn from the market by Bristol-Myers Squibb after rare but severe incidences of hepatotoxicity prompted the FDA to issue nefazodone with a black box warning.

1.7.1 Nefazodone induced hepatotoxicity

The black box warning on the nefazodone label estimated the rate of liver failure as 1 case in 250,000-300,000 patients per year, a rate of three to four times the background rate of liver failure (Food and Drug Administration 09/01/2002). The FDA has also received reports of at least 55 cases of liver failure, including 20 deaths and another 39 cases of less severe liver injury. Case studies indicated that patients presented with nefazodone induced liver injury 1 month to 2 years following initiation of nefazodone treatment. Symptoms of nefazodone induced liver injury included jaundice, raised liver enzymes and malaise. Liver biopsy demonstrated cholestasis, cirrhosis, fibrosis and centrilobular necrosis (Aranda-Michel et al. 1999, Lucena et al. 1999). It was thought that an immune-mediated reaction to the drug was unlikely.

1.7.2 Metabolism and bioactivation of nefazodone and its involvement in DILI

In humans nefazodone is primarily metabolised through hepatic and intestinal CYP450 3A4 (Rotzinger, Baker 2002b) before being excreted into the bile. Several stable circulating metabolites have been identified in humans including meta-chlorophenylpiperazine (mCPP), hydroxynefazodone and a triazoledione metabolite (Franc et al. 1991). It has been shown that both hydroxynefazodone and mCPP have pharmacological properties, with hydroxynefazodone having affinity similar to the parent compound for 5HT_{2A} receptors with both having similar affinity at serotonin reuptake sites (Eison et al. 1990). Nefazodone has a bioavailability of approximately 20% and peak plasma concentrations are reached at approximately 1 hour after dosing (Barbhaiya, Dandekar & Greene 1996).

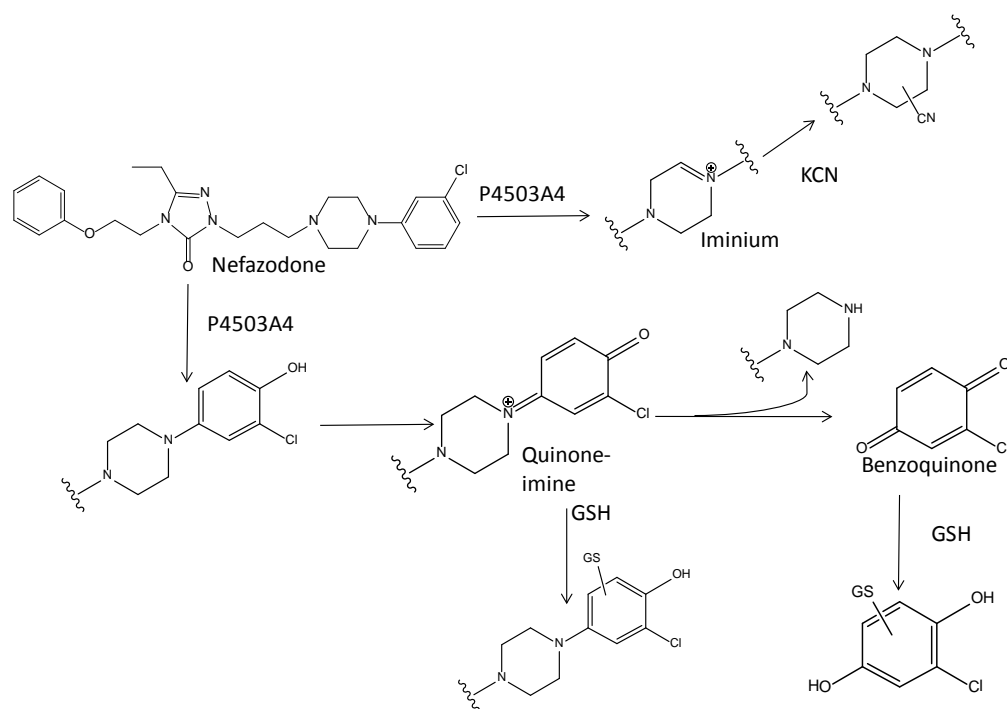


Figure 1.7. Bioactivation of nefazodone to reactive metabolites. Nefazodone is metabolised by CYP450 3A4 to p-OH-nefazodone, which can then be bioactivated via 2 electron addition to reactive quinone-imine species. This can then be further metabolised to benzoquinone. The quinone-imines that are formed can be trapped using GSH and identified using mass spectrometry. Nefazodone can also be metabolised to reactive iminium ions that can be trapped using cyanide. Adapted from Argoti *et al*, 2005.

Nefazodone metabolism via CYP3A4 has been shown to be extensive, with over 20 oxidative metabolites identified in human liver microsomes (HLMs) alone (Li *et al.* 2007). The metabolism of nefazodone has been implicated in its toxicity. Two quinone-imines, benzoquinone and several iminium ions have been identified as possible oxidative metabolites of nefazodone through the trapping of reactive metabolites using GSH and cyanide (Kalgutkar *et al.* 2005b, Bauman *et al.* 2008b, Argoti *et al.* 2005). This implicates a mechanism of toxicity mediated through covalent binding of reactive metabolites of nefazodone in the liver as a cause for

toxicity. Nefazodone displays binding in both HLMs and human hepatocytes, however, as nefazodone is so rapidly turned over covalent binding only represents a small amount of metabolism (Bauman et al. 2009, Obach et al. 2008, Obach et al. 2008). Despite the detection of reactive metabolites and their subsequent covalent binding there has never been a study that provides a definitive relationship between reactive metabolite formation and toxicity.

1.7.3 Parent compound and its involvement in DILI

Although nefazodone reactive metabolites have been identified, the parent compound has also been linked to hepatotoxic effects. Nefazodone has been implicated as a mitochondrial toxin and has also been shown to inhibit efflux transporters *in vitro*, particularly inhibition of the bile salt export pump (BSEP).

Nefazodone has been shown to inhibit complex I of the respiratory chain with an IC_{50} of 14 μ M. A dose response curve of nefazodone in HepG2 cells grown in galactose media, which are more susceptible to mitochondrial toxicity, had an IC_{50} value of 9 μ M compared to 38.4 μ M in HepG2 cells grown in high glucose media. Nefazodone also resulted in significant cell loss, increased ROS and near abolishment of mitochondrial membrane potential at 100X its C_{max} value for a single therapeutic dose (92 μ M) in sandwich cultured hepatocytes (Dyken et al. 2008).

Nefazodone has also been shown to inhibit membrane vesicles expressing BSEP with an IC_{50} of 9 μ M. A similar effect was also observed in sandwich cultured human hepatocytes where nefazodone exhibited a concentration dependent inhibition of taurocholic acid transport into the canaliculi (IC_{50} 14 μ M). Rats that were orally dosed with 75mg/kg showed mean bile acid increases of 167% in the serum one hour

(approximate T_{\max} of nefazodone) after administration, demonstrating the potential of nefazodone to cause inhibit bile acid transport. As membrane vesicles without the capacity for metabolism and sandwich hepatocytes demonstrated similar IC_{50} values, it was assumed that parent drug rather than a metabolite was responsible for the inhibition that was observed. The authors checked for toxicity with and without the presence of 1mM 1-aminobenzotriazole (ABT). Treatment with nefazodone following ABT pre-incubation resulted in a 45% decrease in total protein synthesis whereas nefazodone alone demonstrated full recovery after 24 hours (Kostrubsky et al. 2006). This implied that nefazodone itself is more toxic than its metabolites. However, this study did not investigate the role of metabolism in hepatocytes and whether inhibition re-routed metabolism. Another study into bile acids in sandwich cultured hepatocytes demonstrated that nefazodone may inhibit both influx and efflux transporters and accumulation of deuterium labelled taurocholic acid in the hepatocytes was similar to control values (Ansede et al. 2010).

1.8 BUSPIRONE

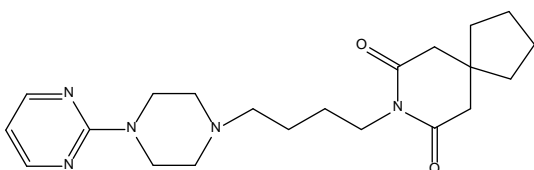


Figure 1.8. Structure of buspirone

Buspirone is an azaspirodecanedione anxiolytic agent (Eison, Temple 1986). It differs from the benzodiazepines, a commonly used class of anxiolytics, in

both structure and pharmacological properties (Eison, Temple 1986). Several studies have shown that buspirone binds with high affinity to the 5-HT_{1A} receptor (Eison et al. 1986, Taylor, Allen & Becker 1984), however, it has a slow onset of action implying a more complex mechanism of action. Buspirone has also been shown to have moderate affinity for brain D₂-dopamine receptors. Buspirone has no

significant affinity for benzodiazepine receptors and does not affect GABA binding *in vitro* and *in vivo* and as such, is used preferentially to the benzodiazepines as it does not use produce the same side-effects of sedation and motor impairment (Goldberg 1984).

Buspirone is administered up to 60mg/day, normally as up to 30mg twice daily. It undergoes extensive first pass metabolism resulting in a bioavailability of only 4% (Gammans, Mayol & Labudde 1986). It has been shown to undergo extensive hepatic metabolism via CYP450 3A4. Work by Kerns *et al* identified 25 metabolites in rat bile, urine and S9 fractions using LC-MS analysis (Kerns et al. 1997) and studies in human liver microsomes (HLMs) have demonstrated that buspirone is metabolised predominantly by CYP3A, with three major routes of metabolism being identified as hydroxylation, *N*-dealkylation and *N*-oxidation (Zhu et al. 2005). It has been demonstrated that some of the metabolites of buspirone are potentially pharmacologically active. Its *N*-dealkylation product, 1-pyrimidinyl-piperazine (1-PP) is known to possess pharmacological activity in rodents where it is responsible for approximately a quarter of the activity of buspirone. Patients do not however, exhibit high levels of 1-PP, so this may not be relevant in humans.

Despite not having any reports of organ-directed toxicity, buspirone demonstrates NADPH-dependent covalent binding to human liver microsomes and human hepatocytes in the same order of magnitude as nefazodone, which has a similar metabolic pathway (Bauman et al. 2009, Obach et al. 2008). Despite the fact that buspirone is metabolised to a para-hydroxy metabolite similar to nefazodone, it seems that buspirone is devoid of the same bioactivation potential and reactive metabolites of buspirone have not been identified (Kalgutkar et al. 2005b).

1.9 BIGUANIDES

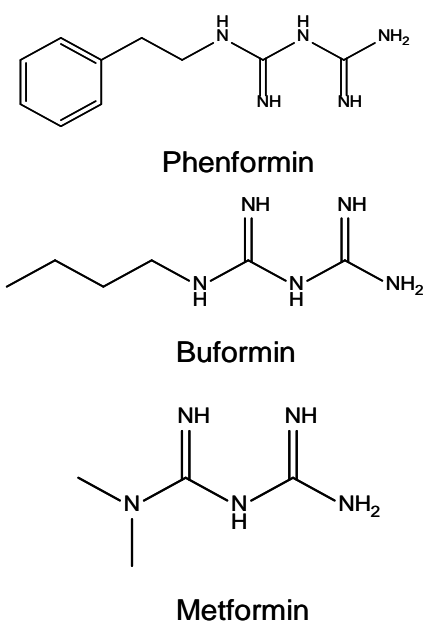


Figure 1.9. Chemical structures of the biguanides

Extracts of *Galega officinalis* (French lilac) have been used to treat symptoms resembling those of diabetes for many centuries (Witters 2001). In 1918 guanidine was shown to possess hypoglycaemic activity in animals, but it was too toxic for use. The less toxic extract galegine, began to be used as an anti-diabetic in the early 1920s. Synthalin A and B, synthetic diguanidines, were found to be tolerated and used clinically in favour of galegine until the early 1930s when insulin use was becoming more common. During

the 1920s several biguanide derivatives were synthesised but it was not until 1957 that metformin and phenformin came to the market, followed a year later by buformin (Witters 2001). Phenformin and buformin were found to be more potent than metformin and therefore were most commonly used.

The biguanides have multiple impacts upon glucose regulation by decreasing intestinal glucose absorption and hepatic glucose efflux, and enhancing peripheral insulin response. Due to their pleiotropic actions, numerous mechanisms of action have been reported in the literature including: inhibition of mitochondrial respiration (El-Mir et al. 2000), reduction of oxidative and nitrative stress (Fujita et al. 2010, Zou et al. 2004), repression of mitochondrial permeability transition and activation of AMP-activated protein kinase (Hawley et al. 2002, Musi et al. 2002, Zhou et al. 2001).

Recently it has been established that AMPK-activators, such as phenformin, have potential as anti-cancer agents. It has been recommended that phenformin enters clinical trials for the treatment of triple negative and ER-positive breast cancer (Caraci et al. 2003, El-Masry, Brown & Dobson 2012).

1.9.1 Biguanides and lactic acidosis

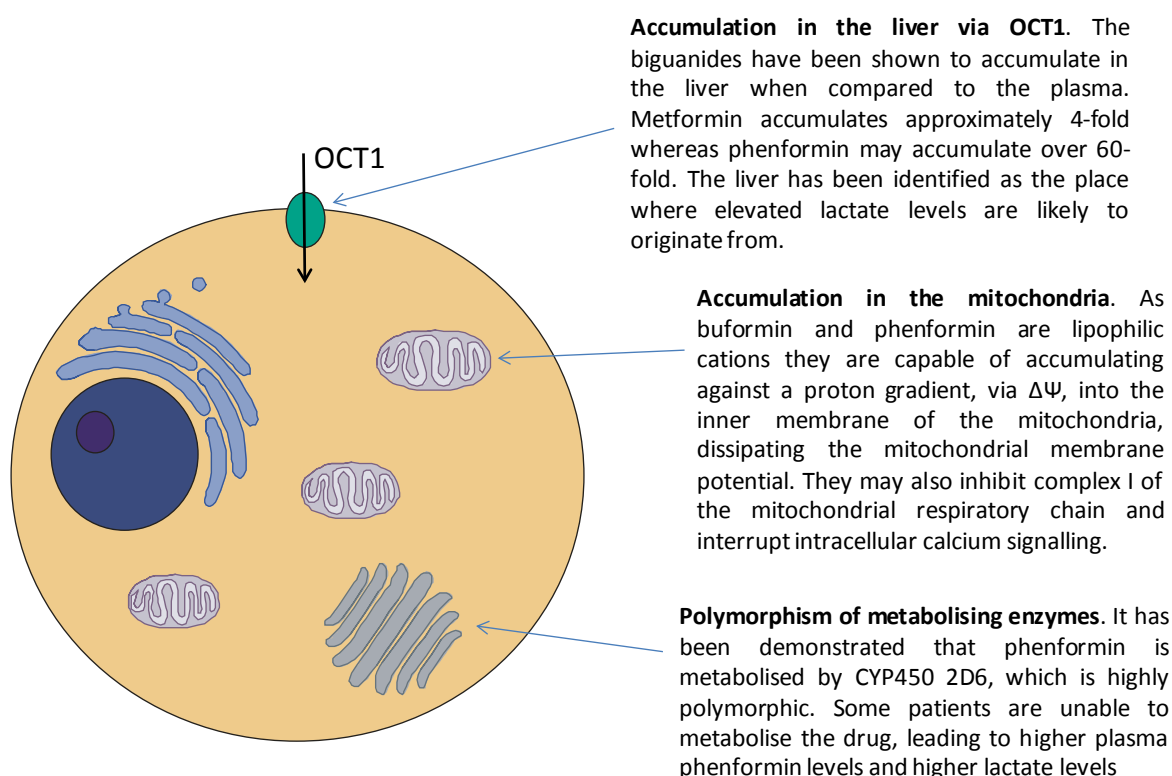


Figure 1.10. Mechanisms that may contribute to phenformin induced lactic acidosis.

The accumulation of phenformin in the liver through accumulation via OCT1 transporters and poor metabolisers of phenformin may lead to increased serum and hepatic concentration of phenformin. Increased hepatic concentrations could then lead to increased mitochondrial accumulation of phenformin via the mitochondrial membrane potential. This could then impair mitochondrial function in the liver leading to lactic acidosis.

Unfortunately, phenformin and buformin were associated a high incidence of lactic acidosis (lactate levels greater than 5mmol/L and serum pH of less than 7.35). The estimated rate of lactic acidosis induced by phenformin is 40-64 cases per 100,000 person years (Bailey 1992). The risk of lactic acidosis associated with metformin is substantially lower at 3.3 cases per 100,000 patient years, a rate that is also lower

than sulfonylurea use (4.8/100,000 patient years) (Lalau 2010) and untreated diabetics, where the incidence of lactic acidosis is 9-16 per 100,000 patient years (Brown et al. 1998). Due to this, buformin and phenformin were withdrawn from most markets in 1977, however, phenformin is still available in Italy, Greece, Brazil, Poland, Portugal, China and Uruguay, where cases of phenformin induced lactic acidosis do still occur. Cases of phenformin induced lactic acidosis may also occur in other countries, where it has been found as a base in Chinese herbal medicines (Ching et al. 2008). Due to the low incidence of lactic acidosis associated with metformin it is still widely used, particularly in obese patients and in combination with the sulfonylureas, and has become a leading treatment for non insulin dependent diabetes mellitus (NIDDM) worldwide.

The toxicity of the biguanides may be related to their mitochondrial mechanisms of action. The biguanides are known to accumulate in the liver. In rats the metformin concentration in the liver was 4 times that in the plasma and for phenformin the concentration in the liver was 61 fold higher than in the plasma (Sogame et al. 2011). Buformin also accumulates in the liver and studies in humans have showed that buformin accumulated up to 25-fold in the liver after an i.v. dose and accumulation was even higher following oral administration (Lintz, Berger & Aenishaenslin 1974). This accumulation is due to active transport of the biguanides into the liver via the organic cation transporter 1 (OCT1). In studies using Oct1(-/-) mice, distribution of metformin to the liver was 30 times lower than OCT1 (+/+) mice (Wang et al. 2002). Using OCT 1(-/-) versus OCT1 (+/+) mice, the liver has also been identified as the organ most likely to be associated with the onset of lactic acidosis (Wang et al. 2003a). Not only do the biguanides accumulate in the liver but there is evidence that they may also accumulate in the mitochondria. The biguanides exist almost entirely

in their cationic form at physiological pH. Phenformin, as a lipophilic cation may therefore undergo accumulation into the mitochondria against a proton gradient via $\Delta\Psi$ up to 100-fold surrounding cytoplasm concentrations (Davidoff 1971). A combination of mitochondrial accumulation and hepatic accumulation could mean that the concentrations seen in liver mitochondria are hundreds of fold higher than plasma concentrations.

In man the biguanides are mainly excreted renally and as such are contra-indicated in patients with renal disease. There have been no metabolites of metformin or buformin identified in man, however, the phenyl ring of phenformin can undergo hydroxylation to 4-hydroxyphenformin and its corresponding *O*-glucuronide (Guest, King & Parke 1979, Alkalay, Volk & Roth 1979). The oxidative metabolism of phenformin is carried out by CYP450 2D6, which is highly polymorphic in nature and approximately 7% of Caucasians are poor metabolisers of CYP450 2D6 substrates. Studies have identified that phenformin plasma concentrations are significantly higher in patients who were also poor metabolisers of debrisoquine (Shah et al. 1980, Oates et al. 1982, Bosisio, Galli Kienle & Galli 1981) (another CYP450 2D6 substrate) and after a single dose of phenformin, patients had higher plasma lactate levels than extensive CYP450 2D6 metabolisers (Idle et al. 1981).

1.10 TOOLS USED TO INVESTIGATE METABOLISM AND TOXICITY

1.10.1 Inhibitors used to investigate mechanisms of toxicity

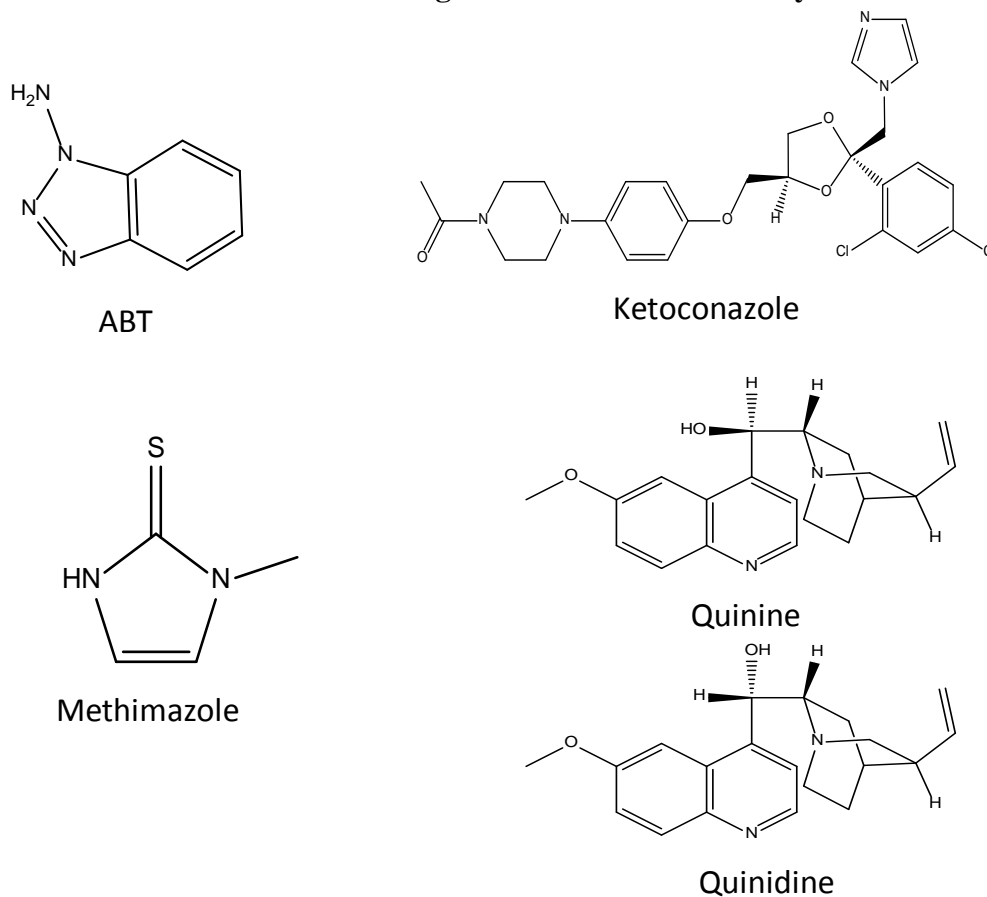


Figure 1.11. Chemical structures of compounds used to inhibit metabolism potential drug-drug interactions.

Chemical inhibitors of metabolism are a useful tool in determining the metabolic pathways of compounds and the effect that inhibition of a pathway can have on cell physiology. A number of chemical inhibitors have been used in this work. Their chemical structure is shown in figure 1.11 and their mechanism of action is described below.

ABT is a non-specific suicide inhibitor of CYP450 enzymes, and works through autocatalytic alkylation of the CYP450 prosthetic haem group resulting in an N-N-

bridged benzyne-protoporphyrin IX adduct. ABT has been extensively used to inhibit CYP450s in a range of in vitro and in vivo studies. It is commonly used in vitro at a concentration of 1mM with a 30 minute pre-incubation, which results in approximately 80% inhibition of total CYP450 activity. Although ABT is a non-specific inhibitor it has greater specificity for some CYP450s than others, and whilst it is thought to almost completely inhibit CYP450 3A4 and CYP450 2A6, it shows a lack of inhibition of CYP450 2C9 (Linder, Renaud & Hutzler 2009).

Ketoconazole is a specific inhibitor of CYP450 3A isoforms at concentrations lower than 5 μ M, although it also has some activity at CYP450 2C9 at low concentrations. It has a mixed-competitive type of inhibition and it has previously been shown that pre-incubation of ketoconazole with microsomes does not result in increased inhibition as with non-competitive inhibitors (Greenblatt et al. 2011).

Methimazole has been identified as a competitive inhibitor of flavin-containing mono-oxygenases (FMOs). FMOs commonly carry out oxidation reactions at nucleophilic groups such as the nitrogen atoms in amines and amides. However, despite its use as an inhibitor of FMOs it has also been shown to inhibit some CYP450s at low concentrations (Guo et al. 1997).

Whilst quinidine has been shown to be a potent and selective competitive inhibitor of CYP450 2D6 in humans, it is much less potent against CYP450 2D2, which is the most abundant CYP450 2D isoform in rats. However, quinine, its optical isomer has been found to inhibit CYP450 2D in rat hepatocytes at a concentration of 100 μ M, whilst the IC₅₀ in hepatocytes is reported to be 300 μ M for both compounds. Both quinine and quinidine have also been identified as inhibitors of isoforms of UGT and

hence can also inhibit the glucuronidation of some compounds (Kobayashi et al. 1989).

1.10.2 Stains and dyes for investigating cell toxicity

Fluorescent microscopy is becoming a valuable tool for assessing the actions of drugs on cell physiology and viability. A number of these dyes have been used in this work and they are described below. Their excitation and emission spectra can be seen in table 1.4.

Name	Excitation (nm)	Emission (nm)
Hoechst 33342	350	461
TMRM	545	580
TOPRO-3 iodide	642	661

Table 1.4. Excitation and emission wavelengths for fluorescent dyes used.

Hoechst 33342 is a nuclear stain which binds to the minor grooves of DNA, with a preference for adenine and thymine rich sequences. It is cell permeable and binds DNA in both alive and dead cells and can therefore be used to identify the position of cells when using fluoroscopy. Hoechst 33342, can also be used as an indicator of cell death in non-dividing cells, such as hepatocytes, as it fluoresces brighter as the nucleus condenses and the DNA becomes more compact.

Tetramethylrhodamine methyl ester (TMRM) is a cell permanent, cationic, red-orange dye that is sequestered into active mitochondria via the mitochondrial membrane potential. TMRM only fluoresces when it reaches the mitochondrial

matrix due to the difference in pH and is therefore an indicator of the presence of a mitochondrial membrane potential.

TOPRO-3 iodide is a carbocyanine monomer nuclear acid stain. It can be used as a live dead indicator due to its impermeability to cell membranes.

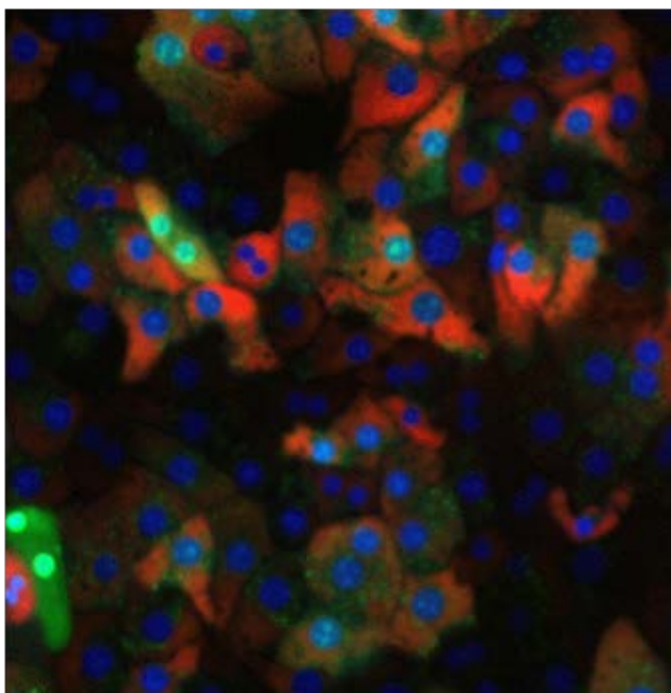


Figure 1.12. Representative composite image of rat hepatocytes stained with Hoechst 33342, TMRM and TOPRO-3 iodide. Blue identifies nuclear staining with Hoechst 33342. Red shows TMRM staining in active mitochondria and green for the nuclear stain and alive/dead indicator TOPRO-3 iodide.

1.11 AIMS

The first two experimental chapters in this thesis describe investigations into the metabolism, irreversible binding and toxicity of nefazodone compared to that of buspirone. The aims of this section of work are:

- To assess reactive metabolite formation from nefazodone and buspirone.
- To assess the irreversible binding of nefazodone and buspirone.

- To assess the species differences between nefazodone toxicity and metabolism in rat and human samples.
- To investigate the relationship between the metabolism, irreversible binding and cytotoxicity of nefazodone.

The final experimental chapter describes work conducted to examine the metabolism of phenformin and whether inhibition of this has an effect on cytotoxicity and lactate production. The aims of this section of work are:

- To determine the full metabolic profile of phenformin in rat hepatocytes.
- To investigate the inhibition of phenformin with CYP450 2D inhibitors.
- To determine whether inhibiting phenformin metabolism would have an effect on cell viability and lactate production.

CHAPTER 2

NEFAZODONE AND BUSPIRONE: REACTIVE METABOLITE FORMATION AND IRREVERSIBLE BINDING IN LIVER MICROSOMES

Contents

2.1 INTRODUCTION.....	42
2.2 MATERIALS AND METHODS.....	45
2.2.1 Materials	45
2.2.2 Preparation of rat liver microsomes	46
2.2.3 Microsomal protein content and CYP450 content	46
2.2.4 Rat liver microsome incubations	46
2.2.5 Rat liver microsome incubations containing trapping agents and inhibitors.....	47
2.2.6 Measurement of covalent binding using solvent exhaustion method	47
2.2.7 Human liver microsome incubations.....	48
2.2.8 Sample preparation for LC-MS.....	48
2.2.9 LC-MS buspirone	48
2.2.10 LC-MS nefazodone in rat liver microsomes	49
2.2.11 LC-MS nefazodone in human liver microsomes	50
2.2.12 Animal work	50
2.2.13 Human ethics	51
2.2.14 Statistics	51
2.3 RESULTS.....	52
2.3.1 Metabolism of buspirone in rat liver microsomes.....	52
2.3.2 Metabolism of nefazodone in rat liver microsomes.....	53
2.3.4 Irreversible binding of nefazodone and buspirone in rat liver microsomes.....	59
2.3.5 Phase I metabolism of nefazodone in human liver microsomes.....	63
2.3.6 Effect of inhibitors on the phase I metabolism of nefazodone in human liver microsomes.....	65
2.4 DISCUSSION.....	68

2.1 INTRODUCTION

Liver microsomes have long been used to assess the possible bioactivation potential of compounds, either through GSH conjugation or irreversible binding studies in the presence and absence of NADPH. The bioactivation of compounds to reactive metabolites is well documented in the literature and many of the drugs which cause DILI are associated with bioactivation. There are several chemical moieties that are liable to undergo bioactivation, which are known as structural alerts. These structural alerts include anilines and analides, arylacetic and arylpropionic acids, hydrazines and hydrazides, thiophenes, nitroaromatics, quinones and quinone-methides (Kalgutkar et al. 2005a).

Nefazodone is an antidepressant that was withdrawn from the market in 2004 following a black box warning for hepatotoxicity. The hepatotoxicity of nefazodone is thought to be mediated through the formation of a reactive quinone-imine via *para*-hydroxylation of the 3-chlorophenylpiperazine moiety, which has been identified through GSH conjugation (figure 2.1) (Kalgutkar et al. 2005b, Bauman et al. 2008a, Argoti et al. 2005, Kalgutkar et al. 2005b). The quinone-imine is then postulated to go on to cause hepatotoxicity through irreversible binding to macromolecules and oxidative stress. The model hepatotoxin, paracetamol, also forms a very well characterised quinone-imine, *N*-acetyl-*p*-benzoquinone-imine (NAPQI). NAPQI has been shown to cause toxicity through depletion of cytosolic and mitochondrial GSH, followed by irreversible binding to important cellular proteins, as well as perturbations in cellular Ca^{2+} homeostasis and mitochondrial function leading to cell death. Other compounds that are known to be bioactivated

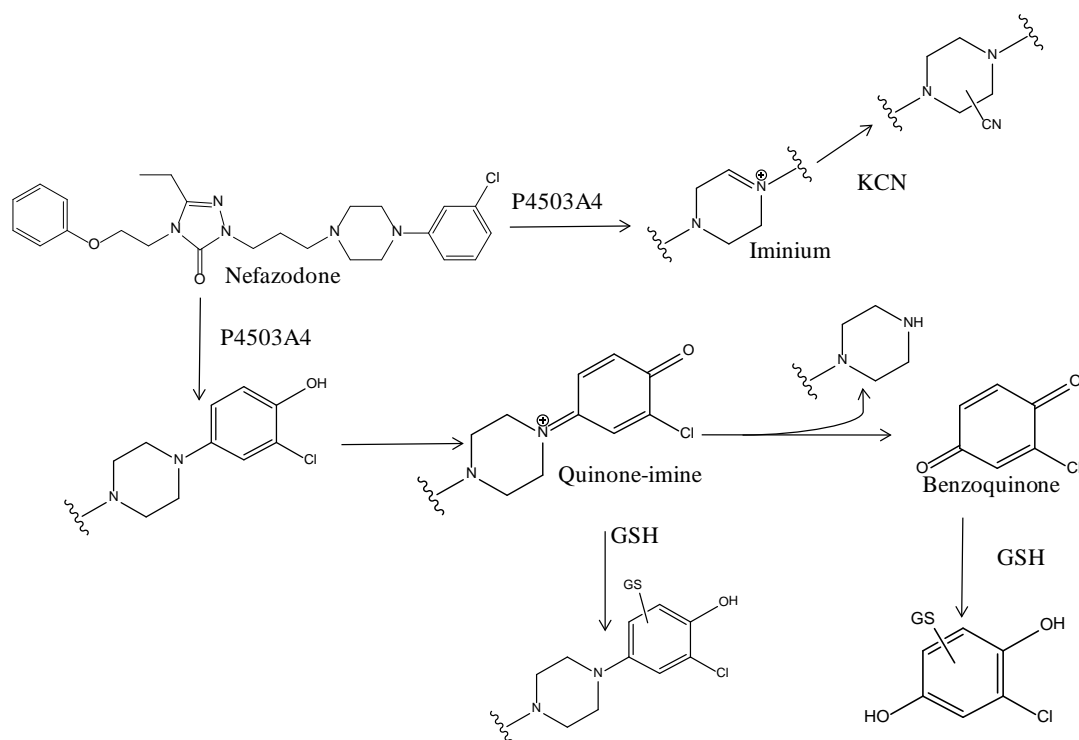


Figure 2.1 Nefazodone bioactivation scheme. Nefazodone has the potential to be bioactivated via CYP450 3A4 to both quinone-imine and iminium reactive metabolites, which can be trapped by GSH and KCN respectively.

via CYP450 enzymes to quinone-imines are diclofenac and indomethacin. The structures of these enzymes can be found in table 2.1.

Nefazodone has also been demonstrated to irreversibly bind to hepatic proteins in human liver microsomes, human S9 fraction and human hepatocytes

(Nakayama et al. 2009, Bauman et al. 2009, Obach et al. 2008) and it is therefore thought that nefazodone toxicity is mediated through the irreversible binding of nefazodone to cellular proteins.

The metabolism of nefazodone is predominantly mediated by CYP450 3A4 (Kalgutkar et al. 2005b, Rotzinger, Baker 2002a), although further metabolism of the circulating metabolite 3-chlorophenylpiperazine has been noted to be mediated through CYP450 2D6 (Von Moltke et al. 1999b). Nefazodone is also an inhibitor of

CYP450 3A4 leading to several known drug interactions (Abernethy et al. 2001, Ashton, Wolin 1996, Helms-Smith, Curtis & Hatton 1996, Von Moltke et al. 1999a) as well as auto-inactivation

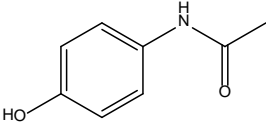
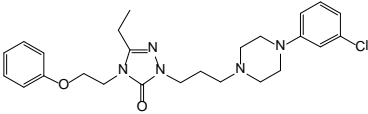
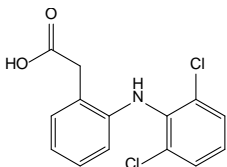
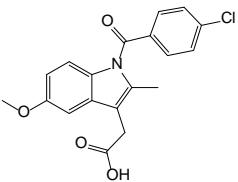
Drug	Structure	Mechanism of bioactivation	References
Paracetamol		2 electron oxidation of para-acetamidophenol substructure by CYPs, peroxidases and cyclooxygenases	Dahlin et al 1984 Corbet et al 1992 Potter and Hinson 1987
Nefazodone		Hydroxylation para to the piperazine nitrogen to generate para-hydroxynefazodone which undergoes 2 electron addition carried out by CYP3A4	Kalgutkar et al Bauman et al
Diclofenac		CYP-catalysed hydroxylation para to the anilide nitrogen to give para hydroxy diclofenac isomers that can undergo CYP or peroxidase mediated oxidation to quinone-imines	Tang et al 1999 Miyamoto et al 1997
Indomethacin		Multipstep process that involves O-demethylation, hydrolysis of the N-acylindole motif and CYP or peroxidase mediated 2 electron addition of the 5-hydroxyindole metabolite	Ju and Uetrecht 1998

Table 2.1. Drugs known to undergo bioactivation to reactive a quinone-imine. Drugs such as paracetamol, nefazodone, diclofenac and indomethacin are known to undergo quinone-imine formation either directly or indirectly following metabolism to a *para*-hydroxy metabolite.

of its own metabolism leading to non-linear pharmacokinetics (Kaul, Shukla & Barbhaiya 1995).

In contrast to nefazodone, buspirone has no reports of specific organ directed toxicity. It is also metabolised through CYP450 3A4 (Zhu et al. 2005) and has the potential to be bioactivated through *para*-hydroxylation on the 1-pyrimidinylpiperazine moiety. However, no GSH conjugates of buspirone have been identified (Kalgutkar et al. 2005b) and it is thought that buspirone is less likely to

undergo the two-electron oxidation required to form a quinone-imine. Despite this buspirone has been demonstrated to irreversibly bind in both human liver microsomes and human hepatocytes (Bauman et al. 2009, Obach et al. 2008).

The aim of this chapter was to assess the phase I metabolic pathways of nefazodone and buspirone in supplemented rat liver microsomes. It also provided the opportunity to examine the difference in bioactivation of the two compounds using GSH trapping and irreversible binding. Finally the bioactivation of nefazodone was assessed in human liver microsomes to confirm the translation of bioactivation in the rat into man.

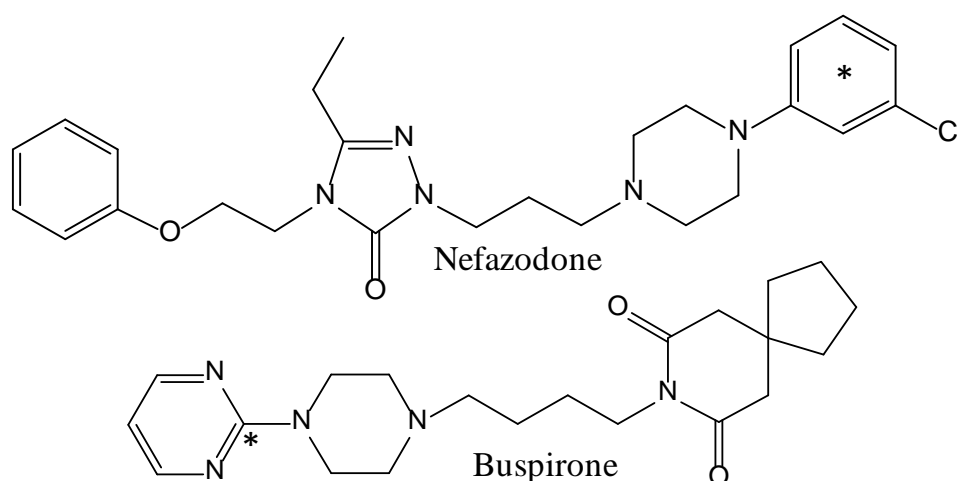


Figure 2.2. Chemical structures of nefazodone and buspirone. * Indicates the position of the radiolabel for irreversible binding experiments.

2.2 MATERIALS AND METHODS

2.2.1 Materials

Buspirone was purchased from Sigma-Aldrich (Poole, Dorset, UK) and nefazodone was kindly purchased by Pfizer from Bosche Scientific (New Jersey, US). [^{14}C]-nefazodone and [^{14}C]-buspirone were supplied by Pfizer (Sandwich, Kent, UK). Human liver microsomes were donated by Pfizer (Sandwich, UK). Liquid

scintillation cocktail Gold Star was purchased from Meridian (Epsom, Surrey, UK). MTS reagent and ATP cell viability assay were purchased from Promega (UK). All other reagents unless otherwise stated were purchased from Sigma-Aldrich (Poole, Dorset, UK). Solvents were purchased from Fischer and were all at least HPLC grade.

2.2.2 Preparation of rat liver microsomes

Rat liver microsomes were prepared from adult male Wistar rats killed by rising levels of CO₂. The livers were removed and placed into ice-cold 0.067M phosphate buffer, pH 7.4, containing 1.15% (w/v) KCl. The livers were then chopped into smaller pieces with a pair of scissors, before being homogenised with a motor-driven homogeniser. This was followed by homogenisation with a manual homogeniser. The homogenate was then centrifuged at 18,000rpm for 25 minutes at 4°C to remove any cellular debris. The resulting supernatant was then centrifuged at 35,000rpm at 4°C to pellet the microsomes. The microsome pellet was then re-suspended by manual homogenisation in phosphate buffer with KCl before being centrifuged at 35,000rpm, for 65 minutes at 4°C. The supernatant was discarded and the microsomes re-suspended in phosphate buffer without KCl and stored at - 80°C until required.

2.2.3 Microsomal protein content and CYP450 content

Microsomal CYP450 content was determined using the procedure described by Omura *et al* (1964). Protein content was determined using a Lowry protein assay (LOWRY *et al.* 1951) and bovine serum albumin was used for the standards.

2.2.4 Rat liver microsome incubations

Microsome incubations were carried out in a final volume of 0.067M phosphate buffer, pH 7.4 and contained a final concentration of 1mg/ml microsomal protein.

All incubations included a final concentration of 5mM MgCl₂ and all but control incubations contained 1mM NADPH. Incubations for metabolism included a concentration of either 100μM nefazodone or buspirone and incubations for covalent binding were carried out using 10μM nefazodone or buspirone and 0.1μCi of corresponding radiolabelled compound. The samples were incubated in a shaking water bath for 60 minutes at 37°C. The reaction was terminated by addition of an equal volume of ice-cold ACN and stored at -20°C.

2.2.5 Rat liver microsome incubations containing trapping agents and inhibitors

Incubations contained either 1mM reduced GSH, 1mM 1-aminobenzotriazole (ABT) or 5μM ketoconazole. Incubations containing ABT were pre-incubated for 15 minutes at 37°C before addition of drug to initiate the reaction. Controls contained no NADPH. The samples were incubated for a further 60 minutes before being terminated using an equal volume of ice-cold ACN.

2.2.6 Measurement of irreversible binding using the solvent exhaustion method

Covalent binding of [¹⁴C]-nefazodone and [¹⁴C]-buspirone was measured using exhaustive solvent extraction method. The samples were centrifuged at 2200rpm, for 10 minutes. 100μl of supernatant was removed for scintillation counting and the supernatants were kept for LC-MS analysis. 3ml of 100% MeOH was added to each pellet and was vortexed and centrifuged again. 100μl of supernatant was removed from each supernatant for scintillation counting and the rest was discarded. 3ml of 70% MeOH was added to the pellet and vortexed before being centrifuged at 2200rpm. Again, 100μl was kept for scintillation counting and the rest was discarded. This process was repeated once more with 70% MeOH after the supernatant was removed and the left over solvent was evaporated in a 60°C oven.

1ml NaOH (1M) was then added to each pellet, vortexed and the protein left to dissolve. 100µl of this was taken for scintillation counting and the protein content was assessed using a Lowry assay (LOWRY et al. 1951). Irreversible binding was calculated as pmol equivalent/mg protein.

2.2.7 Human liver microsome incubations.

Human liver microsome incubations were carried out in a final volume of 1ml in 0.067M phosphate buffer, pH 7.4, and contained a final concentration of 1mg/ml microsomal protein. All incubations included a final concentration of 5mM MgCl₂ and all but control incubations contained NADPH. The samples were incubated in a shaking water bath for 60 minutes at 37°C. For inhibition studies the human liver microsomes were pre-incubated for 15 minutes at 37°C with a final concentration of 1mM ABT or 200µM methimazole with 1mM NADPH. After the pre-incubation period a final concentration of 50µM nefazodone and more NADPH was added and incubated for a further 60 minutes. All incubations were terminated with an equal volume of ice-cold ACN.

2.2.8 Sample preparation for LC-MS

Samples were stored overnight at -20°C to allow any protein to precipitate. The samples were centrifuged at 2200rpm and the supernatant kept. The supernatant was then evaporated under a gentle stream of nitrogen gas. The samples were reconstituted in 300µl of 50% MeOH, before being centrifuged at 14,000rpm. The supernatant was then analysed using LC-MS or LC-MS/MS.

2.2.9 LC-MS buspirone

LC-MS analysis was performed on an API 2000. The LC system consisted of an Agilent Eclipse XDB C18 column (4.6x150mm, 5µ). The aqueous phase was 15mM

ammonium formate (A). The organic solvent (B) was ACN. A gradient separation was used starting initially with 10% B rising to 30% B over 35 minutes and held at 30% for 5 minutes. 25µl of sample was injected onto the column. The flow rate was 1ml/min and the mass spectrometer operated in positive ion mode. The mass spec parameters for buspirone are listed in table 2.2.

Curtain gas (CUR)	30.00
Ion spray voltage (IS)	5000.00
Temperature (TEM)	400.00
Ion source gas 1 (GS1)	30.00
Ion source gas 2 (GS2)	75.00
De-clustering potential (DP)	40.00
Focusing potential (FP)	350.00
Entrance potential (EP)	10.00

Table 2.2 Operating parameters of API2000 for buspirone analysis.

2.2.10 LC-MS nefazodone in rat liver microsomes

LC-MS analysis was performed on an API 2000. The LC system consisted of a Phenomenex phenyl-hexyl column (4.6x150mm, 5µ) and a Perkin Elmer LC-200 quaternary pump. The aqueous phase was 15mM ammonium formate (A) and organic was ACN (B). A gradient separation was run starting at 5% B rising to 70%

Table 2.3. Operating parameters of API2000 for nefazodone analysis

B over 25 minutes. This returned to 5% B at 26 minutes until 30 minutes. The flow rate was 1ml/min. Ionisation was conducted in positive ion mode. The mass spectrometer parameters can be viewed in figure 2.3.

CUR	20.00
IS	5000.00
TEM	400.00
GS1	30.00
GS2	75.00
DP	66.00
FP	250.00
EP	11.50

2.2.11 LC-MS nefazodone in human liver microsomes

LC-MS analysis was performed on an API 4000. The LC system consisted of a Phenomenex phenyl-hexyl column (4.6x150mm, 5 μ) and a Perkin Elmer LC-200 quaternary pump. The aqueous phase was 15mM ammonium formate (A) and organic was ACN (B). A gradient separation was run starting at 5% B rising to 70% B over 25 minutes. This returned to 5% B at 26 minutes until 30 minutes. The flow rate was 1ml/min and the detection was by positive-ion electrospray ionisation, The mass spectrometer parameters can be viewed in table 2.4.

CUR	15.00
IS	4500.00
TEM	400.00
GS1	50.00
GS2	50.00
DP	150.00
EP	10.00

Table 2.4. Operating parameters for API4000 for nefazodone analysis

2.2.12 Animal work

All animal work was carried out according to local ethics policies and in accordance with home office regulation.

2.2.13 Human ethics

All work with human samples was carried out in accordance with local ethics policies.

2.2.14 Statistics

Statistical analysis was undertaken using Stats Direct software. Data was tested for normality using a Shapiro-Wilk test and either a Student's T test (parametric) or Mann-Whitney U test (non-parametric) was used to make comparisons between data sets. An ANOVA (Dunnett's comparison to control) was used to determine significance to control values.

2.3 RESULTS

2.3.1 Metabolism of buspirone in rat liver microsomes

The metabolism of buspirone (m/z 386) in rat liver microsomes (figure 2.3) consisted mainly of hydroxylation reactions. At least 4 [O] buspirone metabolites (m/z 402) were identified consisting of those that had been substituted on both the pyrimidinyl and azaspirone moieties. This was determined by the shift of m/z 123 to m/z 139 through substitution on the azaspirone moiety and a shift of m/z 122 to m/z 138 indicating hydroxylation on the pyrimidine structure. At least 3 [2O] buspirone (m/z 418) metabolites were also identified which contained hydroxylation on both the azaspirone and pyrimidinyl moieties. *N*-dealkylation reactions also took place and 1-pyrimidinyl piperazine (m/z 165) and despyrimidinyl piperazine buspirone (m/z 254) were also detected. Retention times of the compounds can be found in table 2.5. The structures of the metabolites identified in rat liver microsomes can be found in figure 2.4. Appendix 1 contains the AUC for each metabolite. In accordance with the literature , incubations containing GSH (1mM) did not result in the detection of any GSH conjugates of buspirone, despite searching for both addition of 306 and neutral loss of 129.

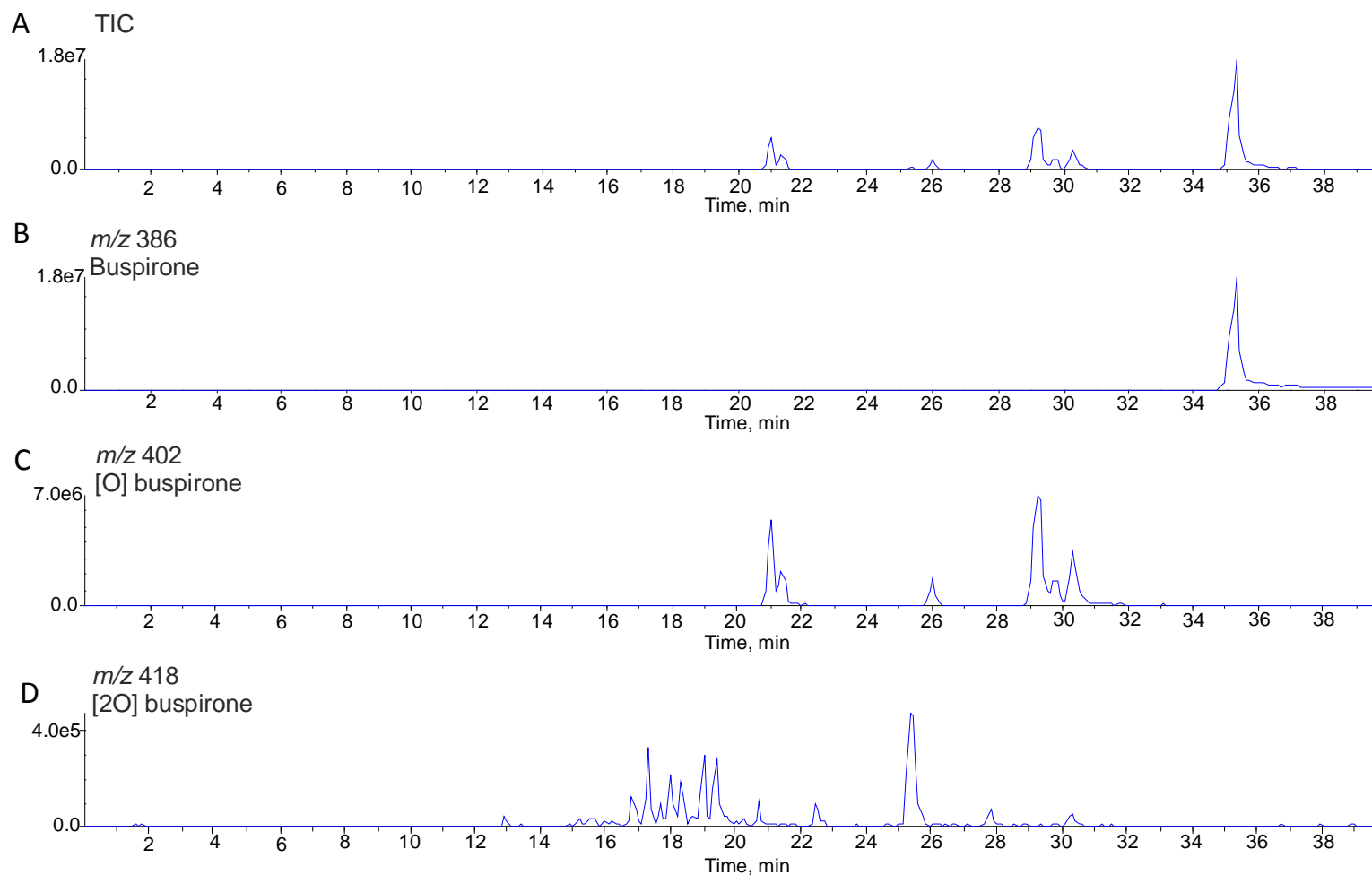


Figure 2.3. LC-MS traces of buspirone metabolites in rat liver microsomes. (A) Total ion current (B) TIC m/z 386 (C) TIC m/z 402 (D) TIC m/z 418.

Name	m/z	Retention time (mins)
1-pyrimidinylpiperazine	165	6.28
[20] buspirone	418	18.35
[20] buspirone	418	18.86
[20] buspirone	418	19.86
[20] buspirone	418	22.691
[O] buspirone	402	24.03
Despyrimidinyl piperazine buspirone	254	25.86
[O] buspirone	402	26.53
[O] buspirone	402	27.53
[O] buspirone	402	29.62
Buspirone	386	35.2

Table 2.5. Metabolites of buspirone identified in rat liver microsomes.

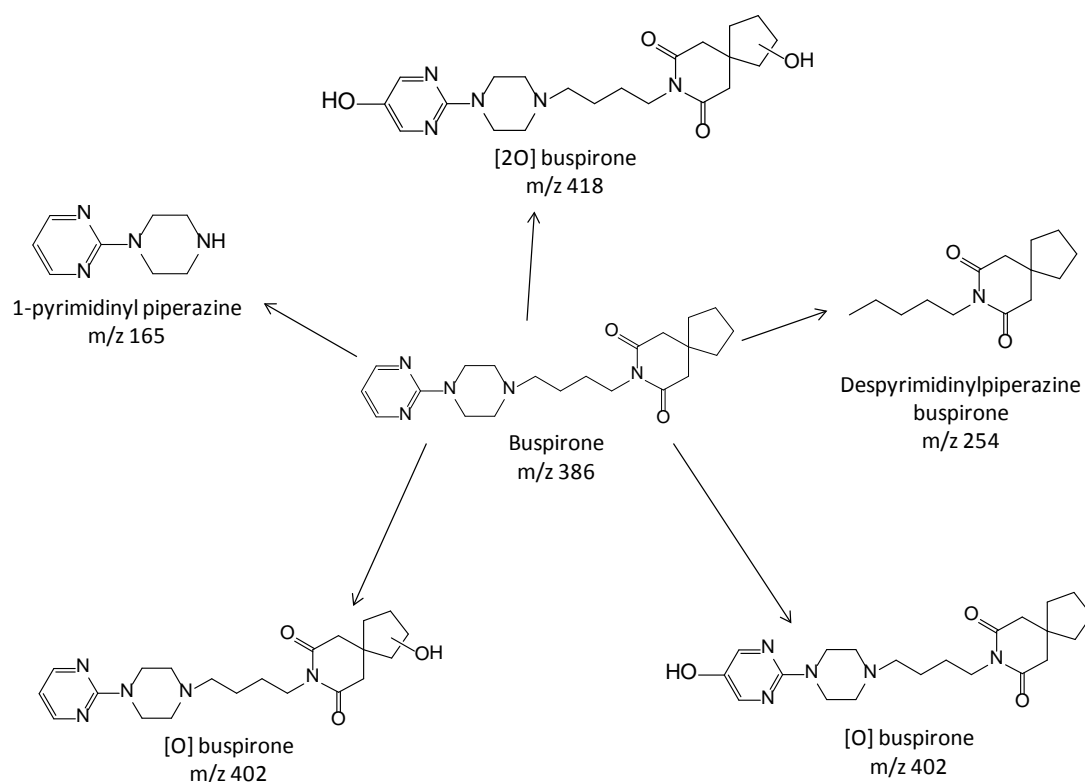


Figure 2.4. Schematic of buspirone metabolites identified in RLMs

2.3.2 Metabolism of nefazodone in rat liver microsomes

Like buspirone, the metabolism of nefazodone mainly consisted of hydroxylation (figure 2.4) and *N*-dealkylation reactions. Nefazodone yielded three [O] nefazodone (m/z 486) products (figure 2.6.). Fragment ions of these metabolites indicated that these consisted of a metabolite with an m/z 274 and one with a fragment ion m/z 290. A fragment ion with an m/z 274 indicates an unsubstituted phenoxyethyl-triazolone-propyl moiety, indicating nefazodone is most likely to be hydroxylated on the chlorophenyl ring. This leads to the possibility of the formation of the *para*-hydroxy metabolite. Two [2O] nefazodone (m/z 502) products were also identified (figure 2.4), although, the location of the additional hydroxyl groups was not determined. Metabolites at m/z 484, [=O] nefazodone, and m/z 292, phenoxyethyl-triazolone *n*-propanol could also be detected. The hydroxylated metabolite of

chlorophenyl piperazine, which has also been reported to undergo bioactivation to a quinone-imine was not detected. The retention times of the metabolites can be found in table 2.6 and the proposed metabolic structures in figure 2.8. Appendix 2 contains the AUC for each metabolite.

In incubations of nefazodone containing GSH (1mM), two GSH conjugates were identified (figure 2.7). The two metabolites had an m/z 807 (GS1) and an m/z 791 (GS2). GS1, [2O] nefazodone GSH had a very weak signal and was only just detectable, however, GS2, [O] nefazodone GSH was more prominent in the sample even though it still only appeared to be present in relatively small amounts compared to other metabolites. These metabolites correspond with the hydroxylated nefazodone products that were formed and suggesting that nefazodone undergoes quinone-imine formation in rat liver microsomes.

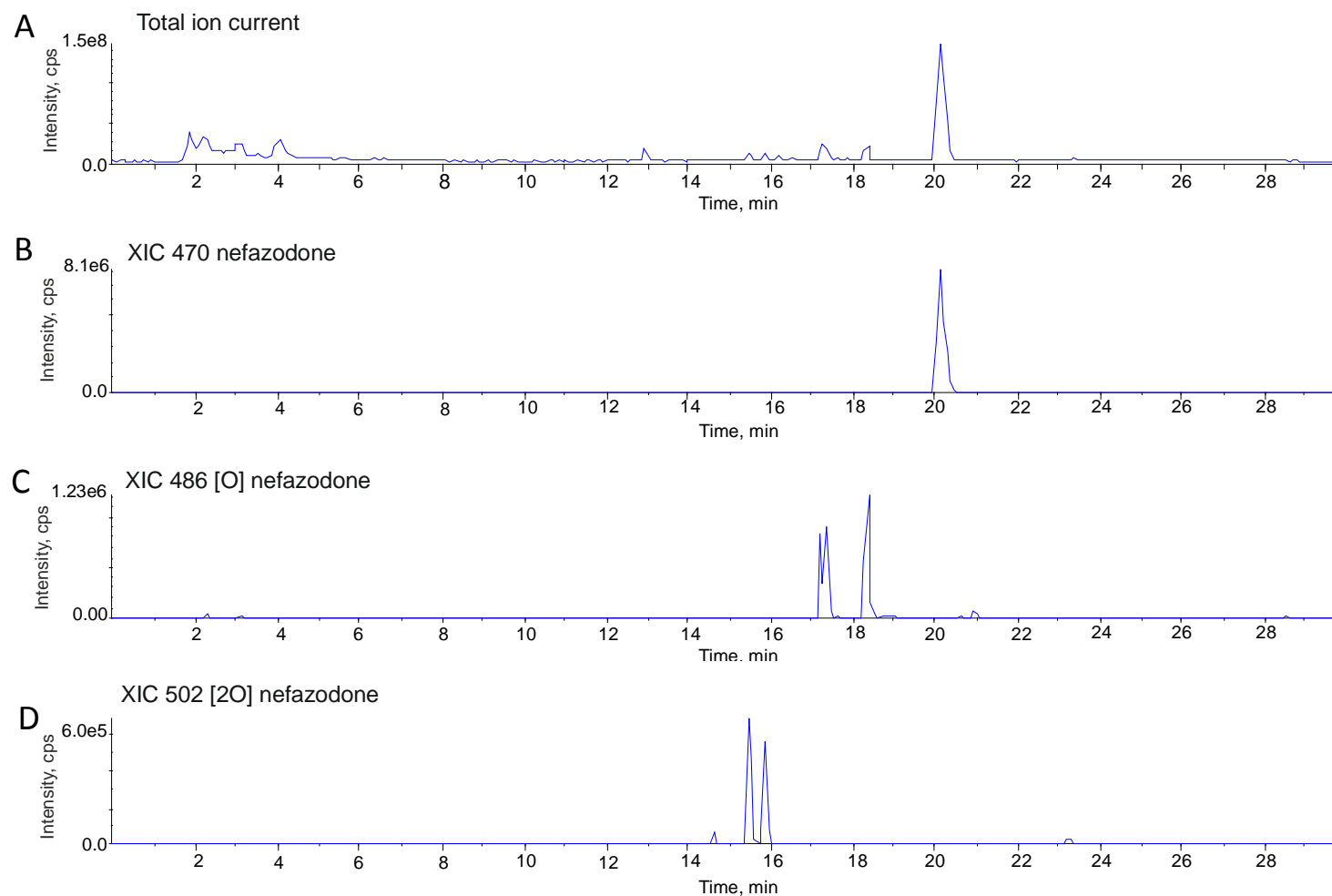


Figure 2.5. Metabolism of nefazodone in rat liver microsomes. (A) Total ion current (B) XIC m/z 470 nefazodone. (C) XIC m/z 486 [O] nefazodone (D) XIC m/z 502 [2O] nefazodone.

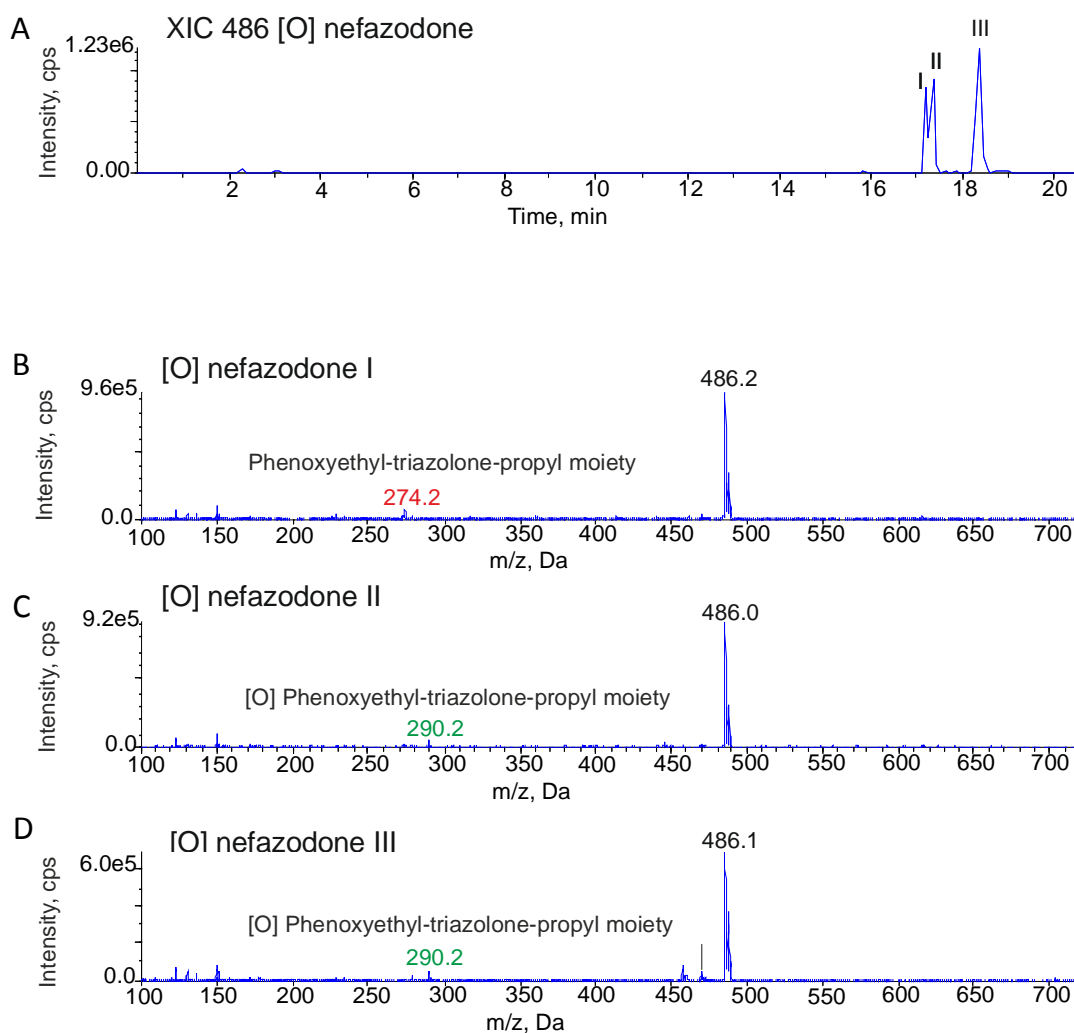


Figure 2.6. Fragmentation of [O] nefazodone metabolites in rat liver microsomes. (A) XIC m/z 486 [O] nefazodone. (B) Fragment ions of [O] nefazodone I (C) Fragment ions of [O] nefazodone II (D) Fragment ions of [O] nefazodone III.

Nefazodone and buspirone: reactive metabolite formation and irreversible binding in liver microsomes

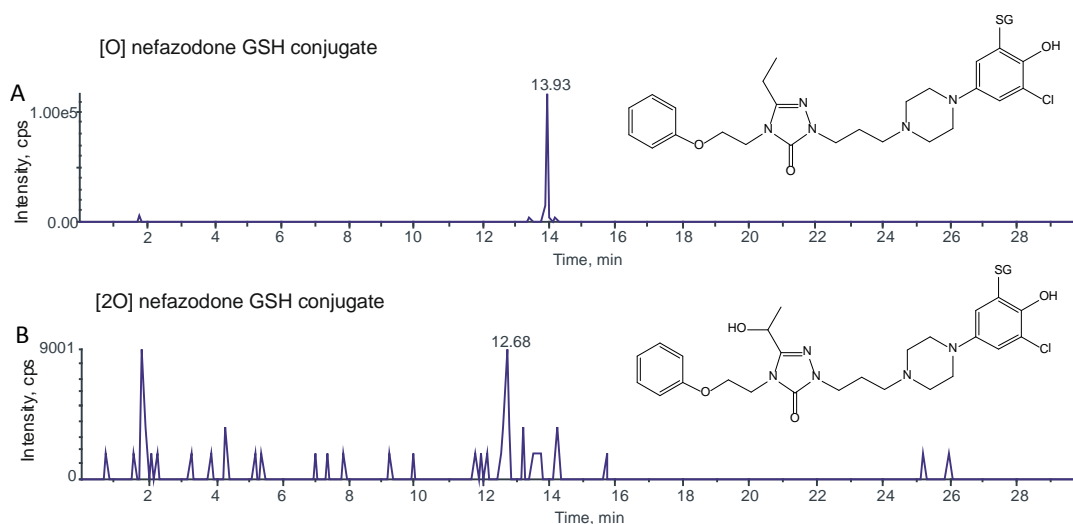


Figure 2.7. GSH conjugates of nefazodone identified in rat liver microsomes. (A) XIC m/z 791 [O] nefazodone GSH conjugate. **(B)** XIC m/z 807 [2O] nefazodone conjugate.

Name	m/z	Retention time (mins)
[2O] nefazodone	502	15.45
[2O] nefazodone	502	15.85
Phenoxyethyltriazolone n-propanol	292	16.19
[O] nefazodone	486	17.19
[O] nefazodone	486	17.34
[O] nefazodone	486	18.34
Nefazodone	470	20.12
[=O] nefazodone	484	20.95

Table 2.6. Metabolites of nefazodone identified in RLMs.

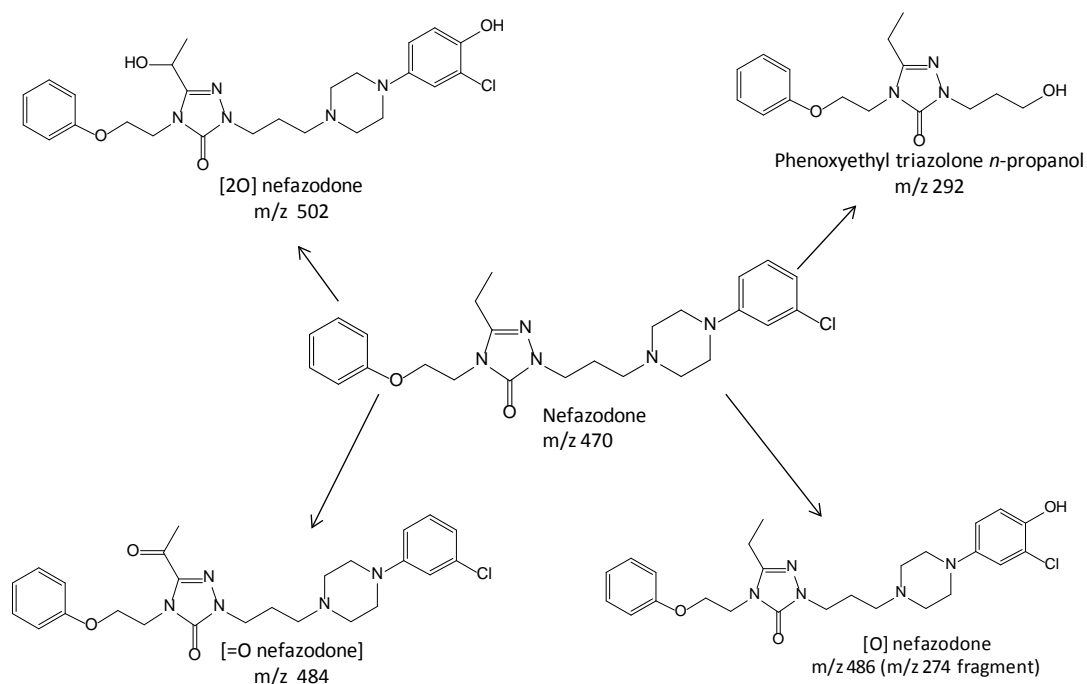


Figure 2.8. Metabolic scheme of nefazodone metabolites identified in RLMs

2.3.4 Irreversible binding of nefazodone and buspirone in rat liver microsomes

Both nefazodone and buspirone demonstrated significant NADPH-dependent irreversible binding in rat liver microsomes (figure 2.9). Although nefazodone and buspirone both displayed irreversible binding, nefazodone exhibited levels of irreversible binding 9-fold higher than those of buspirone (105.54 ± 12.46 pmol equiv/mg protein and 12.76 ± 0.48 pmol equiv/mg protein respectively). Pre-incubation of the microsomes with ABT reduced the irreversible binding of buspirone and nefazodone significantly, so that binding was not significantly different from control values. The CYP450 3A4 inhibitor, ketoconazole, was also added to incubations. Ketoconazole significantly decreased the irreversible binding of buspirone to rat liver microsomal protein when compared to NADPH incubations (5.9 ± 0.23 pmol equiv/mg protein), however this was not the case for nefazodone (73.54 ± 17.96 pmol equiv/mg protein). Nefazodone and buspirone covalent binding

was also significantly decreased when GSH was added to the incubations (16.13±2.63 pmol equiv/mg protein and 8.65 ± 0.19 pmol equiv/mg protein respectively).

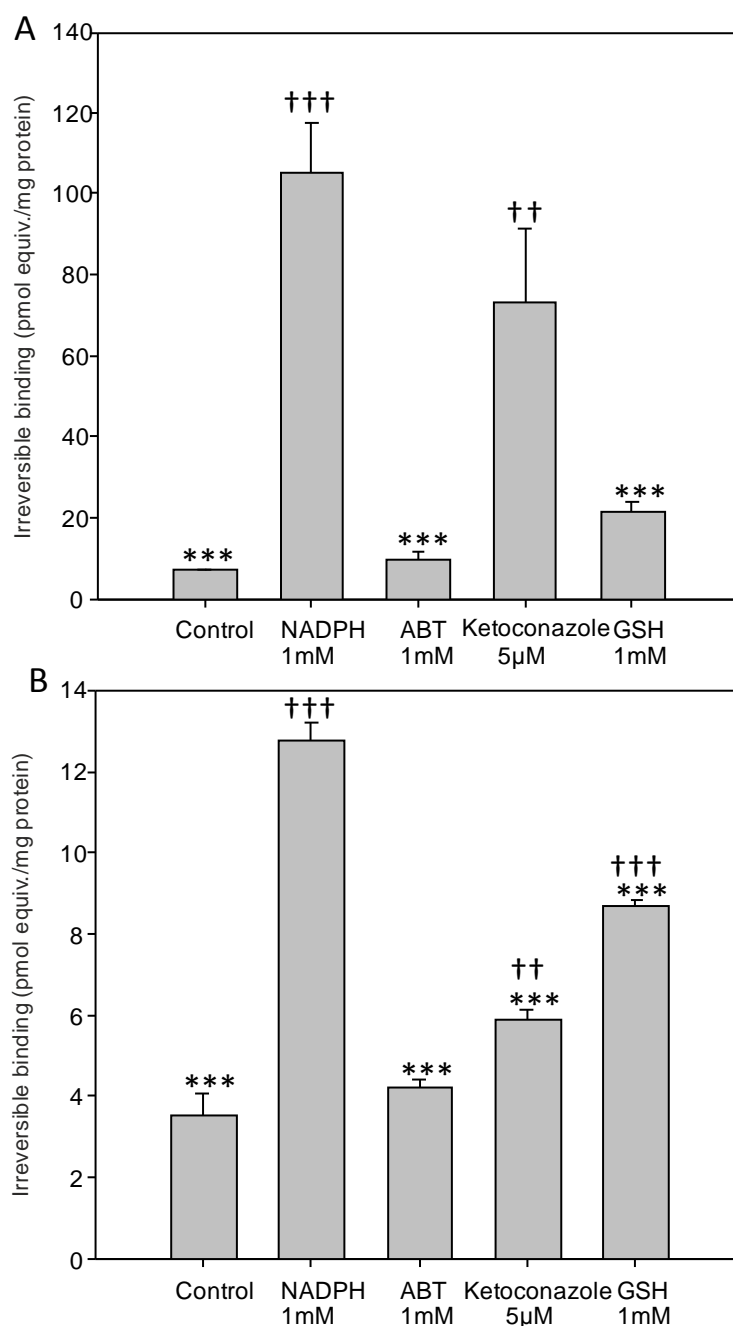


Figure 2.9. Irreversible binding of nefazodone (A) and buspirone (B) in rat liver microsomes. Data is expressed as pmol equivalent/mg protein and is taken from 3 independent isolations. * $P < 0.05$, ** $P < 0.01$, *** $P < 0.001$ versus NADPH. † $P < 0.05$ †† $P < 0.01$ ††† $P < 0.001$ versus control. Statistical significance was determined using ANOVA (Dunnett's comparison to control).

2.3.5 Phase I metabolism of nefazodone in human liver microsomes

The metabolism of nefazodone in human liver microsomes was similar to that in rat liver microsomes and consisted of hydroxylation (figure 2.10) and *N*-dealkylation reactions. There were also 3 [O] nefazodone metabolites in human liver microsomes and as in rat liver microsomes the most polar of these had an unsubstituted phenoxyethyl-triazolone propyl moiety (figure 2.11). Unlike in rat liver microsomes, however, there was only one [2O] nefazodone metabolite detected, which appeared to be hydroxylated on both the chlorophenylpiperazine and the phenoxyethyl-triazolone propyl moiety. The products of *N*-dealkylation reactions could also be identified.

In incubations containing GSH (1mM) two GSH conjugates were detected. As in rat liver microsomes these were the products of [O] nefazodone and [2O] nefazodone. The GSH conjugates were easier to detect in the human liver microsomes which allowed for a better fragmentation pattern (figure 2.12). The unsubstituted phenoxyethyl-triazolone-propyl fragment of m/z 274 can be clearly seen in the fragmentation pattern of the [O] nefazodone GSH conjugate (m/z 791), whilst a m/z 290 fragment, indicating hydroxylation on both the chlorophenylphenylpiperazine and phenoxy-ethyl-triazolone-propyl moieties, can be identified in the [2O] nefazodone GSH conjugate (m/z 807).

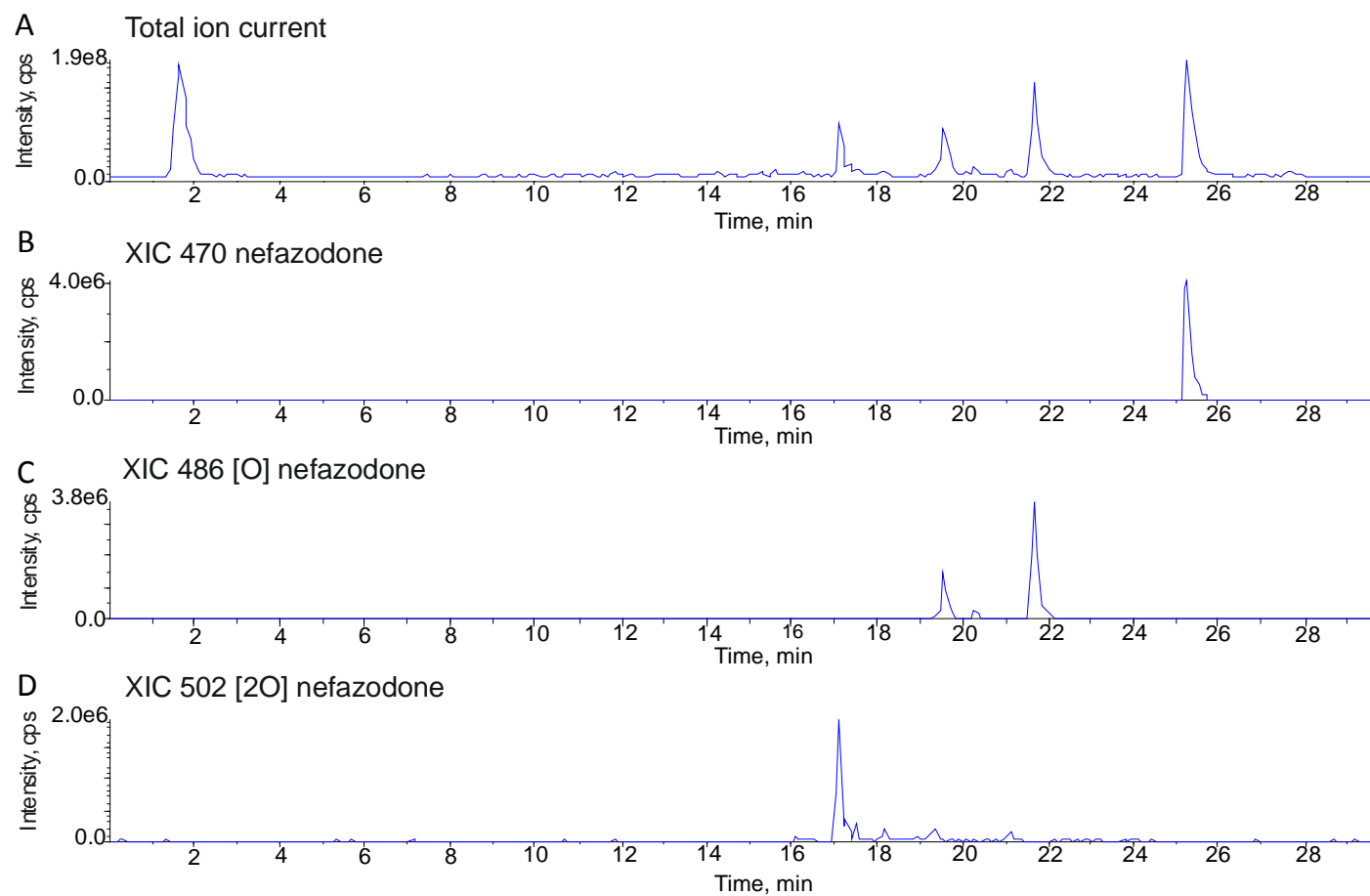


Figure 2.10. Hydroxylated metabolites of nefazodone in human liver microsomes. (A) Total ion current of nefazodone metabolism. (B) XIC m/z 470 nefazodone (C) XIC m/z 486 [O] nefazodone. (D) XIC m/z 502 [2O] nefazodone.

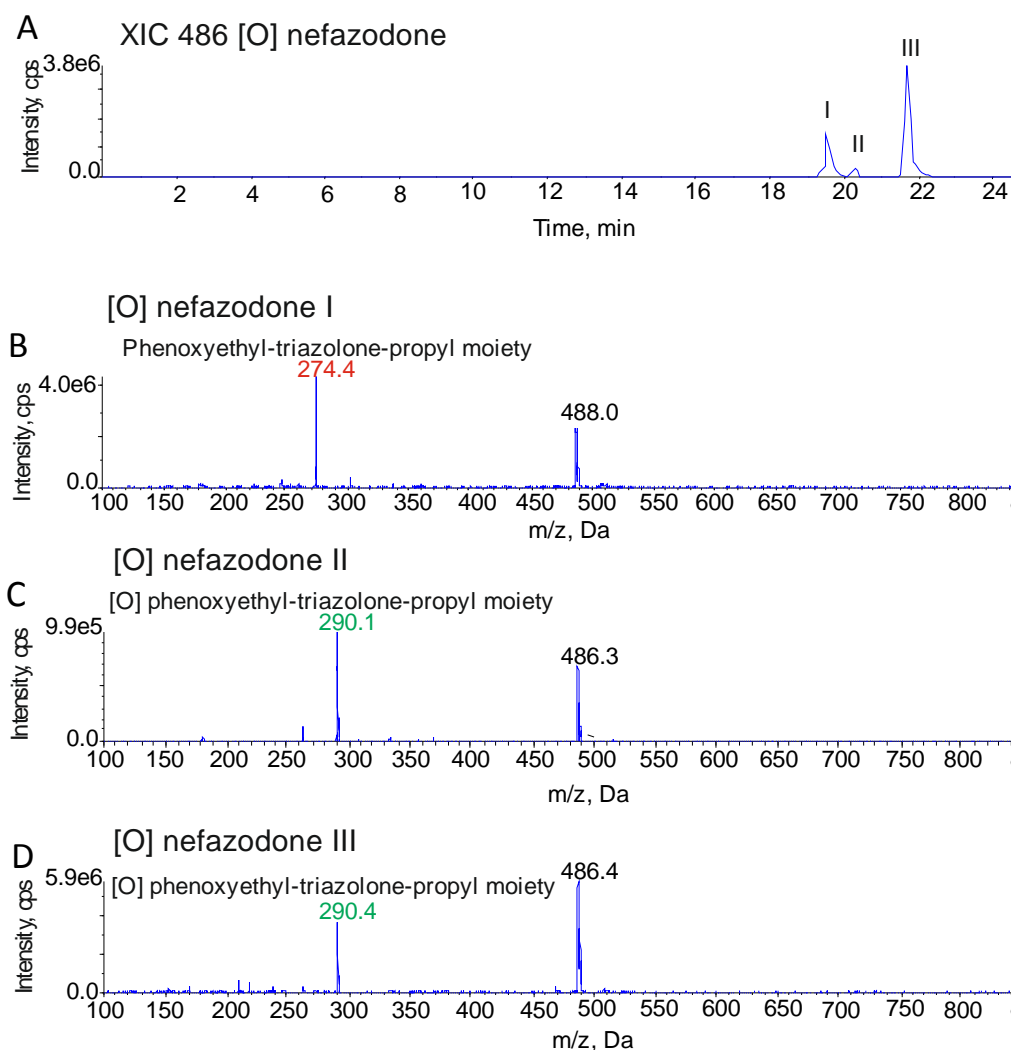


Figure 2.11. Fragment ions of [O] nefazodone in human liver microsomes. (A) XIC m/z 486 [O] nefazodone. (B) Fragment ions of [O] nefazodone I with a fragment ion of m/z 274 indicating an unsubstituted phenoxyethyl-triazolone propyl fragment. (C) Fragment ions of [O] nefazodone II. (D) Fragment ions of [O] nefazodone III.

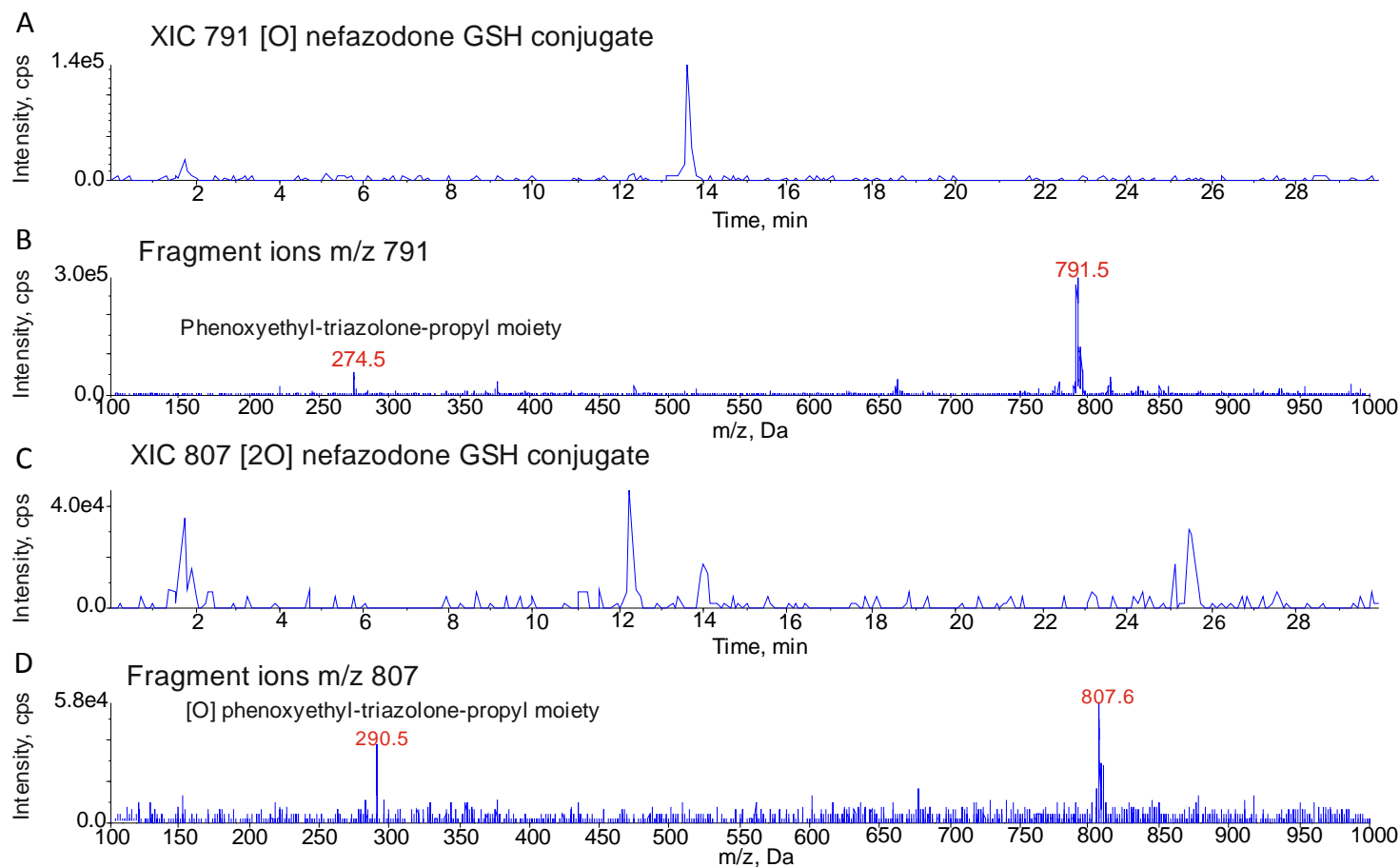


Figure 2.12. GSH conjugates of nefazodone in human liver microsomes. (A) XIC m/z 791 [O] nefazodone GSH conjugate. (B) Fragment ions of the [O] nefazodone GSH conjugate. (C) XIC m/z 807 [20] nefazodone GSH conjugate. (D) Fragment ions of the [20] nefazodone GSH conjugate.

2.3.6 Effect of inhibitors on the phase I metabolism of nefazodone in human liver microsomes

Incubation of nefazodone with the inhibitors ABT and methimazole in human liver microsomes led to the decreased metabolism of nefazodone (figure 2.13). Based on the ratios to parent compound, it appeared that ABT almost completely abolished metabolism. Without the use of a quantitative method it was difficult to determine by how much the turnover was reduced, however, the only metabolite that could be detected following ABT pre-incubation of the human liver microsomes was a [O] nefazodone metabolite. This corresponded with the [O] nefazodone I metabolite which has a fragment at m/z 274, making it the [O] nefazodone metabolite that is most likely to undergo bioactivation. Despite this the ratio of the peak to nefazodone was greatly diminished (0.307 to 0.021) and there is a high probability that in these incubations, turnover to [O] nefazodone I was reduced to a great extent.

Inclusion of methimazole in the incubation reduced metabolism to some degree. It reduced turnover to [O] nefazodone metabolites but the main effect was on the major peak [2O] nefazodone peak at 17.1 minutes, where the ratio of the peak to the parent compound was reduced from 0.245 to 0.027. Methimazole is an inhibitor of human FMO and, there is a possibility that the [2O] nefazodone is an N-oxide, due to the decrease in the ratio to the parent. As such it is tentatively suggested that the [2O] nefazodone metabolite is formed via *N*-oxidation followed by sequential hydroxylation.

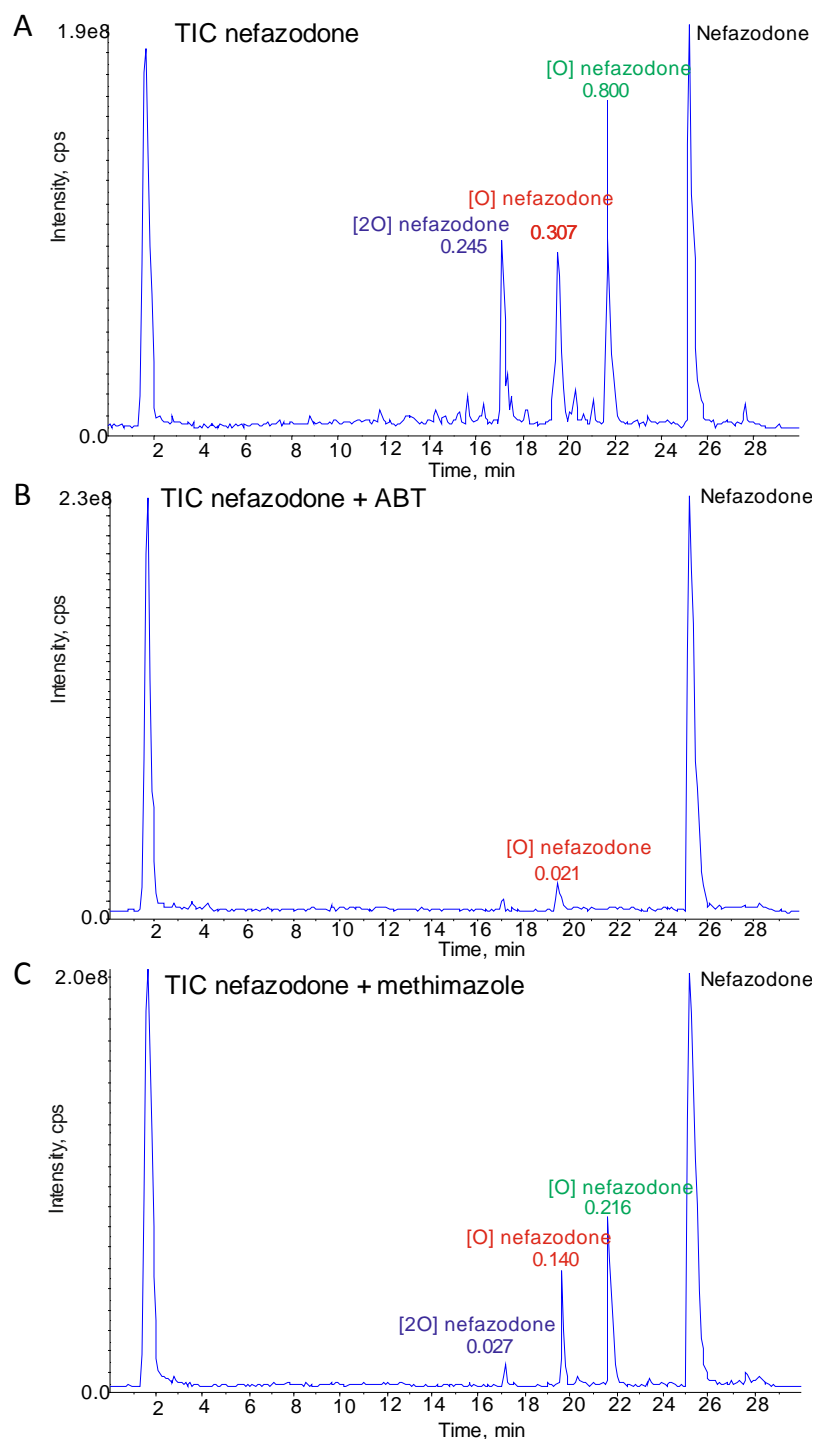


Figure 2.13. Effect of inhibitors on nefazodone metabolism in human liver microsomes. (A) Total ion current nefazodone metabolism in human liver microsomes. (B) Total ion current of nefazodone metabolism following ABT pre-incubation. (C) Total ion current of nefazodone metabolism following pre-incubation with methimazole. Numbers represent the ratio of the major hydroxylate metabolite to the parent peak.

2.4 DISCUSSION

The investigations in this chapter aimed to assess the metabolism and bioactivation of nefazodone and buspirone in rat liver microsomes and to further assess the bioactivation of nefazodone in human liver microsomes. This demonstrated that nefazodone formed both GSH conjugates in rat and human liver microsomes and also demonstrated significant irreversible binding in rat liver microsomes. In contrast buspirone, did not produce any GSH conjugates and although significant irreversible binding was noted this was several times lower than that of nefazodone.

The metabolism of nefazodone and buspirone in liver microsomes mainly consists of hydroxylation and *N*-dealkylation reactions. The hydroxylation of nefazodone is of particular interest as it has been suggested that the *para*-hydroxylation of nefazodone, followed by bioactivation is responsible for its hepatotoxicity (Kalgutkar et al. 2005b, Bauman et al. 2008a, Argoti et al. 2005). Buspirone, which has a pyrimidinylpiperazine ring instead of a phenylpiperazine ring, has also been shown to have a *para*-hydroxy metabolite but has not been shown to be bioactivated (Kalgutkar et al. 2005b). Both drugs are metabolised by CYP450 3A4 (Zhu et al. 2005, Rotzinger, Baker 2002a, Von Moltke et al. 1999a, Kalgutkar et al. 2005a) and it is thought that a potential reason for the difference between the toxicity profiles of nefazodone and buspirone is due to their differing bioactivation potential.

Analysis of the metabolism of nefazodone in rat and human liver microsomes demonstrated three [O] nefazodone metabolites. One of these had a fragment ion with *m/z* 274, indicating an unsubstituted phenoxyethyl-triazolone-propyl fragment and, therefore, hydroxylation on the phenylpiperazine ring. Hydroxylation of nefazodone *para* to the piperazine nitrogen leads to the possibility of two electron

oxidation to a reactive quinone-imine. To determine whether a quinone-imine was formed, incubations were carried out in the presence of excess GSH to trap the reactive metabolite. This identified two GSH adducts, one formed from [O] nefazodone and one from [2O] nefazodone, in both rat and human liver microsomes. This corresponded with the bioactivation pathway that has previously been identified (Kalgutkar et al. 2005b, Bauman et al. 2008b, Argoti et al. 2005). Buspirone also produced several hydroxylated metabolites, and it is likely that one of these was a *para*-hydroxy metabolite on the pyrimidinyl piperazine, signified by a shift from m/z 122 to m/z 138 in the fragmentation pattern. Unlike nefazodone, in the trapping experiments no GSH conjugates of buspirone could be identified.

As the formation of *N*-oxides of nefazodone has been reported, inhibitor studies with the CYP450 inhibitor, ABT, and the FMO inhibitor, methimazole, were undertaken. ABT reduced considerably the metabolism of nefazodone and only a [O] metabolite could be detected, but this metabolite also produced a less intense peak on the LC-MS when compared to parent compound. Whilst ABT almost abolished the metabolism of nefazodone, the most noticeable effect of methimazole was on the peak corresponding to [2O] nefazodone. It is a possibility that the m/z 502 metabolite is an *N*-oxide that undergoes subsequent hydroxylation. However, although methimazole is widely reported to be an inhibitor of FMOs it has also been shown to inhibit CYP450 3A4 (Guo, Z et al. 1997). It is, therefore, not possible to state with certainty whether the [2O] nefazodone is a result of *N*-oxide formation.

To reinforce the observation that nefazodone can be bioactivated by rat liver microsomes whilst buspirone is not, irreversible binding studies were undertaken using [^{14}C] nefazodone and buspirone. These studies demonstrated that nefazodone and buspirone both exhibit significant NADPH-dependent irreversible binding

compared to control values. However, the irreversible binding of buspirone was 9-fold lower than that of nefazodone. Incubation with the non-specific suicide CYP450 inhibitor, ABT, significantly attenuated irreversible binding, further providing evidence that bioactivation via CYP450 enzymes are involved in the bioactivation of nefazodone. As expected, following identification of GSH adducts, GSH also significantly prevented the irreversible binding of nefazodone to rat liver microsome protein. The specific CYP450 3A4 inhibitor, ketoconazole, significantly reduced the binding of buspirone, but not nefazodone. It is possible whilst buspirone is metabolised by the same isoform in rat and human, that nefazodone is metabolised by either a different CYP450 in rat or a different CYP450 3A isoform than CYP450 3A1 which is the main isoform present in rat liver. Several discrepancies between the metabolism of rats and humans exist in regards to CYP450 3A. The well known CYP450 3A4 inducer rifampicin does not seem to induced CYP450 3A1 (Lu, Li 2001) and other model substrates of CYP450 3A4 metabolism are not metabolised by CYP450 3A1 (Guengerich 1997).

Quinone-imines, and their subsequent irreversible binding, have been implicated in the toxicity of several compounds (table 2.1). As a result the formation of quinone-imines and irreversible binding in liver microsomes highlights the potential role of reactive metabolite formation in nefazodone induced liver injury. The most commonly investigated quinone-imine is NAPQI and its formation from paracetamol and subsequent covalent binding is well documented. NAPQI has been demonstrated to bind to mitochondrial proteins causing disruption of cellular processes and activation of cell death pathways. While irreversible binding and the modification of cellular proteins by electrophilic reactive metabolites is undoubtedly important in eliciting the toxicity of some drugs, the usefulness of *in vitro* irreversible binding

data to predict the toxicity is debated (Nakayama et al. 2009, Obach et al. 2008, Usui et al. 2009). Although a definitive link between the bioactivation of paracetamol, the resulting irreversible binding and hepatotoxicity has been well established it is not so clear cut for other compounds. In fact the regioisomer of paracetamol, 3'-hydroxyacetanilide, also undergoes bioactivation to a reactive metabolite and displays irreversible binding, but is not hepatotoxic to mice. Irreversible binding studies in liver microsomes between hepatotoxic and non-hepatotoxic drugs shows that irreversible binding alone cannot distinguish between the hepatotoxic and non-hepatotoxic compounds. In fact a study by Obach *et al* showed that the non-hepatotoxin diphenhydramine exhibits higher irreversible binding in human liver microsomes than nefazodone and the hepatotoxin diclofenac (Obach et al. 2008). Separation of the groups of compounds cannot be improved by UDPGA or GSH (Obach et al. 2008, Usui et al. 2009). Multiplication of the irreversible binding by daily dose of the compound improves the distinction between the hepatotoxic and non-hepatotoxic drugs, however, it is well documented that the dose of the drug is related to toxicity.

It must also be taken into account that liver microsomes do not possess a full complement of metabolising enzymes. Non-microsomal enzymes can play both a role in bioactivation and detoxification of reactive metabolites, as such, liver microsomes cannot always predict accurately how a drug will be metabolised *in vivo*. For example, raloxifene undergoes CYP450 3A4 mediated bioactivation of its phenolic groups *in vitro* to yield a reactive quinoid species (Chen et al. 2002). *In vivo*, however, glucuronidation of the phenolic groups in the gut and liver contributes to the principal elimination mechanism of raloxifene (Dalvie et al. 2008). This may explain the low levels of idiosyncratic toxicity observed with raloxifene.

From this data included in this chapter we can begin to build a decision tree similar to those that are used in industry (figure 2.14). Both of these compounds demonstrate significant NADPH-dependent binding when compared to control values, however there is a difference in GSH conjugation and dose. Whilst nefazodone forms GSH conjugates which are indicative of bioactivation, whilst buspirone does not, it could be argued that nefazodone has a clear detoxification pathway via GSH, whereas buspirone irreversibly binds without a clear detoxification method present. Dose must also be taken into account when making any such decisions. The highest dose recommended for use with nefazodone is 10-fold that of buspirone and therefore it is more likely that buspirone would be taken forward into further testing from these investigations. However, based on this data nefazodone would still likely proceed with caution as the dose started on is much lower and a decision cannot be made on irreversible binding alone.

In conclusion, nefazodone demonstrated both reactive metabolite formation to quinone-imines and irreversible binding in liver microsomes. On the other hand although buspirone exhibited significant irreversible binding this was small in comparison to nefazodone and no GSH conjugates of buspirone were identified. This implies that bioactivation of nefazodone is responsible for its toxicity, however, a definitive link between irreversible binding and toxicity cannot be determined from liver microsomes alone. To investigate the relationship between bioactivation of

Nefazodone and buspirone: reactive metabolite formation and irreversible binding in liver microsomes

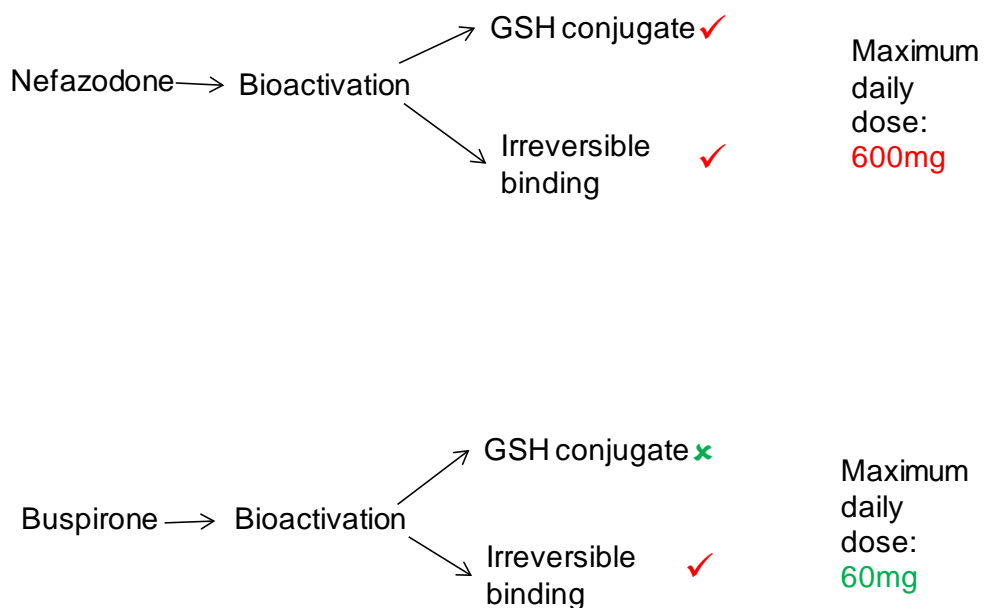


Figure 2.14. Overview of bioactivation of buspirone and nefazodone in rat liver microsomes.(DeLeve, Kaplowitz 1991)(DeLeve, Kaplowitz 1991)

nefazodone and cytotoxicity, the next chapter (chapter 3) will employ the use of primary rat and human hepatocytes. This will provide a complete set of metabolising enzymes to explore bioactivation of irreversible binding to a further extent, alongside the assessment of cytotoxicity

CHAPTER 3

NEFAZODONE AND BUSPIRONE: REACTIVE
METABOLITE FORMATION AND TOXICITY TO
HEPATOCYTES

3.1 INTRODUCTION.....	78
3.2 MATERIALS AND METHODS.....	80
3.2.1 Materials	80
3.2.2 Rat Hepatocyte isolations	80
3.2.3 Rat hepatocyte incubations	81
3.2.4 Irreversible binding in rat hepatocytes.....	82
3.2.5 Human hepatocyte isolations	82
3.2.6 Human hepatocyte incubations.....	82
3.2.7 Buspirone LC-MS method	83
3.2.8 Nefazodone LC-MS method	83
3.2.9 Cellular GSH determination	84
3.2.10 Protein determination	84
3.2.11 Cultured hepatocyte isolation	84
3.2.12 Cellomics analysis	85
3.2.13 Animal Work	85
3.2.14 Human Ethics Approval.....	86
3.2.15 Statistical analysis	86
3.3 RESULTS.....	86
3.3.1 Metabolism of buspirone in freshly isolated rat hepatocytes.....	86
3.3.2 The metabolism of nefazodone in freshly isolated rat hepatocytes	94
3.3.3 The metabolism of nefazodone in freshly isolated human hepatocytes.....	98
3.3.4 Effect of ABT on nefazodone metabolism in human hepatocytes	104
3.3.5 Effect of nefazodone and buspirone on cellular toxicity and GSH levels in rat hepatocytes.....	107
3.3.6 The effect of ABT on nefazodone cytotoxicity in freshly isolated rat hepatocytes	110
3.3.7 Irreversible binding in freshly isolated rat hepatocytes	112
3.3.8 The effect of ABT on toxicity and irreversible binding of nefazodone in freshly isolated rat hepatocytes	115
3.3.9 Cytotoxicity of nefazodone and buspirone in cultured rat hepatocytes using Cellomics technology	117
3.3.10 Cytotoxicity of nefazodone in freshly isolated human hepatocytes	122
3.3.11 Comparison of nefazodone toxicity in human and rat hepatocytes	122
3.4 DISCUSSION.....	125
3.4.1 Metabolism	125

3.4.1.1 Reactive metabolite formation and GSH depletion.....	125
3.4.1.2. Irreversible binding	128
3.4.4 Mitochondrial toxicity.....	130
3.4.3 BSEP inhibition	131
3.4.4 Conclusion.....	132

3.1 INTRODUCTION

The previous chapter identified that nefazodone metabolites irreversibly binds to protein and that this was significantly reduced when GSH was included in the incubation. GSH adducts of nefazodone were also identified in RLMs, therefore, identifying reactive metabolite formation as a potential cause of nefazodone hepatotoxicity. In contrast to buspirone, irreversible binding was 9-fold lower than nefazodone and no GSH conjugates of buspirone were identified, providing evidence of the possibility that the differing bioactivation potentials of nefazodone and buspirone are responsible for their different safety profiles. This has led to the hypothesis that reactive metabolite formation and irreversible binding are responsible for the differences in nefazodone and buspirone toxicity.

The clearance of nefazodone is principally through hepatic and intestinal metabolism by CYP450 3A4 (Rotzinger, Baker 2002b, Mayol et al. 1994). Nefazodone is extensively metabolised to a number of hydroxy metabolites, and it has been shown that following *para*-hydroxylation, nefazodone can undergo bioactivation to a quinone-imine reactive metabolite species (Kalgutkar et al. 2005b, Bauman et al. 2008b, Argoti et al. 2005). It has also been demonstrated that nefazodone irreversibly binds to liver S9 fraction and human hepatocytes (Bauman et al. 2009). Although in the previous chapter we concentrated on the GSH adducts of nefazodone evidence has been presented to suggest that nefazodone forms an iminium ion as several adducts of nefazodone have been identified using cyanide trapping (Argoti et al. 2005). However, there are other proposed mechanisms in the literature that suggest that the parent compound was the cause of hepatotoxicity in patients taking nefazodone. Indeed, Dykens *et al*, 2008 (Dykens et al. 2008) demonstrated that

nefazodone could elicit its toxicity through inhibition of complex I of the oxidative phosphorylation chain causing a collapse of the mitochondrial membrane potential and Kostrubsky *et al*, 2006 (Kostrubsky *et al*. 2006) have shown that nefazodone inhibits its own excretion into the bile through the bile salt export pump (BSEP) causing an accumulation, not only of nefazodone, but also of toxic bile salts in the liver. In neither case did the metabolism of the compound make it more toxic.

Buspirone, an anti-anxiety drug introduced in the 1980s, is also metabolised by CYP450 3A4 (Zhu *et al*. 2005) to several hydroxy metabolites and like nefazodone has the potential to undergo *para*-hydroxylation that can lead to the formation of a quinone-imine reactive metabolite species. However, unlike nefazodone, buspirone has not been associated with any reported cases of organ-directed toxicity and studies have not identified a buspirone reactive metabolite (Kalgutkar *et al*. 2005b). Despite this both nefazodone and buspirone have been reported to irreversibly bind to human hepatocytes at similar levels (Bauman *et al*. 2009, Obach *et al*. 2008) and the result of this study suggested that it is the differing daily dose, the recommended nefazodone dose (up to 600mg a day) being 10 times the daily dose of buspirone (up to 60mg a day), that results in their differences in toxicity.

Due to the conflicting arguments in the literature about the production of reactive metabolites and their link to toxicity, the irreversible binding and metabolism of nefazodone was investigated to try and provide a definitive link between reactive metabolite formation and the hepatotoxicity of nefazodone.

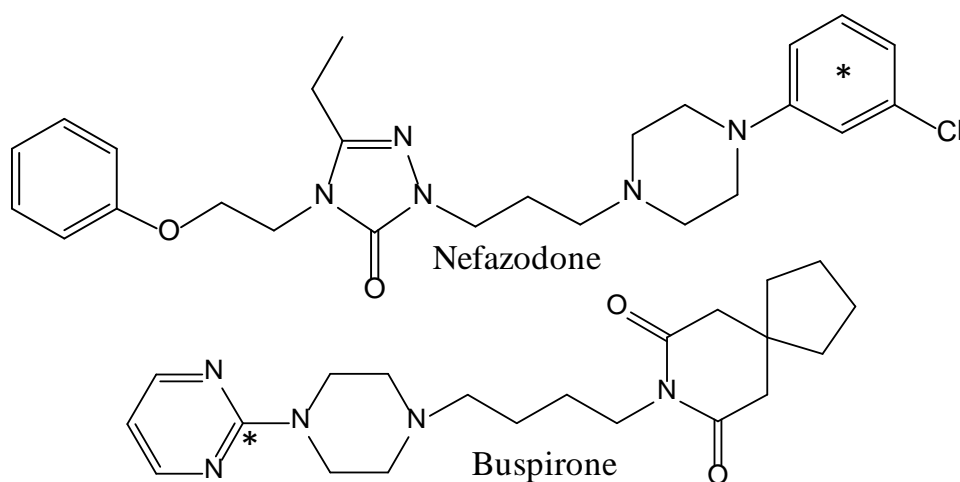


Figure 3.1 Chemical structures of nefazodone and buspirone. * Indicates the position of the radiolabel.

3.2 MATERIALS AND METHODS

3.2.1 Materials

Nefazodone was kindly purchased by Pfizer from Bosche Scientific (New Jersey, USA). Buspirone and methapyrilene were purchased from Sigma Aldrich (Poole, UK). [^{14}C] radiolabels were provided by Pfizer. Collagenase was purchased from Roche (UK). CellTiter-Glo® Luminescent Cell Viability (ATP) Assay was purchased from Promega (UK). All other reagents were purchased from Sigma-Aldrich (Poole, UK) unless otherwise stated. Solvents were purchased from Fischer Scientific and were all at least HPLC grade. Animals were purchased from Charles River (UK).

3.2.2 Rat Hepatocyte isolations

Rat hepatocytes were isolated as previously described by Williams *et al* (2007)(Williams et al. 2007). Male Wistar rats were anaesthetised using sodium pentobarbital (60mg/ml 1 μ l/g i.p). The hepatic portal vein was cannulated and the liver was perfused for 9 mins at a constant flow rate of 40 ml/min with a wash buffer

containing Hanks' balanced salt solution, 5.8mM HEPES and 4.5mM NaHCO₃. The wash step was followed by a collagenase perfusion using wash buffer with 5mM CaCl₂, 0.5mg/ml Collagenase A and 0.072 mg/ml trypsin inhibitor until the liver was visually judged to be digested. All wash and digestion solutions were kept at 37°C throughout the perfusion. The liver was then excised and the liver capsule removed to release the cells. The cells were then re-suspended in 50ml of wash buffer supplemented with DNase I (0.1mg/ml) and filtered through 125µm nylon mesh. The cell suspensions were then left to settle for 10 min on ice before the supernatant was removed. The cells were re-suspended in wash-DNase I and centrifuged at 50g for 2 mins. This was repeated twice more with wash buffer alone. The cells were re-suspended in incubation buffer (wash buffer with 1mM MgSO₄·7H₂O). Hepatocyte viability was assessed by trypan blue exclusion and only used when viability was greater than 80%.

3.2.3 Rat hepatocyte incubations

Experimental hepatocyte incubations contained a total volume of 6ml with a concentration of 2x10⁶cells/ml. For dose response studies there was a final concentration range of 0-500µM nefazodone or buspirone. For studies investigating the effect of 1-aminobenzotriazole (ABT) hepatocytes were incubated with 0-200µM final concentration of nefazodone or buspirone following pre-incubation for 30 minutes with ABT (1mM). Hepatocytes were incubated for 6 hours at 37°C, under normal atmospheric conditions and 180rpm. Viability was assessed using trypan blue exclusion and ATP assay. Samples (1ml) were also taken to determine cellular GSH content. Remaining hepatocyte suspension was quenched with an equal volume of ice-cold methanol for metabolism.

3.2.4 Irreversible binding in rat hepatocytes

Hepatocytes were incubated (as above) with 200µM cold drug and 0.1µCi [¹⁴C] nefazodone or buspirone for 0, 0.5, 1, 2, 4 or 6 hours and cells were then processed as above. Remaining hepatocyte suspension was used for analysis of irreversible binding.

3.2.5 Human hepatocyte isolations

Liver tissue from patients that had undergone liver resection was washed with 1-2L of 1x HEPES buffer at 50-75ml/min with no re-circulation. The liver was then perfused with re-circulated collagenase perfusion for approximately 20 minutes until the liver was soft and hepatocytes could be easily removed from the liver. The hepatocytes were then filtered through a 125µM nylon mesh. The cells were then washed 3 times in ice-cold William's E media before being transferred to incubation buffer and washed twice more. Cells were used for incubations if viability, as assessed by trypan blue, was greater than 90%.

3.2.6 Human hepatocyte incubations

Human hepatocytes were incubated with 0-200µM nefazodone for 6 hours in incubation buffer. After 6 hours viability, GSH content and metabolism was assessed. Cells were only used at 6 hours if control viability was greater than 60%. For ABT incubations, hepatocytes were pre-incubated at 37°C for 30mins, before addition of either 100 or 200µM nefazodone.

Patient number	Sex	Age	Medications (excluding chemotherapy)	Chemotherapy
3	M	73	Tamsulosin/heparin	Capecitabine, oxaliplatin, irinotecan, cetuximab
4	F	51	-	-
6	M	73	Atenolol	Capecitabine, oxaliplatin
9	M	53	Valproate/simvastatin/salmeterol/salbutamol	-

Table 3.1. Donor information for human hepatocyte incubations. Human hepatocyte donors were all undergoing liver resection for hepatic cancer. Healthy liver tissue removed during resections was used to isolate hepatocytes.

3.2.7 Buspirone LC-MS method

LC-MS/MS analysis was performed on an API 2000. The LC system consisted of an Agilent Eclipse XDB C18 column (4.6x150mm, 5 μ). The aqueous phase was 15mM ammonium formate (A). The organic solvent (B) was acetonitrile (ACN). A gradient separation was used starting initially with 10% B rising to 30% B over 35 minutes and held at 30% for 5 minutes. 25 μ l of sample was injected onto the column. The ion-spray was operated at +5000 v and a temperature of 400°C. MS/MS was used to extract ions according to m/z found in Kerns *et al*, 1997.

3.2.8 Nefazodone LC-MS method

The LC system consisted Phenomenex Luna phenyl-hexyl column (4.6x100mm, 5 μ) with a Perkin Elmer pump and autosampler attached to an API2000 mass spectrometer. The mobile phase consisted of 15mM ammonium formate (A) and

ACN (B). A gradient separation was run beginning at 5% B and rising to 70% B over 25 minutes, the gradient returned to 5% B over the next minute and then ran at 5% B until 30 minutes.

3.2.9 Cellular GSH determination

Hepatocytes were spun at 1000rpm for 2 minutes and the supernatant was removed and discarded. The pellet was lysed with 10mM HCl and vortexed. A fifth was removed to be kept for protein determination and replaced with 6.5% 5'-sulfosalicylic acid (SSA) to precipitate the protein. After 10 minutes on ice the samples were spun for 5 minutes at 14,000rpm and the supernatant kept for analysis. The GSH content was measured as according to Vandeputte *et al* (Vandeputte et al. 1994) and was measured at a wavelength of 412nm. Standards ranged from 0-40 nmol/ml. GSH content was normalised to protein content of the cell.

3.2.10 Protein determination

Protein content was determined using a Lowry assay (LOWRY et al. 1951) as in chapter 2.

3.2.11 Cultured hepatocyte isolation

Hepatocytes for cell culture were isolated from male Han Wistar rats weighing between 200-350g. Rats were anaesthetised using isoflurane in an induction chamber before being moved to a nose cone for maintenance. A V-shaped incision was made in the abdomen and the guts moved to one-side. A loose tie was placed around the portal vein before the diaphragm was cut. A cannula was placed in the hepatic portal vein and tied in place before the removal of the heart to allow free loss of perfusion buffers. The liver was perfused with HBSS (-CaCl₂/-MgCl₂) at a flow rate of

25ml/min until the liver was completely blanched and free of blood. The liver was then perfused with digestion media (HBSS with 5mM CaCl₂ and collagenase type II) until visually well digested, before being removed and placed in collection media (HBSS with 5mM CaCl₂ and 10,000U DNase). Hepatocytes were teased from the liver using a scapel blade into media containing DNase and filtered through a 100µ mesh. The hepatocytes were centrifuged a 30g for 5 minutes before being washed and spun again. The hepatocytes were then centrifuged at 60g for 10 minutes in a percoll gradient to separate the alive and dead cells. The cells were washed twice more in attachment media before being counted using a Guava machine. The cells were seeded at a density of 0.25x10⁶ cells/ml into collagen-coated 96-well plates in attachment media and placed in the incubator at 37°C/5% CO₂. After a minimum of 2 hours the attachment media was removed and replaced with basal media (no FBS). The cells were then left to settle before dosing.

3.2.12 Cellomics analysis

Hepatocytes were dosed with a final concentration of 0-100µM nefazodone or buspirone dissolved in 0.1% DMSO for 24, 48 or 72 hours. At each time point the media was removed and replaced with basal media containing Hoechst 33342 (1 in 10000), TMRM (1 in 200) and TO-PRO 3 iodide (1 in 1000). Plates were then returned to the incubator for 20 minutes to allow uptake of the dyes. The plates were then read using Cellomics technology.

3.2.13 Animal Work

All animal work was carried out according to local ethics policies and in accordance with home office regulation.

3.2.14 Human Ethics Approval

All work with human samples was carried out in accordance with local ethics policies.

3.2.15 Statistical analysis

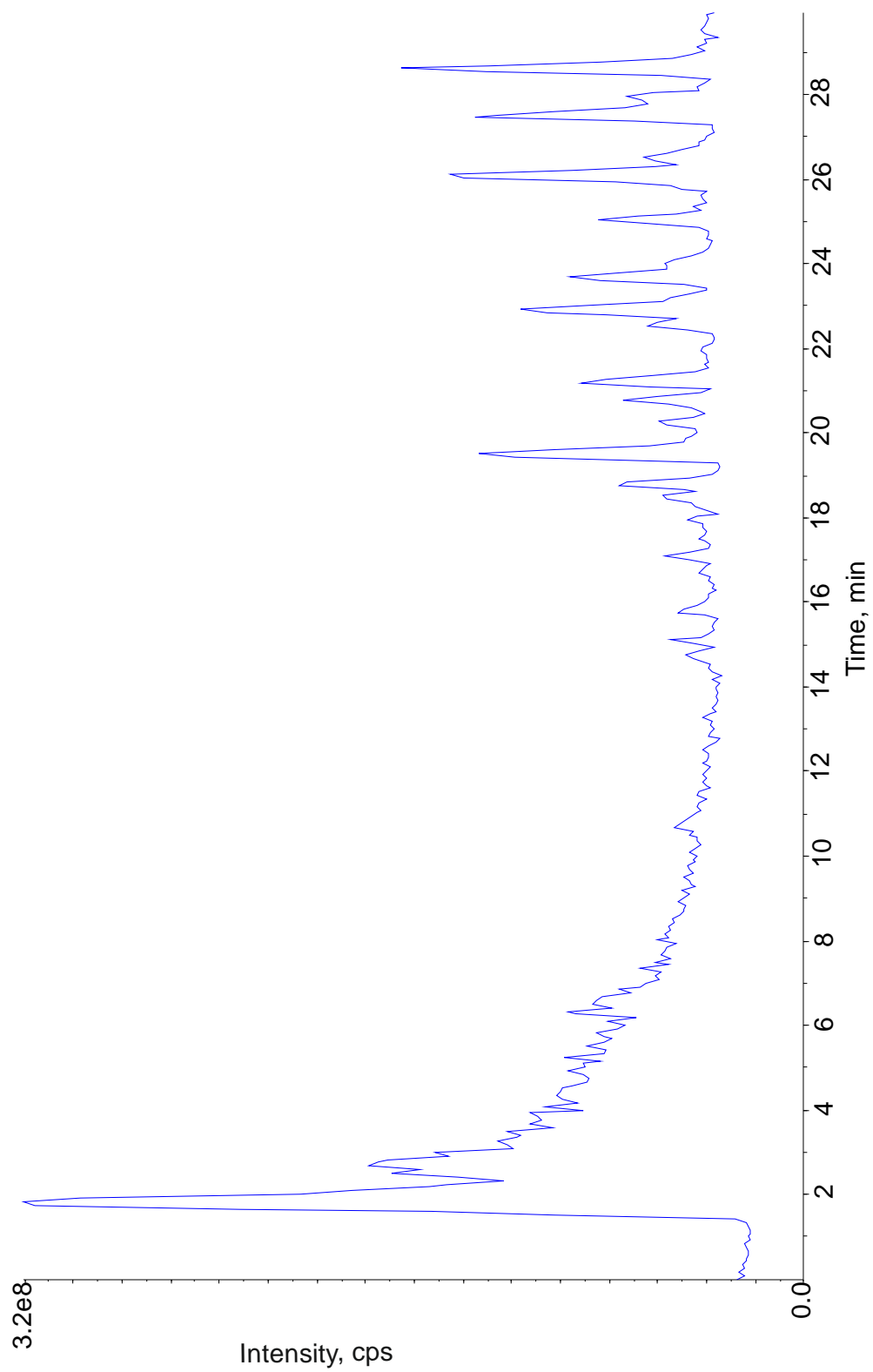
Statistical analysis was undertaken using Stats Direct software. Data was tested for normality using a Shapiro-Wilks test and either a Student's T test (parametric) or Mann-Whitney U test (non-parametric) was used to make comparisons between data sets. An ANOVA (Dunnett's comparison to control) was used to determine significance to control values.

3.3 RESULTS

3.3.1 Metabolism of buspirone in freshly isolated rat hepatocytes

The metabolism of 100 μ M and 200 μ M buspirone was investigated in rat hepatocytes in suspension. Identification of the metabolites of buspirone were based upon the previous work of Kerns et al (Kerns et al. 1997), who identified several buspirone metabolites in rat bile and urine and rat liver S9 preparations. Buspirone (m/z 386) exhibited extensive turn over in rat hepatocytes to several phase I and II metabolites through hydroxylation, *N*-dealkylation, catechol *O*-methylation and glucuronidation. Several [O] buspirone, m/z 402 (figure 3.3) and [2O] buspirone, m/z 418 were identified. The fragment ions of these metabolites indicated that hydroxylation occurred on both the azaspirone and pyrimidinyl moieties, a shift of m/z 123 to m/z 139 indicating hydroxylation on the azaspirone structure and a shift of m/z 122 to m/z 138 indicating hydroxylation on the pyrimidine structure. Buspirone was also turned over to several [2O, OCH₃] metabolites (m/z 448), thought to be formed

through the sequential hydroxylation and *O*-methylation of the buspirone molecule. Buspirone also underwent *N*-dealkylation reactions to 1-pyrimidinyl-piperazine (*m/z* 165), despyrimidinyl buspirone (*m/z* 308) and despyrimidinyl piperazine buspirone (*m/z* 254). Phase II reactions consisted mainly of glucuronidation reactions (fig 3.4), confirmed by neutral loss of 176 amu. [O] buspirone glucuronide (*m/z* 578) , [2O] buspirone glucuronide (*m/z* 594), [O, OCH₃] buspirone glucuronide (*m/z* 608) and [2O, OCH₃] buspirone glucuronide (*m/z* 624) were all identified and corresponded with the phase I metabolites present. Despite hydroxylation of the pyrimidinyl moiety and therefore the possibility of para-hydroxy buspirone formation, no GSH conjugates of buspirone were identified. The AUC values for each metabolite can be found in appendix III.



Name	m/z	Retention time
1-pyrimidinylpiperazine	165	6.36
[2O] buspirone glucuronide	594	14.8
[2O, OCH3] buspirone glucuronide	624	16.5
[2O] buspirone glucuronide	594	17.1
[2O] buspirone	418	17.5
[2O] buspirone	418	18
[2O] buspirone	418	18.5
[2O, OCH3] buspirone glucuronide	624	18.8
[2O] buspirone	418	18.9
[2O] buspirone glucuronide	594	19.6
[2O, OCH3] buspirone	448	19.8

[2O] buspirone	418	20.2
[O] buspirone	402	20.8
[2O, OCH3] buspirone	448	20.9
[2O, OCH3] buspirone glucuronide	624	21.1
[O] buspirone	402	21.2
[2O] buspirone	418	22.6
[O] buspirone glucuronide	578	22.9
[O] buspirone	402	23.7
[O, OCH3] buspirone glucuronide	608	24.1
Despyrimidinyl buspirone	308	25
[2O] buspirone	418	25
[O, OCH3] buspirone	432	25.3
[O] buspirone	402	26.1

[O] buspirone	402	27.5
Despyrimidinylpiperazine	254	27.9
Buspirone	386	28.6

Table 3.2. Buspirone metabolites identified from rat hepatocyte incubations.

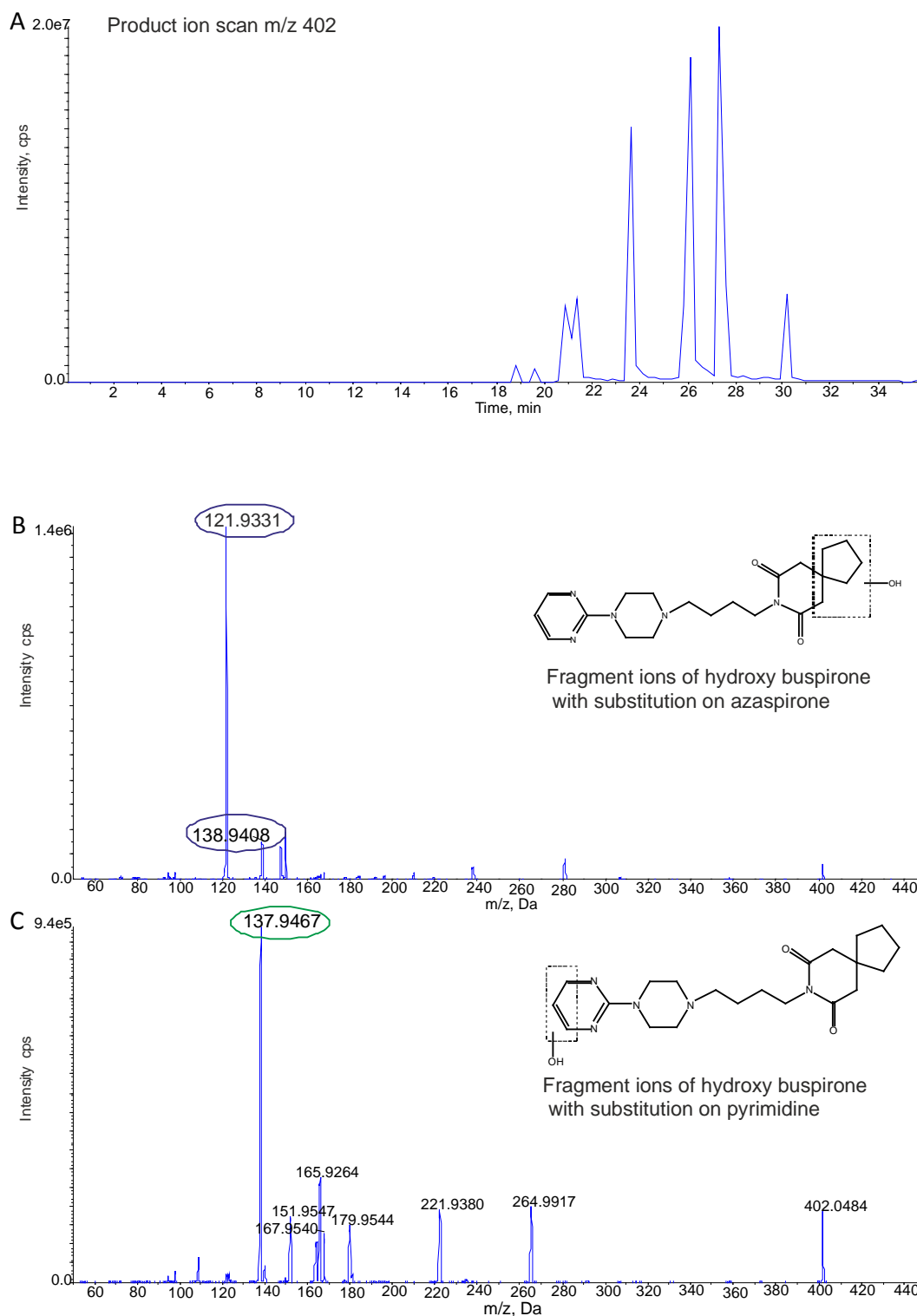


Figure 3.3 Product ion scan m/z 402 and fragment ions of [O] buspirone. (A) TIC for product ion scan of m/z 402. (B) Fragment ions of [O] buspirone substituted on the azaspirone moiety. Fragment ions related to the m/z 122 (unsubstituted pyrimidine) and m/z 139 (hydroxylated azaspirone moiety) are highlighted in purple. (C) Fragment ions of [O] buspirone substituted on the pyrimidine moiety. The fragment ion m/z 138 (hydroxylated pyrimidine) is highlighted in green.

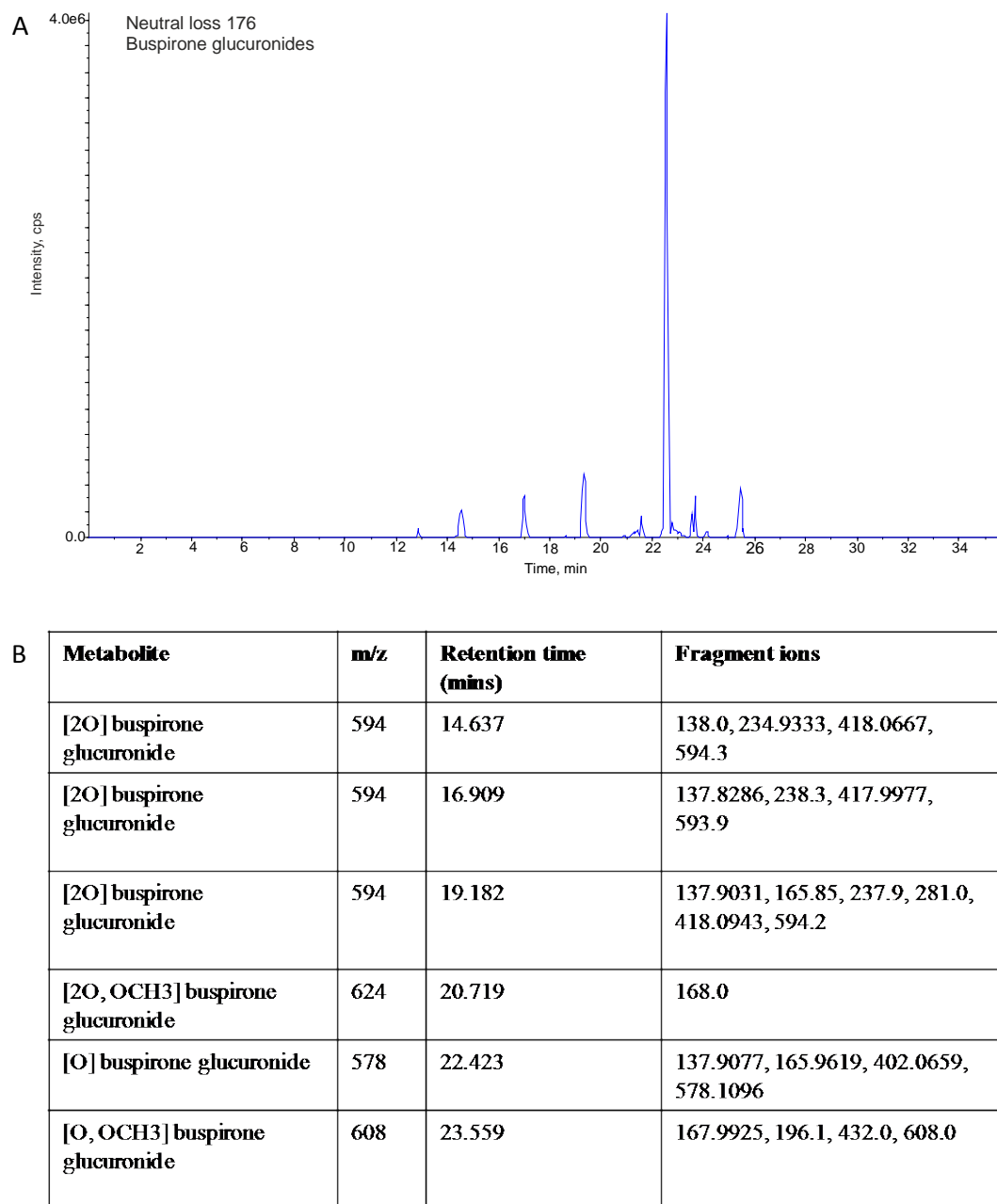
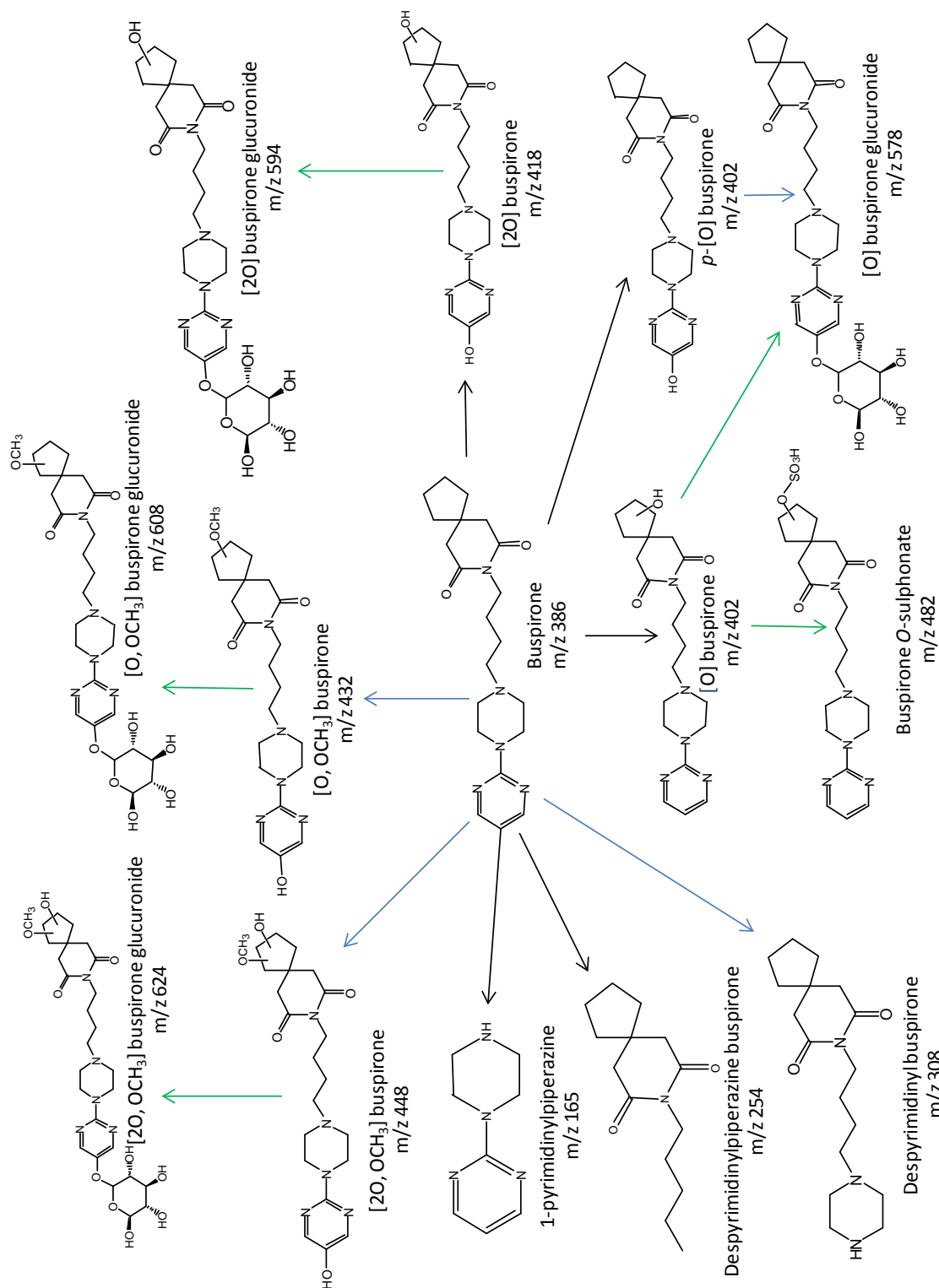


Figure 3.4. Glucuronide metabolites of buspirone in primary rat hepatocytes. (A) Neutral loss scans of 176u for identification of glucuronide metabolites. (B) Identified glucuronide metabolites and their fragment ions.



3.3.2 The metabolism of nefazodone in freshly isolated rat hepatocytes

In rat hepatocytes the metabolic profile of nefazodone was concentration dependent, with a different metabolism profile appearing with 100 μ M and 200 μ M incubations (figure 3.6). The major pathways of metabolism appear to be similar to buspirone and consist mainly of hydroxylation, *N*-dealkylation and glucuronidation. Hydroxy metabolites of nefazodone are particularly important to the theory that nefazodone causes toxicity through reactive metabolite formation, particularly those with a fragment ion of *m/z* 274 indicating an unsubstituted phenoxyethyl-triazolone-propyl moiety. A lack of hydroxylation of the phenoxyethyl-triazolone-propyl fraction (*m/z* 274) indicates that hydroxylation has probably occurred in the chlorophenylpiperazine ring and therefore hydroxylated metabolites with a fragment ion at *m/z* 274 may be *para*-hydroxylated and have the potential to form a reactive quinine-imine species. At 100 μ M nefazodone only one [O] nefazodone peak was prominent (peak 9) which appeared to consist of a mixture of at least two co-eluting [O] nefazodone metabolites, which yielded both the *m/z* 274 and *m/z* 290. In the 200 μ M incubations a second [O] nefazodone peak was also present that consisted only of the *m/z* 290 fragment indicating hydroxylation on the phenoxyethyl-triazolone-propyl moiety and, therefore, this metabolite is unlikely to undergo bioactivation. One of the [O] nefazodone metabolites underwent a sulphation reaction to yield an *O*-sulphonate metabolite (*m/z* 566) which gave a prominent peak in the 100 μ M sample (peak 7) but was less abundant at 200 μ M. The *O*-sulphonate yielded a fragment ion of *m/z* 274 indicating the presence of the unsubstituted phenoxyethyl-triazolone-propyl fragment. Two of the [O] nefazodone metabolites also underwent glucuronidation, forming peaks 3 and 4 (*m/z* 662). There were also two [2O] nefazodone metabolites which were prominent in both 100 μ M and 200 μ M

incubations (peaks 5 and 6). These both underwent glucuronidation to $[M+H]^+$ m/z 678, although glucuronidation appeared to be less in the 200 μ M incubations. Several carbonyl metabolites were also present. Phenoxy-triazolone carboxylic acid (peak 8) was a prominent peak in both 100 μ M and 200 μ M incubations but the triazolone ethylcarbonyl derivative (peak 12), a product of sequential hydroxylation and dehydrogenation was only found in the 200 μ M incubation. The di-oxygenated ($[O, =O]$) metabolite (m/z 500, peak 10) co-eluted with other metabolites but clearly displayed the phenoxyethyl-ketotriazolone-propyl fragment (m/z 288) and could be confirmed as a metabolite due to the characteristic double peak of ^{+35}Cl and ^{+37}Cl seen with chlorinated compounds. A deschlorophenyl metabolite (m/z 360) and 3-chlorophenylpiperazine (m/z 197) were also identified in both concentrations of hepatocyte samples, co-eluting with other metabolites in peaks 1 and 2, respectively. 3-chlorophenylpiperazine is also thought to be hydroxylated to a *para*-hydroxy metabolite, however $[O]$ 3-chlorophenylpiperazine was not identified in any of the rat hepatocyte samples. Whether this was due to the absence of the metabolite or because it was too polar to be detected was not determined. Unlike in RLM incubations (chapter 2) no GSH conjugates of nefazodone could be identified in rat hepatocyte isolations. There is a possibility that this is due to the high turnover of nefazodone to glucuronides and sulphonates in hepatocytes and GSH conjugates are not formed in the same manner as in RLM incubations where GSH is the only phase II reaction available. Table 3.3 details the metabolites identified in rat hepatocytes dosed with 200 μ M nefazodone and a metabolic scheme in figure 3.7 and appendix IV contains the AUC of each nefazodone metabolite.

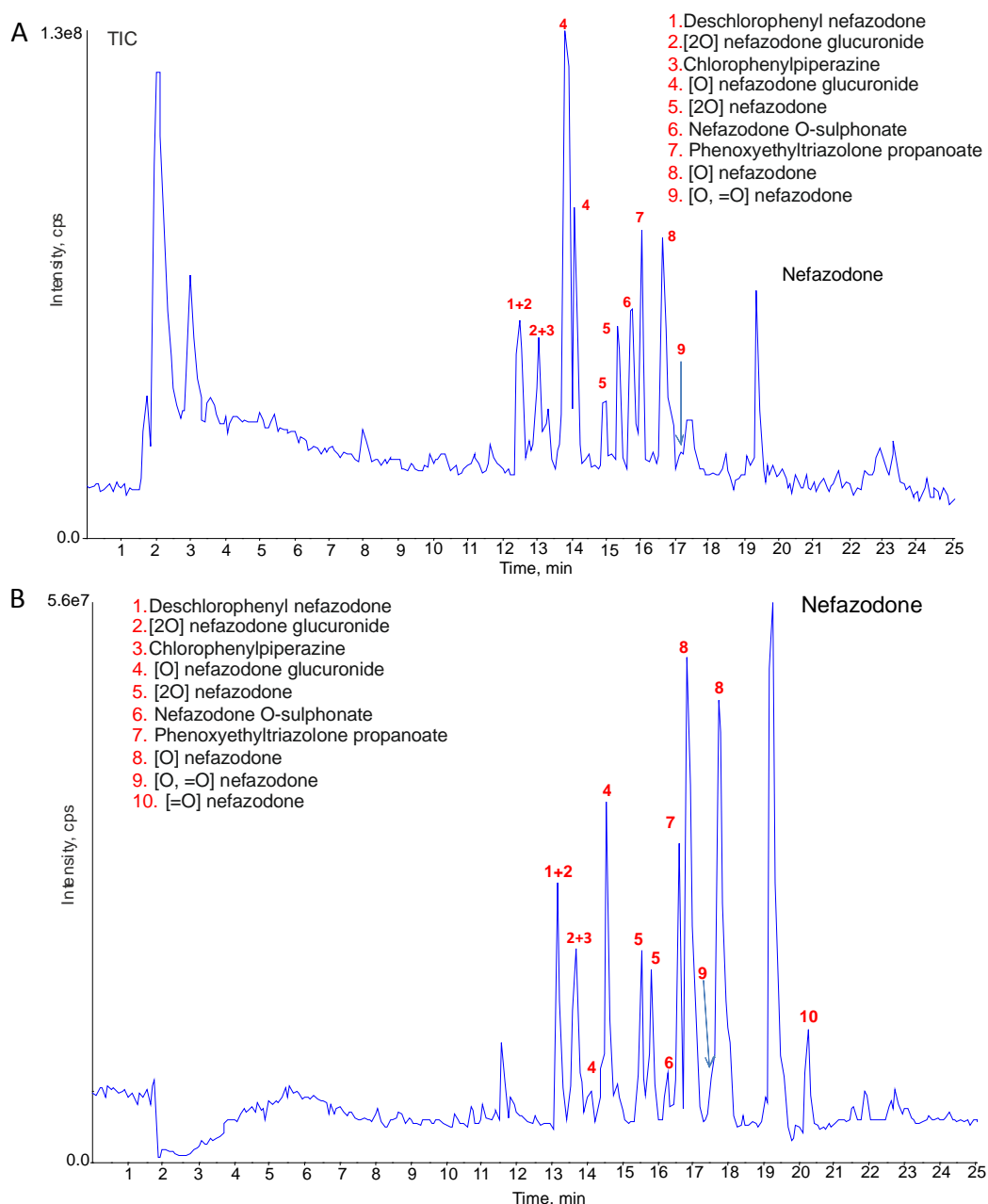
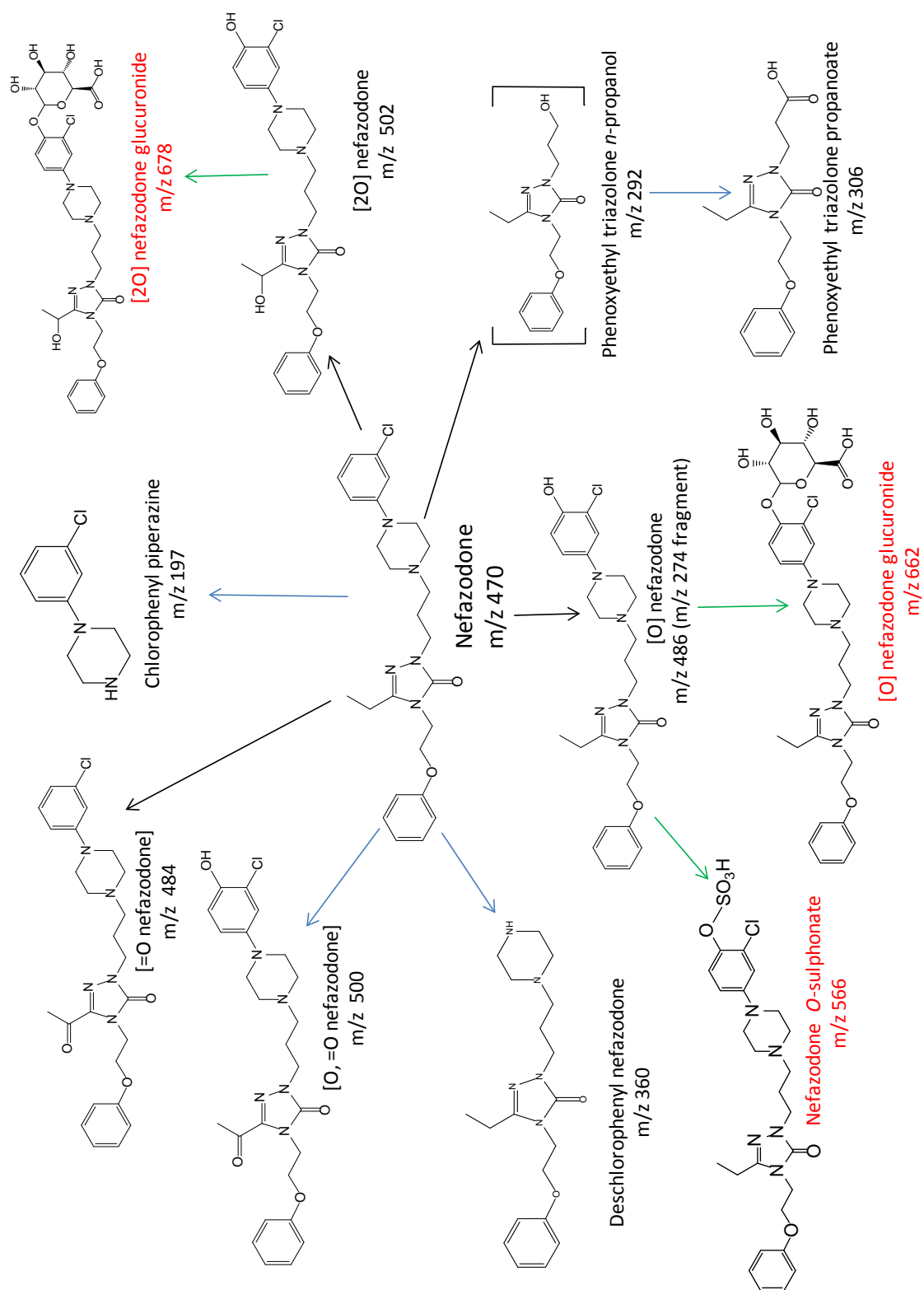


Figure 3.6. Representation of the total ion current of (A) 100 μ M and (B) 200 μ M nefazodone in freshly isolated rat hepatocytes.

Number	Name	m/z	Retention (mins)	time
1	Deschlorophenyl nefazodone	360	13.18	
2	[2O] nefazodone glucuronide	678	13.31	
2	[2O] nefazodone glucuronide	678	13.67	
3	Chlorophenylpiperazine	197	13.66	
4	[O] nefazodone glucuronide	662	14.60	
4	[O] nefazodone glucuronide	662	14.61	
5	[2O] nefazodone	502	15.52	
5	[2O] nefazodone	502	15.84	
6	Nefazodone O-sulphonate	566	16.34	
7	Phenoxyethyltriazolone propanoate	306	16.61	
8	[O] nefazodone	486	16.68	
9	[O, =O] nefazodone	500	17.56	
8	[O] nefazodone	486	17.71	
Nefazodone	Nefazodone	470	19.24	
10	[=O] nefazodone	484	20.27	

Table 3.3. Metabolites of nefazodone in rat hepatocytes



3.3.3 The metabolism of nefazodone in freshly isolated human hepatocytes

The metabolism of nefazodone in human hepatocytes was extensive and as in the rat the metabolite profile was concentration dependent. The retention times of all the metabolites are summarised in table 3.4 and the AUC of each metabolite can be found in appendix V. Several differences existed between the turnover of nefazodone in rat and human hepatocytes (figure 3.8). The major difference between the incubations at 100 μ M nefazodone was a difference in the production of mono-oxygenated metabolites (m/z 486). Whereas rat hepatocytes produced 1 major and 3 minor metabolites corresponding to an m/z 486, human hepatocytes produced 3 major and 1 minor [O] nefazodone metabolite. This is also in contrast to HLMS where 3 [O] nefazodone metabolites were detected (chapter 2). The [O] nefazodone metabolites can be seen in figure 3.7. The most polar of the four [O] metabolites (I and II) produced a fragment ion with m/z 274 and the least polar [O] metabolites (III and IV) had the fragment ion m/z 290. The phase II metabolites of [O] nefazodone were much less prominent than in rat hepatocytes although the *O*-sulphonate (peak 11) and the two glucuronides (peaks labelled 7) were still present. Five di-oxygenated metabolites were identified consisting of 2 [2O] nefazodone and 3 [O, =O] nefazodone metabolites. There was also a glucuronide conjugate of [2O] nefazodone detectable. The 3 [O, =O] nefazodone metabolites are represented in figure 3.9. Metabolite I exhibited a fragment ion with an m/z of 288 representing phenoxyethyl-ketopropyl triazolone. Metabolite II only had a fragment ion present at m/z 274 indicating unchanged phenoxyethyl-propyltriazolone, whilst metabolite III had a fragment ion at m/z 304 indicating the presence of phenoxyethyl-oxyketopropyltriazolone following both hydroxylation and carbonyl formation on

the phenoxyethyl-propyltriazolone moiety. Unlike in rat hepatocytes a [3O] nefazodone metabolite was detected (m/z 518). The [3O] nefazodone metabolite had a fragment ion of m/z 290 indicating that only one of the hydroxylation reactions was present on the phenoxyethyl-propyl triazolone structure, but it could not be identified where the other hydroxylation reactions occurred based on the fragmentation pattern. As in rat hepatocyte isolations no GSH conjugates were identified in the human hepatocyte incubations.

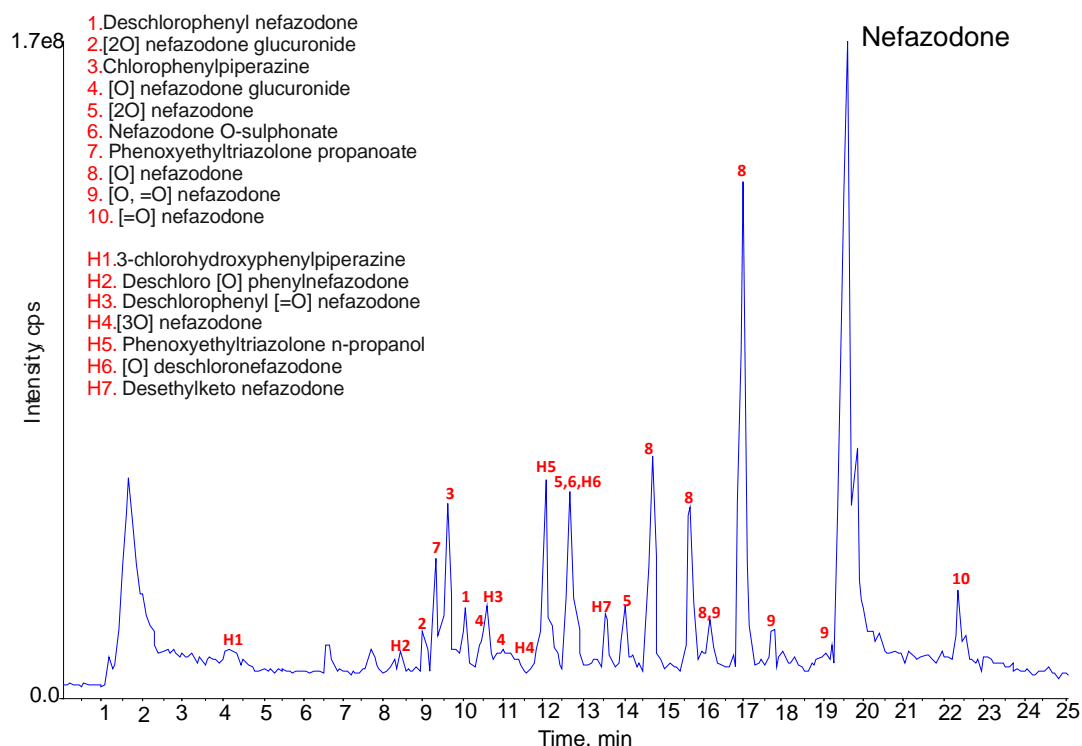


Figure 3.8. Total ion current of nefazodone and metabolites in freshly isolated human hepatocytes (from patient 3).

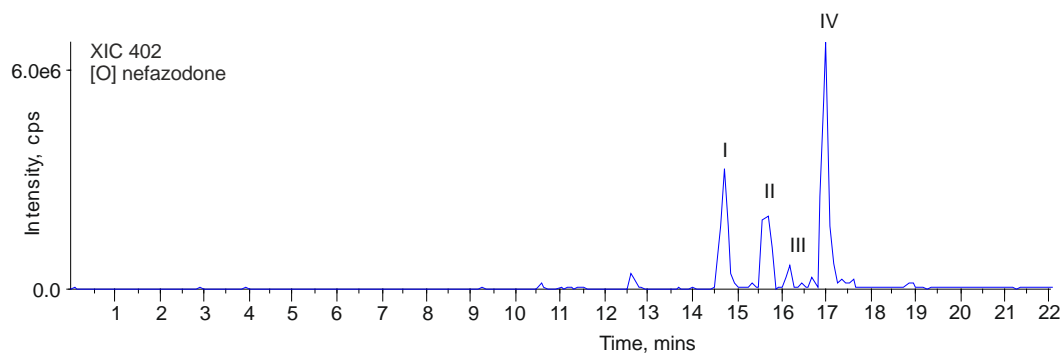


Figure 3.9. [O] nefazodone metabolites identified in human hepatocyte samples. Four [O] nefazodone metabolites were identified in patient samples. The most polar metabolites (I and II) produced the fragment ion m/z 274 indicating an unsubstituted phenoxyethyl-triazolone-propyl fragment, whilst the less polar metabolites (III and IV) displayed the fragment ion m/z 290 indicating oxidation of the phenoxyethyl-triazolone-propyl moiety.

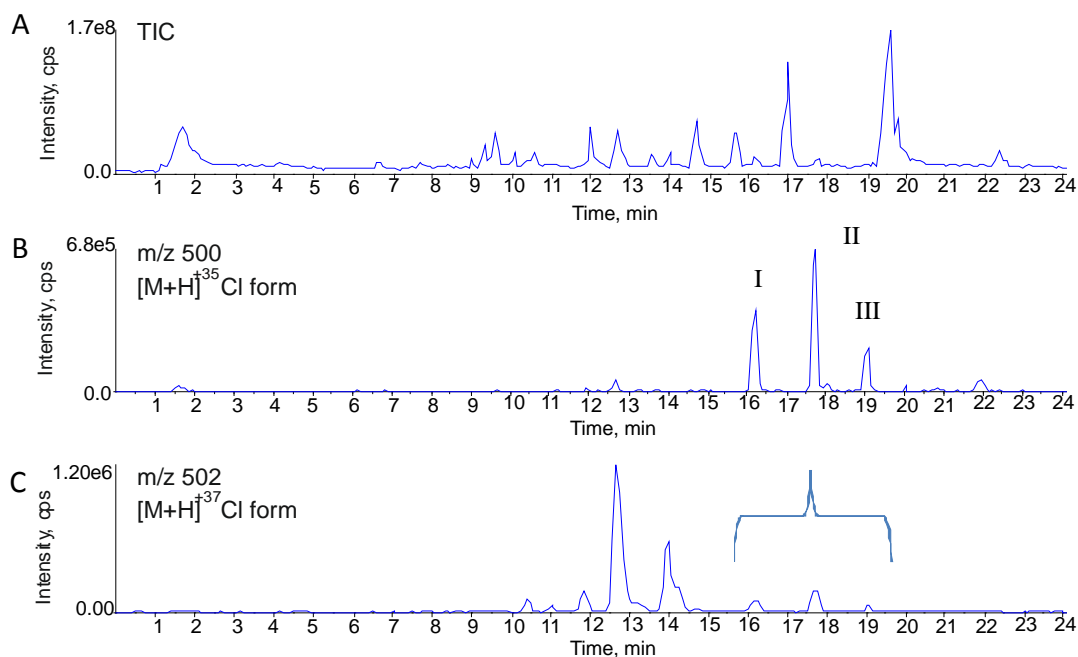
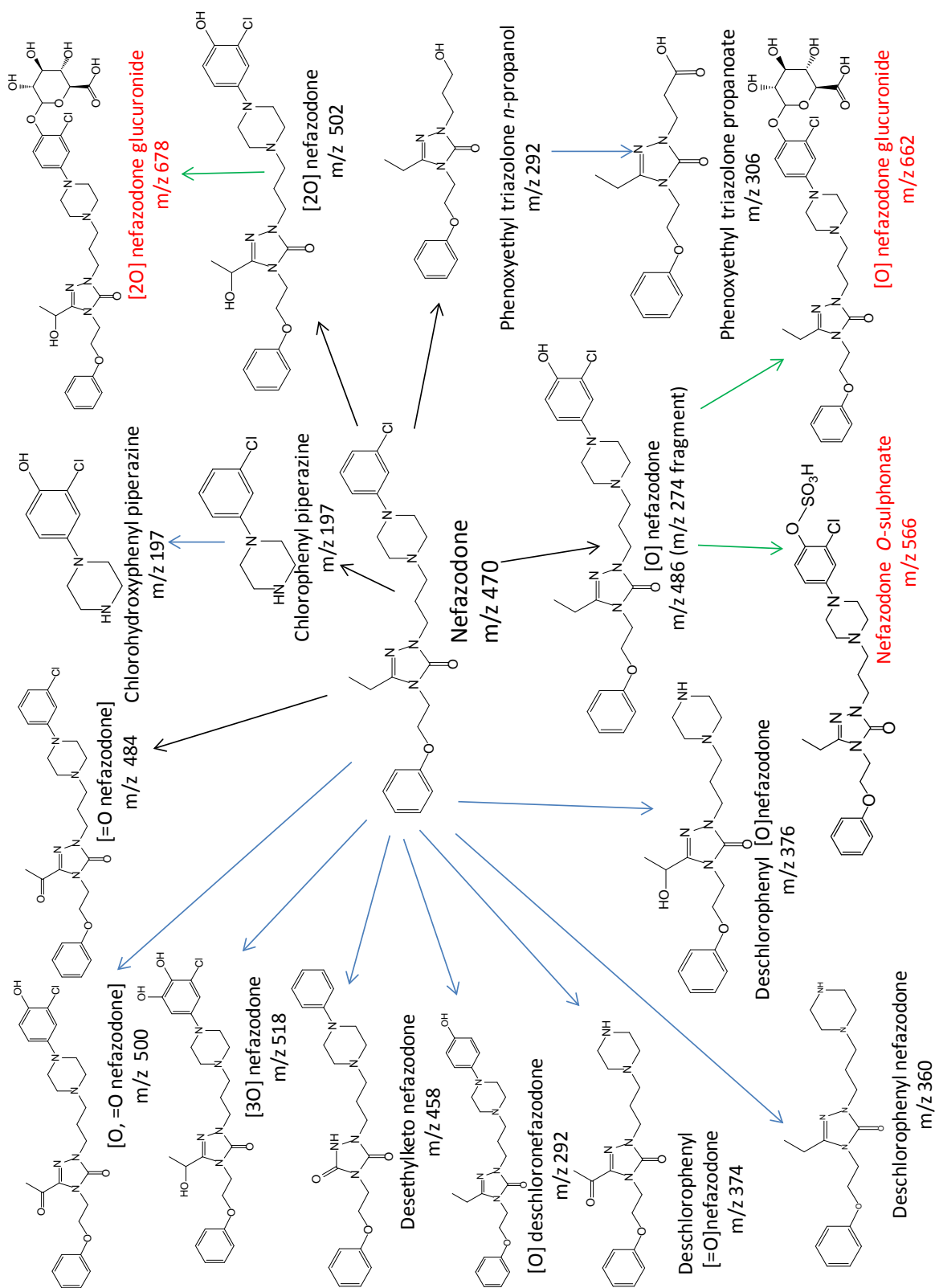


Figure 3.10. [=O,O] nefazodone metabolites identified in human hepatocyte samples. 3
[=O, O] nefazodone metabolites were identified in human hepatocyte samples. I demonstrated a fragment ion of m/z 288, II a fragment ion of m/z 274 and III a fragment ion of m/z 304. (A) Total ion current of nefazodone in human hepatocytes. (B) m/z 500 ^{+35}Cl form of [=O, O] nefazodone. (C) m/z 502 ^{+37}Cl form of [=O,O] nefazodone highlighted.

Number	Name	m/z	Retention time (mins)
H1	3-chlorohydroxyphenylpiperazine	213	4.25
H2	Deschloro [O] phenyl nefazodone	376	8.43
2	[2O] nefazodone glucuronide	678	9.08
7	Phenoxyethyltriazolone propanoate	306	9.34
3	Chlorophenylpiperazine	197	9.60
1	Deschlorophenyl nefazodone	360	10.09
4	[O] nefazodone glucuronide	662	10.58
H3	Deschlorophenyl [=O] nefazodone	374	10.69
4	[O] nefazodone glucuronide	662	11.18
H4	[3O] nefazodone	518	11.30
H5	Phenoxyethyltriazolone n-propanol	292	12.02
5	[2O] nefazodone	502	12.62
6	Nefazodone O-sulphonate	566	12.62
H6	[O] deschloronefazodone	451	12.78
H7	Desethylketo nefazodone	458	13.54
5	[2O] nefazodone	502	14.01
8	[O] nefazodone	486	14.68
8	[O] nefazodone	486	15.65

8	[O] nefazodone	486	16.17
9	[O, =O] nefazodone	500	16.23
8	[O] nefazodone	486	17.00
9	[O, =O] nefazodone	500	17.73
9	[O, =O nefazodone]	500	19.07
Nefazodone	Nefazodone	470	19.58
10	[=O] nefazodone	484	22.36

Table 3.4. Nefazodone metabolites identified in human hepatocyte isolations.



3.3.4 Effect of ABT on nefazodone metabolism in human hepatocytes

The pre-incubation of the hepatocytes with ABT effectively inhibited turnover of nefazodone, the major exception to this was [O] nefazodone I, which appears not be inhibited by ABT and was deemed not be a CYP450 3A4 mediated reaction, being catalysed by either an ABT insensitive CYP450 or another phase I metabolising enzyme.

3.3.5 Effect of nefazodone and buspirone on cellular toxicity and GSH levels in rat hepatocytes

A reduction in cellular GSH concentration can indicate the depletion of GSH through conjugation to reactive metabolites. If the cells are thought to be dying through depletion of GSH and exposure to covalent protein modification the cells exhibit a significant decrease in cellular GSH concentration before cell death occurs, however, cell death can also be the cause of GSH depletion as GSH leaks from dead cells. The trend in viability and GSH depletion for nefazodone and buspirone can be seen in figure 3.12. Both nefazodone and buspirone significantly deplete GSH, however, the trend in GSH depletion is very different. Nefazodone exhibits significant cell toxicity at 200 μ M after 6 hours, however, buspirone only begins to exhibit significant toxicity after reaching concentrations of 1mM, much higher than the 0.0045 μ M serum C_{\max} reached after a single dose of 20mg buspirone. Nefazodone did significantly deplete GSH but the depletion of GSH followed toxicity very closely and as a result of this trend it is likely that the GSH depletion seen with nefazodone is likely to be a consequence and not a cause of cell death. Unexpectedly, buspirone also significantly depleted GSH; however, this occurred in the absence of

cytotoxicity. This indicates that GSH depletion could be a potential mechanism for buspirone mediated cell death at high buspirone doses.

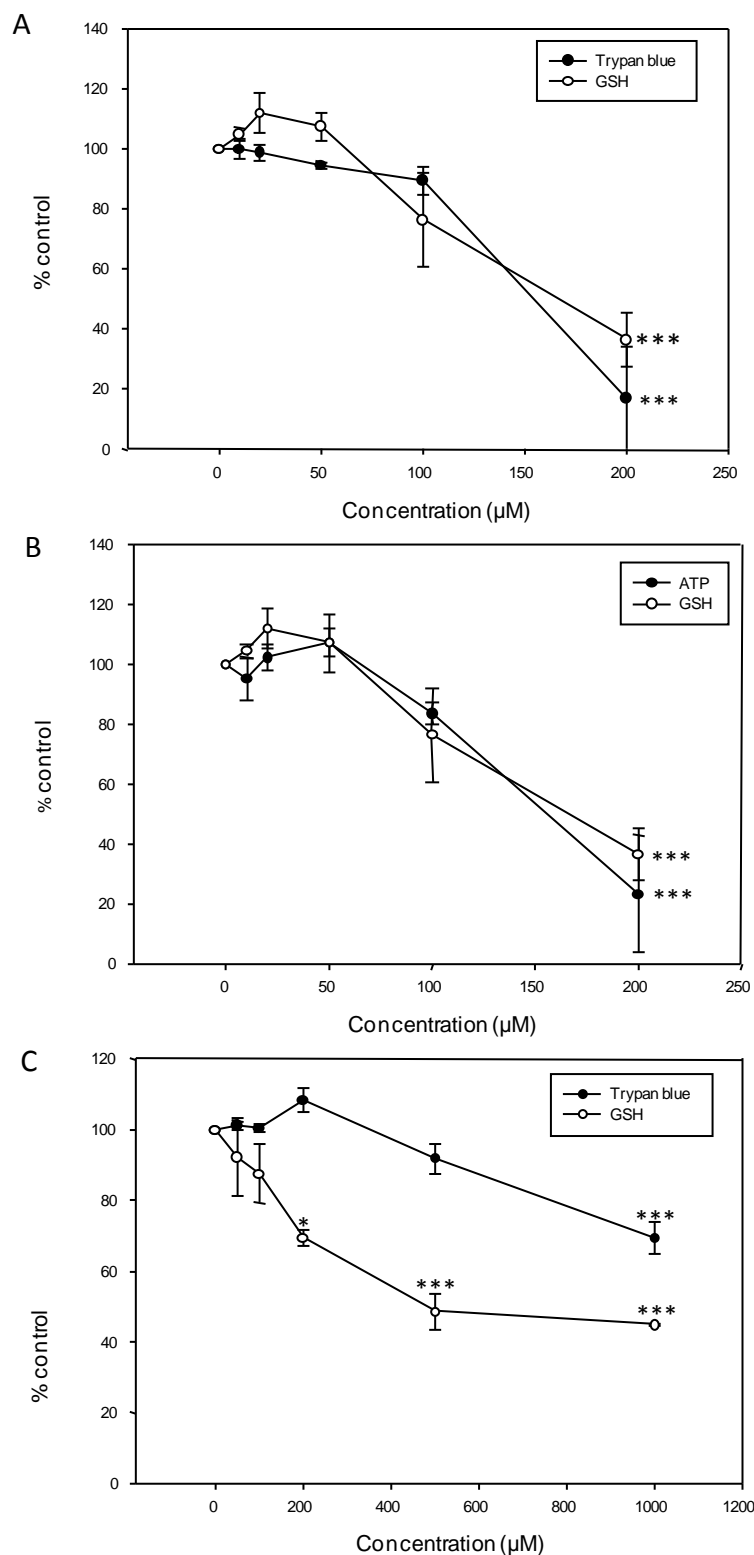


Figure 3.12. The effect of nefazodone and buspirone on cell viability and cellular GSH levels. Hepatocytes were dosed with 0-200μM nefazodone or buspirone for 6 hours and the viability was assessed for nefazodone using trypan blue exclusion (A) and cellular ATP content (B) and compared to cellular GSH levels. Buspirone (C) was assessed using trypan blue and compared to GSH. Both viability (●) and GSH levels (○) are expressed as % control values. Values are mean±SEM from 4 independent isolations. ***P<0.001determined using ANOVA (Dunnet's multiple comparison to control).

3.3.6 The effect of ABT on nefazodone cytotoxicity in freshly isolated rat hepatocytes

Incubations of nefazodone in the presence and absence of a 30 minute pre-incubation with ABT (1mM) demonstrated a decrease in cell viability determined by both trypan blue exclusion and cellular ATP content (figure 3.13). Cell viability was not significantly different in control incubations in the presence and absence of ABT, $99.5 \pm 2.33\%$ control and $94.5 \pm 10.5\%$ control for trypan blue exclusion and ATP content respectively. A significant decrease in cell viability was observed when hepatocytes were pre-incubated with ABT with both $20\mu\text{M}$ ($98.75 \pm 2.72\%$ control vs $88.25 \pm 1.55\%$ control), $50\mu\text{M}$ ($94.5 \pm 1.19\%$ control vs $79.75 \pm 2.56\%$ control) and $100\mu\text{M}$ ($89.5 \pm 4.59\%$ control vs $41 \pm 3.84\%$ control) using trypan blue exclusion and $50\mu\text{M}$ ($107.25 \pm 9.8\%$ control vs $74.25 \pm 4.66\%$ control) and $100\mu\text{M}$ ($83.75 \pm 3.7\%$ control vs $36.0 \pm 13.40\%$ control) using assessment of ATP content.

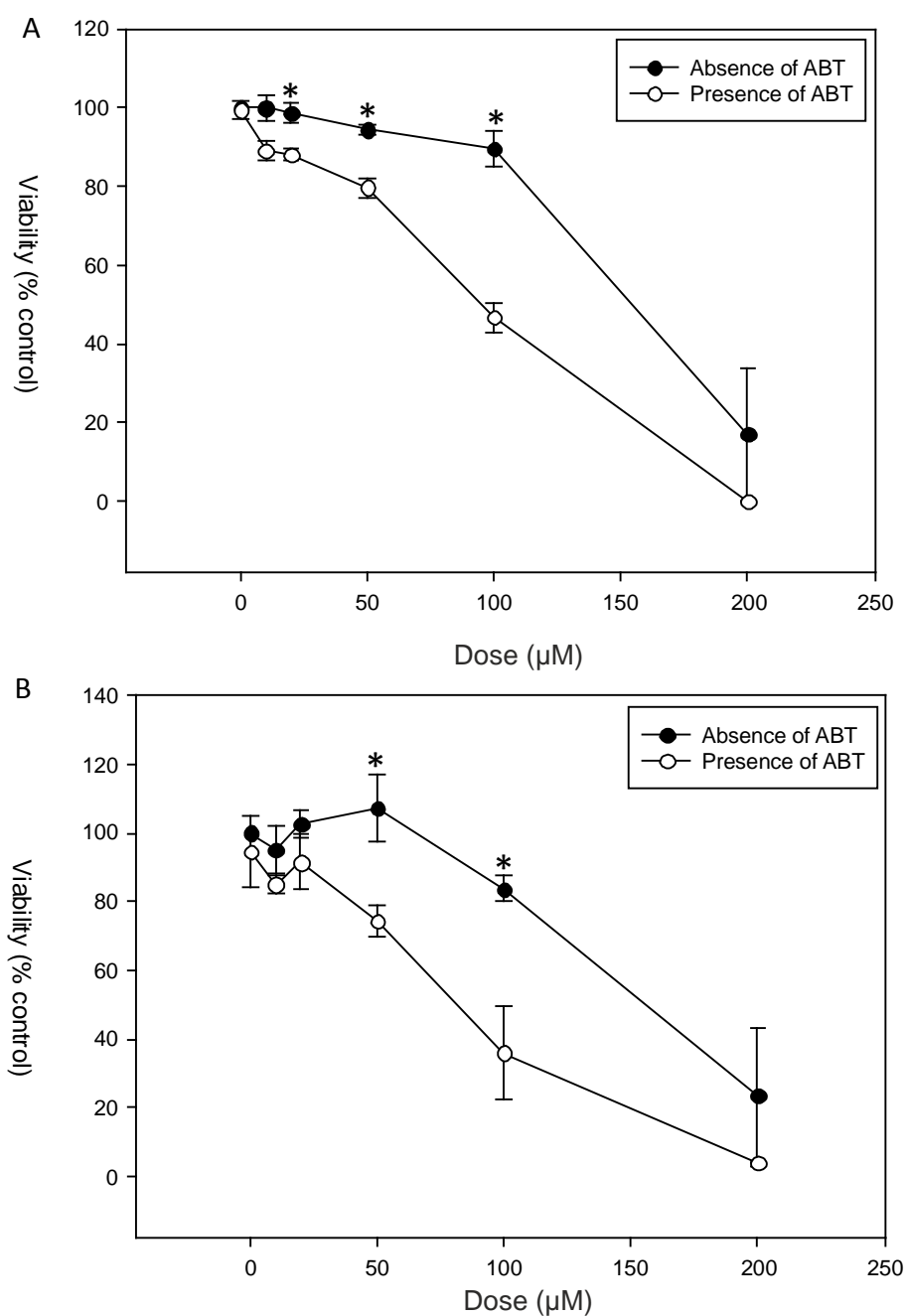


Figure 3.13. The effect of ABT on the toxicity of nefazodone in freshly isolated hepatocytes. Freshly isolated hepatocytes were incubated with 0-200μM nefazodone over 6 hours in the absence (●) and presence (○) of 1mM ABT and viability was determined using trypan blue exclusion (A) and cellular ATP content (B). Values are mean ± SEM from 4 independent isolations. *P<0.05 determined using a Mann Whitney U test.

3.3.7 Irreversible binding in freshly isolated rat hepatocytes

In freshly isolated rat hepatocytes both nefazodone and buspirone exhibited significant irreversible binding at 6 hours. Despite significant irreversible binding of buspirone at 6 hours there was no significant decrease in cell viability which was 99.33 ± 1.33 % control viability (figure 3.14). In contrast nefazodone exhibited significant irreversible binding (117.54 ± 15.32 pmol equiv./mg protein) and a significant decrease in cell viability (19.25 ± 18.26 % control viability) at 6 hours (figure 3.11). Surprisingly when a comparison between the irreversible binding of nefazodone and buspirone was carried out there was no significant difference between the irreversible binding at any time point, despite a significant difference in cytotoxicity elicited by the two drugs from 2 hours onwards (figure 3.15).

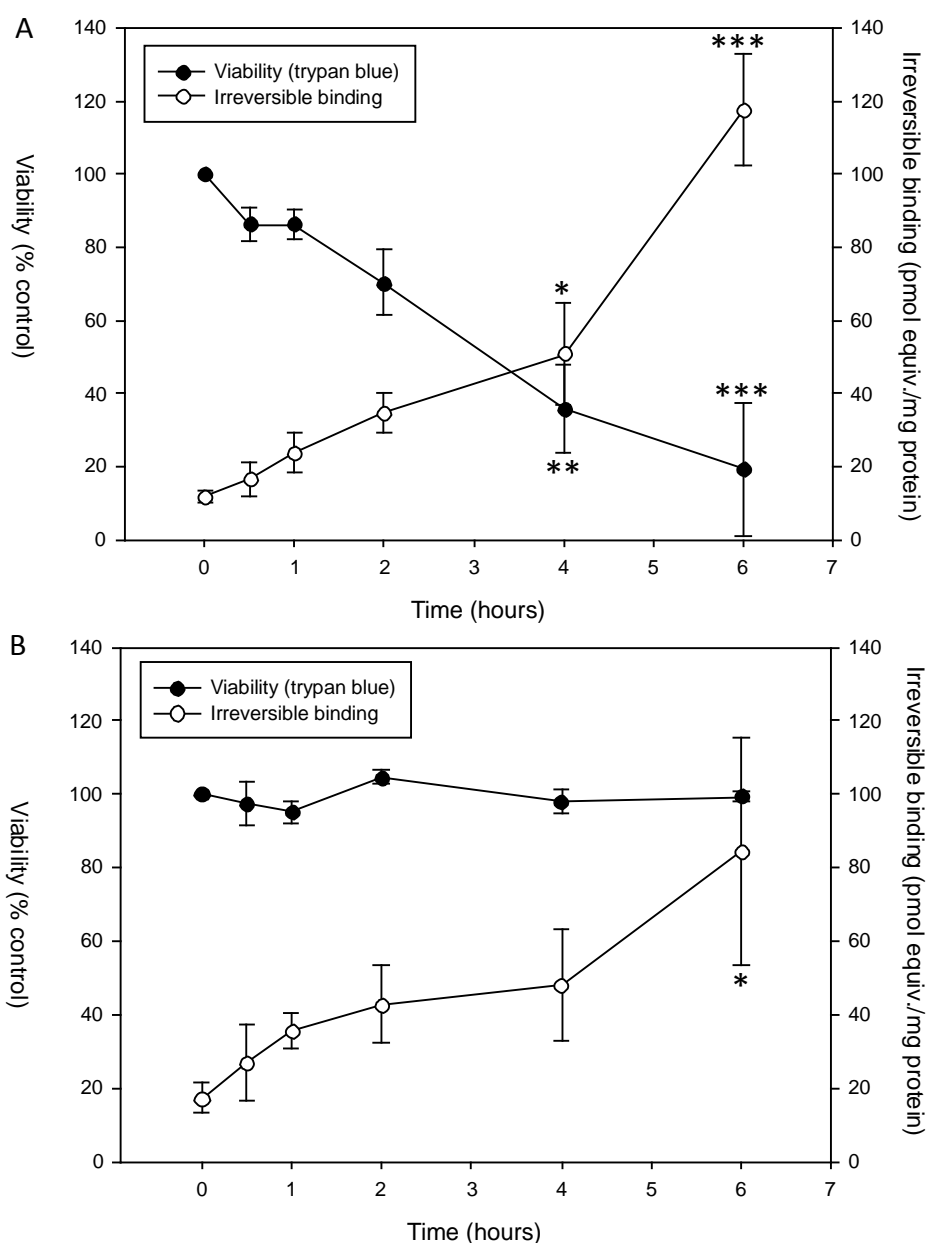


Figure 3.14. Comparison of the irreversible binding and cell viability in freshly isolated rat hepatocytes treated with nefazodone and buspirone. Freshly isolated rat hepatocytes were incubated with 200 μ M nefazodone (A) or buspirone (B) and 0.1 μ Ci of the corresponding [14 C] labelled compound for 0-6 hours. Viability was determined using trypan blue exclusion is expressed as % control values. Irreversible binding is expressed as pmol equiv/mg protein. Values are mean \pm SEM from 4 independent isolations. Significance to control values was determined using an ANOVA (Dunnett's multiple comparison to control). *P<0.05, **P<0.01, ***P<0.001.

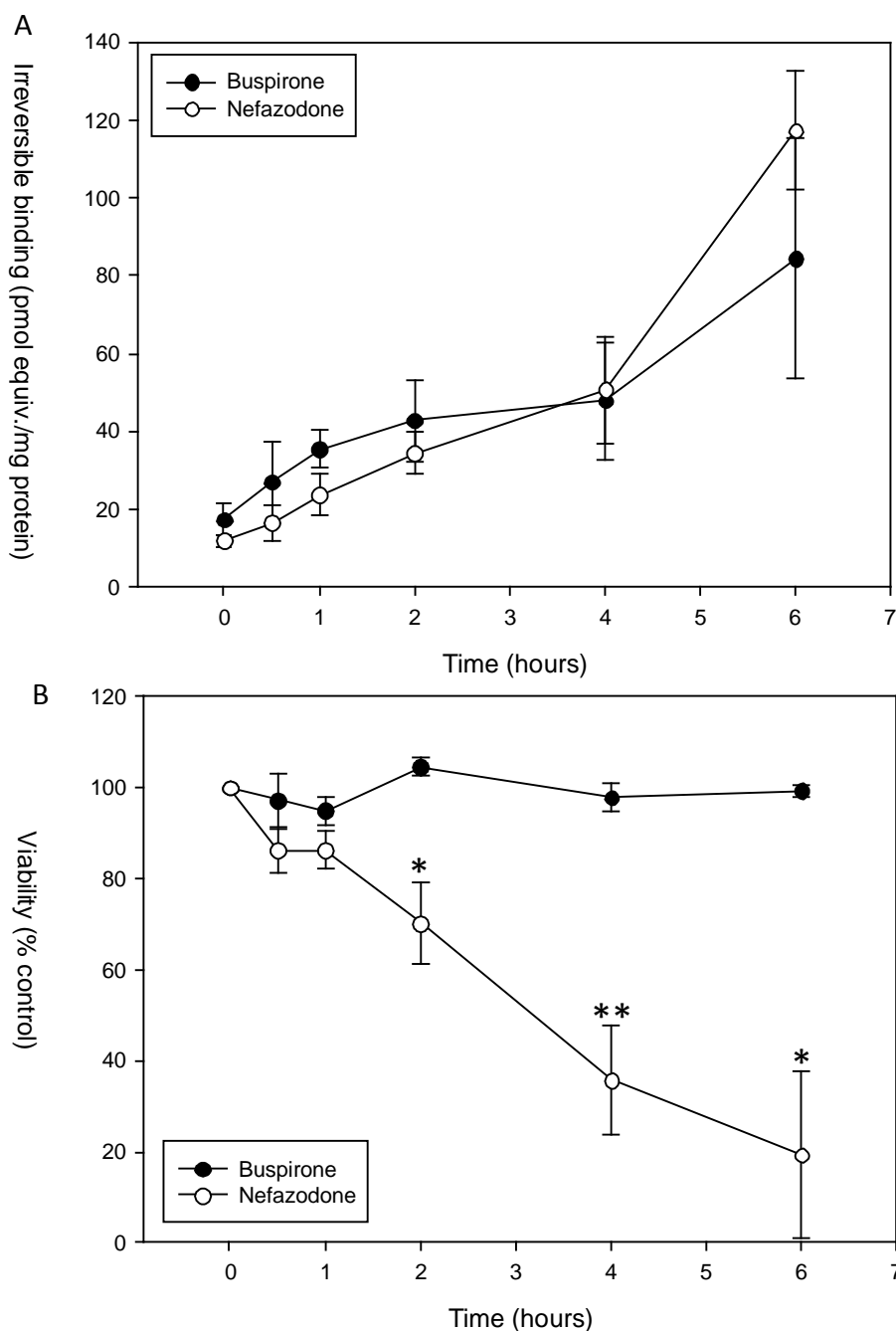


Figure 3.15. Comparison of irreversible binding and cell viability of freshly isolated rat hepatocytes treated with nefazodone and buspirone. Freshly isolated rat hepatocytes were incubated with 200 μ M nefazodone or buspirone and 0.1 μ Ci of the corresponding [14 C] radiolabelled compound for 0-6 hours. Irreversible binding (A) is expressed as pmol equiv./mg protein. Cell viability (B) was determined by trypan blue exclusion and is expressed as % control values. Values are mean \pm SEM and are from 4 independent isolations. Significance between nefazodone and buspirone was determined using an unpaired t-test. *P<0.05 **P<0.01.

3.3.8 The effect of ABT on toxicity and irreversible binding of nefazodone in freshly isolated rat hepatocytes

To determine whether CYP450s are involved in the metabolic activation and irreversible binding of nefazodone, hepatocytes were pre-incubated with ABT (1mM) for 30 minutes. The pre-incubation with ABT significantly reduced the irreversible binding of nefazodone from 117.54 ± 15.32 pmol equiv./mg protein to 49.34 ± 4.64 pmol equiv./mg protein. However, the viability of the hepatocytes also decreased (figure 3.16) indicating that the irreversible binding may not be the cause of nefazodone toxicity in rat hepatocytes. Use of the positive control, methapyrilene, demonstrated that pre-incubation with ABT could prevent metabolic activation and hence cytotoxicity of compounds where a reactive metabolite is a known cause of toxicity (Graham et al. 2008) (figure 3.17).

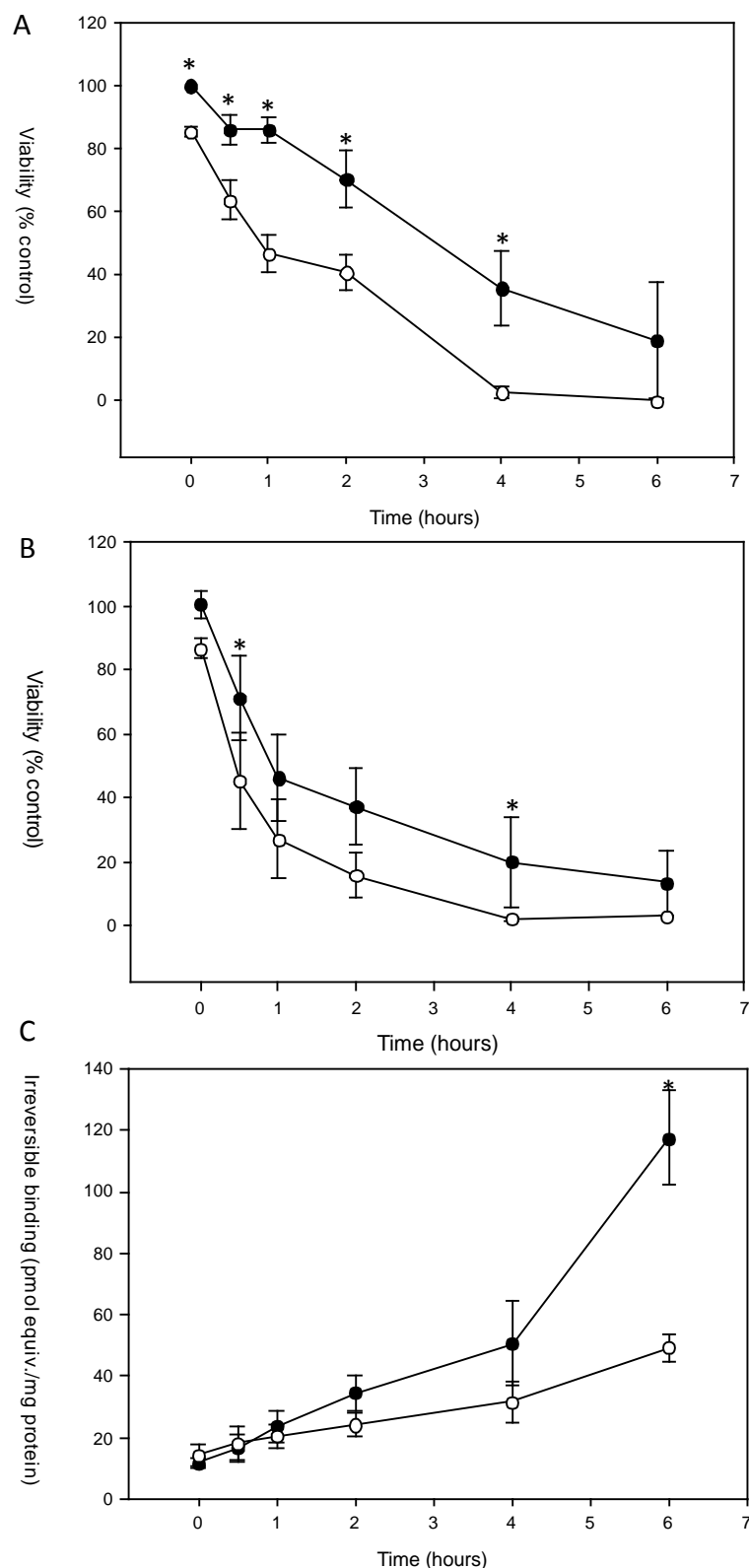


Figure 3.16. Effect of ABT on cytotoxicity and irreversible binding in freshly isolated rat hepatocytes. Freshly isolated rat hepatocytes were incubated with 200 μ M nefazodone and 0.1 μ Ci [14 C] nefazodone for 0-6 hours in the presence (○) and absence (●) of 1mM ABT. Viability was determined via trypan blue exclusion (A) and ATP content (B) and is expressed as % control. Irreversible binding (C) is expressed as pmol equiv/mg protein. Values are mean \pm SEM from 4 independent isolations. *P<0.05 nefazodone vs nefazodone + ABT determined using a Mann Whitney U test.

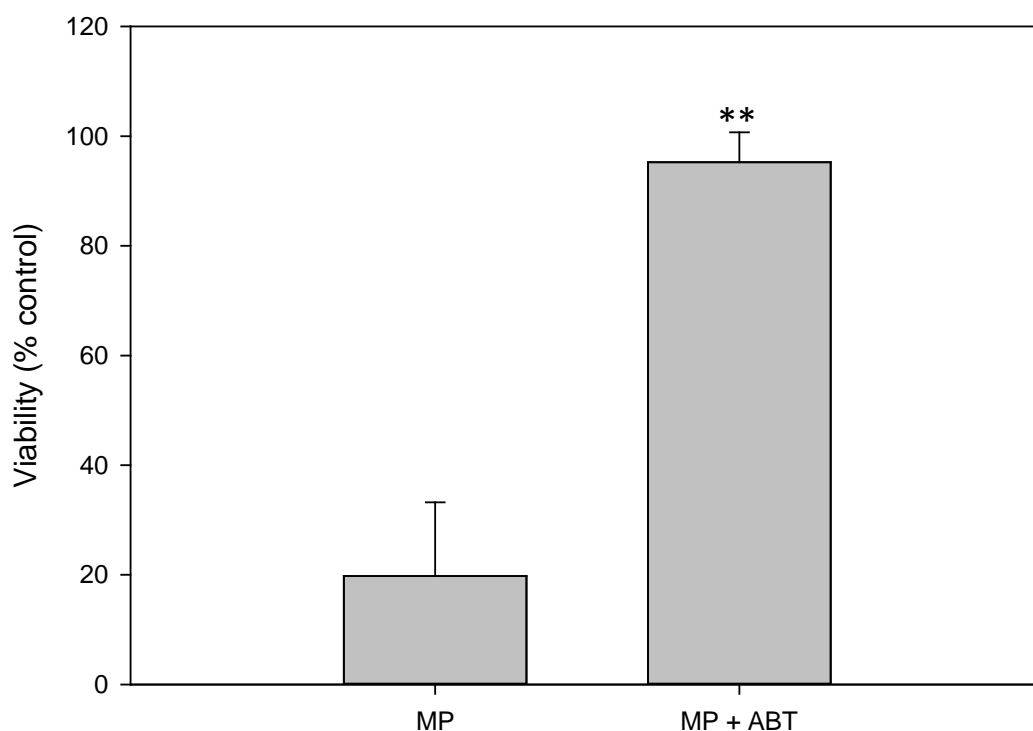


Figure 3.17. Effect of ABT on cells treated with methapyrilene. Freshly isolated rat hepatocytes were incubated with 200 μ M methapyrilene for 6 hours and viability was assessed by trypan blue exclusion. ** $P < 0.01$. MP, 200 μ M methapyrilene; MP+ABT, 200 μ M methapyrilene + 1mM ABT.

3.3.9 Cytotoxicity of nefazodone and buspirone in cultured rat hepatocytes using Cellomics technology

Cultured hepatocytes from Han Wistar rats were incubated with nefazodone and buspirone (0-100 μ M) for 24-72 hours. Figure 3.18. shows representative images of hepatocytes dosed with 0.1% DMSO, 100 μ M nefazodone and 100 μ M buspirone at 24hours. The hepatocytes were stained by Hoechst 33342 for nuclei and nuclear condensation, TMRM for mitochondrial membrane potential and TO-PRO-3 iodide for cell membrane integrity. The images show that the hepatocytes treated with 0.1% DMSO vehicle exhibit round normal shaped morphology, with a healthy

mitochondrial membrane potential and living cells with membrane integrity. Cells treated with buspirone produced similar imaging results as the 0.1% DMSO vehicle. On the other hand hepatocytes treated with 100 μ M nefazodone displayed nuclear condensation, dissipation of the mitochondrial membrane potential and a lack of cell membrane integrity. The hepatocyte images were analysed using ArrayScan software and the mean object intensity was used to assess Hoechst 33342, mean target intensity for TMRM and mean total target intensity for TO-PRO-3 iodide. Using Hoechst 33342 to assess nuclear condensation nefazodone (100 μ M) demonstrated a significantly increased fluorescence signal compared to 0.1% DMSO vehicle control (24hrs, 300.85 \pm 21.15 % control; 48hrs, 413.84 \pm 21.15 % control; 72hrs, 365.79 \pm 8.0 % control), whereas buspirone did not exhibit significantly increased fluorescence at any dose or time point. Cells stained with TO-PRO-3 iodide also indicated significance at all time points with nefazodone (100 μ M; 24hrs, 411.08 \pm 67.25 % control; 48hrs, 425.61 \pm 70.68 % control; 72hrs, 493.97 \pm 152.87 % control) indicating cell permeability, but not with buspirone. Significantly decreased TMRM fluorescence, indicated mitochondrial dysfunction in cells treated with nefazodone (100 μ M; 24hrs, 44.20 \pm 4.68 % control; 48hrs, 47.43 \pm 5.02 % control; 72hrs, 57.75 \pm 12.85 % control) (figure 3.19) but not with buspirone when compared to 0.1% DMSO controls (figure 3.20).

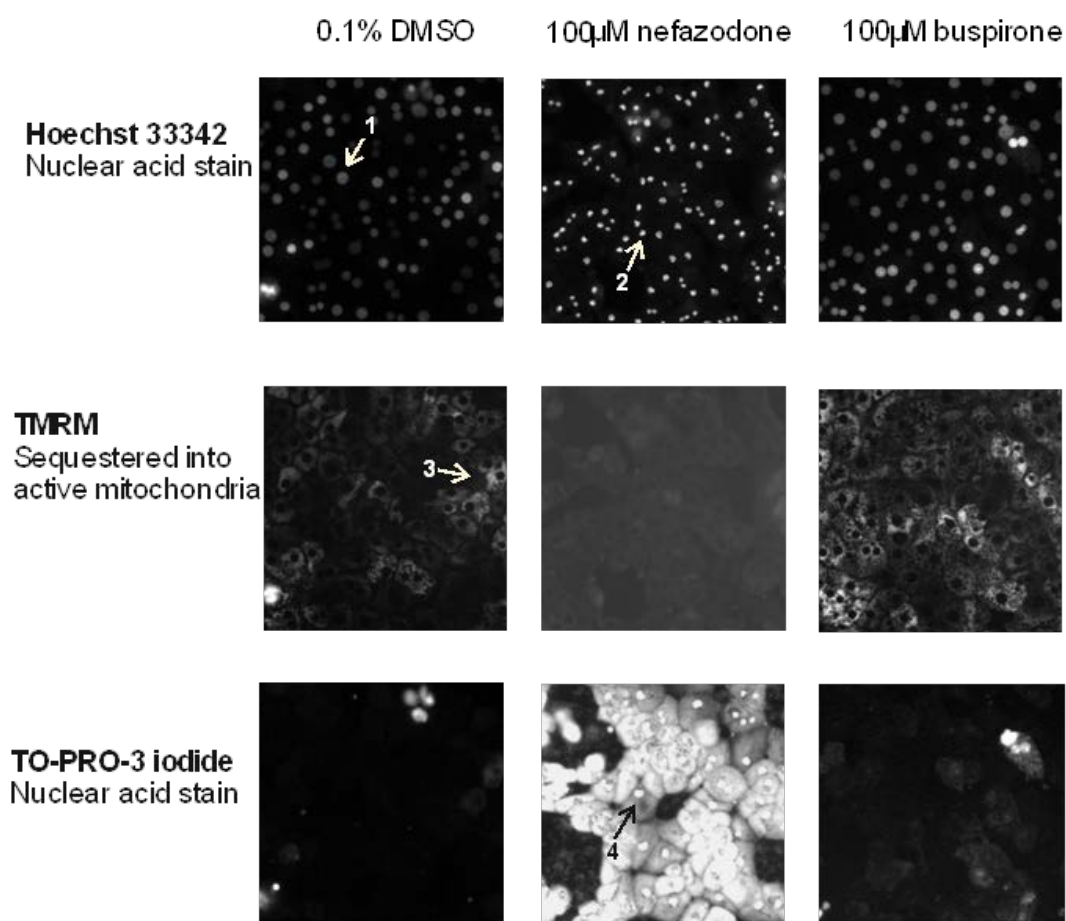


Figure 3.18. Images of cultured hepatocytes treated with 100µM nefazodone or buspirone after 24 hours. Representative images of hepatocytes treated for 24 hours with 0.1% DMSO (left column), 100µM nefazodone (middle column) and 100µM buspirone (right column). They were stained with Hoechst 33342 for nuclei (1st row), TMRM or mitochondrial membrane potential (2nd row) and TO-PRO-3 iodide to indicate membrane permeability. 1 indicates staining of hepatocytes with Hoechst 33342 with normal morphology. 2 demonstrates hepatocytes with a condensed nucleus following cell death stained with Hoechst 33342. 3 shows hepatocytes with normal mitochondrial membrane potential stained with TMRM, which cannot be seen in nefazodone treated cells. 4 shows cells with TO-PRO-3 iodide staining indicating disruption to the cell membrane and therefore TO-PRO-3 iodide staining of nuclear acids, which is not demonstrated in control (0.1% DMSO) treated cells.

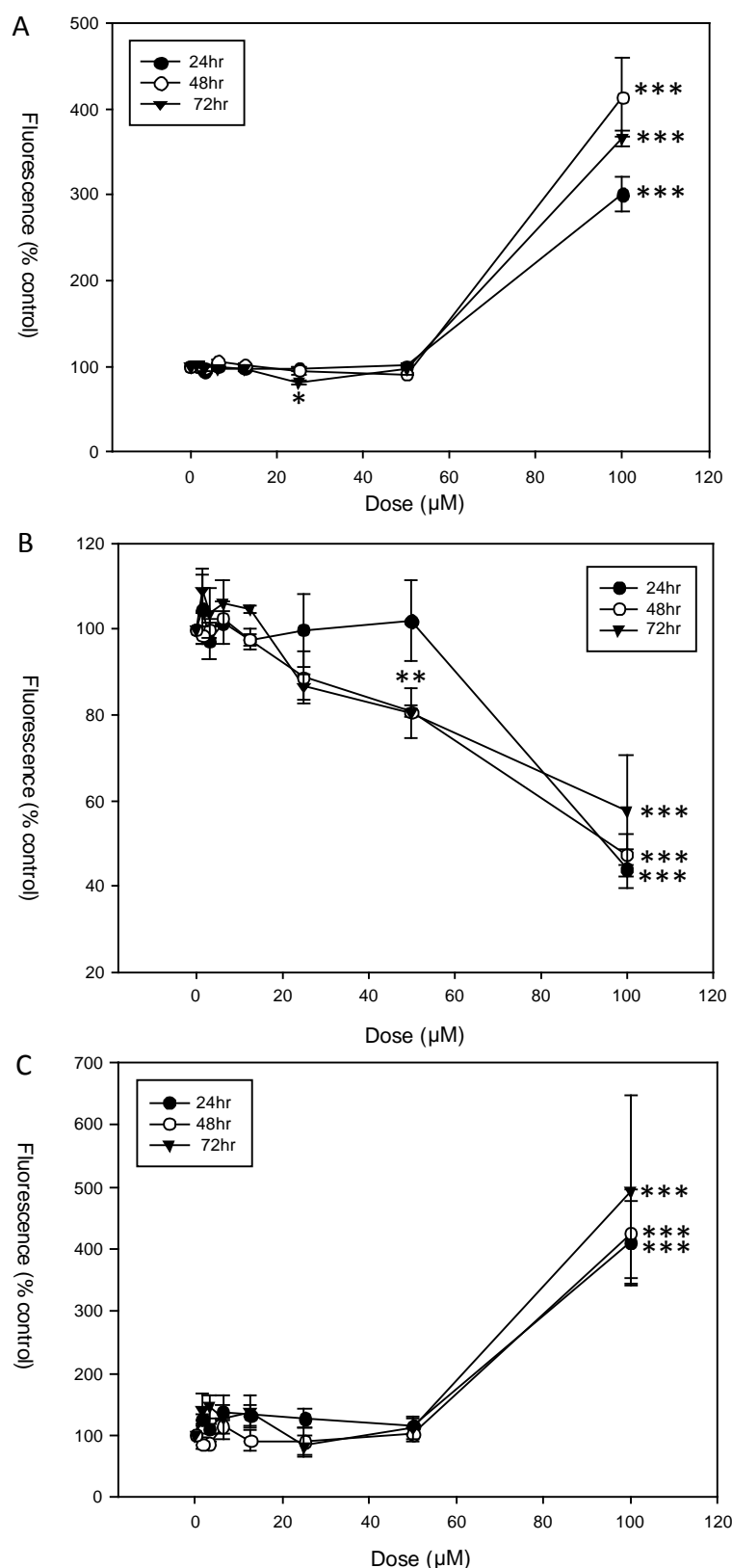


Figure 3.19. The cytotoxicity of nefazodone in cultured rat hepatocytes assessed using Cellomics technology. Hepatocytes from male Han Wistar rats were cultured with 0-100μM nefazodone for 24, 48 and 72 hours and assessed using (A) Hoechst 33324, (B) TMRM and (C) TO-PRO-3 iodide and expressed as % of control values. Data is from 3 independent isolations and is expressed as mean ± SEM.

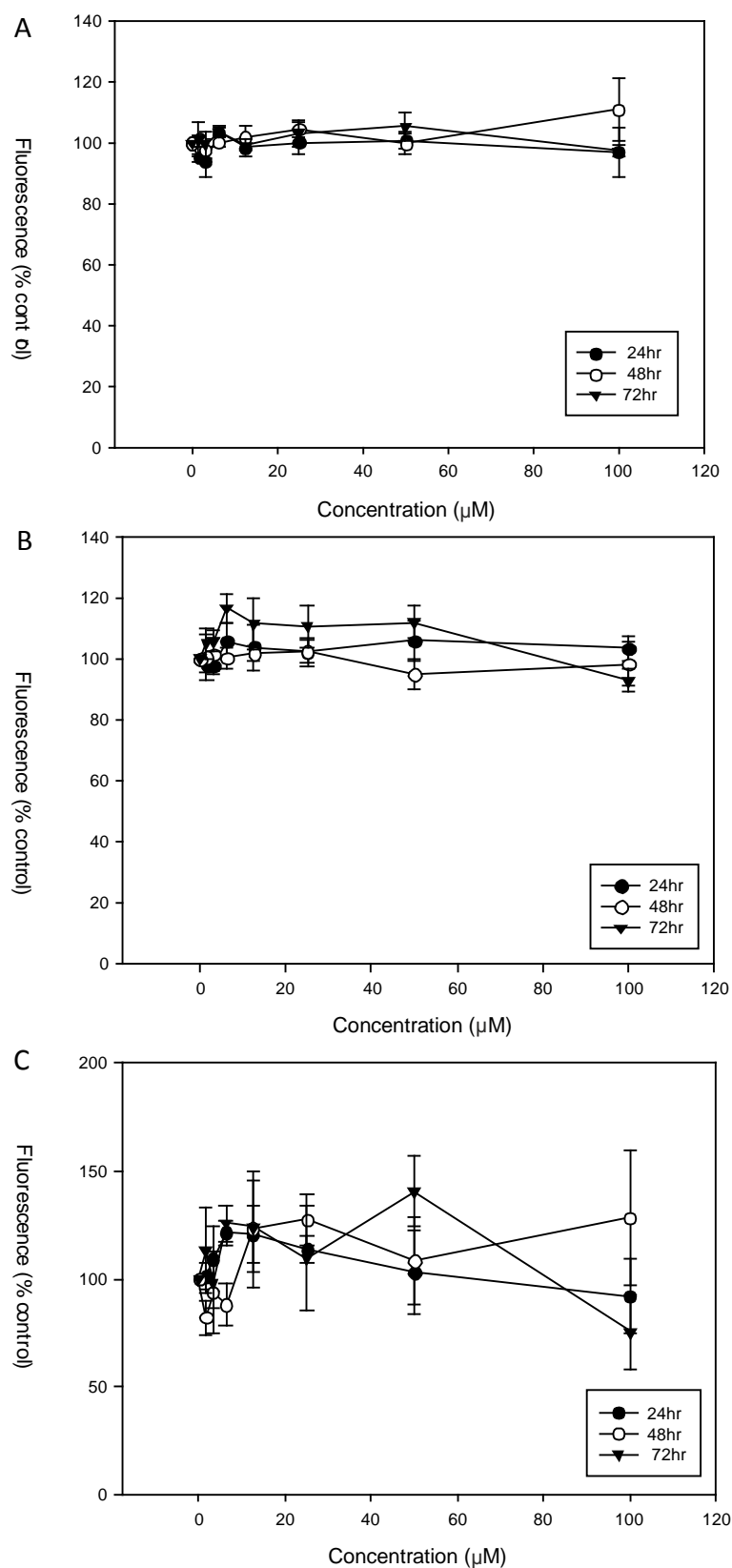


Figure 3.20. The cytotoxicity of buspirone in cultured rat hepatocytes assessed using Cellomics technology. Hepatocytes from male Han Wistar rats were cultured with 0-100 μM for 24, 48 and 72 hours and assessed using (A) Hoechst 33324, (B) TMRM and (C) TO-PRO-3 iodide and expressed as % of control values. Data is from 3 independent isolations and is expressed as mean \pm SEM.

3.3.10 Cytotoxicity of nefazodone in freshly isolated human hepatocytes

The toxicity of nefazodone in human hepatocytes was evaluated using a dose response of nefazodone (0-200 μ M) over 6 hours in suspension cells. There was significant toxicity in cells dosed with 100 and 200 μ M nefazodone (figure 3.21), using both trypan blue exclusion and ATP assay. Significant GSH depletion occurred, however, the GSH concentration in the hepatocytes was much lower than expected, possibly due to the age and health of the patients in combination with the isolation procedure (figure 3.22.). Despite this, the trend still indicated that GSH depletion was not the cause of cell death, the same relationship that is seen in rat hepatocytes between GSH and cytotoxicity.

3.3.11 Comparison of nefazodone toxicity in human and rat hepatocytes

The toxicity of nefazodone towards human and rat hepatocytes (figure 3.23) was very similar, with near complete cell death at 200 μ M nefazodone. There was a trend towards increased toxicity in human hepatocytes using both trypan blue exclusion and to greater extent ATP content, but neither measures of viability were significant.

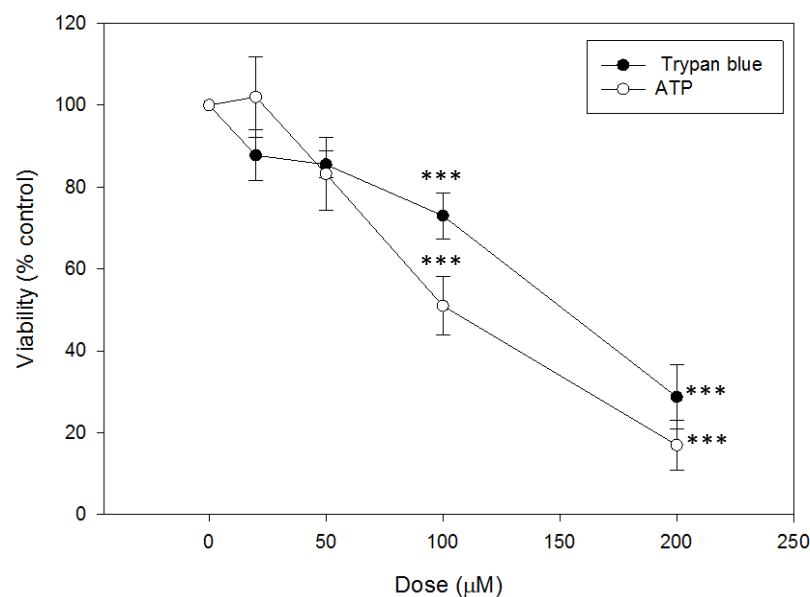


Figure 3.21. Effect of nefazodone on the viability of freshly isolated human hepatocytes. Human hepatocytes were treated with 0-200μM nefazodone for 6 hours and viability was assessed using trypan blue exclusion (●) and ATP content (○). Data is mean ± SEM from 4 independent isolations and expressed as % control values. *** P<0.001 determined using ANOVA (Dunnet's comparison to control)

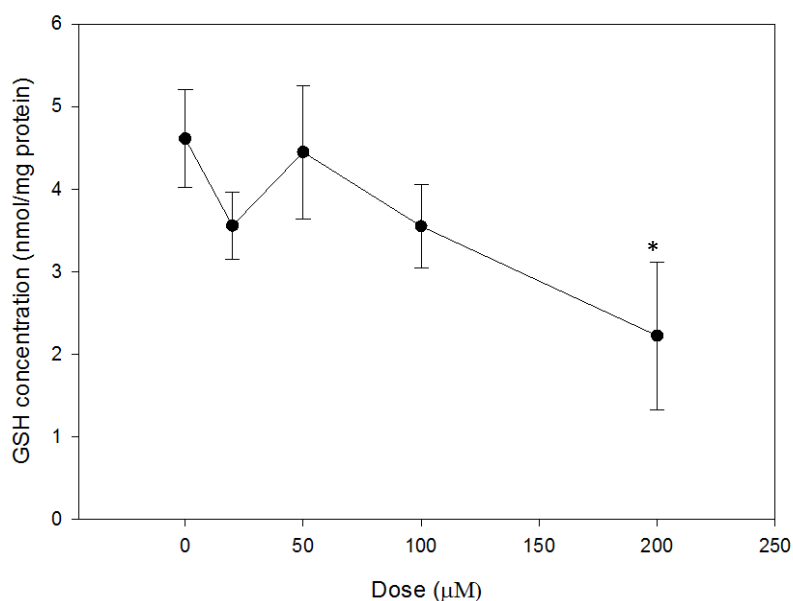


Figure 3.22. GSH concentrations in human hepatocytes treated with nefazodone. Human hepatocytes were treated with 0-200μM nefazodone and GSH concentration tested. Data is mean ± SEM and from 4 independent isolations and expressed as nmol/mg protein. *P<0.05 determined using ANOVA (Dunnet's comparison to control).

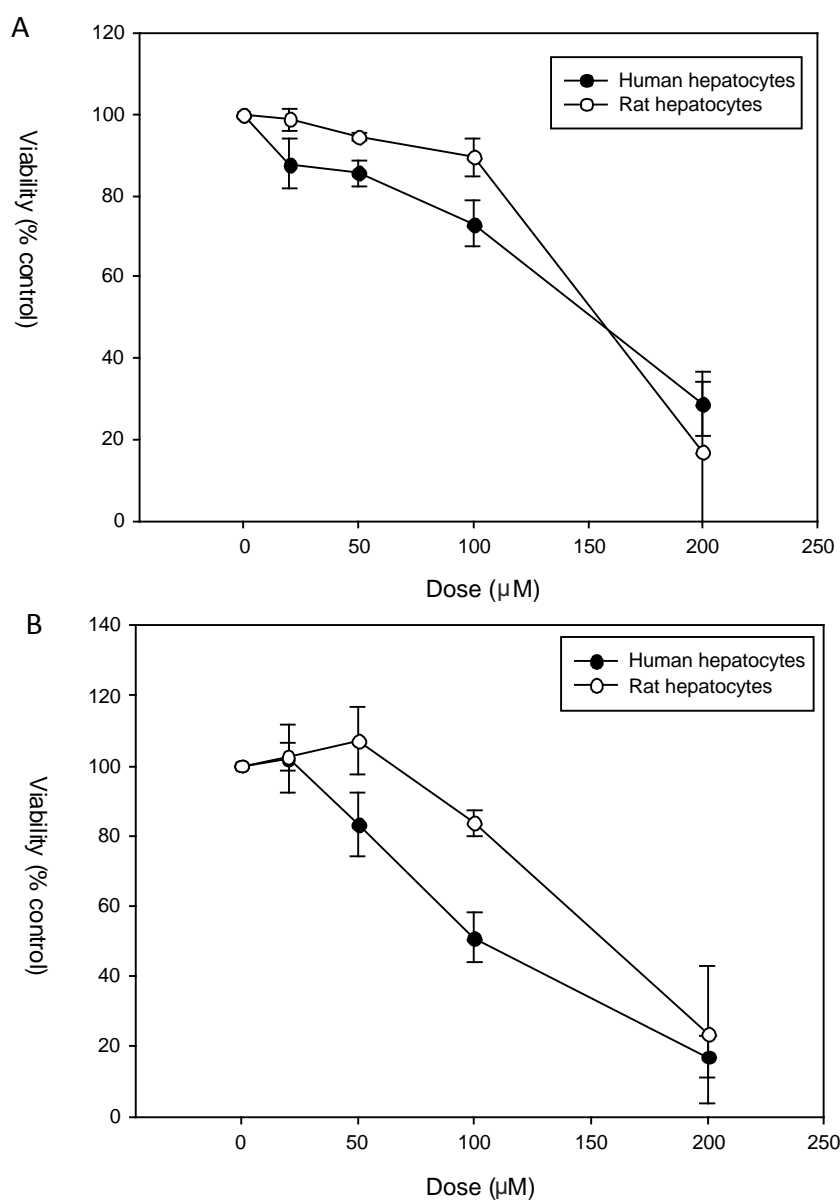


Figure 3.23. Comparison of the toxicity of nefazodone in freshly isolated rat and human hepatocytes. Human and rat hepatocytes were treated with 0-200μM nefazodone and viability was assessed with (A) trypan blue exclusion and (B) ATP content. Data is mean ± SEM from 4 independent isolations and data is presented as % control viability.

3.4 DISCUSSION

The principle aims of the work described in this chapter was to provide a link between reactive metabolite formation, irreversible binding and the toxicity elicited by nefazodone. In the previous chapter, it was demonstrated that nefazodone could produce reactive metabolite species in rat and human liver microsomes. This has been previously well documented but a link between the observed bioactivation in liver microsomes and toxicity has never been demonstrated. Trying to elucidate the mechanisms through which nefazodone induces toxicity may help to inform development of safe drugs in the future.

3.4.1 Metabolism

3.4.1.1 Reactive metabolite formation and GSH depletion

It is widely recognised that nefazodone, but not buspirone, can form reactive metabolites in human liver microsomes. In accordance with the literature, in chapter 2 we demonstrated that a hydroxynefazodone glutathione conjugate and a dihydroxynefazodone glutathione conjugate could be formed in both human and rat liver microsomes. In rat hepatocytes nefazodone and buspirone both demonstrated extensive turnover, with hydroxylation, *N*-dealkylation and glucuronidation prevailing as the predominant pathways of drug metabolism. In both rat and human hepatocytes hydroxynefazodone was formed with an *m/z* 274 indicating an unsubstituted phenoxyethyl-propyltriazolone fragment making the most likely place of hydroxylation the chlorophenylpiperazine moiety. Hydroxylation of the chlorophenylpiperazine moiety *para* to the piperazinyl nitrogen can lead to quinone-imine formation, which can be detected through the corresponding GSH adduct (Baillie, Davis 1993). Unlike in human and rat liver microsomes no GSH conjugates could be detected in either rat or human hepatocytes. Despite several sources

identifying both *p*-hydroxy nefazodone and *p*-dihydroxy nefazodone in rat and human liver microsomes (Kalgutkar et al. 2005b, Bauman et al. 2008a, Argoti et al. 2005). GSH conjugates of nefazodone have never previously been identified in hepatocytes, and a study in cultured human hepatocytes also only identified glucuronide and sulphate formation from nefazodone metabolites (Kostrubsky et al. 2006). This may be due to the availability of cytosolic phase II metabolising enzymes in hepatocytes that are not present in liver microsomes, resulting in glucuronide and sulphate formation rather than the formation of a GSH conjugate. There is also the possibility that the nefazodone GSH conjugates are unstable and the difference in processing time between liver microsomes and hepatocytes results in their degradation, therefore resulting in no detection. As discussed below, buspirone produced both significant irreversible binding and GSH depletion in rat hepatocytes, however, as with liver microsomes, no GSH conjugates of buspirone were detected. Hydroxylation on the pyrimidinyl moiety of some of the hydroxybuspirone metabolites was evident from a shift from *m/z* 122 to 138 in the fragmentation pattern indicating the potential for buspirone to undergo bioactivation to a quinone-imine. In light of the irreversible binding and GSH depletion caused by buspirone it is possible that buspirone does produce a GSH adduct that is too unstable to be detected using current LC-MS methods.

GSH is an essential molecule for cellular function and survival. As the most abundant reducing molecule in hepatocytes (concentrations of approximately 10mM) it is vital for maintaining the redox balance of the cell (Han et al. 2006). It is also a major anti-oxidant quenching both endogenous oxidant species and endogenous induced oxidative stress, as well as conjugating reactive metabolites produced by xenobiotics (DeLeve, Kaplowitz 1991). It can also modulate signalling cascades and

the susceptibility of cells to cell death signals, and plays an important role in apoptosis (Circu, Aw 2008). It has been shown that quinone-imines, such as NAPQI, can attack and irreversibly bind to the cysteinyl residues of cellular proteins. Hepatocytes preferentially conjugate the NAPQI formed following metabolism of paracetamol to GSH conjugates, however, when a large amount of NAPQI is produced this overwhelms the cells leading to depletion of the cellular GSH concentration. Once cellular GSH levels become depleted, NAPQI is then free to bind to cellular proteins, leading to cell death.

Despite a lack of GSH conjugates of nefazodone and buspirone both compounds significantly depleted GSH compared to control values in rat hepatocyte suspensions. The depletion of GSH by nefazodone mirrors the cytotoxicity of nefazodone, and there was no significant decrease of GSH concentrations preceding hepatocyte cell death. This trend indicates that the depletion of GSH is likely to be due to the release of GSH into the surrounding media when the cells die and therefore the depletion of GSH by nefazodone is probably a consequence and not a cause of cell death.

Buspirone, however, depleted GSH in a manner that suggests GSH depletion is a cause of cell death. Unlike nefazodone, significant depletion of GSH occurred before significant cell death. It is a possibility that buspirone does not directly conjugate GSH but rather increases ROS formation, and GSH is depleted through the reduction of ROS and subsequent oxidation of GSH to GSSG.

3.4.1.2. Irreversible binding

Nefazodone demonstrates time, concentration and NADPH-dependent inactivation of CYP450 3A4 in human liver microsomes (Von Moltke et al. 1999a). These characteristics are consistent with the observed non-linear pharmacokinetics of nefazodone in humans upon dose escalation (Kaul, Shukla & Barbhuiya 1995), as well as a wide variety of drug-drug interactions between nefazodone and a number of CYP450 3A4 substrates (Abernethy et al. 2001, Helms-Smith, Curtis & Hatton 1996). It is thought that this is mediated by the quinone-imine species that nefazodone has been shown to produce in liver microsomes, via irreversible binding to CYP450 3A4, leading to auto-inactivation, or to critical cellular proteins leading to hepatotoxicity.

A time course of the irreversible binding and toxicity of nefazodone over 6 hours revealed that irreversible binding of GSH increases with a concomitant decrease in hepatocyte viability. This mimics the trend seen in other well documented cases, where reactive metabolite formation and subsequent irreversible binding of a compound leads to cell death.

To identify that bioactivation through CYP450s and resulting irreversible binding was the cause of the cytotoxicity observed in rat hepatocytes, the irreversible binding study was repeated following pre-incubation with the non-specific CYP450 inhibitor ABT, as well as positive control samples containing methapyrilene. Methapyrilene is a known rat hepatotoxin and is bioactivated, in rat hepatocytes, to a reactive thiophene metabolite that can bind to macromolecules leading to cell death (Graham et al. 2008). Pre-incubation of rat hepatocytes with ABT has been shown to prevent the toxicity of methapyrilene to rat hepatocytes. These experiments yielded surprising results as although ABT sufficiently prevented both the toxicity of

methapyrilene and the irreversible binding of nefazodone as expected, it did not prevent the toxicity of nefazodone in hepatocytes. Further experiments in hepatocytes revealed that pre-incubating hepatocytes with ABT resulted in a significant increase in toxicity at concentrations as low as 20 μ M nefazodone. This trend in increased toxicity was also observed in human hepatocytes, however, due to the constraints of retrieving human liver for hepatocyte isolations and the difficulty in getting hepatocytes to survive to 6 hours, following a 30 minute pre-incubation with ABT it was not possible to get more data the effects of ABT in human hepatocytes.

Surprisingly buspirone also demonstrated significant irreversible binding in rat hepatocyte incubations, although unlike nefazodone there was no impact on the viability of the hepatocytes. The irreversible binding of buspirone was much higher than that observed in rat liver microsomes (chapter 2). It is a possibility that buspirone irreversibly binds to cytosolic proteins found in hepatocytes and not to the CP450 enzymes found in the endoplasmic reticulum.

It has previously been shown that nefazodone and buspirone both exhibit high levels of irreversible binding in human hepatocytes. In human hepatocytes it was calculated that the daily body burden of buspirone (3.8mg/kg) was actually higher than nefazodone (3.6mg/kg) due to the higher turnover of nefazodone to metabolites and hence a smaller fraction of the metabolites of nefazodone are reactive metabolites (Bauman et al. 2009). However, it is important to note that the irreversible binding of a drug to cellular protein does not necessarily lead to toxicity. 3-hydroxyacetanilide, a region-isomer of paracetamol, irreversibly binds to hepatic proteins in rodents without inducing hepatotoxicity. The difference in the location of the binding is important in this case, with 3-hydroxyacetanilide binding primarily to cytosolic

proteins, whilst paracetamol binds primarily to proteins in the mitochondria, which are important in regulating cell death (Tirmenstein, Nelson 1989). Nakayama et al, investigated the risk posed by irreversible binding using a using a zone classification system, which used daily dose and irreversible binding in human liver microsomes, human hepatocytes and rat liver *in vivo* (Nakayama et al. 2009). They identified that hepatocytes provided the best correlation between irreversible binding, dose and toxicity of the drug, however, the system still placed 7 out of 37 drugs (19%) in the wrong category. It is therefore important that irreversible binding studies are taken into consideration with a variety of other *in vitro* tests and the formation of reactive metabolites and irreversible binding alone is not used as an indicator of toxicity. Indeed a study that includes a panel of *in vitro* assays to determine likelihood of toxicity, identified nefazodone as a potential risk in all but one assay and of all the compounds tested it flagged the most warning signals for potential toxicity (Thompson et al. 2012). In this panel nefazodone gave positive results for all the identified ways that nefazodone could potentially cause toxicity, giving positive results for toxicity in THLE null cells as well as THLE CYP3A4 cells, demonstrated greater toxicity in galactose rather than glucose grown HepG2 cells and gave a positive result for the inhibition of BSEP in transporter assays (Thompson et al. 2012).

3.4.4 Mitochondrial toxicity

The data that was gathered in cultured rat hepatocytes using Cellomics technology, indicated that 100µM nefazodone abolished the mitochondrial membrane potential, determined using TMRM, whilst buspirone had no effect on the mitochondria at equivalent concentrations. Nefazodone treatment also resulted in cell death that was characterised by nuclear condensation and disruption of cellular membrane potential.

Due to the time points used it is unclear whether mitochondrial involvement in nefazodone cell death was a result of direct or indirect mitochondrial toxicity, however, there is evidence that nefazodone is a mitochondrial toxin. Work done by Dykens *et al* showed that, in HepG2 cells, nefazodone had IC₅₀ values of 38.4µM and 9µM in cells grown in glucose and galactose containing media respectively (Dykens et al. 2008). Cells grown in high glucose media are not dependent on ATP production through OXPHOS and are therefore less susceptible to mitochondrial toxicity. This can be revealed using cells grown in galactose media, where the cells are forced to undergo OXPHOS to produce their ATP requirements (Marroquin et al. 2007). Further investigation identified that nefazodone inhibits complex I of the OXPHOS chain. Inhibition of complex I, which prevents electron flow to ubiquinone, leads to an accumulation of NADH which may lead enhanced formation of ROS and therefore cell death. The use of HepG2 cells to carry out these experiments, which have little or no CYP450 mediated metabolism, indicates that nefazodone itself, and not a reactive metabolite, is toxic to the mitochondria.

3.4.3 BSEP inhibition

The argument that nefazodone itself causes drug induced liver injury and not the reactive metabolite has been suggested previously and mechanisms of injury other than reactive metabolite formation and irreversible binding have been proposed. Kostrubsky *et al*, investigated the effect nefazodone had on the bile salt export pump (BSEP). Following experiments in vesicles expressing BSEP and using sandwich cultured hepatocytes to assess the transport of taurocholic acid into the canaliculi they found that the IC₅₀ values were similar in both systems, and concluded that parent compound must be responsible for BSEP inhibition. Using sandwich cultured hepatocytes they also demonstrated that 24 hours post nefazodone dose, cells pre-

incubated with ABT had a 45% decrease in protein synthesis, whereas hepatocytes treated with nefazodone alone had returned to the same levels as control values. They also found no evidence of a GSH conjugate in their system and concluded that this may be due to the high rate of glucuronidation and sulphation in the hepatocytes preventing the bioactivation of *p*-hydroxy metabolites (Kostrubsky et al. 2006).

It is also a possibility that a combination of the above mechanisms is a possibility. Inhibition of BSEP and other export pumps could lead to an accumulation of bile salts which have also been shown to be mitochondrial toxins, leading to a collapse of the mitochondrial membrane potential and cell death.

3.4.4 Conclusion

The aim of this chapter was to determine whether there was a link between reactive metabolite formation, irreversible binding and toxicity of nefazodone in hepatocytes and compare this to the non-hepatotoxin buspirone.

Following experiments with rat liver microsomes in chapter 2 it can be suggested that reactive metabolite formation might be responsible for the hepatotoxicity observed with nefazodone; i.e. the differences in the bioactivation potential of *para*-hydroxy nefazodone and buspirone could explain the differences in the toxicity. However, experiments with hepatocytes suggest an alternative mechanism, as they do not support this conclusion. Indeed, analysis of the relationship between metabolism and toxicity suggest that the parent compound might be responsible. Other mechanistic possibilities by which nefazodone parent compound may cause hepatotoxicity are through inhibition of the BSEP transporter or through interference with the mitochondrial OXPHOS.

CHAPTER 4

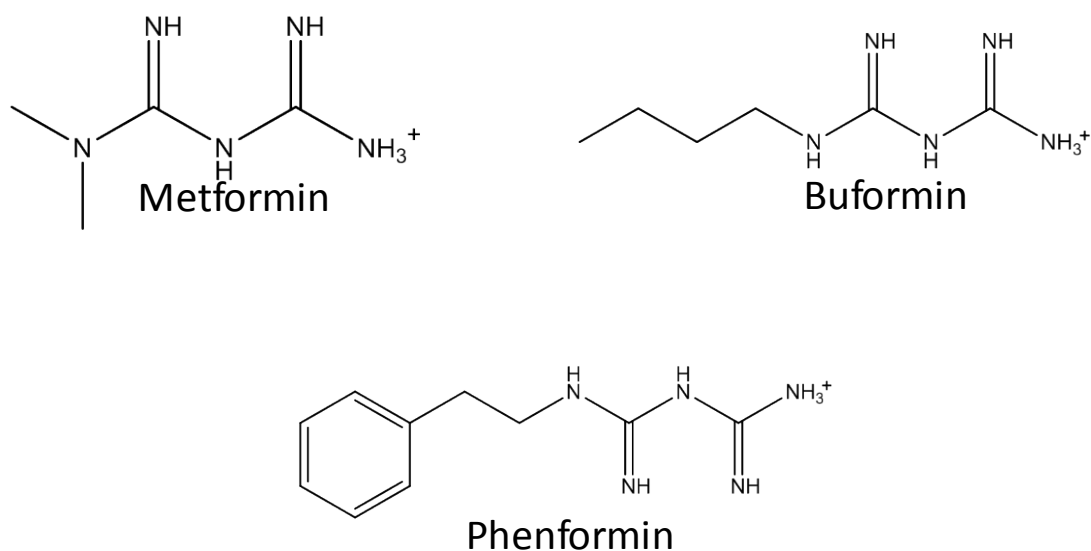
PHENFORMIN: PARENT COMPOUND AND ITS ROLE IN MITOCHONDRIAL TOXICITY

Table of Contents

4.1 INTRODUCTION	135
4.2 MATERIALS AND METHODS	139
4.2.1 Materials	139
4.2.2. Rat hepatocyte isolations for suspension hepatocytes	139
4.2.3 Suspension hepatocyte incubations	139
4.2.5. Cellomics analysis	140
4.2.6. HPLC and LC-MS sample preparation	140
4.2.7 HPLC method	140
4.2.8. LC-MS method.....	141
4.2.9 Lactate measurement	141
4.2.10 Animal work.....	141
4.2.11 Statistical analysis	142
4.3 RESULTS.....	143
4.3.1 Effect of the biguanides on mitochondria in cultured rat hepatocytes.....	143
4.3.2 The metabolism of phenformin in primary rat hepatocytes	147
4.3.3 Investigations of quinine and quinidine as CYP450 2D inhibitors in rat hepatocytes	151
4.3.4. Effect of CYP2D inhibition on turnover of phenformin in suspension rat hepatocytes.....	156
4.3.5 Effects of CYP2D6 inhibition on the toxicity of phenformin in suspension rat hepatocytes.....	157
4.3.6. Effect of phenformin on lactate levels in suspension hepatocytes	158
4.4 DISCUSSION.....	159

4.1 INTRODUCTION

Phenformin is an anti-diabetic agent belonging to the biguanide class. It came to the market in the 1950s and quickly became the leading compound in its class due to its superior efficacy. Unfortunately it became apparent that phenformin was associated with an increased risk of lactic acidosis (lactate levels greater than 5mmol/L and serum pH of less than 7.35). This estimated to be between 40-64 cases per 100,000 patient years (Bailey 1992), substantially higher than the 3.3 cases per 100,000



patient years associated with metformin.

Figure 4.1. Chemical structures of the biguanides.

The guanidinium group gives the biguanides a cationic charge at physiological pH. This coupled with the relatively high lipophilicity of phenformin it is able to be accumulated into mitochondria up to 100-fold against a concentration gradient (Davidoff 1971), probably via $\Delta\Psi$. Phenformin has also been demonstrated to accumulate up to 61-fold in the liver of rats (Sogame et al. 2011) via OCT1 (Wang et al. 2002, Wang et al. 2003b, Sogame et al. 2009). An investigation carried out in 30

diabetic patients to try and clarify the relationship between serum biguanide levels and increased lactate concentrations could demonstrate no relationship between the serum biguanide level, administered dose and time of administration. There was also no correlation between biguanide levels and lactate increase. Whilst the serum levels were only slightly above the therapeutic range expected with phenformin, both liver and kidney concentrations of phenformin showed highly toxic levels of the drug (Irsigler, Kritz & Regal 1979), demonstrating that biguanide accumulation in the liver also occurs in humans. An accumulation in both the liver, followed by the liver mitochondria, could mean that mitochondrial concentrations reach several thousand fold that of plasma concentrations, causing interference with energy production and lactate metabolism through inhibition of complex 1 of the mitochondrial respiratory chain (El-Mir et al. 2000, Dykens, J.A., Jamieson, J., Marroquin, L., Nadanaciva, S., Billis, P.A., Will, Y. 2008, Owen, Doran & Halestrap 2000). In the case of phenformin this accumulation in the mitochondria could be further exacerbated by metabolism.

Phenformin has been shown to be undergo hepatic metabolism to *p*-hydroxy phenformin in man, rats, guinea pigs and dogs (Shah, Evans & Oates 1985, Guest, King & Parke 1979, Alkalay, Volk & Roth 1979, Oates et al. 1982) and in man this metabolism takes place through CYP450 2D6 (Shah, Evans & Oates 1985, Oates et al. 1982). CYP450 2D6 is a highly polymorphic enzyme and this can lead to different patients outcomes treated with the same drug, ranging from a lack of clinical effect to severe toxicity. Perhaps one of the most well documented of these cases is that of perhexilene. Perhexilene is hydroxylated by CYP450 2D6 so that it can undergo excretion. However, PMs lack the capacity to metabolise perhexilene causing an accumulation of perhexilene in tissues, eventually leading to steatosis and

peripheral neuropathy. However, identification of CYP450 2D6 PMs and therapeutic drug monitoring has enabled this drug to be re-introduced in some countries. Table 4.1 identifies other compounds that have been demonstrated to be metabolised by CYP450 2D6 and the clinical effect of polymorphisms in this enzyme (Shah, Oates & Idle 1982, Morgan, Reshef & Shah 1984).

In a study of healthy volunteers given a single dose of phenformin a significant correlation between CYP450 2D6 PM phenotype and higher lactate levels has been demonstrated (Idle et al. 1981, Shah, Evans & Oates 1985, Shah et al. 1980). A combination of PM phenotype and accumulation in liver mitochondria could potentially lead to toxic concentrations of phenformin in the liver causing mitochondrial toxicity in the form of lactic acidosis.

Drug	Indication	Clinical effect of CYP2D6 polymorphism	References
Perhexilene	Anti-anginal	Mono-hydroxylation of perhexilene carried out almost exclusively by CYP2D6. Accumulates in PMs leading to steatosis and peripheral neuropathy.	Shah <i>et al</i> , 1982; Morgan, Reshef, Shah, 1984.
Haloperidol	Anti-psychotic	PMs show an increased risk of pseudoparkinsonism and over-sedation, whilst lower therapeutic efficacy is seen with an increasing number of active CYP2D6 genes.	Brockmüller <i>et al</i> , 2002; Spina <i>et al</i> , 1992.
Tamoxifen	Anti-cancer	Pro-drug tamoxifen is metabolised to its active form endoxifen by <i>N</i> -demethylation and 4-hydroxylation, both reactions carried out by CYP2D6. A smaller therapeutic effect is observed in PMs.	Sterns and Rae, 2008.
Phenformin	Anti-diabetic	Lack of hydroxylation via CYP2D6 leads to higher plasma lactate levels and increased risk of lactic acidosis.	Idle <i>et al</i> , 1981, Shah <i>et al</i> , 1980; Shah <i>et al</i> 1985
Tramadol	Analgesic	Tramadol undergoes <i>O</i> -demethylation to <i>O</i> -desmethyltramadol, which is 200 times more potent at the μ opioid receptors. In PMs tramadol has been reported to have a much lower analgesic effect.	Stamer <i>et al</i> , 2007

Table 4.1. Clinical effects of CYP2D6 polymorphisms. CYP2D6 is responsible for the metabolism of 25% of drugs, therefore several important clinical consequences of CYP2D6 polymorphisms are known to occur. These range from reduced efficacy through to severe toxicity.

Recently, there has been a renewed interest in phenformin as an anti-cancer drug. AMPK activators, such as phenformin, have been demonstrated to induce either cell cycle arrest or apoptosis in various cell cancer lines of different genetic origin (Caraci et al. 2003, Appleyard et al. 2012, El-Masry, Brown & Dobson 2012). This has led to phenformin being recommended for clinical trials for the treatment of ER-positive and triple negative breast cancer.

The aims of this chapter were primarily to assess the biguanides as tools for investigations of mitochondrial toxicity in primary hepatocyte suspensions. Initially the propensity for the biguanides to dissipate the mitochondrial membrane potential

was established in cultured hepatocytes using TMRM. This allowed phenformin to be taken forward as a tool for assessing mitochondrial dysfunction in primary hepatocytes.

4.2 MATERIALS AND METHODS

4.2.1 Materials

Phenformin, quinine and quinidine were purchased from Sigma-Aldrich (Poole, UK). ATP assay was purchased from Promega (UK). Collagenase type II was purchased from Worthington Biochemical Corporation. Cellomics dyes, Hoechst 33342, TMRM and TO-PRO 3 iodide, and 10x HBSS were all purchased from Invitrogen (UK). Lactate assay was purchased from Sigma-Aldrich (Poole, UK). Biocoat collagen coated plates were purchased from VWR (UK). Solvents were purchased from Fischer Scientific and were all HPLC grade and above. All other reagents were purchased from Sigma-Aldrich (Poole, UK) unless otherwise stated.

4.2.2. Rat hepatocyte isolations for suspension hepatocytes

Rat hepatocytes were isolated from male Wistar rats as in chapter 3.2.2 and only used if viability was greater than 80% as assessed by trypan blue exclusion.

4.2.3 Suspension hepatocyte incubations

Hepatocytes were incubated with 50-1000 μ M phenformin in the absence and presence of 100 μ M quinine for 6 hours in incubation buffer and only used if control values were greater than 60% as assessed by trypan blue exclusion at 6 hours. After 6 hours viability was assessed using trypan blue exclusion and ATP content and samples for metabolism were taken.

4.2.4 Cultured hepatocyte isolation

Hepatocytes isolated at Pfizer for hepatocyte culture were isolated as in chapter 3.2.11.

4.2.5. Cellomics analysis

Hepatocytes were dosed with 0-200 μ M phenformin dissolved in basal media for 24, 48 or 72 hours. At each time point the media was removed and replaced with basal media containing Hoechst 33342 (1 in 10000), TMRM (1 in 200) and TO-PRO 3 iodide (1 in 1000). Plates were then returned to the incubator for 20 minutes to allow uptake of the dyes. The plates were then read using Cellomics technology.

4.2.6. HPLC and LC-MS sample preparation

At the end of the incubation period samples were stopped by the addition of an equal volume of ice-cold ACN and were then stored at -20°C overnight to precipitate protein. The samples were then spun at 2200rpm for 10 minutes and the supernatant removed. The supernatant was then dried down under a gentle stream of nitrogen gas. Once the samples were dried they were reconstituted in 300 μ l dH₂O and centrifuged twice at 14,000 rpm for 5 minutes to remove any remaining debris. The samples were then run on either the HPLC or mass spec. Samples not run immediately were stored at -20°C until analysis.

4.2.7 HPLC method

The HPLC system consisted of a Phenomenex Gemini-NX C18 column (4.6x250mm, 5 μ), a Dionex HPLC, with auto-sampler and UV detection which was set at 236nm. The mobile phase consisted of 0.1% formic acid (A) and 90% methanol 10% ACN (B) with a flow rate of 0.9ml/min. A step wise gradient was run beginning at 5% B and rising to 30% B at 10 minutes. This was then increased further to 70% B at 15 minutes and 100% B at 16 minutes. It was held at 100% B for

1 minute before being returned to 5% B at 18 minutes. The column was then left to re-equilibrate for the next sample until 25 minutes.

4.2.8. LC-MS method

LC-MS analysis was undertaken with an API2000 attached to a Perkin-Elmer LC system. The LC method was the same as section 4.2.7. The MS was operated in positive ion mode. The operating parameters are in table 4.2 below.

CUR	30.00
IS	5000V
TEM	400°C
GS1	30
GS2	75
DP	100
FP	250
EP	10

Table 4.2. Operating parameters for phenformin mass spectrometry.

4.2.9 Lactate measurement

Lactate was measured using a Lactate Assay Kit from Sigma-Aldrich. Samples were snap frozen in liquid nitrogen and stored at -80°C until needed. 200µl of sample was vortexed and centrifuged at 14,000rpm for 10 minutes to remove insoluble material. The sample was then passed through a 10kDa cut-off spin filter to remove any lactate dehydrogenase. The lactate was then measured according to manufacturer's instructions.

4.2.10 Animal work

All animal work was undertaken in accordance with Home Office regulations and local ethics committee procedures.

4.2.11 Statistical analysis

Statistical analysis was undertaken using Stats Direct software. Data was tested for normality using a Shapiro-Wilk test and either a Student's T test (parametric) or Mann Whitney U test (non-parametric) was used to make comparisons between data sets. An ANOVA (Dunnett's comparison to control), for parametric data, or Kruskal-Wallis, for non-parametric data, was used to determine significance to control values.

4.3 RESULTS

4.3.1 Effect of the biguanides on mitochondria in cultured rat hepatocytes

The effects of the biguanides on cytotoxicity and the mitochondrial membrane potential were assessed using cultured rat hepatocytes and Cellomics analysis (figure 4.2-4.). The hepatocytes were incubated with 0-200 μ M of metformin, buformin or phenformin for 24-72 hours. Cytotoxicity was assessed using Hoechst 33342 and the mitochondrial membrane potential using TMRM. Metformin did not induce either significant toxicity or dissipation of the mitochondrial membrane potential at any concentration or time point (figure 4.2). 200 μ M buformin was significantly cytotoxic at all time points (24 hours, 146.238 ± 11.882 % control; 48 hours, 306.575 ± 19.359 % control; 72 hours, 290.312 ± 59.216 % control) but only depleted the mitochondrial membrane potential at 48 and 72 hours (48 hours, 24.241 ± 7.391 % control; 72 hours, 2.356 ± 0.769) (figure 4.3). 200 μ M phenformin showed significant cytotoxicity at all time points but no other concentration of phenformin demonstrated significant toxicity (figure 4.4). The mitochondrial membrane potential was significantly decreased in hepatocytes dosed with 200 μ M phenformin at 24 hours (1.028 ± 0.39 % control) and 48 hours (2.13 ± 0.32 % control). At 72 hours phenformin demonstrated loss of mitochondrial membrane potential at 50 μ M (60.50 ± 5.98 % control), 100 μ M (65.08 ± 3.59 % control) and 200 μ M (3.21 ± 1.21 % control). The significant depletion of mitochondrial membrane potential before onset of cytotoxicity implies that in cultured hepatocytes the dissipation of the mitochondrial membrane potential is a possible cause of cell death. Based on these results phenformin was taken forward to use as a tool for the assessment of mitochondrial toxicity in primary rat hepatocytes.

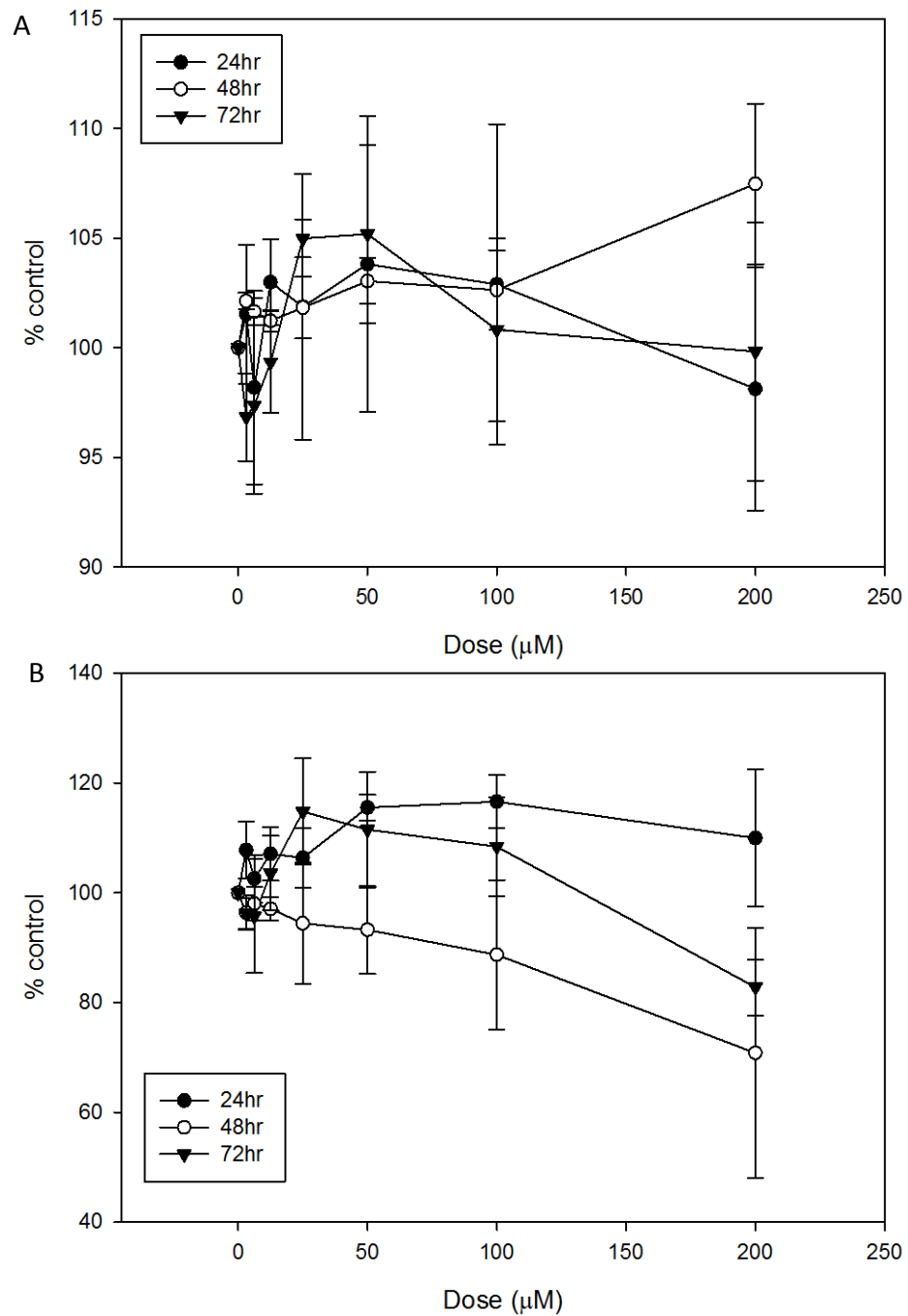


Figure 4.2. Cellomics analysis of metformin in cultured rat hepatocytes. (A) Hoechst staining for cytotoxicity metformin. (B) TMRM intensity in hepatocytes treated with metformin. Data is % control values and is expressed as mean \pm SEM. Data is from 3 independent isolations.

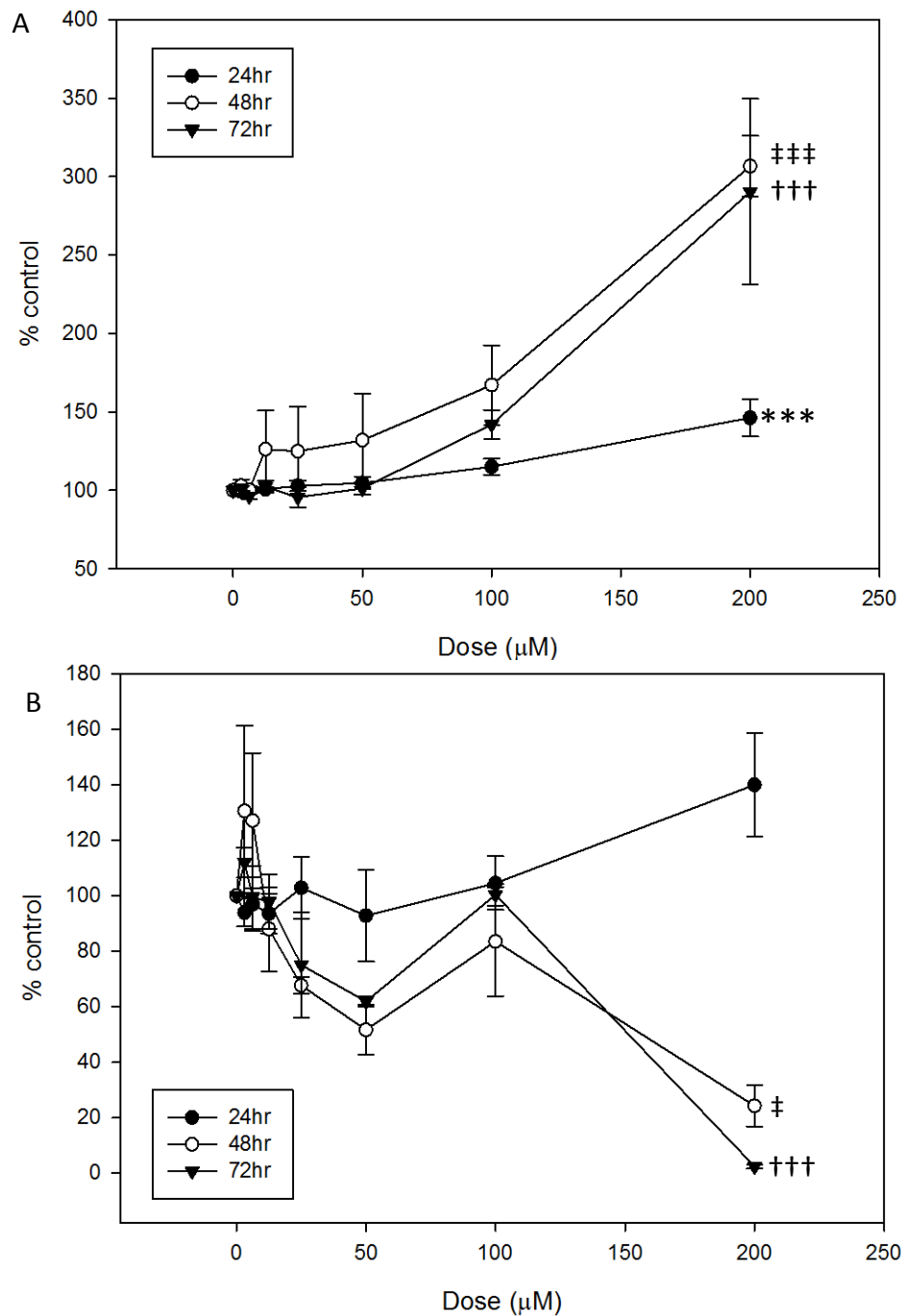


Figure 4.3. Cellomics analysis of buformin in cultured rat hepatocytes. (A) Hoechst staining for cytotoxicity of buformin. (B) TMRM intensity in hepatocytes treated with buformin. Data is % control values and is expressed as mean \pm SEM. Data is from 3 independent isolations. Significance was determined using ANOVA (Dunnett's comparison to control) *** $P < 0.001$ 24hours; ‡ $P < 0.05$ ‡‡‡ $P < 0.001$ 48 hours; ††† $P < 0.001$ 72 hours.

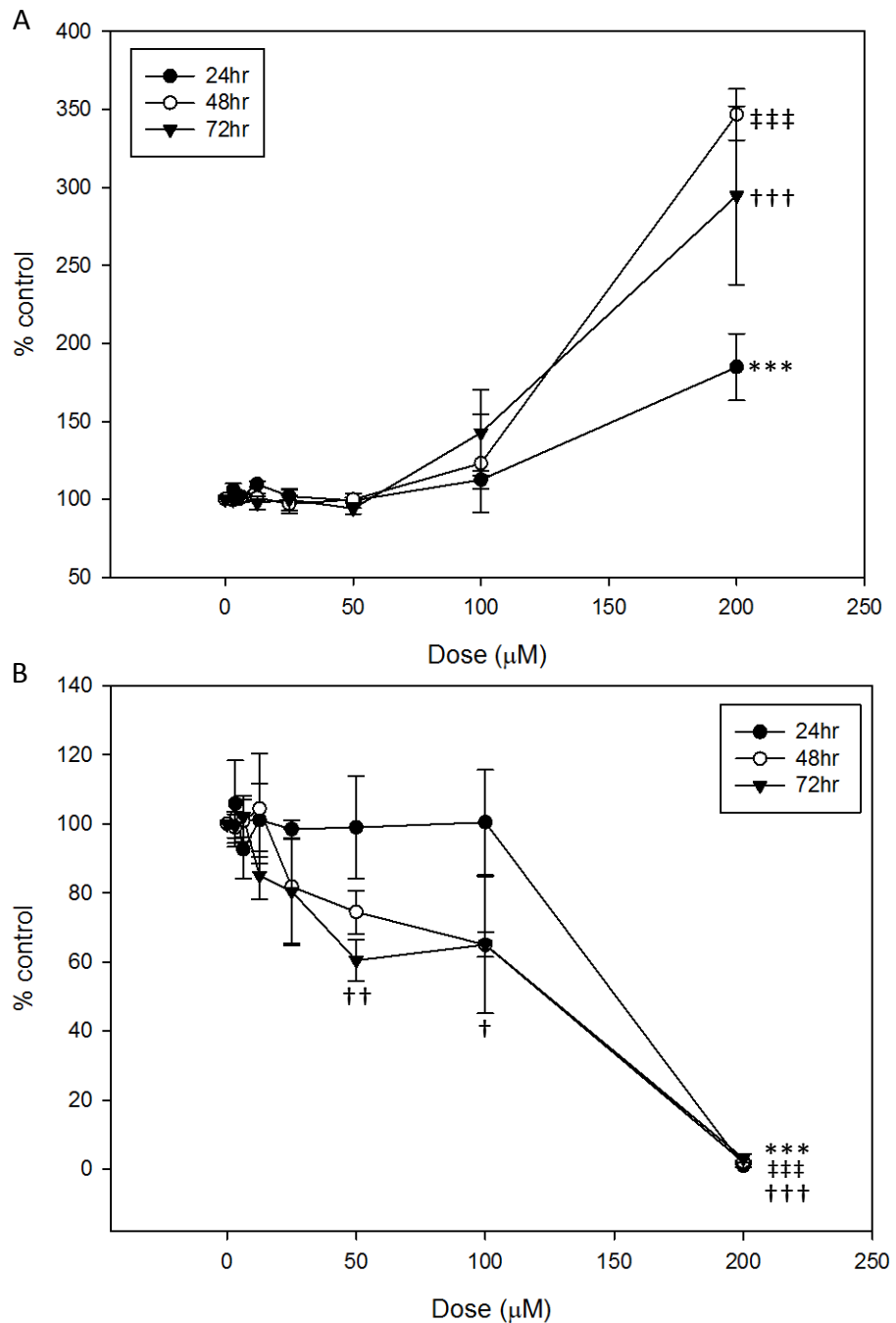


Figure 4.4. Cellomics analysis of phenformin in cultured rat hepatocytes. (A) Hoechst staining for cytotoxicity of phenformin. (B) TMRM intensity in hepatocytes treated with phenformin. Data is % control values and is expressed as mean \pm SEM. Data is from 3 independent isolations. Significance was determined using ANOVA (Dunnett's comparison to control) *** $P < 0.001$ 24hours; ††† $P < 0.001$ 48 hours; † $P < 0.05$ †† $P < 0.01$ ††† $P < 0.001$ 72 hours.

4.3.2 The investigation of metabolism of phenformin in primary rat hepatocytes

The metabolism of phenformin was determined in freshly isolated suspension rat hepatocytes between 50-1000 μ M. In this system phenformin was completely turned over at concentrations of 200 μ M and less to 3 metabolites (M1-M3) demonstrated in figure 4.6. Metabolites M1-M3 were all identified through searches for m/z 60, $[C(NH_2)_3]^+$, a fragment ion distinctive to the biguanide class of drugs (figure 4.5). All 3 of these metabolites were discovered to be glucuronides. M1 (m/z 398) was determined to be an [OH] phenformin glucuronide and is assumed to be the 4'-OH-phenformin that has previously been identified. Novel metabolites M2 (m/z 414) and M3 (m/z 428) were determined to be a [2OH] phenformin glucuronide and a [OH, OMe] phenformin glucuronide respectively.

At concentrations greater than 200 μ M the metabolism of phenformin to both phase I and phase II metabolites became saturated. In these samples the phase I aglycones of the glucuronide metabolites M1 and M3 could be identified (figure 4.7). In samples containing 1000 μ M phenformin the phase I metabolites [OH] phenfomin (M4) and [OH, OMe] phenformin (M5) were determined. Again the [OH] metabolite is assumed to be 4'-OH-phenformin. The fragment ions of each of the metabolites can be found in table 4.3.

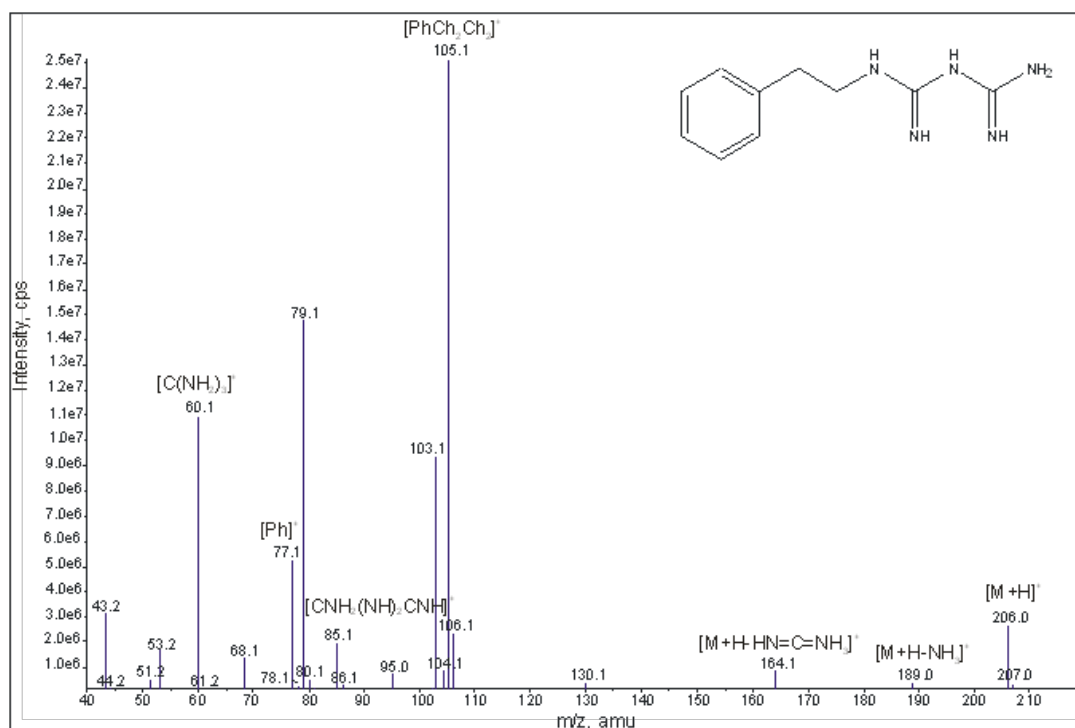


Figure 4.5. Product ion spectra of [M+H]⁺ ions of phenformin. Important fragments are highlighted in brackets.

	Metabolite	m/z	Fragment ions
M1	[OH] phenformin glucuronide	398	60.2, 121.1, 180.0, 205.0, 222.0, 398.1
M2	[2OH] phenformin glucuronide	414	137.1, 196.0, 218.1, 238.1, 414.1
M3	[OH, OMe] phenformin glucuronide	428	60.1, 121.1, 151.1, 210.1, 222.1, 235.1, 252.1, 398.0, 428.1
M4	[OH] phenformin	222	60.1, 77.1, 91.1, 93.1, 103.1, 121.1, 180.1, 222.0
M5	[OH, OMe] phenformin	252	60.1, 91.2, 119.2, 151.0, 252.1

Table 4.3. Fragment ions of phenformin metabolites identified in freshly isolated rat hepatocytes.

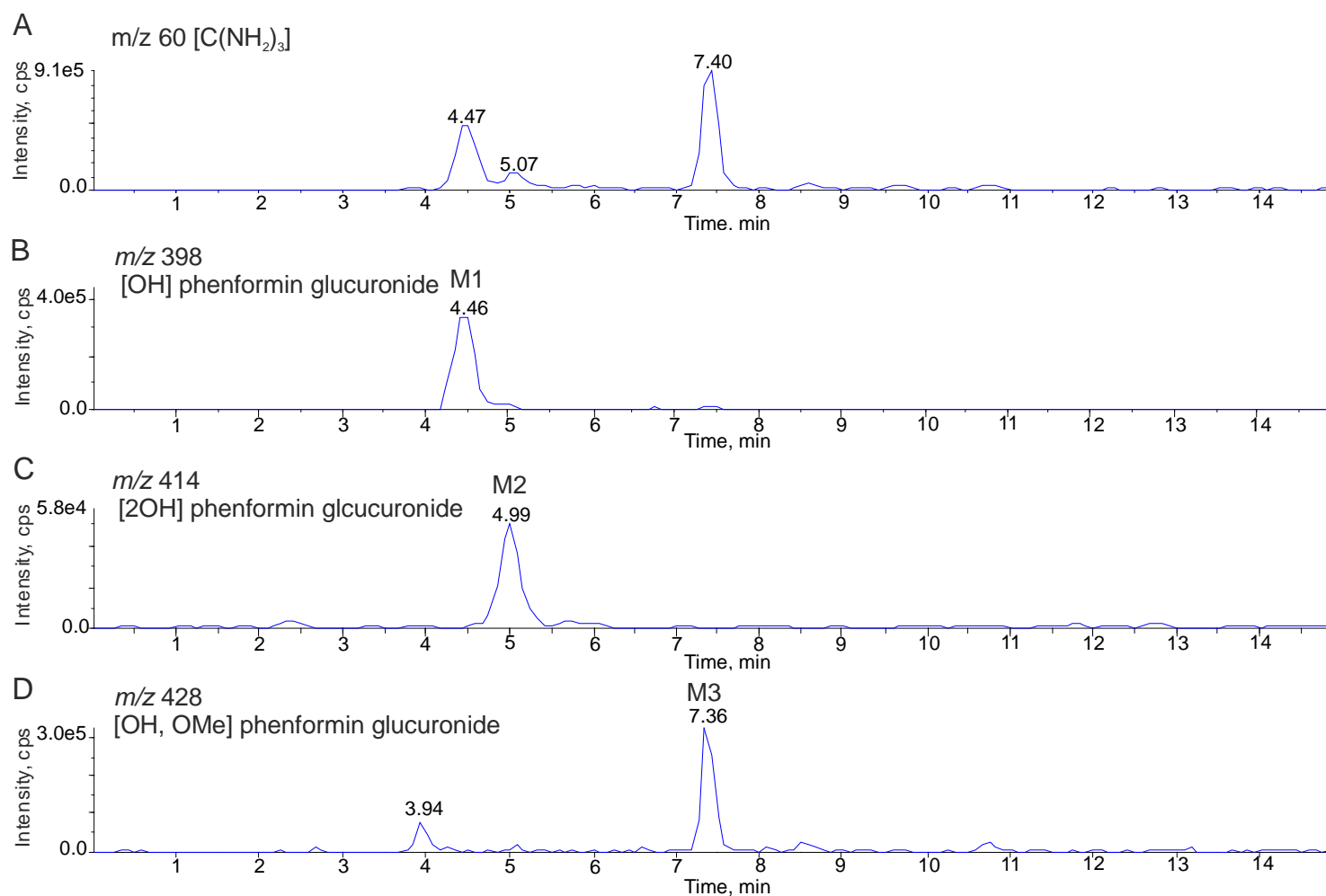


Figure 4.6. Representative traces of 100 μ M phenformin metabolites identified in rat hepatocytes. (A) Extracted ion current m/z 60 (B) [OH] phenformin glucuronide (m/z 398) (C) [2OH] phenformin glucuronide (m/z 414) (D) [O, OMe] phenformin glucuronide.

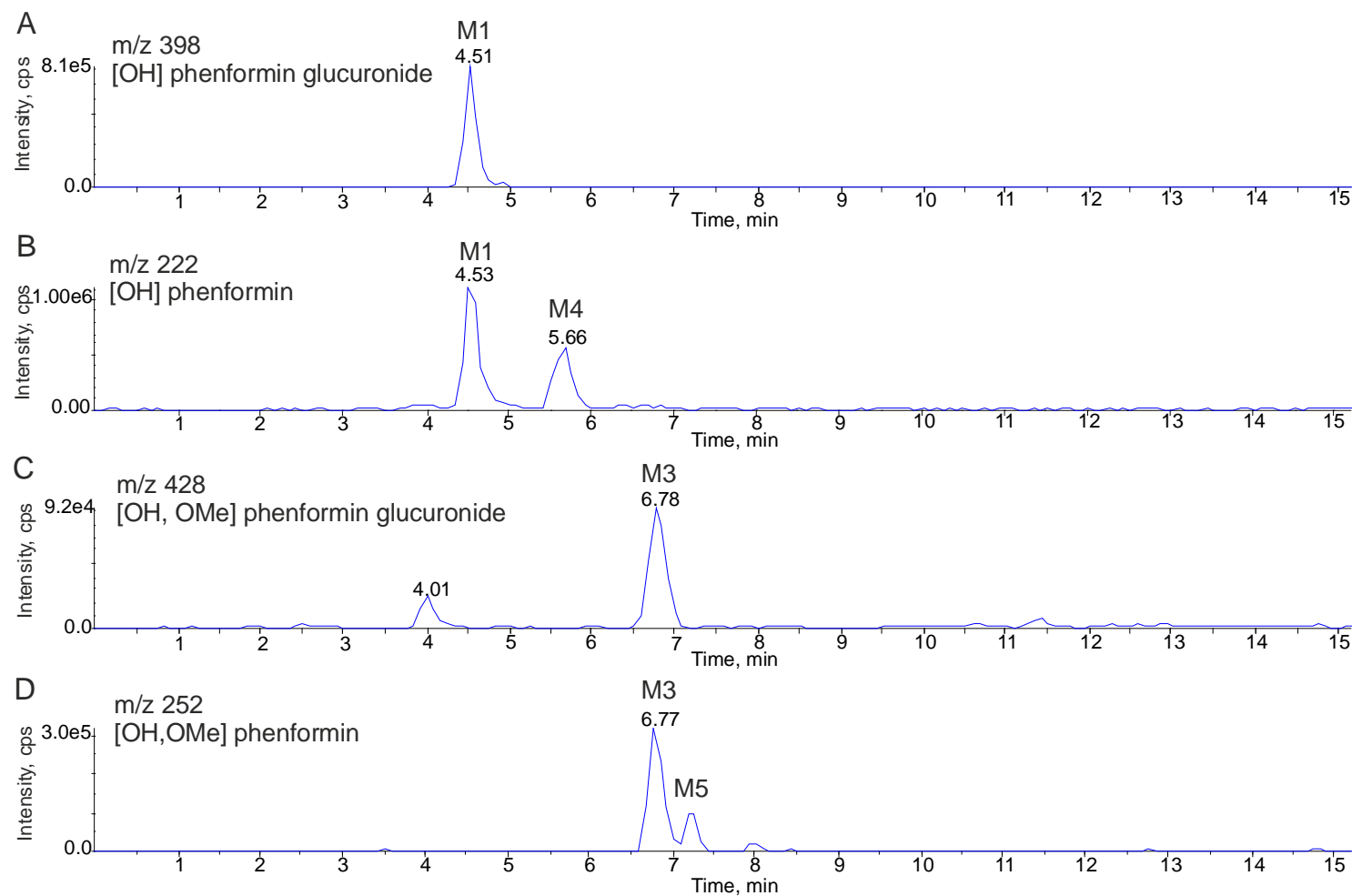


Figure 4.7. Representative traces of 1000 μ M phenformin metabolites identified in rat hepatocytes. (A) XIC m/z 398 [OH] phenformin glucuronide. (B) XIC m/z 222 [OH] phenformin. (C) XIC 428 [OH, OMe] phenformin glucuronide. (D) XIC m/z 252 [OH, OMe] phenformin.

4.3.3 Investigations of quinine and quinidine as CYP450 2D inhibitors in rat hepatocytes

Quinidine is a well known CYP450 2D6 inhibitor in humans and is widely used in both human and rodent samples. However, it has been reported that its stereoisomer quinine is a more potent CYP450 2D inhibitor in the rat. To investigate the inhibitory properties of quinine and quinidine on phenformin metabolism, inhibition studies were undertaken in the rat hepatocytes and the metabolism assessed using HPLC and LC-MS. Quinine was clearly the most effective inhibitor of phenformin in rat hepatocytes (figure 4.9 and 4.10) with only small amounts of metabolites detectable using HPLC and LC-MS.. Additionally, it appears to partially inhibit the glucuronidation of the small amount of hydroxyphenformin that was produced. Based on the intensity of metabolite peaks quinidine (figure 4.8 and 4.12) was much less effective as an inhibitor of phenformin hydroxylation than quinine (figure 4.11.). It did, however, completely prevent further oxidation of hydroxyphenformin to the catechol intermediate. Like quinine, it also appeared to inhibit glucuronidation of the hydroxyphenformin that was formed.

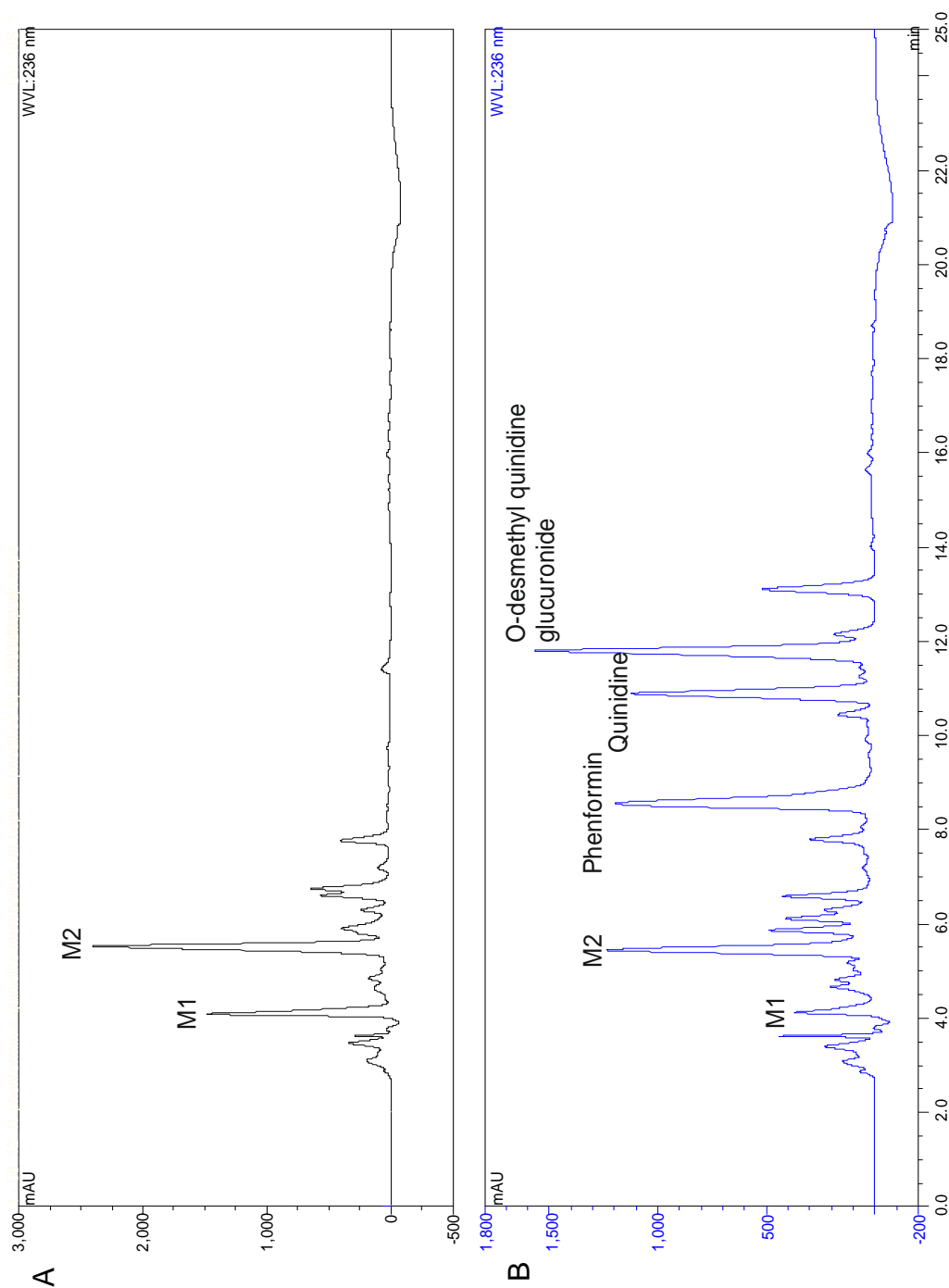
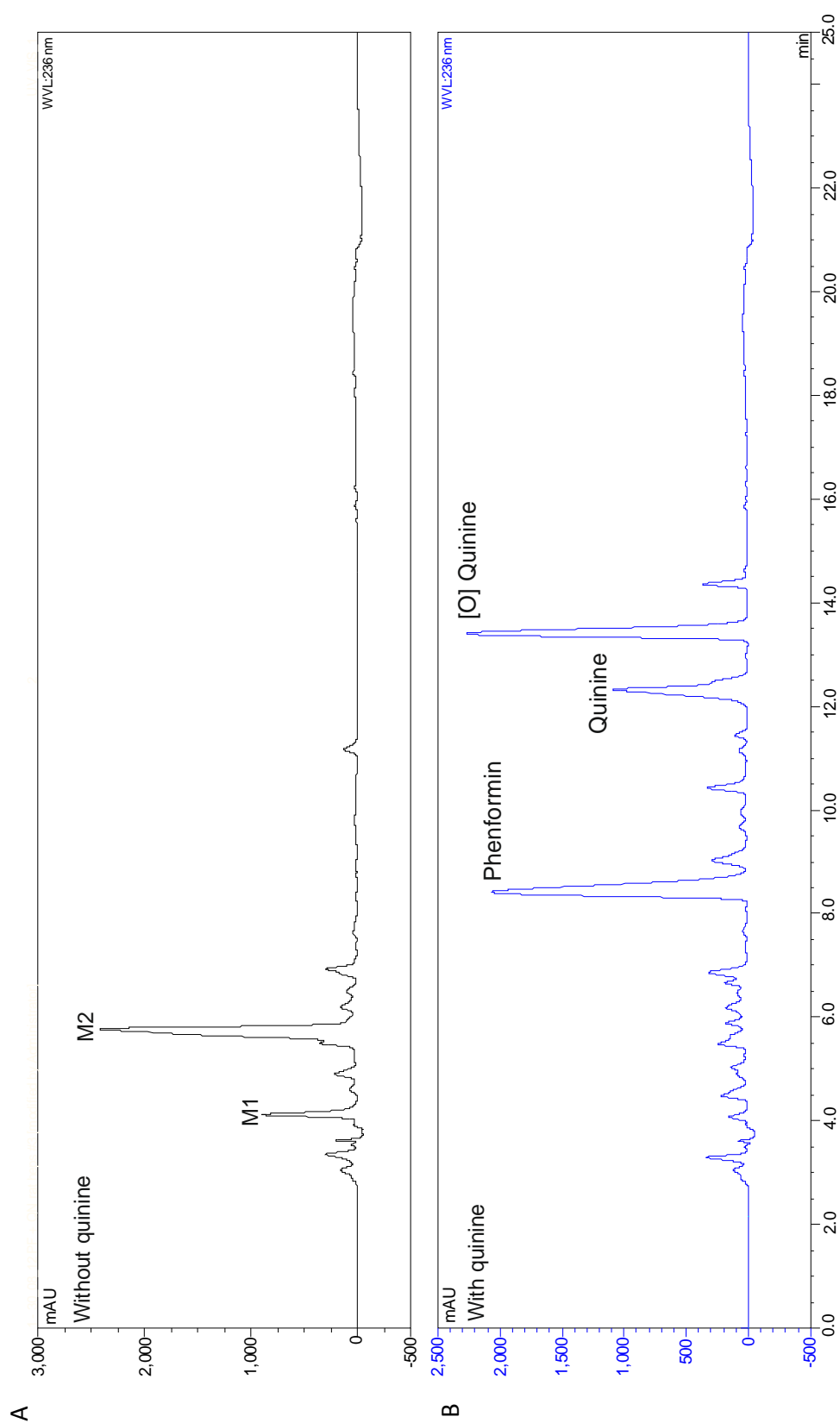


Figure 4.8. Representation of HPLC trace of phenformin (100 μM) turnover in the absence and presence of quinidine. (A) HPLC of 100 μM phenformin without quinidine (B) HPLC of 100 μM phenformin with quinidine.



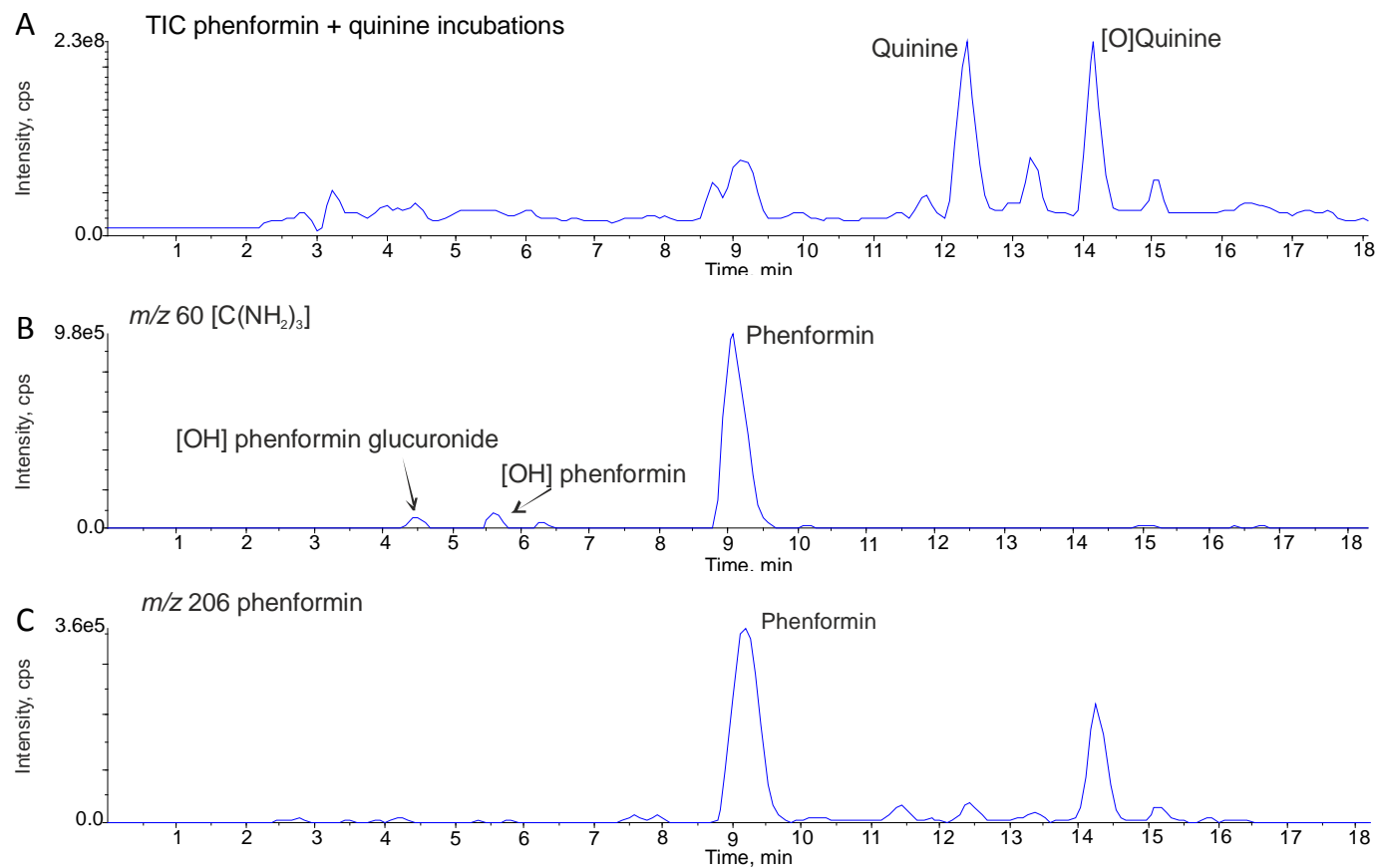


Figure 4.10. Inhibition of phenformin metabolism by quinine in rat hepatocytes. (A) TIC of phenformin and quinine in rat hepatocytes (B) XIC m/z 60. (C) XIC m/z 206 phenformin.

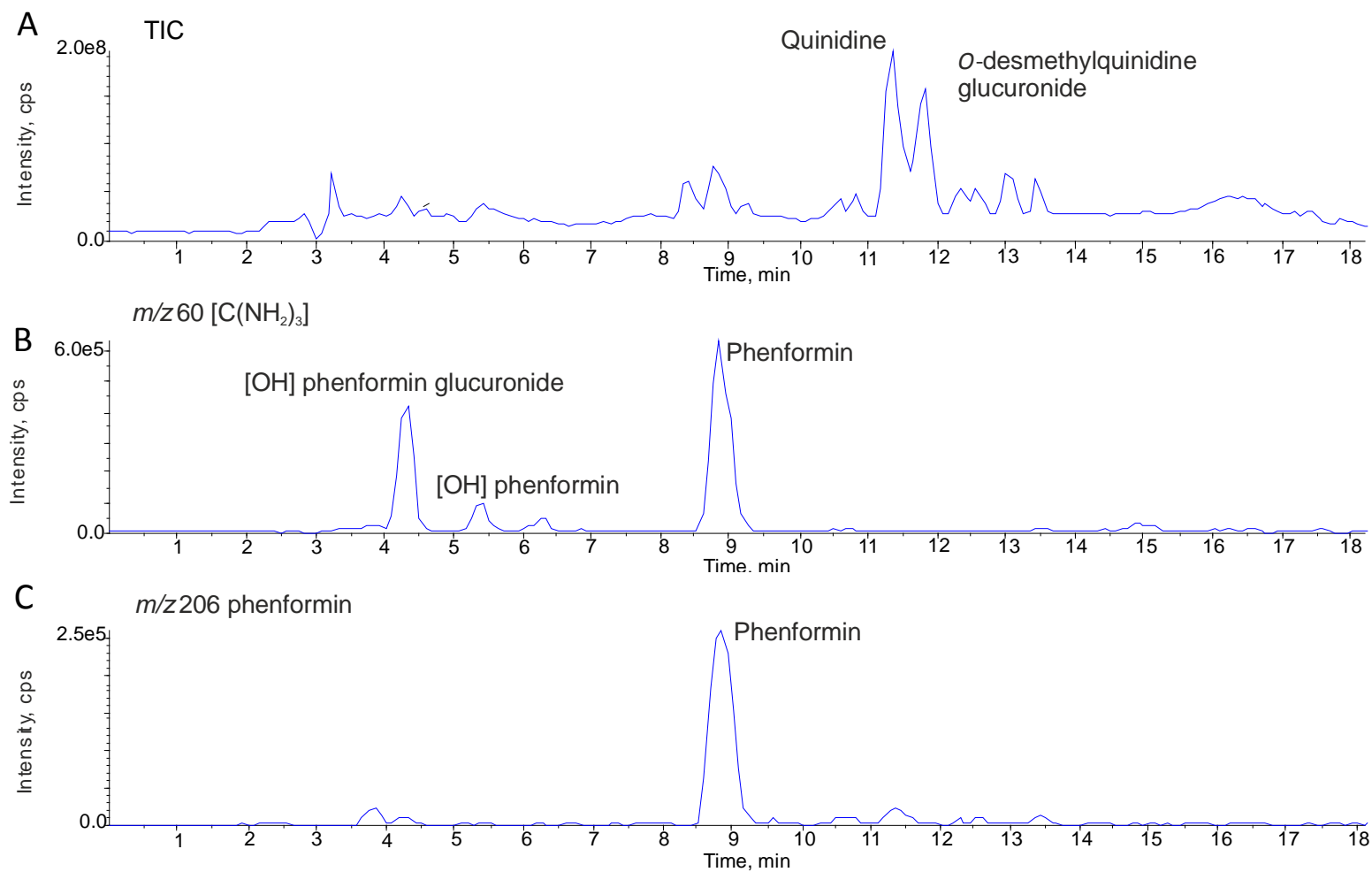


Figure 4.11. Inhibition of phenformin metabolism by quinidine in rat hepatocytes. (A) TIC of phenformin and quinidine in rat hepatocytes. (B) XIC m/z 60 $[C(NH_2)_3]$ (C) XIC m/z 206 phenformin.

4.3.4. Effect of CYP2D inhibition on turnover of phenformin in suspension rat hepatocytes

The inhibition of the turnover of 0-1000 μ M phenformin by quinine (100 μ M) was assessed using HPLC (figure 4.13). The difference between the AUC of phenformin in samples without and with quinine was investigated. Quinine had a significant effect on the turnover of phenformin in hepatocytes dosed with 100 μ M (0 ± 0 without quinine vs 318.03 ± 87.85 with quinine) and 200 μ M (47.30 ± 47.30 without quinine vs 648.80 ± 121.28 with quinine) phenformin. Quinine also seemed to have an effect at 500 μ M (714.90 ± 214.91 without quinine vs 1128.89 ± 68.38 with quinine) 1000 μ M (13320.96 ± 48.11 without quinine vs 1400.17 ± 26.67 with quinine) but this was not significant (figure 4.12).

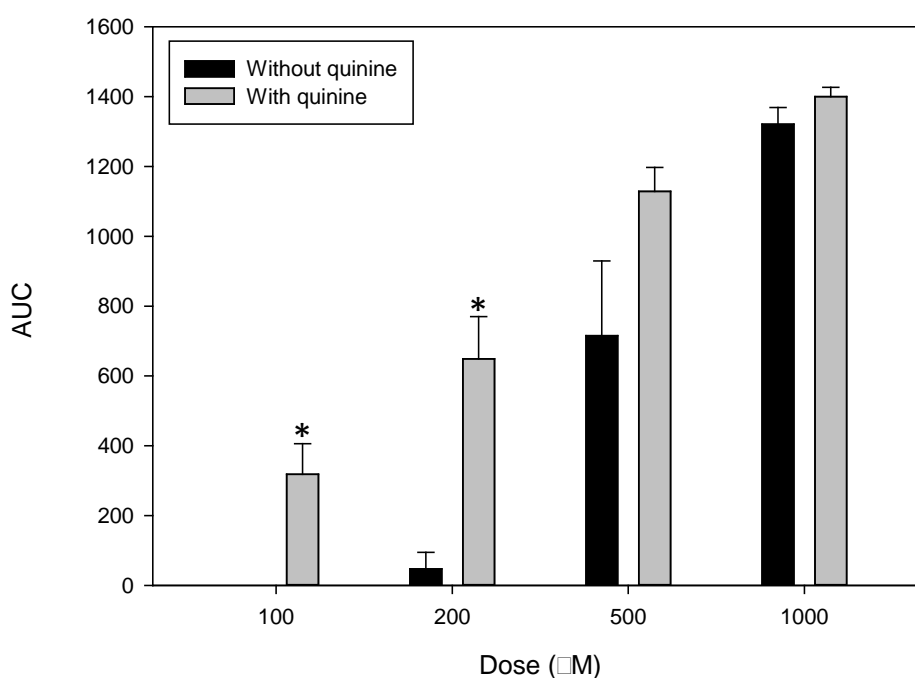


Figure 4.12. Effect of quinine on the turnover of phenformin in rat hepatocytes. Hepatocytes were treated with 0-1000 μ M phenformin in the presence of quinine (100 μ M) and the difference in turnover assessed by AUC of phenformin peak. Data is mean AUC \pm SEM from four independent isolations. Statistical significance was determined using a Mann Whitney U test. *P<0.05

4.3.5 Effects of CYP2D6 inhibition on the toxicity of phenformin in suspension rat hepatocytes

The effect of 0-1000 μ M phenformin on the viability of suspension was investigated in the presence and absence of quinine using trypan blue exclusion (figure 4.13.). Quinine concentrations of 0-100 μ M were initially tested for cytotoxicity and it was determined that none of these concentrations were cytotoxic. The viability of hepatocytes treated with 100 μ M quinine after 6 hours were $101.28 \pm 2.89\%$ control (n=4). Phenformin was only significantly cytotoxic to hepatocytes at 500 μ M and above, however when the hepatocytes were incubated in the presence of quinine only 1000 μ M phenformin was significant compared to control values. This demonstrated a trend towards decreased cell viability when cells were incubated in the presence of quinine but this decrease was not significant at any concentration.

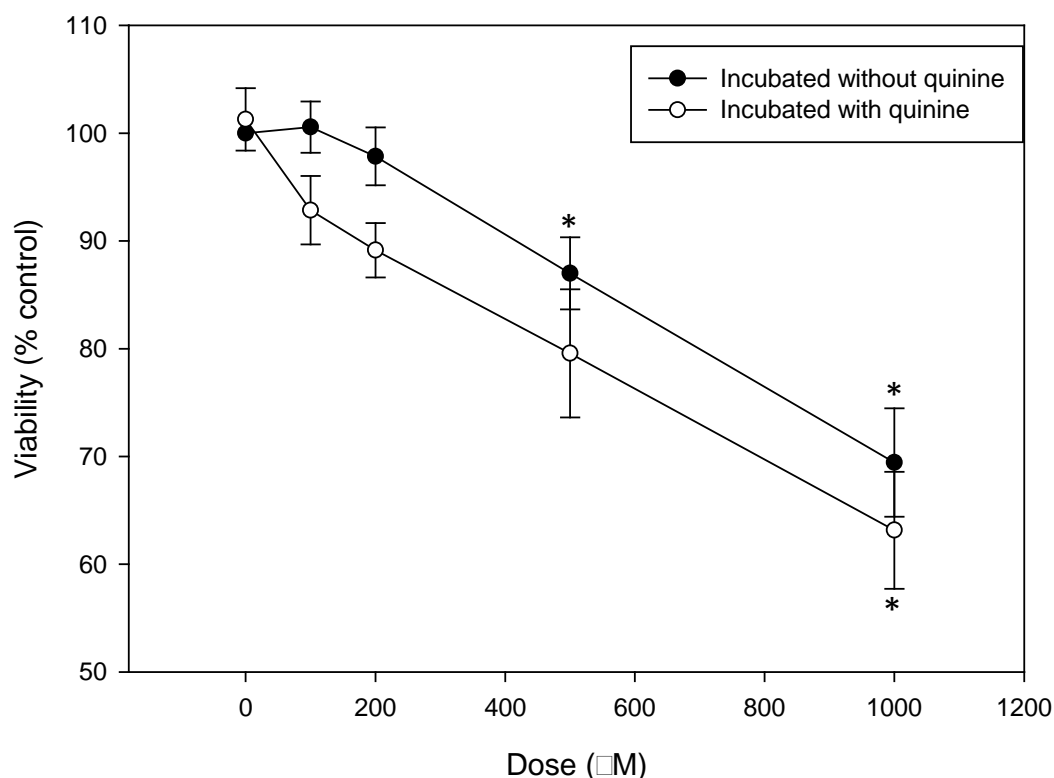


Figure 4.13. Cell viability of hepatocytes treated with phenformin in the presence (○) and absence (●) of phenformin. Data is expressed as mean \pm SEM % control and are from 7 independent isolations. Significance to control was determined using Kruskal-Wallis $*P < 0.05$. Significance between data points was determined using Mann Whitney U test but the difference between the data was not significant.

4.3.6. Effect of phenformin on lactate levels in suspension hepatocytes

The lactate levels of hepatocytes treated with phenformin did not appear to increase until 1000 μ M phenformin when lactate concentrations were elevated 3.2 fold that of control values. When phenformin was incubated with quinine the lactate concentration of the cell was considerably higher than with phenformin alone. The most noticeable difference was at 500 μ M phenformin where the lactate concentration in the presence of quinine was 2.7 fold that of phenformin alone (figure 4.14).

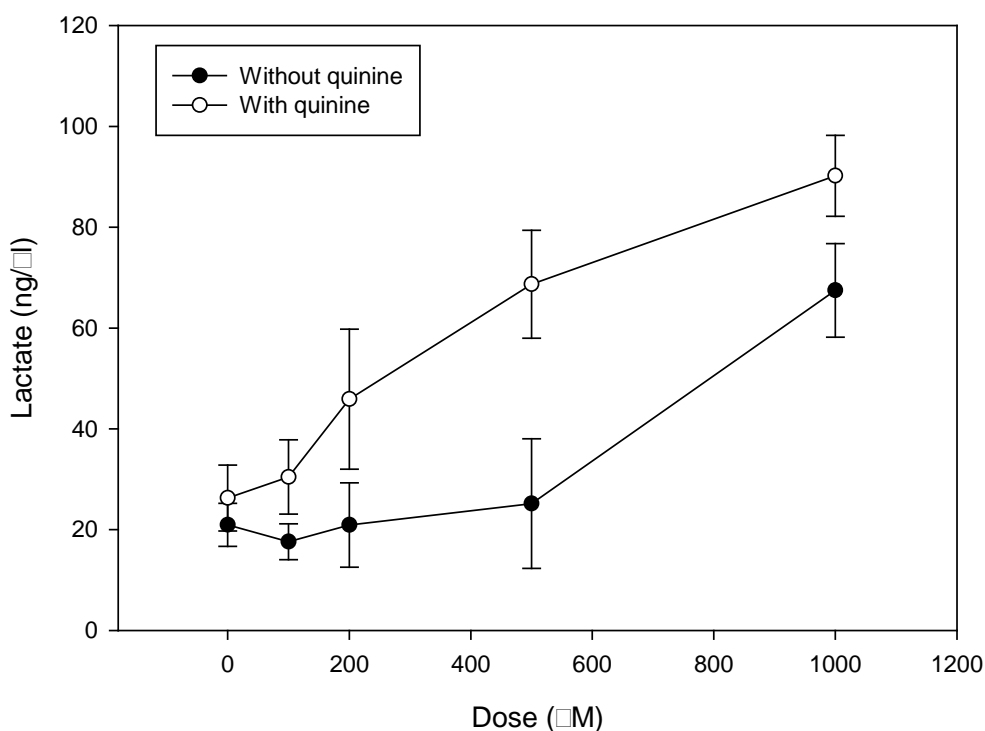


Figure 4.14. Concentration of lactate in hepatocytes treated phenformin in the presence (\circ) and absence (\bullet) of quinine. Data is expressed as ng/ μ l and is mean \pm SEM from two independent isolations.

4.4 DISCUSSION

The principal aims of this chapter were to establish whether there was a link between inhibition of phenformin metabolism and mitochondrial toxicity. Phenformin had a high turnover in rat hepatocytes, which could be inhibited with inclusion of quinine in the incubation. Increased phenformin concentrations in hepatocytes, as measured by HPLC, correlated with an increase in lactate concentrations. In cultured hepatocytes there was also evidence that phenformin dissipates the mitochondrial membrane potential which may have a role in phenformin induced lactic acidosis.

Phenformin was metabolised in rat hepatocytes to five detectable metabolites. At lower concentrations of phenformin (<200 μ M) the metabolites consisted completely of glucuronides and it was only when the concentration became high enough to saturate metabolism (>200 μ M) that the aglycones of the glucuronide metabolites became detectable. Previous studies of phenformin metabolites have only identified hydroxyphenformin and the corresponding glucuronide as metabolites (Guest, King & Parke 1979, Alkalay, Volk & Roth 1979). In rat hepatocytes, however, hydroxyphenformin underwent both further hydroxylation and methylation reactions. Whether these metabolites would be formed *in vivo* or whether the reduced environment of hepatocyte suspension leads to further metabolic transformations remains to be seen.

Plasma concentrations of phenformin do not always correlate with an onset of lactic acidosis (Irsigler, Kritz & Regal 1979). The identification of OCT1 in the transport of metformin (Sogame et al. 2009) and more recently the accumulation of phenformin in the liver of rats leading to concentrations 61-fold those in the serum (Sogame et al. 2011) suggest that the source of lactic acidosis may be in the liver,

this is supported by a case study that estimated that liver concentrations were 24-26 fold that of serum phenformin concentrations (Irsigler, Kritz & Regal 1979). Lactate concentrations in hepatocytes increased >3-fold in hepatocytes treated with high (1000 μ M) concentrations of phenformin, compared to control.

Studies of metabolism of phenformin in humans showed that phenformin hydroxylation was mediated by the same enzyme as debrisoquine (Shah, Evans & Oates 1985, Shah et al. 1980, Oates et al. 1982), which is now known to be CYP450 2D6. CYP450 2D6 is responsible for the metabolism of approximately 25% of drugs, but is highly polymorphic. The population can be split into 4 metabolising groups, poor metabolisers (PMs), intermediate metabolisers (IMs), extensive metabolisers (EMs) and ultra-rapid metabolisers (UMs) (Ingelman-Sundberg 2005). CYP2D6 polymorphisms significantly affect the pharmacokinetics of approximately 50% of the CYP2D6 substrates that are used in the clinic (Ingelman-Sundberg 2005), some of the clinical consequences of CYP450 2D6 polymorphisms are demonstrated in figure 4.2. Patients with PM phenotype, which account for approximately 7% of the Caucasian population (Bradford 2002, Sachse et al. 1997), are more likely to develop toxicity due to higher drug plasma or organ concentrations whilst UMs, 1-2% of the Caucasian population (Bradford 2002), are more likely to suffer as a result of lack of efficacy or toxicity resulting from the production of a toxic metabolite. To mimic poor metaboliser phenotype *in vitro*, the metabolism of phenformin was inhibited using quinine in rat hepatocytes. Including quinine in the incubations significantly increased hepatocyte phenformin concentrations. The increase in phenformin concentration was associated with enhanced hepatocyte lactate concentrations. At concentrations of 200-500 μ M phenformin incubated with quinine the lactate concentration increased >x2 phenformin alone.

As demonstrated in cultured rat hepatocytes, phenformin dissipated the mitochondrial membrane potential as measured by TMRM. As phenformin exists in its cationic form at physiological pH, it is a possibility that phenformin can accumulate in the mitochondria against the concentration gradient due to $\Delta\Psi_m$ (Davidoff 1971). Accumulation of other lipophilic cationic drugs such as perhexilene and amiodarone, cause 'OXPHOS uncoupling', which results in a reduction of ATP-synthesis as the re-entry of protons within the mitochondrial matrix bypasses ATP synthase. This explains why the toxicity of the biguanides correlates with lipophilicity, with the most polar biguanide, metformin, the only one to remain on the market. Furthermore, the biguanides are also capable of inhibition of complex I of the mitochondrial transport chain (Dyken, J.A., Jamieson, J., Marroquin, L., Nadanaciva, S., Billis, P.A., Will, Y. 2008, Owen, Doran & Halestrap 2000) J.A. et al. 2000). It has been established that inhibition of complex I leads to inhibition of gluconeogenesis (Owen, Doran & Halestrap 2000). PM phenotype followed by successive accumulation into the liver and then the mitochondria could therefore lead to a concentration of phenformin in the mitochondria several thousand fold that in the serum. This could be enough to inhibit complex I sufficiently to induce lactic acidosis.

The inhibition of gluconeogenesis by the biguanides is part of their primary pharmacology. The inhibition of complex I and OXPHOS uncoupling by the biguanides alters the AMP:ATP ratio which activates AMPK. AMPK becomes activated when the AMP:ATP ratio is altered in favour of AMP, normally during cellular stress, such as hypoxia and ischemia, when ATP production drops. The AMPK pathway leads to the activation of glycolysis for ATP production and the inhibition of gluconeogenesis. This helps to reduce blood glucose levels in diabetics,

hence controlling hyperglycaemia (Hawley et al. 2002, Zhou et al. 2001). However, in PM phenotypes the concentration of phenformin may be enough to inhibit gluconeogenesis to the extent where lactic acidosis is induced.

Recently, the interest in phenformin has been renewed, due to the reports of its potential uses as chemotherapeutic agent for cancer treatment. AMPK activators such as phenformin, can induce apoptosis or cell-cycle arrest in various cancer cell lines of different genetic origin (Caraci et al. 2003, Appleyard et al. 2012, El-Masry, Brown & Dobson 2012). As a result phenformin has been recommended for clinical trials in the treatment of ER-positive and triple negative breast cancer. Genotyping patients for CYP450 2D6 phenotype could help to improve the treatment regimen of patients receiving phenformin and result in a safer re-introduction into the clinic. In conclusion, increased phenformin concentrations achieved by inhibition of CYP450 2D in rat hepatocytes does lead to increased lactate concentrations. This demonstrates the importance of the liver concentration of phenformin in inducing lactic acidosis in patients.

CHAPTER 5

CONCLUDING DISCUSSION

Table of Contents

5.1 INTRODUCTION	165
5.2 EXPLORING THE DIFFERENCES BETWEEN NEFAZODONE AND BUSPIRONE CYTOTOXICITY.	167
5.3 THE USE OF THE BIGUANIDES AS MODEL COMPOUNDS TO STUDY MITOCHONDRIAL TOXICITY.....	171
5.4 FUTURE INVESTIGATIONS: BIOACCUMULATION IN THE MITOCHONDRIA.....	173
5.5 CONCLUDING REMARKS	174

5.1 INTRODUCTION

Adverse drug reactions (ADRs) are a major problem to pharmaceutical companies and health services alike. They account for the attrition of drugs during pre-clinical development as well as the withdrawal of marketed drugs. In the UK, it is reported that 6.5% of hospital admissions are attributable to ADRs (Pirmohamed et al. 2004). ADRs can affect any system within the body; however, the liver is frequently a target of drug toxicity. Drug induced hepatotoxicity is the most cited cause for the removal of drugs from the market and is hard to predict from pre-clinical and clinical testing (Jaeschke et al. 2002). Clinical surveillance in the US has indicated that 50% of acute liver failures are due to drugs. The majority (36%) are caused through paracetamol overdose but 16% of these are idiosyncratic reactions (Ostapowicz et al. 2002).

It is widely accepted that bioactivation plays a role in drug induced liver injury. The ability of a drug to become bioactivated is a function of its chemistry and the structural alerts that lead to bioactivation are well defined (Kalgutkar et al. 2005a). Despite this, the potential of a drug to be bioactivated and cause toxicity is a complex one and many drugs are bioactivated but are not hepatotoxic. Idiosyncratic hepatotoxicity caused by bioactivation is likely to be due to where the drug binds in the cell as well as a function of the patient's biology. This uncertainty in the role of bioactivation and irreversible binding makes it difficult to predict which drugs will be toxic. Further investigations into the roles of bioactivation and mechanisms of toxicity need to be further established.

There is a growing awareness of the role of mitochondria in drug toxicity. Drugs such as troglitazone, diclofenac, nimesulide, valproic acid and amiodarone are all

now known to involve a mitochondrial component in their toxicity. Drugs can affect the mitochondria through a variety of mechanisms, with many causing mitochondrial damage through a mixture of these. Mitochondrial dysfunction often affects the liver due to the high concentrations of xenobiotics to which the liver is exposed. Of the drugs removed from the market due to hepatotoxicity, mitochondrial toxicity will be involved in several cases (Dykens, J.A. and Will, Y et al. 2007).

The aims of this thesis were two-fold:

1. To investigate the role of bioactivation in nefazodone cytotoxicity (chapters 2 and 3).

This led to the characterisation of the bioactivation pathway of nefazodone in both rat and human liver microsomes. The ability of nefazodone to irreversibly bind to hepatic protein was assessed and the formation of quinone-imines was identified through GSH trapping. The bioactivation of nefazodone was further investigated in freshly isolated rat and human hepatocyte suspensions. Assessment of reactive metabolite formation, irreversible binding, total GSH content and cytotoxicity revealed that the parent compound was more cytotoxic towards hepatocytes than its metabolites.

2. To investigate mechanisms underlying mitochondrial toxicity (chapter 4)

The known mitochondrial toxins, the biguanides, were selected for these studies. Phenformin, in particular, was investigated due to the greater cytotoxicity observed in cell line and cultured hepatocytes (chapter 4) vs the other biguanides (Dykens et al. 2008). Difficulties of assessing parent compound cytotoxicity in freshly isolated hepatocytes had to be taken into account (due to the higher metabolic capability vs

cell lines); therefore, studies into the metabolism of phenformin were undertaken. Also, cytotoxicity and lactic acid formation was examined in the presence and absence of CYP450 2D inhibition, as phenformin causes lactic acidosis rather than overt hepatotoxicity in the clinic.

Bioactivation, irreversible binding and mitochondrial liability in *in vitro* models can give hazard signals with specific compounds, but as this work demonstrates, the complete mechanism must be examined using both model compounds and non-toxic analogues, in order to gain a more thorough pathogenesis. This emphasises the fact that although knowledge of *in vitro* liabilities of compounds can help in pre-clinical decision making, attrition of a compound during pre-clinical testing, for example, due to bioactivation potential alone could prevent the development of useful drugs. This highlights the need for a battery of tests in pre-clinical decision making involving both reactive metabolite formation and mitochondrial toxicity.

5.2 EXPLORING THE DIFFERENCES BETWEEN NEFAZODONE AND BUSPIRONE CYTOTOXICITY.

The ability of nefazodone, but not buspirone, to be bioactivated is thought to be the reason for the difference in their safety profiles (Kalgutkar et al. 2005b). Nefazodone has also been associated with mitochondrial dysfunction (Dykens et al. 2008) and transporter inhibition (Kostrubsky et al. 2006) and these studies identified parent compound as the toxic agent (figure 5.1). The aims of this section of work were to establish the link between nefazodone bioactivation and cytotoxicity.

The work carried out in chapter 2 demonstrated the bioactivation of nefazodone. In supplemented rat and human liver microsomes, GSH conjugates of nefazodone were identified. Significant irreversible binding of radiolabelled nefazodone to rat liver microsomes also confirmed bioactivation. In concordance with other studies

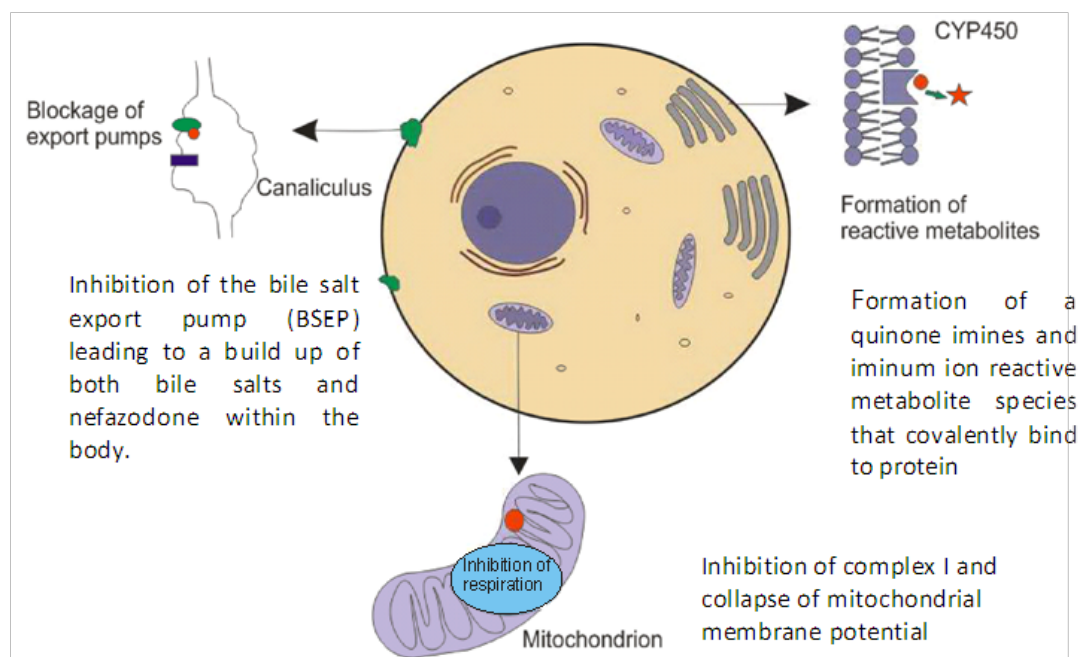


Figure 5.1. Proposed mechanisms of nefazodone mediated liver injury. There are three proposed mechanisms of nefazodone mediated liver injury in the literature. Nefazodone can undergo bioactivation to a quinone-imine that may cause hepatotoxicity through covalent binding to protein. Nefazodone has also been shown to inhibit complex I of the OXPHOS chain and BSEP in vitro, independently of hepatic metabolism.

(Kalgutkar et al. 2005b), GSH conjugates of buspirone were not identified, even though *para* hydroxylation was deemed to have taken place. Buspirone did exhibit significant NADPH dependent irreversible binding as compared to control values, however, this was several fold lower than the binding displayed by nefazodone. From these studies it did appear as though the bioactivation of nefazodone, but not buspirone could be the cause of cytotoxicity, however, liver microsomes do not contain a full complement of metabolising enzymes. Therefore, the use of primary

hepatocytes was employed to investigate the bioactivation and cytotoxicity of nefazodone and buspirone (chapter 3).

Metabolism studies carried out in primary rat hepatocytes did not identify any GSH conjugates of nefazodone, despite their previous discovery in liver microsomes. It is postulated that this is due to a high rate of glucuronidation and sulfation prevailing over bioactivation and GSH conjugation. As with liver microsomes buspirone did not produce a GSH conjugate. Despite a lack of GSH conjugation both nefazodone and buspirone both displayed significant irreversible binding over time. Buspirone also caused significant GSH depletion without causing a reduction in cell viability until concentrations reaching 1mM (200,000x serum C_{\max}). In contrast, the increase in irreversible binding of nefazodone and corresponding decrease in cell viability seemed to indicate that bioactivation was a possible mechanism for cytotoxicity. The use of the CYP450 inhibitor, ABT, decreased irreversible binding but paradoxically decreased cell viability. In this primary rat hepatocyte model of nefazodone toxicity it was therefore deemed that reactive metabolite formation was not the cause of cytotoxicity.

Nefazodone cytotoxicity was also assessed in primary human hepatocytes. In human hepatocytes nefazodone exhibited similar cytotoxicity to rat hepatocytes. Metabolism studies were also undertaken and as with rat hepatocytes, no GSH conjugates of nefazodone were identified. Due to the limitations of the availability of liver and suitable hepatocyte isolations, inhibition of nefazodone metabolism using ABT could only be carried out once, but this demonstrated the same pattern of increased cytotoxicity as in rat hepatocytes.

Concluding discussion

Type of reaction	Effect on cells	Seen with nefazodone
Hepatocellular	Direct effect or production by enzyme-drug adduct leads to cell dysfunction, membrane dysfunction, cytotoxic T-cell response	Yes
Cholestasis	Injury to canalicular membrane and transporters	Yes
Immunoallergic	Enzyme-drug adducts on cell surface induce IgE response	No
Granulomatous	Macrophages, lymphocytes infiltrate hepatic lobule	Yes
Microvesicular fat	Altered mitochondrial respiration, β -oxidation leads to lactic acidosis and triglyceride accumulation	No
Steatohepatitis	Multifactorial	Yes
Autoimmune	Cytotoxic lymphocyte response directed at hepatocyte membrane components	No
Fibrosis	Activation of stellate cells	Yes
Vascular collapse	Causes ischemic or hypoxic injury	Yes
Oncogenesis	Encourages tumour formation	No
Mixed	Cytoplasmic and canalicular injury, direct damage to bile ducts	Yes

Table 5.1. The clinical presentation of nefazodone induced liver injury.

Drug induced hepatotoxicity can mimic natural disease processes making a diagnosis of DILI difficult. Bioactivation and/or mitochondrial dysfunction are generally thought to be an initiating factor and it is a possibility that in humans a mixture of causes for nefazodone hepatotoxicity exist (table 5.1). Case studies indicate that the onset of nefazodone injury occurs between 4 and 28 weeks after initiation of nefazodone treatment and patients presented with symptoms of jaundice and malaise (Aranda-Michel et al. 1999, Aranda-Michel et al. 1999, Lucena et al. 1999, Eloubeidi, Gaede & Swaim 2000, Schirren, Baretton 2000, Tzimas, Dion & Deschênes 2003). Histopathological findings from patients with liver injury suggest that the idiosyncratic reaction in patients is due to mixed aetiologies. Centrilobular necrosis, which is commonly associated with DILI, was identified in all patients. Many patients also exhibited cholestasis, demonstrating a disruption of bile flow, possibly through an inhibition of BSEP by nefazodone. Some patients also had ballooning

degeneration, which is commonly seen in patients with non-alcoholic steatohepatitis, and is, therefore, likely to be as a result of mitochondrial damage to the cell.

Whilst it can be concluded that in rat hepatocytes reactive metabolite formation is not responsible for cytotoxicity, it very difficult to extrapolate this to the clinic. The mechanism of nefazodone hepatotoxicity in patients could not be fully elucidated and it is likely that, in humans, nefazodone toxicity is mediated through a variety of different mechanisms. The case of buspirone also highlights that whilst it is important to be aware of the irreversible binding and bioactivation potential of a compound, irreversible binding alone should not be used as a determining factor for drug failure in pre-clinical safety testing.

5.3 THE USE OF THE BIGUANIDES AS MODEL COMPOUNDS TO STUDY MITOCHONDRIAL TOXICITY

There is an ever increasing awareness of the involvement of the mitochondria in DILI. Mitochondria can be involved in DILI either as a direct target of toxicity or indirectly through initiation of cell death pathways. This is highlighted through the association of nefazodone with mitochondrial liabilities. However, due to the complex nature of nefazodone metabolism it is not an ideal compound for investigating mitochondrial toxicity and, therefore, the known mitochondrial toxins, the biguanides, were chosen as tools for exploring mitochondrial toxicity in primary hepatocytes.

Initially, work was carried out to investigate the effect of the biguanides on the mitochondrial membrane potential in cultured hepatocytes. In agreement with the literature (Dykens et al. 2008), this showed that phenformin and buformin were the most potent inducers of mitochondrial dysfunction and cytotoxicity, hence it was

decided that phenformin should be taken forward to study mitochondrial dysfunction. Investigations in primary hepatocytes have to take into account hepatic metabolism and consequently initial investigations explored the metabolism of phenformin. The turnover of phenformin in rat hepatocytes was high and consisted mainly of hydroxylation and subsequent glucuronidation. Previous investigations into the metabolism of phenformin identified 4-hydroxy phenformin and the corresponding glucuronide as the metabolites of phenformin (Guest, King & Parke 1979, Alkalay, Volk & Roth 1979) but in rat hepatocytes further hydroxylation and *O*-methylation reactions took place.

Previously, studies have identified CYP450 2D6 as being responsible for the metabolism of phenformin in man. CYP450 2D6 is highly polymorphic and it has been reported that people with a CYP450 2D6 poor metaboliser phenotype, have higher serum lactate concentrations (Idle et al. 1981, Shah, Evans & Oates 1985, Shah et al. 1980, Oates et al. 1982). To mimic CYP450 2D6 poor metaboliser phenotype in the rat hepatocytes, phenformin was co-incubated with quinine. Inhibition of metabolism did not significantly decrease the cell viability of hepatocytes incubated with phenformin; however, as phenformin is not an overt hepatotoxin this was not a surprising result. The enhanced phenformin concentrations arising from inhibition of CYP450 2D did correspond with an increase in lactate production in hepatocytes.

5.4 FUTURE INVESTIGATIONS: BIOACCUMULATION IN THE MITOCHONDRIA

It has long been established that compounds can accumulate in the mitochondria via the mitochondrial membrane potential. Fluorescent dyes, such as TMRM, use the mitochondrial membrane potential to accumulate in the mitochondria where they lose their positive charge and fluoresce. These dyes are commonly used to assess the presence of a mitochondrial membrane in isolated mitochondria and intact cells. However, cationic lipophilic compounds are able to accumulate in the mitochondria in the same way. In fact, as mitochondrial $\Delta\Psi$ can be as great as -180mV, as much as a 1000-fold concentration gradient can form across the inner membrane (Dykens et al.2008). Lipophilic anionic compounds do not cross as easily into the mitochondria as they are restricted by the outer membrane, but once inside the inter-membrane space their movement into the mitochondria can be facilitated by mitochondrial anion carrier proteins. As the pH of the mitochondria is pH 8, this traps charged molecules and bioaccumulation can occur.

Investigation into accumulation of xenobiotics within mitochondria using model compounds could help not only to predict mitochondrial liabilities but may also be useful as a pharmacological target. In chapter 4 it was demonstrated that increased concentrations of phenformin lead to increased lactate levels. The biguanides are known to accumulate into the liver via OCT1 (Sogame et al. 2011, Sogame et al. 2009) and it has been demonstrated in isolated heart mitochondria that phenformin can accumulate against a concentration gradient into the mitochondria (Davidoff 1971). This means that the biguanides could accumulate in liver mitochondria several thousand-fold the plasma C_{max} . The biguanides as a class show increasing frequency of lactic acidosis as lipophilicity increases. The biguanides all have a

cationic charge at physiological pH, but the phenyl group on phenformin makes it much more lipophilic than its clinically safer counterpart metformin. Unfortunately, the metabolism of phenformin in metabolically competent cells, such as primary hepatocytes would not make it an ideal tool to investigate such accumulation. Conversely buformin, where the metabolically soft phenyl group is replaced by a butyl group, may be more suitable for such studies.

5.5 CONCLUDING REMARKS

Idiosyncratic reactions are not only a function of the chemistry of a drug but also the biology of the patient. Whilst much of this thesis has focussed on the potential toxicity caused through bioactivation to reactive metabolites, it has also demonstrated that mimicking CYP450 2D6 poor metabolisers, a function of the patient, can induce mitochondrial dysfunction.

The investigations into the bioactivation and nefazodone and buspirone, ultimately concluded that in rat hepatocytes, at least, nefazodone is not responsible for cytotoxicity, but also highlighted the problems of predicting toxicity from bioactivation. The fact that buspirone demonstrated irreversible binding to the same extent as nefazodone in hepatocytes highlights this point. It still remains that in most cases the implications of bioactivation and irreversible binding of a compound cannot be predicted. Irreversible binding can only be a biomarker of bioactivation and not of toxicity. Whilst it is important to consider bioactivation potential and irreversible binding, toxicity studies incorporating these factors must be taken into account. Another important consideration is the predicted dose of the compound. If the dose is expected to be high then the daily body burden of a reactive metabolite is likely to be much higher and, therefore, more likely to overwhelm cellular defences.

Investigations into mitochondrial toxicity, using phenformin, demonstrated the patient component of idiosyncratic drug reactions. The inhibition of metabolism of phenformin demonstrated the increased likelihood of mitochondrial dysfunction that could be faced by CYP450 2D6 poor metabolisers. However, it was demonstrated that phenformin was not a suitable tool for the assessment of mitochondrial dysfunction in primary rat hepatocytes.

The investigations presented in this thesis highlight the importance of understanding the role of drug bioactivation. Knowledge of drug bioactivation helps to further influence whether a drug should be progressed to clinical trials, however, a decision should be made in the context of other safety assessments. A more thorough understanding of the relationship between bioactivation potential and how this relates to clinical situations is required. A greater understanding of *in vitro* systems, and the tools we use to assess them, allows them to be used in an appropriate way in drug discovery and development. Ultimately understanding these *in vitro* tests and the model compounds used to assess them will help us to bridge the gap to man.

APPENDIX I

AUC values for buspirone metabolites produced in rat liver microsomes.

Name	Peak AUC	Percent total peak area (%)
Buspirone	1.87E+08	37.30077993
1-pyrimidinylpiperazine	2.03E+07	4.049229051
[2O] buspirone	1.71E+06	0.341092693
[2O] buspirone	2.55E+06	0.508646999
[2O] buspirone	3.54E+06	0.706121716
[2O] buspirone	6.43E+06	1.282588315
[O] buspirone	8.88E+07	17.71288373
Despyrimidinylpiperazine	1.57E+07	3.131669758
[O] buspirone	2.06E+07	4.109069874
[O] buspirone	9.46E+07	18.86980632
[O] buspirone	6.01E+07	11.98811162

APPENDIX II

AUC values for nefazodone metabolites produced in rat liver microsomes.

Name	Peak AUC	Percent total peak area (%)
Nefazodone	8.17E+07	62.4569987
[2O] nefazodone	6.19E+06	4.732054124
[2O] nefazodone	3.51E+06	2.683281095
Phenoxyethyltriazolone n-propanol	2.51E+06	1.918813546
[O] nefazodone	2.09E+07	15.97737176
[O] nefazodone	9.89E+06	7.560584053
[O] nefazodone	1.15E+06	0.879137681
[=O] nefazodone	1.63e+006	1.246082104

APPENDIX III

AUC values for buspirone metabolites produced in rat hepatocytes

Name	Peak AUC	Percent total peak area (%)
1-pyrimidinylpiperazine	7.60E+07	7.320150641
[2O] buspirone glucuronide	1.01E+07	0.972809493
[2O, OCH3] buspirone glucuronide	4.29E+05	0.041320324
[2O] buspirone glucuronide	9.52E+06	0.916945186
[2O] buspirone	1.27E+07	1.223235699
[2O] buspirone	1.38E+07	1.329185248
[2O] buspirone	8.73E+06	0.840854146
[2O, OCH3] buspirone glucuronide	3.27E+05	0.031495911
[2O] buspirone	4.62E+06	0.444988105
[2O] buspirone glucuronide	2.20E+07	2.118990975
[2O, OCH3] buspirone	1.41E+06	0.135808058
[2O] buspirone	2.50E+07	2.40794429
[O] buspirone	3.59E+07	3.457808
[2O, OCH3] buspirone	1.33E+06	0.128102636
[2O, OCH3] buspirone glucuronide	6.04E+05	0.058175934
[O] buspirone	7.52E+07	7.243096424
[2O] buspirone	3.36E+07	3.236277125
[O] buspirone glucuronide	1.05E+08	10.11336602
[O] buspirone	7.51E+07	7.233464647
[O, OCH3] buspirone glucuronide	1.28E+07	1.232867476
Despyrimidinyl buspirone	1.67E+06	0.160850679
[2O] buspirone	5.88E+07	5.66348497
[O, OCH3] buspirone	8.39E+06	0.808106104
[O] buspirone	1.35E+08	13.00289916
[O] buspirone	1.18E+08	11.36549705
Despyrimidinylpiperazine	2.82E+07	2.716161159
Buspirone	1.64E+08	15.79611454

APPENDIX IV

AUC values for nefazodone metabolites produced in rat hepatocytes

Name	Peak AUC	Percent total peak area (%)
Nefazodone	1.60E+07	16.11717184
Deschlorophenyl nefazodone	1.03E+07	10.37542937
[2O] nefazodone glucuronide	6.17E+05	0.621518439
[2O] nefazodone glucuronide	2.06E+05	0.207508587
Chlorophenylpiperazine	3.88E+06	3.908414171
[O] nefazodone glucuronide	3.55E+06	3.575997502
[O] nefazodone glucuronide	3.50E+06	3.52563134
[2O] nefazodone	4.96E+06	4.99632327
[2O] nefazodone	4.04E+06	4.069585889
Nefazodone O-sulphonate	4.42E+05	0.445236872
Phenoxyethyltriazolone propanoate	3.33E+06	3.354386389
[O] nefazodone	2.10E+07	21.15378804
[O, =O] nefazodone	7.48E+05	0.753477783
[O] nefazodone	2.67E+07	26.89553051
[=O] nefazodone	3.14e+006	3.162994973

APPENDIX V

AUC values for nefazodone metabolites produced in human hepatocytes

Name	Peak AUC	Percent total peak area (%)
Nefazodone	1.61E+08	36.80757184
Hydroxychlorophenylpiperazine	4.88E+06	1.115658078
Deschloro [O] phenyl nefazodone	2.60E+06	0.594407993
[2O] nefazodone glucuronide	1.19E+06	0.272055966
Phenoxyethyltriazolone propanoate	6.67E+06	1.524885119
Chlorophenylpiperazine	2.63E+07	6.012665463
Deschlorophenylpiperazine nefazodone	6.69E+06	1.529457488
[O] nefazodone glucuronide	7.23E+06	1.652911456
[3O] nefazodone	1.23E+06	0.281200704
Phenoxyethyltriazolone n-propanol	9.84E+06	2.249605633
[2O] nefazodone	1.79E+07	4.09227041
Nefazodone O-sulphonate	6.68E+06	1.527171304
Desethylketo nefazodone	1.06E+07	2.423355662
[2O] nefazodone	1.15E+07	2.629112275
[O] nefazodone	3.61E+07	8.253126357
[O] nefazodone	2.54E+07	5.80690885
[O] nefazodone	4.85E+06	1.108799524
[O, = O] nefazodone	3.66E+06	0.836743559
[O] nefazodone	8.45E+07	19.31825976
[O, = O] nefazodone	6.51E+06	1.488306166
[O, =O] nefazodone	2.08E+06	0.475526394
[=O] nefazodone	1.25e+007	2.857730733

BIBLIOGRAPHY

- Abernethy, D.R., Barbey, J.T., Franc, J., Brown, K.S., Feirrer, I., Ford, N. & Salazar, D.E. 2001, "Loratadine and terfenadine interaction with nefazodone: Both antihistamines are associated with QTc prolongation", *Clinical pharmacology and therapeutics*, vol. 69, no. 3, pp. 96-103.
- Alkalay, D., Volk, J. & Roth, W. 1979, "Metabolism, plasma or serum levels, and elimination of phenformin in guinea pigs, rats, and dogs", *Journal of pharmaceutical sciences*, vol. 68, no. 2, pp. 156-160.
- Ansede, J.H., Smith, W.R., Perry, C.H., St Claire III, R.L. & Brouwer, K.R. 2010, "An in vitro assay to assess transporter-based cholestatic hepatotoxicity using sandwich-cultured rat hepatocytes", *Drug Metabolism and Disposition*, vol. 38, no. 2, pp. 276-280.
- Appleyard, M.V.C.L., Murray, K.E., Coates, P.J., Wullschleger, S., Bray, S.E., Kernohan, N.M., Fleming, S., Alessi, D.R. & Thompson, A.M. 2012, "Phenformin as prophylaxis and therapy in breast cancer xenografts", *British journal of cancer*, vol. 106, no. 6, pp. 1117-1122.
- Aranda-Michel, J., Koehler, A., Bejarano, P.A., Poulos, J.E., Luxon, B.A., Khan, C.M., Ee, L.C., Balistreri, W.F. & Weber Jr., F.L. 1999, "Nefazodone-induced liver failure: Report of three cases", *Annals of Internal Medicine*, vol. 130, no. 4 I, pp. 285-288.
- Argoti, D., Liang, L., Conteh, A., Chen, L., Bershas, D., Yu, C.-., Vouros, P. & Yang, E. 2005, "Cyanide trapping of iminium ion reactive intermediates followed by detection and structure identification using liquid chromatography-tandem mass spectrometry (LC-MS/MS)", *Chemical research in toxicology*, vol. 18, no. 10, pp. 1537-1544.
- Ashton, A.K. & Wolin, R.E. 1996, "Nefazodone-induced carbamazepine toxicity [3]", *American Journal of Psychiatry*, vol. 153, no. 5, pp. 733.
- Bailey, C.J. 1992, "Biguanides and NIDDM", *Diabetes care*, vol. 15, no. 6, pp. 755-772.
- Baillie, T.A. & Davis, M.R. 1993, "Mass spectrometry in the analysis of glutathione conjugates", *Biological mass spectrometry*, vol. 22, no. 6, pp. 319-325.
- Barbhaiya, R.H., Dandekar, K.A. & Greene, D.S. 1996, "Pharmacokinetics, absolute bioavailability, and disposition of [¹⁴C]nefazodone in humans", *Drug Metabolism and Disposition*, vol. 24, no. 1, pp. 91-95.
- Bauman, J.N., Frederick, K.S., Sawant, A., Walsky, R.L., Cox, L.M., Obach, R.S. & Kalgutkar, A.S. 2008a, "Comparison of the bioactivation potential of the

- antidepressant and hepatotoxin nefazodone with aripiprazole, a structural analog and marketed drug", *Drug Metabolism and Disposition*, vol. 36, no. 6, pp. 1016-1029.
- Bauman, J.N., Frederick, K.S., Sawant, A., Walsky, R.L., Cox, L.M., Obach, R.S. & Kalgutkar, A.S. 2008b, "Comparison of the bioactivation potential of the antidepressant and hepatotoxin nefazodone with aripiprazole, a structural analog and marketed drug", *Drug Metabolism and Disposition*, vol. 36, no. 6, pp. 1016-1029.
- Bauman, J.N., Kelly, J.M., Tripathy, S., Zhao, S.X., Lam, W.W., Kalgutkar, A.S. & Obach, R.S. 2009, "Can in vitro metabolism-dependent covalent binding data distinguish hepatotoxic from nonhepatotoxic drugs? An analysis using human hepatocytes and liver S-9 fraction", *Chemical research in toxicology*, vol. 22, no. 2, pp. 332-340.
- Becker, C.M. & Harris, R.A. 1983, "Influence of valproic acid on hepatic carbohydrate and lipid metabolism", *Archives of Biochemistry and Biophysics*, vol. 223, no. 2, pp. 381-392.
- Bosisio, E., Galli Kienle, M. & Galli, G. 1981, "Defective hydroxylation of phenformin as a determinant of drug toxicity", *Diabetes*, vol. 30, no. 8, pp. 644-649.
- Bourdi, M., Chen, W., Peter, R.M., Martin, J.L., Buters, J.T.M., Nelson, S.D. & Pohl, L.R. 1996, "Human cytochrome P450 2E1 is a major autoantigen associated with halothane hepatitis", *Chemical research in toxicology*, vol. 9, no. 7, pp. 1159-1166.
- Bradford, L.D. 2002, "CYP2D6 allele frequency in European Caucasians, Asians, Africans and their descendants", *Pharmacogenomics*, vol. 3, no. 2, pp. 229-243.
- Brown, J.B., Pedula, K., Barzilay, J., Herson, M.K. & Latare, P. 1998, "Lactic acidosis rates in type 2 diabetes.", *Diabetes care*, vol. 21, no. 10, pp. 1659.
- Bulera, S.J., Birge, R.B., Cohen, S.D. & Khairallah, E.A. 1995, "Identification of the mouse liver 44-kDa acetaminophen-binding protein as a subunit of glutamine synthetase", *Toxicology and applied pharmacology*, vol. 134, no. 2, pp. 313-320.
- Caraci, F., Chisari, M., Frasca, G., Chiechio, S., Salomone, S., Pinto, A., Sortino, M.A. & Bianchi, A. 2003, "Effects of phenformin on the proliferation of human tumor cell lines", *Life Sciences*, vol. 74, no. 5, pp. 643-650.
- Chen, Q., Ngui, J.S., Doss, G.A., Cai, X., Wang, R.W., DiNinno, F.P., Blizzard, T.A., Hammond, M.L., Stearns, R.A., Evans, D.C., Baillie, T.A. & Tang, W. 2002, "Cytochrome P450 3A4-mediated bioactivation of raloxifene: Irreversible enzyme inhibition and thiol adduct formation", *Chemical research in toxicology*, vol. 15, no. 7, pp. 907-914.

- Ching, C., Lai, C., Poon, W., Wong, E.N.P., Yan, W., Chan, A.Y.W. & Mak, T.W.L. 2008, "Hazards posed by a banned drug-phenformin is still hanging around", *HONG KONG MEDICAL JOURNAL*, vol. 14, no. 1, pp. 50.
- Christie, G. & Judah, J. 1954, "Mechanism of action of carbon tetrachloride on liver cells", *Proceedings of the Royal Society of London. Series B-Biological Sciences*, vol. 142, no. 907, pp. 241-257.
- Circu, M.L. & Aw, T.Y. 2008, "Glutathione and apoptosis", *Free Radical Research*, vol. 42, no. 8, pp. 689-706.
- Copple, I.M., Goldring, C.E., Jenkins, R.E., Chia, A.J.L., Randle, L.E., Hayes, J.D., Kitteringham, N.R. & Park, B.K. 2008, "The hepatotoxic metabolite of acetaminophen directly activates the keap1-Nrf2 cell defense system", *Hepatology*, vol. 48, no. 4, pp. 1292-1301.
- Corcoran, G.B., Chung, S.-. & Salazar, D.E. 1987, "Early inhibition of the Na⁺/K⁺-ATPase ion pump during acetaminophen-induced hepatotoxicity in rat", *Biochemical and biophysical research communications*, vol. 149, no. 1, pp. 203-207.
- Corkey, B.E., Hale, D.E., Glennon, M.C., Kelley, R.I., Coates, P.M., Kilpatrick, L. & Stanley, C.A. 1988, "Relationship between unusual hepatic acyl coenzyme A profiles and the pathogenesis of Reye syndrome", *Journal of Clinical Investigation*, vol. 82, no. 3, pp. 782-788.
- Cribb, A.E., Nuss, C.E., Alberts, D.W., Lamphere, D.B., Grant, D.M., Grossman, S.J. & Spielberg, S.P. 1996, "Covalent binding of sulfamethoxazole reactive metabolites to human and rat liver subcellular fractions assessed by immunochemical detection", *Chemical research in toxicology*, vol. 9, no. 2, pp. 500-507.
- Cribb, A.E., Spielberg, S.P. & Griffin, G.P. 1995, "N4-hydroxylation of sulfamethoxazole by cytochrome P450 of the cytochrome P4502C subfamily and reduction of sulfamethoxazole hydroxylamine in human and rat hepatic microsomes", *Drug Metabolism and Disposition*, vol. 23, no. 3, pp. 406-414.
- Crompton, M. 1999, "The mitochondrial permeability transition pore and its role in cell death.", *Biochemical Journal*, vol. 341, no. Pt 2, pp. 233.
- Dalvie, D., Kang, P., Zientek, M., Xiang, C., Zhou, S. & Obach, R.S. 2008, "Effect of intestinal glucuronidation in limiting hepatic exposure and bioactivation of raloxifene in humans and rats", *Chemical research in toxicology*, vol. 21, no. 12, pp. 2260-2271.
- Davidoff, F. 1971, "Effects of guanidine derivatives on mitochondrial function. 3. The mechanism of phenethylbiguanide accumulation and its relationship to in

- vitro respiratory inhibition.", *Journal of Biological Chemistry*, vol. 246, no. 12, pp. 4017-4027.
- Davis, R., Whittington, R. & Bryson, H.M. 1997, "Nefazodone. A review of its pharmacology and clinical efficacy in the management of major depression", *Drugs*, vol. 53, no. 4, pp. 608-636.
- DeLeve, L.D. & Kaplowitz, N. 1991, "Glutathione metabolism and its role in hepatotoxicity", *Pharmacology and Therapeutics*, vol. 52, no. 3, pp. 287-305.
- Dietze, E.C., Schäfer, A., Omichinski, J.G. & Nelson, S.D. 1997a, "Inactivation of glyceraldehyde-3-phosphate dehydrogenase by a reactive metabolite of acetaminophen and mass spectral characterization of an arylated active site peptide", *Chemical research in toxicology*, vol. 10, no. 10, pp. 1097-1103.
- Dietze, E.C., Schäfer, A., Omichinski, J.G. & Nelson, S.D. 1997b, "Inactivation of glyceraldehyde-3-phosphate dehydrogenase by a reactive metabolite of acetaminophen and mass spectral characterization of an arylated active site peptide", *Chemical research in toxicology*, vol. 10, no. 10, pp. 1097-1103.
- Dyken, J.A., Jamieson, J., Marroquin, L., Nadanaciva, S., Billis, P.A., Will, Y. 2008, "Biguanide-induced mitochondrial dysfunction yields increased lactate production and cytotoxicity of aerobically-poised HepG2 cells and human hepatocytes in vitro", *Toxicology and applied pharmacology*, vol. 233, no. 2, pp. 203-210.
- Dyken, J.A., Jamieson, J.D., Marroquin, L.D., Nadanaciva, S., Xu, J.J., Dunn, M.C., Smith, A.R. & Will, Y. 2008, "In vitro assessment of mitochondrial dysfunction and cytotoxicity of nefazodone, trazodone, and buspirone", *Toxicological Sciences*, vol. 103, no. 2, pp. 335-345.
- Dyken, J.A. & Will, Y. 2008, *Drug induced mitochondrial dysfunction*, 1st edn, Wiley.
- Edwards, P.J. & Sturino, C. 2011, "Managing the liabilities arising from Structural alerts: A safe philosophy for medicinal chemists", *Current medicinal chemistry*, vol. 18, no. 20, pp. 3116-3135.
- Eison, A.S., Eison, M.S., Torrente, J.R., Wright, R.N. & Yocca, F.D. 1990, "Nefazodone: Preclinical pharmacology of a new antidepressant", *Psychopharmacology bulletin*, vol. 26, no. 3, pp. 311-315.
- Eison, A.S. & Temple, D.L. 1986, "Buspirone: Review of its pharmacology and current perspectives on its mechanism of action", *American Journal of Medicine*, vol. 80, no. 3 B, pp. 1-9.
- Eison, A.S., Eison, M.S., Stanley, M. & Riblet, L.A. 1986, "Serotonergic mechanisms in the behavioral effects of buspirone and gepirone", *Pharmacology Biochemistry and Behavior*, vol. 24, no. 3, pp. 701-707.

- Eliasson, E. & Kenna, J.G. 1996, "Cytochrome P450 2E1 is a cell surface autoantigen in halothane hepatitis", *Molecular pharmacology*, vol. 50, no. 3, pp. 573-582.
- El-Masry, O.S., Brown, B.L. & Dobson, P.R.M. 2012, "Effects of activation of AMPK on human breast cancer cell lines with different genetic backgrounds", *Oncology Letters*, vol. 3, no. 1, pp. 224-228.
- El-Mir, M.-., Nogueira, V., Fontaine, E., Avéret, N., Rigoulet, M. & Leverve, X. 2000, "Dimethylbiguanide inhibits cell respiration via an indirect effect targeted on the respiratory chain complex I", *Journal of Biological Chemistry*, vol. 275, no. 1, pp. 223-228.
- Eloubeidi, M.A., Gaede, J.T. & Swaim, M.W. 2000, "Reversible nefazodone-induced liver failure", *Digestive diseases and sciences*, vol. 45, no. 5, pp. 1036-1038.
- Evans, D.C., Watt, A.P., Nicoll-Griffith, D.A. & Baillie, T.A. 2004, "Drug-Protein Adducts: An Industry Perspective on Minimizing the Potential for Drug Bioactivation in Drug Discovery and Development", *Chemical research in toxicology*, vol. 17, no. 1, pp. 3-16.
- Food and Drug Administration
09/01/2002, <http://www.fda.gov/downloads/Safety/MedWatch/SafetyInformation/SafetyAlertsforHumanMedicalProducts/UCM171084.pdf>.
- Forman, H.J., Zhang, H. & Rinna, A. 2008, "Glutathione: Overview of its protective roles, measurement, and biosynthesis", *Molecular Aspects of Medicine*, .
- Franc, J.E., Duncan, G.F., Farnen, R.H. & Pittman, K.A. 1991, "High-performance liquid chromatographic method for the determination of nefazodone and its metabolites in human plasma using laboratory robotics", *Journal of Chromatography - Biomedical Applications*, vol. 570, no. 1, pp. 129-138.
- Fromenty, B., Berson, A. & Pessayre, D. 1997, "Microvesicular steatosis and steatohepatitis: Role of mitochondrial dysfunction and lipid peroxidation", *Journal of Hepatology, Supplement*, vol. 26, no. 1, pp. 13-22.
- Fromenty, B. & Pessayre, D. 1995, "Inhibition of mitochondrial beta-oxidation as a mechanism of hepatotoxicity", *Pharmacology and Therapeutics*, vol. 67, no. 1, pp. 101-154.
- Fujita, Y., Hosokawa, M., Fujimoto, S., Mukai, E., Abudukadier, A., Obara, A., Ogura, M., Nakamura, Y., Toyoda, K., Nagashima, K., Seino, Y. & Inagaki, N. 2010, "Metformin suppresses hepatic gluconeogenesis and lowers fasting blood glucose levels through reactive nitrogen species in mice", *Diabetologia*, vol. 53, no. 7, pp. 1472-1481.

- Funk, C., Pantze, M., Jehle, L., Ponelle, C., Scheuermann, G., Lazendic, M. & Gasser, R. 2001a, "Troglitazone-induced intrahepatic cholestasis by an interference with the hepatobiliary export of bile acids in male and female rats. Correlation with the gender difference in troglitazone sulfate formation and the inhibition of the canalicular bile salt export pump (Bsep) by troglitazone and troglitazone sulfate", *Toxicology*, vol. 167, no. 1, pp. 83-98.
- Funk, C., Ponelle, C., Scheuermann, G. & Pantze, M. 2001b, "Cholestatic potential of troglitazone as a possible factor contributing to troglitazone-induced hepatotoxicity: In vivo and in vitro interaction at the canalicular bile salt export pump (Bsep) in the rat", *Molecular pharmacology*, vol. 59, no. 3, pp. 627-635.
- Gammans, R.E., Mayol, R.F. & Labudde, J.A. 1986, "Metabolism and disposition of buspirone", *American Journal of Medicine*, vol. 80, no. 3 B, pp. 41-51.
- Gardner, I., Zahid, N., MacCrimmon, D. & Uetrecht, J.P. 1998, "A comparison of the oxidation of clozapine and olanzapine to reactive metabolites and the toxicity of these metabolites to human leukocytes", *Molecular pharmacology*, vol. 53, no. 6, pp. 991-998.
- Gibson, G. & Skett, P. 2001, *Introduction to drug metabolism*, 3rd edn, Nelson Thornes Publishers.
- Gill, H.J., Hough, S.J., Naisbitt, D.J., Maggs, J.L., Kitteringham, N.R., Pirmohamed, M. & Park, B.K. 1997, "The relationship between the disposition and immunogenicity of sulfamethoxazole in the rat", *Journal of Pharmacology and Experimental Therapeutics*, vol. 282, no. 2, pp. 795-801.
- Goldberg, H.L. 1984, "Buspirone hydrochloride: A unique new anxiolytic agent. Pharmacokinetics, clinical pharmacology, abuse potential and clinical efficacy", *Pharmacotherapy*, vol. 4, no. 6, pp. 315-324.
- Graham, E.E., Walsh, R.J., Hirst, C.M., Maggs, J.L., Martin, S., Wild, M.J., Wilson, I.D., Harding, J.R., Kenna, J.G., Peter, R.M., Williams, D.P. & Park, B.K. 2008, "Identification of the thiophene ring of methapyrilene as a novel bioactivation-dependent hepatic toxicophore", *Journal of Pharmacology and Experimental Therapeutics*, vol. 326, no. 2, pp. 657-671.
- Greenblatt, D.J., Zhao, Y., Venkatakrishnan, K., Duan, S.X., Harmatz, J.S., Parent, S.J., Court, M.H. & Von Moltke, L.L. 2011, "Mechanism of cytochrome P450-3A inhibition by ketoconazole", *Journal of Pharmacy and Pharmacology*, vol. 63, no. 2, pp. 214-221.
- Gross, A., Jockel, J., Wei, M.C. & Korsmeyer, S.J. 1998, "Enforced dimerization of BAX results in its translocation, mitochondrial dysfunction and apoptosis", *The EMBO journal*, vol. 17, no. 14, pp. 3878-3885.

- Guengerich, F.P. 1997, "Comparisons of catalytic selectivity of cytochrome P450 subfamily enzymes from different species", *Chemico-biological interactions*, vol. 106, no. 3, pp. 161-182.
- Guest, D., King, L.J. & Parke, D.V. 1979, "Metabolism of phenformin in the rat and guinea pig", *Xenobiotica*, vol. 9, no. 11, pp. 681-693.
- Gunawan, B.K., Liu, Z.X., Han, D., Hanawa, N., Gaarde, W.A. & Kaplowitz, N. 2006, "c-Jun N-terminal kinase plays a major role in murine acetaminophen hepatotoxicity", *Gastroenterology*, vol. 131, no. 1, pp. 165-178.
- Guo, Z., Raeissi, S., White, R.B. & Stevens, J.C. 1997, "Orphenadrine and methimazole inhibit multiple cytochrome P450 enzymes in human liver microsomes", *Drug Metabolism and Disposition*, vol. 25, no. 3, pp. 390-393.
- Gupta, S., Rogers, L.K., Taylor, S.K. & Smith, C.V. 1997, "Inhibition of carbamyl phosphate synthetase-I and glutamine synthetase by hepatotoxic doses of acetaminophen in mice", *Toxicology and applied pharmacology*, vol. 146, no. 2, pp. 317-327.
- Halmes, N.C., Hinson, J.A., Martin, B.M. & Pumford, N.R. 1996, "Glutamate dehydrogenase covalently binds to a reactive metabolite of acetaminophen", *Chemical research in toxicology*, vol. 9, no. 2, pp. 541-546.
- Han, D., Hanawa, N., Saberi, B. & Kaplowitz, N. 2006, "Mechanisms of liver injury. III. Role of glutathione redox status in liver injury", *American Journal of Physiology - Gastrointestinal and Liver Physiology*, vol. 291, no. 1, pp. G1-G7.
- Hawley, S.A., Gadalla, A.E., Olsen, G.S. & Hardie, D.G. 2002, "The antidiabetic drug metformin activates the AMP-activated protein kinase cascade via an adenine nucleotide-independent mechanism", *Diabetes*, vol. 51, no. 8, pp. 2420.
- Hayden, P.J., Ichimura, T., McCann, D.J., Pohl, L.R. & Stevens, J.L. 1991, "Detection of cysteine conjugate metabolite adduct formation with specific mitochondrial proteins using antibodies raised against haloethane metabolite adducts", *Journal of Biological Chemistry*, vol. 266, no. 28, pp. 18415-18418.
- Helms-Smith, K.M., Curtis, S.L. & Hatton, R.C. 1996, "Apparent interaction between nefazodone and cyclosporine.", *Annals of Internal Medicine*, vol. 125, no. 5, pp. 424.
- Houtkooper, R.H. & Vaz, F.M. 2008, "Cardiolipin, the heart of mitochondrial metabolism", *Cellular and Molecular Life Sciences*, vol. 65, no. 16, pp. 2493-2506.
- Idle, J.R., Oates, N.S., Shah, R.R. & Smith, R.L. 1981, "Is there a genetic predisposition to phenformin-induced lactic acidosis?", *British journal of clinical pharmacology*, vol. 11, no. 4, pp. 418P-419P.

- Ingelman-Sundberg, M. 2005, "Genetic polymorphisms of cytochrome P450 2D6 (CYP2D6): Clinical consequences, evolutionary aspects and functional diversity", *Pharmacogenomics Journal*, vol. 5, no. 1, pp. 6-13.
- Irsigler, K., Kritz, H. & Regal, H. 1979, "Biguanide-induced and associated lactic acidosis: Serum and tissue biguanide levels in hyperlactaemia and lactic acidosis", *Wiener klinische Wochenschrift*, vol. 91, no. 2, pp. 59-65.
- Jaeschke, H., Gores, G.J., Cederbaum, A.I., Hinson, J.A., Pessayre, D. & Lemasters, J.J. 2002, "Mechanisms of hepatotoxicity", *Toxicological Sciences*, vol. 65, no. 2, pp. 166-176.
- Jancovaa, P., Anzenbacherb, P. & Anzenbacherovaa, S. 2010, "Phase II drug metabolizing enzymes", *Biomed.Pap.Med.Fac.Univ.Palacky.Olomouc.Czech.Repub*, vol. 154, pp. 103-116.
- Kalgutkar, A.S. & Didiuk, M.T. 2009, "Structural alerts, reactive metabolites, and protein covalent binding: How reliable are these attributes as predictors of drug toxicity?", *Chemistry and Biodiversity*, vol. 6, no. 11, pp. 2115-2137.
- Kalgutkar, A.S., Gardner, I., Obach, R.S., Shaffer, C.L., Callegari, E., Henne, K.R., Mutlib, A.E., Dalvie, D.K., Lee, J.S., Nakai, Y., O'Donnell, J.P., Boer, J. & Harriman, S.P. 2005a, "A comprehensive listing of bioactivation pathways of organic functional groups", *Current Drug Metabolism*, vol. 6, no. 3, pp. 161-225.
- Kalgutkar, A.S., Henne, K.R., Lame, M.E., Vaz, A.D.N., Collin, C., Soglia, J.R., Zhao, S.X. & Hop, C.E.C.A. 2005b, "Metabolic activation of the nontricyclic antidepressant trazodone to electrophilic quinone-imine and epoxide intermediates in human liver microsomes and recombinant P4503A4", *Chemico-Biological Interactions*, vol. 155, no. 1-2, pp. 10-20.
- Kalgutkar, A.S. & Soglia, J.R. 2005, "Minimising the potential for metabolic activation in drug discovery", *Expert Opinion on Drug Metabolism and Toxicology*, vol. 1, no. 1, pp. 91-142.
- Kalgutkar, A.S., Vaz, A.D.N., Lame, M.E., Henne, K.R., Soglia, J., Zhao, S.X., Abramov, Y.A., Lombarde, F., Collin, C., Hendsch, Z.S. & Hop, C.E.C.A. 2005a, "Bioactivation of the nontricyclic antidepressant nefazodone to a reactive quinone-imine species in human liver microsomes and recombinant cytochrome P450 3A4", *Drug Metabolism and Disposition*, vol. 33, no. 2, pp. 243-253.
- Kalgutkar, A.S., Vaz, A.D.N., Lame, M.E., Henne, K.R., Soglia, J., Zhao, S.X., Abramov, Y.A., Lombarde, F., Collin, C., Hendsch, Z.S. & Hop, C.E.C.A. 2005b, "Bioactivation of the nontricyclic antidepressant nefazodone to a reactive quinone-imine species in human liver microsomes and recombinant

- cytochrome P450 3A4", *Drug Metabolism and Disposition*, vol. 33, no. 2, pp. 243-253.
- Kassahun, K., Pearson, P.G., Tang, W., McIntosh, I., Leung, K., Elmore, C., Dean, D., Wang, R., Doss, G. & Baillie, T.A. 2001, "Studies on the metabolism of troglitazone to reactive intermediates in vitro and in vivo. Evidence for novel biotransformation pathways involving quinone methide formation and thiazolidinedione ring scission", *Chemical research in toxicology*, vol. 14, no. 1, pp. 62-70.
- Kaul, S., Shukla, U.A. & Barbhuiya, R.H. 1995, "Nonlinear pharmacokinetics of nefazodone after escalating single and multiple oral doses", *Journal of clinical pharmacology*, vol. 35, no. 8, pp. 830-839.
- Kawai, K., Kawasaki-Tokui, Y., Odaka, T., Tsuruta, F., Kazui, M., Iwabuchi, H., Nakamura, T., Kinoshita, T., Ikeda, T., Yoshioka, T., Komai, T. & Nakamura, K.-. 1997, "Disposition and metabolism of the new oral antidiabetic drug troglitazone in rats, mice and dogs", *Arzneimittel-Forschung/Drug Research*, vol. 47, no. 4, pp. 356-368.
- Kenna, J.G. 1997, "Immunoallergic drug-induced hepatitis: Lessons from halothane", *Journal of Hepatology, Supplement*, vol. 26, no. 1, pp. 5-12.
- Kerns, E.H., Rourick, R.A., Volk, K.J. & Lee, M.S. 1997, "Buspirone metabolite structure profile using a standard liquid chromatographic-mass spectrometric protocol", *Journal of Chromatography B: Biomedical Applications*, vol. 698, no. 1-2, pp. 133-145.
- Kitteringham, N.R., Powell, H., Clement, Y.N., Dodd, C.C., Tettey, J.N., Pirmohamed, M., Smith, D.A., McLellan, L.I. & Kevin Park, B. 2000, "Hepatocellular response to chemical stress in CD-1 mice: Induction of early genes and γ -glutamylcysteine synthetase", *Hepatology*, vol. 32, no. 2, pp. 321-333.
- Kobayashi, S., Murray, S., Watson, D., Sesardic, D., Davies, D.S. & Boobis, A.R. 1989, "The specificity of inhibition of debrisoquine 4-hydroxylase activity by quinidine and quinine in the rat is the inverse of that in man", *Biochemical pharmacology*, vol. 38, no. 17, pp. 2795-2799.
- Kostrubsky, S.E., Strom, S.C., Kalgutkar, A.S., Kulkarni, S., Atherton, J., Mireles, R., Feng, B., Kubik, R., Hanson, J., Urda, E. & Mutlib, A.E. 2006, "Inhibition of hepatobiliary transport as a predictive method for clinical hepatotoxicity of nefazodone", *Toxicological Sciences*, vol. 90, no. 2, pp. 451-459.
- Kostrubsky, V.E., Vore, M., Kindt, E., Burliegh, J., Rogers, K., Peter, G., Altrogge, D. & Sinz, M.W. 2001, "The effect of troglitazone biliary excretion on metabolite distribution and cholestasis in transporter-deficient rats", *Drug Metabolism and Disposition*, vol. 29, no. 12, pp. 1561-1566.

- Kramer, J.A., Sagartz, J.E. & Morris, D.L. 2007, "The application of discovery toxicology and pathology towards the design of safer pharmaceutical lead candidates", *Nature Reviews Drug Discovery*, vol. 6, no. 8, pp. 636-649.
- Labbe, G., Pessayre, D. & Fromenty, B. 2008, "Drug-induced liver injury through mitochondrial dysfunction: Mechanisms and detection during preclinical safety studies", *Fundamental and Clinical Pharmacology*, vol. 22, no. 4, pp. 335-353.
- Lalau, J.D. 2010, "Lactic acidosis induced by metformin: incidence, management and prevention", *Drug Safety*, vol. 33, no. 9, pp. 727-740.
- Landin, J.S., Cohen, S.D. & Khairallah, E.A. 1996, "Identification of a 54-kDa mitochondrial acetaminophen-binding protein as aldehyde dehydrogenase", *Toxicology and applied pharmacology*, vol. 141, no. 1, pp. 299-307.
- Lasser, K.E., Allen, P.D., Woolhandler, S.J., Himmelstein, D.U., Wolfe, S.M. & Bor, D.H. 2002, "Timing of new black box warnings and withdrawals for prescription medications", *Journal of the American Medical Association*, vol. 287, no. 17, pp. 2215-2220.
- Leist, M., Single, B., Castoldi, A.F., Kühnle, S. & Nicotera, P. 1997, "Intracellular adenosine triphosphate (ATP) concentration: a switch in the decision between apoptosis and necrosis", *The Journal of experimental medicine*, vol. 185, no. 8, pp. 1481-1486.
- Li, P., Nijhawan, D., Budihardjo, I., Srinivasula, S.M., Ahmad, M., Alnemri, E.S. & Wang, X. 1997, "Cytochrome c and dATP-dependent formation of Apaf-1/caspase-9 complex initiates an apoptotic protease cascade", *Cell*, vol. 91, no. 4, pp. 479-489.
- Li, A.C., Shou, W.Z., Mai, T.T. & Jiang, X.-. 2007, "Complete profiling and characterization of in vitro nefazodone metabolites using two different tandem mass spectrometric platforms", *Rapid Communications in Mass Spectrometry*, vol. 21, no. 24, pp. 4001-4008.
- Linder, C.D., Renaud, N.A. & Hutzler, J.M. 2009, "Is 1-Aminobenzotriazole an appropriate in vitro tool as a nonspecific cytochrome P450 inactivator?", *Drug Metabolism and Disposition*, vol. 37, no. 1, pp. 10-13.
- Lintz, W., Berger, W. & Aenishaenslin, W. 1974, "Butylbiguanide concentration in plasma, liver, and intestine after intravenous and oral administration to man", *European journal of clinical pharmacology*, vol. 7, no. 6, pp. 433-448.
- LOWRY, O.H., ROSEBROUGH, N.J., FARR, A.L. & RANDALL, R.J. 1951, "Protein measurement with the Folin phenol reagent", *The Journal of biological chemistry*, vol. 193, no. 1, pp. 265-275.

- Lu, C. & Li, A.P. 2001, "Species comparison in P450 induction: Effects of dexamethasone, omeprazole, and rifampin on P450 isoforms 1A and 3A in primary cultured hepatocytes from man, Sprague-Dawley rat, minipig, and beagle dog", *Chemico-biological interactions*, vol. 134, no. 3, pp. 271-281.
- Lucena, M.I., Andrade, R.J., Gomez-Outes, A., Rubio, M. & Cabello, M.R. 1999, "Acute liver failure after treatment with nefazodone", *Digestive diseases and sciences*, vol. 44, no. 12, pp. 2577-2579.
- Maggs, J.L., Williams, D., Pirmohamed, M. & Park, B.K. 1995, "The metabolic formation of reactive intermediates from clozapine, a drug associated with agranulocytosis in man", *Journal of Pharmacology and Experimental Therapeutics*, vol. 275, no. 3, pp. 1463-1475.
- Manchanda, T., Hess, D., Dale, L., Ferguson, S.G. & Rieder, M.J. 2002, "Haptenation of sulfonamide reactive metabolites to cellular proteins", *Molecular pharmacology*, vol. 62, no. 5, pp. 1011-1026.
- Marroquin, L.D., Hynes, J., Dykens, J.A., Jamieson, J.D. & Will, Y. 2007, "Circumventing the crabtree effect: Replacing media glucose with galactose increases susceptibility of hepG2 cells to mitochondrial toxicants", *Toxicological Sciences*, vol. 97, no. 2, pp. 539-547.
- Martin, J.L., Kenna, J.G., Martin, B.M., Thomassen, D., Reed, G.F. & Pohl, L.R. 1993, "Halothane hepatitis patients have serum antibodies that react with protein disulfide isomerase", *Hepatology*, vol. 18, no. 4, pp. 858-863.
- Martin, J.L., Pumford, N.R., LaRosa, A.C., Martin, B.M., Gonzaga, H.M.S., Beaven, M.A. & Pohl, L.R. 1991, "A metabolite of halothane covalently binds to an endoplasmic reticulum protein that is highly homologous to phosphatidylinositol-specific phospholipase C- α but has no activity", *Biochemical and biophysical research communications*, vol. 178, no. 2, pp. 679-685.
- Masubuchi, Y., Nakayama, S. & Horie, T. 2002, "Role of mitochondrial permeability transition in diclofenac-induced hepatocyte injury in rats", *Hepatology*, vol. 35, no. 3, pp. 544-551.
- Matthews, A.M., Hinson, J.A., Roberts, D.W. & Pumford, N.R. 1997, "Comparison of covalent binding of acetaminophen and the regioisomer 3'-hydroxyacetanilide to mouse liver protein", *Toxicology letters*, vol. 90, no. 1, pp. 77-82.
- Mayol, R.F., Cole, C.A., Luke, G.M., Colson, K.L. & Kerns, E.H. 1994, "Characterization of the metabolites of the antidepressant drug nefazodone in human urine and plasma", *Drug Metabolism and Disposition*, vol. 22, no. 2, pp. 304-311.

- Meister, A. & Anderson, M.E. 1983, "Glutathione", *Annual Review of Biochemistry*, vol. Vol. 52, pp. 711-760.
- Miller, J.L. & Trepanier, L.A. 2002, "Inhibition by atovaquone of CYP2C9-mediated sulphamethoxazole hydroxylamine formation", *European journal of clinical pharmacology*, vol. 58, no. 1, pp. 69-72.
- Morgan, M.Y., Reshef, R. & Shah, R.R. 1984, "Impaired oxidation of debrisoquine in patients with perhexiline liver injury", *Gut*, vol. 25, no. 10, pp. 1057-1064.
- Musi, N., Hirshman, M.F., Nygren, J., Svanfeldt, M., Bavenholm, P., Rooyackers, O., Zhou, G., Williamson, J.M., Ljunqvist, O. & Efendic, S. 2002, "Metformin increases AMP-activated protein kinase activity in skeletal muscle of subjects with type 2 diabetes", *Diabetes*, vol. 51, no. 7, pp. 2074.
- Naisbitt, D.J., Farrell, J., Gordon, S.F., Maggs, J.L., Burkhart, C., Pichler, W.J., Pirmohamed, M. & Park, B.K. 2002, "Covalent binding of the nitroso metabolite of sulfamethoxazole leads to toxicity and major histocompatibility complex-restricted antigen presentation", *Molecular pharmacology*, vol. 62, no. 3, pp. 628-637.
- Nakayama, S., Atsumi, R., Takakusa, H., Kobayashi, Y., Kurihara, A., Nagai, Y., Nakai, D. & Okazaki, O. 2009, "A zone classification system for risk assessment of idiosyncratic drug toxicity using daily dose and covalent binding", *Drug Metabolism and Disposition*, vol. 37, no. 9, pp. 1970-1977.
- Nicolaou, M., Andress, E.J., Zolneriks, J.K., Dixon, P.H., Williamson, C. & Linton, K.J. 2012, "Canalicular ABC transporters and liver disease", *Journal of Pathology*, vol. 226, no. 2, pp. 300-315.
- Oates, N.S., Shah, R.R., Idle, J.R. & Smith, R.L. 1982, "Genetic polymorphism of phenformin 4-hydroxylation", *Clinical pharmacology and therapeutics*, vol. 32, no. 1, pp. 81-89.
- Obach, R.S., Kalgutkar, A.S., Soglia, J.R. & Zhao, S.X. 2008, "Can in vitro metabolism-dependent covalent binding data in liver microsomes distinguish hepatotoxic from nonhepatotoxic drugs? An analysis of 18 drugs with consideration of intrinsic clearance and daily dose", *Chemical research in toxicology*, vol. 21, no. 9, pp. 1814-1822.
- Olson, H., Betton, G., Robinson, D., Thomas, K., Monro, A., Kolaja, G., Lilly, P., Sanders, J., Sipes, G., Bracken, W., Dorato, M., Van Deun, K., Smith, P., Berger, B. & Heller, A. 2000, "Concordance of the toxicity of pharmaceuticals in humans and in animals", *Regulatory Toxicology and Pharmacology*, vol. 32, no. 1, pp. 56-67.
- Orrenius, S. 2004, "Mitochondrial regulation of apoptotic cell death", *Toxicology letters*, vol. 149, no. 1-3, pp. 19-23.

- Ostapowicz, G., Fontana, R.J., Schioødt, F.V., Larson, A., Davern, T.J., Han, S.H.B., McCashland, T.M., Shakil, A.O., Hay, J.E., Hynan, L., Crippin, J.S., Blei, A.T., Samuel, G., Reisch, J., Lee, W.M., Santyanarayana, R., Caldwell, C., Shick, L., Bass, N., Rouillard, S., Atillasoy, E., Flamm, S., Benner, K.G., Rosen, H.R., Martin, P., Stribling, R., Schiff, E.R., Torres, M.B., Navarro, V., McGuire, B., Chung, R., Abraczinskas, D. & Dienstag, J. 2002, "Results of a prospective study of acute liver failure at 17 tertiary care centers in the United States", *Annals of Internal Medicine*, vol. 137, no. 12, pp. 947-954.
- Owen, M.R., Doran, E. & Halestrap, A.P. 2000, "Evidence that metformin exerts its anti-diabetic effects through inhibition of complex 1 of the mitochondrial respiratory chain", *Biochemical Journal*, vol. 348, no. 3, pp. 607-614.
- Ozdemirler, G., Aykac, G., Uysal, M. & Oz, H. 1994, "Liver lipid peroxidation and glutathione-related defence enzyme systems in mice treated with paracetamol", *Journal of Applied Toxicology*, vol. 14, no. 4, pp. 297-299.
- PALADE, G.E. 1953, "An electron microscope study of the mitochondrial structure.", *The journal of histochemistry and cytochemistry : official journal of the Histochemistry Society*, vol. 1, no. 4, pp. 188-211.
- Palmeira, C.M. & Rolo, A.P. 2004, "Mitochondrially-mediated toxicity of bile acids", *Toxicology*, vol. 203, no. 1-3, pp. 1-15.
- Park, B.K., Boobis, A., Clarke, S., Goldring, C.E.P., Jones, D., Kenna, J.G., Lambert, C., Lavery, H.G., Naibitt, D.J. & Nelson, S. 2011, "Managing the challenge of chemically reactive metabolites in drug development", *Nature Reviews Drug Discovery*, vol. 10, no. 4, pp. 292-306.
- Park, B.K., Kitteringham, N.R., Maggs, J.L., Pirmohamed, M. & Williams, D.P. 2005, *The role of metabolic activation in drug-induced hepatotoxicity*.
- Parmar, D.V., Ahmed, G., Khandkar, M.A. & Katyare, S.S. 1995, "Mitochondrial ATPase: a target for paracetamol-induced hepatotoxicity", *European Journal of Pharmacology: Molecular Pharmacology*, vol. 293, no. 3, pp. 225-229.
- Pirmohamed, M., James, S., Meakin, S., Green, C., Scott, A.K., Walley, T.J., Farrar, K., Park, B.K. & Breckenridge, A.M. 2004, "Adverse drug reactions as cause of admission to hospital: Prospective analysis of 18 820 patients", *British Medical Journal*, vol. 329, no. 7456, pp. 15-19.
- Pirmohamed, M., Williams, D., Madden, S., Templeton, E. & Park, B.K. 1995, "Metabolism and bioactivation of clozapine by human liver in vitro", *Journal of Pharmacology and Experimental Therapeutics*, vol. 272, no. 3, pp. 984-990.
- Prabhu, S., Fackett, A., Lloyd, S., McClellan, H.A., Terrell, C.M., Silber, P.M. & Li, A.P. 2002, "Identification of glutathione conjugates of troglitazone in human hepatocytes", *Chemico-biological interactions*, vol. 142, no. 1-2, pp. 83-97.

- Preininger, K., Sting, H., Englisch, R., Fürnsinn, C., Graf, J., Waldhäusl, W. & Roden, M. 1999, "Acute troglitazone action in isolated perfused rat liver", *British journal of pharmacology*, vol. 126, no. 1, pp. 372-378.
- Rashed, M.S., Myers, T.G. & Nelson, S.D. 1990, "Hepatic protein arylation, glutathione depletion, and metabolite profiles of acetaminophen and a non-hepatotoxic regioisomer, 3'-hydroxyacetanilide, in the mouse.", *Drug Metabolism and Disposition*, vol. 18, no. 5, pp. 765-770.
- Regan, S.L., Maggs, J.L., Hammond, T.G., Lambert, C., Williams, D.P. & Park, B.K. 2010, "Acyl glucuronides: The good, the bad and the ugly", *Biopharmaceutics and Drug Disposition*, vol. 31, no. 7, pp. 367-395.
- Reilly, T.P., Lash, L.H., Doll, M.A., Hein, D.W., Woster, P.M. & Svensson, C.K. 2000, "A role for bioactivation and covalent binding within epidermal keratinocytes in sulfonamide-induced cutaneous drug reactions", *Journal of Investigative Dermatology*, vol. 114, no. 6, pp. 1164-1173.
- Robertson, J.D. & Orrenius, S. 2000, "Molecular mechanisms of apoptosis induced by cytotoxic chemicals", *CRC critical reviews in toxicology*, vol. 30, no. 5, pp. 609-627.
- Robertson, J.D., Orrenius, S. & Zhivotovsky, B. 2000, "Review: nuclear events in apoptosis", *Journal of structural biology*, vol. 129, no. 2-3, pp. 346-358.
- Rotzinger, S. & Baker, G.B. 2002a, "Human CYP3A4 and the metabolism of nefazodone and hydroxynefazodone by human liver microsomes and heterologously expressed enzymes", *European Neuropsychopharmacology*, vol. 12, no. 2, pp. 91-100.
- Rotzinger, S. & Baker, G.B. 2002b, "Human CYP3A4 and the metabolism of nefazodone and hydroxynefazodone by human liver microsomes and heterologously expressed enzymes", *European Neuropsychopharmacology*, vol. 12, no. 2, pp. 91-100.
- Sachse, C., Brockmöller, J., Bauer, S. & Roots, I. 1997, "Cytochrome P450 2D6 variants in a Caucasian population: Allele frequencies and phenotypic consequences", *American Journal of Human Genetics*, vol. 60, no. 2, pp. 284-295.
- Salinas, A.E. & Wong, M.G. 1999, "Glutathione S-transferases - A review", *Current medicinal chemistry*, vol. 6, no. 4, pp. 279-309.
- Scherrmann, J.-. 2009, "Transporters in absorption, distribution, and elimination", *Chemistry and Biodiversity*, vol. 6, no. 11, pp. 1933-1942.
- Schirren, C.A. & Baretton, G. 2000, "Nefazodone-induced acute liver failure [8]", *American Journal of Gastroenterology*, vol. 95, no. 6, pp. 1596-1597.

- Shah, R.R., Evans, D.A.P. & Oates, N.S. 1985, "The genetic control of phenformin 4-hydroxylation", *Journal of medical genetics*, vol. 22, no. 5, pp. 361-366.
- Shah, R.R., Oates, N.S. & Idle, J.R. 1982, "Impaired oxidation of debrisoquine in patients with perhexiline neuropathy", *British medical journal*, vol. 284, no. 6312, pp. 295-299.
- Shah, R.R., Oates, N.S., Idle, J.R. & Smith, R.L. 1980, "Genetic impairment of phenformin metabolism", *Lancet*, vol. 1, no. 8178, pp. 1147.
- Sogame, Y., Kitamura, A., Yabuki, M. & Komuro, S. 2011, "Liver uptake of Biguanides in rats", *Biomedicine and Pharmacotherapy*, vol. 65, no. 6, pp. 451-455.
- Sogame, Y., Kitamura, A., Yabuki, M. & Komuro, S. 2009, "A comparison of uptake of metformin and phenformin mediated by hOCT1 in human hepatocytes", *Biopharmaceutics and Drug Disposition*, vol. 30, no. 8, pp. 476-484.
- Stieger, B., Meier, Y. & Meier, P.J. 2007, "The bile salt export pump", *Pflügers Archiv European Journal of Physiology*, vol. 453, no. 5, pp. 611-620.
- Summan, M. & Cribb, A.E. 2002, "Novel non-labile covalent binding of sulfamethoxazole reactive metabolites to cultured human lymphoid cells", *Chemico-biological interactions*, vol. 142, no. 1-2, pp. 155-173.
- Taylor, D.P., Allen, L.E. & Becker, J.A. 1984, "Changing concepts of the biochemical action of the anxiolytic drug, buspirone", *Drug Development Research*, vol. 4, no. 1, pp. 95-108.
- Tettey, J.N., Maggs, J.L., Rapeport, W.G., Pirmohamed, M. & Park, B.K. 2001, "Enzyme-induction dependent bioactivation of troglitazone and troglitazone quinone in vivo", *Chemical research in toxicology*, vol. 14, no. 8, pp. 965-974.
- Thompson, R.A., Isin, E.M., Li, Y., Weidolf, L., Page, K., Wilson, I., Swallow, S., Middleton, B., Stahl, S., Foster, A.J., Dolgos, H., Weaver, R. & Kenna, J.G. 2012, "In Vitro Approach to Assess the Potential for Risk of Idiosyncratic Adverse Reactions Caused by Candidate Drugs", *Chemical research in toxicology*, .
- Tirmenstein, M.A. & Nelson, S.D. 1989, "Subcellular binding and effects on calcium homeostasis produced by acetaminophen and a nonhepatotoxic regioisomer, 3'-hydroxyacetanilide, in mouse liver.", *Journal of Biological Chemistry*, vol. 264, no. 17, pp. 9814.
- Toyokuni, S. 1999, "Reactive oxygen species-induced molecular damage and its application in pathology", *Pathology international*, vol. 49, no. 2, pp. 91-102.

- Tsokos-Kuhn, J.O., Hughes, H., Smith, C.V. & Mitchell, J.R. 1988, "Alkylating toxins and the liver plasma membrane calcium pump/calcium atpase.", *Advances in Experimental Medicine and Biology*, vol. 232, pp. 151-158.
- Tzimas, G.N., Dion, B. & Deschênes, M. 2003, "Early onset, nefazodone-induced fulminant hepatic failure [7]", *American Journal of Gastroenterology*, vol. 98, no. 7, pp. 1663-1664.
- Uetrecht, J.P., Shear, N.H. & Zahid, N. 1993, "N-chlorination of sulfamethoxazole and dapsone by the myeloperoxidase system", *Drug Metabolism and Disposition*, vol. 21, no. 5, pp. 830-834.
- Usui, T., Mise, M., Hashizume, T., Yabuki, M. & Komuro, S. 2009, "Evaluation of the potential for drug-induced liver injury based on in vitro covalent binding to human liver proteins", *Drug Metabolism and Disposition*, vol. 37, no. 12, pp. 2383-2392.
- Vandeputte, C., Guizon, I., Genestie-Denis, I., Vannier, B. & Lorenzon, G. 1994, "A microtiter plate assay for total glutathione and glutathione disulfide contents in cultured/isolated cells: Performance study of a new miniaturized protocol", *Cell biology and toxicology*, vol. 10, no. 5-6, pp. 415-421.
- Vergani, D., Mieli-Vergani, G. & Alberti, A. 1980, "Antibodies to the surface of halothane-altered rabbit hepatocytes in patients with severe halothane-associated hepatitis", *New England Journal of Medicine*, vol. 303, no. 2, pp. 66-71.
- Von Moltke, L.L., Greenblatt, D.J., Granda, B.W., Grassi, J.M., Schmider, J., Harmatz, J.S. & Shader, R.I. 1999a, "Nefazodone, meta-chlorophenylpiperazine, and their metabolites in vitro: Cytochromes mediating transformation, and P450-3A4 inhibitory actions", *Psychopharmacology*, vol. 145, no. 1, pp. 113-122.
- Von Moltke, L.L., Zalma, A., Granda, B.W., Grassi, J.M., Shader, R.I. & Greenblatt, D.J. 1999b, "Meta-chloro-phenylpiperazine (mCPP): P450-3A-dependent formation from nefazodone and trazodone; P450-2D6-dependent clearance", *Clinical pharmacology and therapeutics*, vol. 65, no. 2, pp. 144.
- Walgren, J.L., Mitchell, M.D. & Thompson, D.C. 2005, "Role of metabolism in drug-induced idiosyncratic hepatotoxicity", *CRC critical reviews in toxicology*, vol. 35, no. 4, pp. 325-361.
- Wang, D.S., Jonker, J.W., Kato, Y., Kusuhara, H., Schinkel, A.H. & Sugiyama, Y. 2002, "Involvement of organic cation transporter 1 in hepatic and intestinal distribution of metformin", *Journal of Pharmacology and Experimental Therapeutics*, vol. 302, no. 2, pp. 510-515.

- Wang, D.-., Kusuhara, H., Kato, Y., Jonker, J.W., Schinkel, A.H. & Sugiyama, Y. 2003a, "Involvement of organic cation transporter 1 in the lactic acidosis caused by metformin", *Molecular pharmacology*, vol. 63, no. 4, pp. 844-848.
- Wang, D.-., Kusuhara, H., Kato, Y., Jonker, J.W., Schinkel, A.H. & Sugiyama, Y. 2003b, "Involvement of organic cation transporter 1 in the lactic acidosis caused by metformin", *Molecular pharmacology*, vol. 63, no. 4, pp. 844-848.
- Williams, D.P. 2006, "Toxicophores: Investigations in drug safety", *Toxicology*, vol. 226, no. 1, pp. 1-11.
- Williams, D.P., Antoine, D.J., Butler, P.J., Jones, R., Randle, L., Payne, A., Howard, M., Gardner, I., Blagg, J. & Park, B.K. 2007, "The metabolism and toxicity of furosemide in the wistar rat and CD-1 mouse: A chemical and biochemical definition of the toxicophore", *Journal of Pharmacology and Experimental Therapeutics*, vol. 322, no. 3, pp. 1208-1220.
- Williams, D.P., Kitteringham, N.R., Naisbitt, D.J., Pirmohamed, M., Smith, D.A. & Park, B.K. 2002, "Are chemically reactive metabolites responsible for adverse reactions to drugs?", *Current Drug Metabolism*, vol. 3, no. 4, pp. 351-366.
- Williams, D.P., Pirmohamed, M., Naisbitt, D.J., Maggs, J.L. & Park, B.K. 1997, "Neutrophil cytotoxicity of the chemically reactive metabolite(s) of clozapine: Possible role in agranulocytosis", *Journal of Pharmacology and Experimental Therapeutics*, vol. 283, no. 3, pp. 1375-1382.
- Williams, D.P., Pirmohamed, M., Naisbitt, D.J., Uetrecht, J.P. & Park, B.K. 2000, "Induction of metabolism-dependent and -independent neutrophil apoptosis by clozapine", *Molecular pharmacology*, vol. 58, no. 1, pp. 207-216.
- Witters, L.A. 2001, "The blooming of the French lilac", *Journal of Clinical Investigation*, vol. 108, no. 8, pp. 1105-1107.
- Yuan, L. & Kaplowitz, N. 2008, "Glutathione in liver diseases and hepatotoxicity", *Molecular Aspects of Medicine*, .
- Zhao Chao Liu & Uetrecht, J.P. 1995, "Clozapine is oxidized by activated human neutrophils to a reactive nitrenium ion that irreversibly binds to the cells", *Journal of Pharmacology and Experimental Therapeutics*, vol. 275, no. 3, pp. 1476-1483.
- Zhou, G., Myers, R., Li, Y., Chen, Y., Shen, X., Fenyk-Melody, J., Wu, M., Ventre, J., Doebber, T. & Fujii, N. 2001, "Role of AMP-activated protein kinase in mechanism of metformin action", *Journal of Clinical Investigation*, vol. 108, no. 8, pp. 1167-1174.
- Zhu, M., Zhao, W., Jimenez, H., Zhang, D., Yeola, S., Dai, R., Vachharajani, N. & Mitroka, J. 2005, "Cytochrome P450 3A-mediated metabolism of buspirone in

Bibliography

human liver microsomes", *Drug Metabolism and Disposition*, vol. 33, no. 4, pp. 500-507.

Zou, M.-., Kirkpatrick, S.S., Davis, B.J., Nelson, J.S., Wiles IV, W.G., Schlattner, U., Neumann, D., Brownlee, M., Freeman, M.B. & Goldman, M.H. 2004, "Activation of the AMP-activated protein kinase by the anti-diabetic drug metformin in vivo: Role of mitochondrial reactive nitrogen species", *Journal of Biological Chemistry*, vol. 279, no. 42, pp. 43940-43951.